UNIVERSITÀ DEGLI STUDI DI NAPOLI

"FEDERICO II"

DIPARTIMENTO DI FARMACIA

Dottorato di Ricerca in

"Scienza del Farmaco"

Ciclo XXVIII 2013-2016

"Quali-quantitative determination and structural characterization of microalgal toxins in environmental matrices"

Dr. Antonia Mazzeo

Tutor

Prof.ssa

Carmela Dell'Aversano

Coordinator

Prof.ssa

Maria Valeria D'Auria

Table of contents

Table List

Figure List

Summary

"Harmful Algal Blooms" (HABs) are massive proliferations of marine microalgae producing biotoxins. These natural phenomena, occurring under particular climatic and environmental conditions, represent a worldwide problem since they pose serious threats to human health and heavily affect economy of coastal areas. Humans may be affected by marine biotoxins through three main exposure routes: the oral route through consumption of contaminated seafood, the respiratory route through inhalation of aerosolized toxins, and the dermal route through direct contact with microalgae and/or contaminated seawater. However, for some marine biotoxins the mechanism through which they exert their toxicity has not been clarified yet.

The *Ostreopsis* phenomenon currently represents the major HAB-related threat to humans in the Mediterranean area. Since the late 1990s, blooms of *Ostreopsis* cf. *ovata* have been repetitively recorded all along the Italian coastlines as well as along the Mediterranean coasts of Spain, France, Croatia, Greece and North Africa. Concomitantly, a severe respiratory syndrome has been observed in humans requiring in some cases hospitalization. Previous studies have demonstrated that *O.* cf. *ovata* produces congeners of palytoxin (PLTX), (ovatoxins and an isobaric PLTX), one of the most potent marine toxins so far known, originally isolated from soft corals belonging to the genus *Palythoa.* However, inhalatory toxicity of PLTX and its congeners was completely unknown and the mechanism through which they harm humans through inhalation is still matter of speculation. The increasing spread of the *Ostreopsis* phenomenon and the ever-growing number of ovatoxins (OVTXs) being discovered makes the need of evaluating their toxicity urgent. The availability of sufficient amounts of well characterized reference material is the cornerstone for the achievement of toxicity data.

Beside PLTX congeners, a wide array of marine biotoxins present serious concern for humans. As a result, National and Local authorities in charge of safeguarding public health have enacted monitoring and risk management programs of toxin with the purpose of limiting adverse impacts of HABs; these regulations require routine monitoring of shellfish for toxins and the analysis of water samples for the presence of toxin-producing microalgae. However, the analysis of shellfish and the analysis of microalgae presents number of technical and practical limitations; for these reasons, in recent years, passive sampling (*Solid Phase Adsorption Toxins Tracking,* SPATT) has been investigated as an alternative mean to highlight the presence of toxic microalgae directly in seawater.

In this frame, the aim of this thesis was:

- to investigate the mechanism through which *O.* cf. *ovata* and *Palythoa* spp. and the toxins they produce exert their toxicity;
- to determine toxin profile and content of *Ostreopsis* spp. strains from South-East Mediterranean Sea (Cyprus Island and Lebanon), New Zealand and Australia to serve the double purpose of evaluating the risk they present to humans and investigating the presence of novel PLTX analogues by LC-$HRMS^n$;
- to use SPATT methods for detection of marine biotoxins;
- to perform preliminary studies toward isolation of PLTX congeners.

Investigation of the toxicity mechanism of *O.* cf. *ovata* and *Palythoa* spp.

In Chapter 2 the potentially active role of the mucilaginous matrix produced by *O.* cf. *ovata*, has been for the first time investigated. In order to better elucidate toxicity dependence on direct/indirect contact, the role of the mucilaginous matrix and the potential differences in toxicity along the growth curve of *O.* cf. *ovata*, a toxic bioassay during exponential, stationary and late stationary phases was carried out. Simultaneously, a molecular assay was performed to quantify intact cells or to exclude the presence of the cells. Liquid Chromatography-High Resolution Mass Spectrometry (LC-HRMS) analyses were also carried out to evaluate toxin profile and content in the different treatments. As a result, a higher mortality of model organism (*Artemia salina* nauplii) was also observed, especially during the late stationary phase, when direct contact between the model organism and intact microalgal cells occurred ($LC_{50\text{-}48h}$ < 4 cells/ml on *A. salina*). Also growth medium devoid of microalgal cells but containing *O.* cf. *ovata* mucilage caused significant toxic effects. This finding was also supported by chemical analyses which showed the highest toxin content in pellet extract (95%) and around 5% of toxins in the growth medium holding mucous, while the growth medium devoid of both cells and mucilage did not contain any detectable toxins. Additionally, the connection between mucilaginous matrix and the thecal plates, pores and trychocysts was explored by way of atomic force microscopy (AFM) to investigate the cell surface at a sub-nanometer resolution, providing a pioneering description of cellular features.

In Chapter 3 LC-HRMS analysis of both soft coral and seawater from a home marine aquarium involved in a whole family poisoning is reported. Several anecdotal reports exist of aquarium hobbyists that experienced severe respiratory distress and/or skin

injury following cleaning operation of home aquaria containing *Palythoa* sp. soft corals as well as hundreds of cases of respiratory illness and/or dermatitis have been recorded in proximity to the sea concomitantly with algal blooms of *Ostreopsis* spp. in the Mediterranean area. Both *Palythoa* spp. and *Ostreopsis* spp. contain congeners of PLTX whose inhalation hazard is however unknown. In this study, we demonstrate the presence of high levels of PLTXs (PLTX and hydroxy-PLTX) in both soft coral and seawater collected in the marine aquarium. Due to the high toxin levels found in seawater, a procedure for a rapid and efficient determination of palytoxin in seawater was developed. A comparison of symptoms of *Palythoa*- and *Ostreopsis*-related inhalatory poisonings showed many similarities including fever, respiratory distress, nausea, and flu-like symptoms. From the chemical and symptomatological data reported herein it is reasonable to hold PLTXs responsible for respiratory disorders following inhalation. Although the exact mechanism through which PLTX congeners exert their inhalatory toxicity is still unknown, this represents a step toward demonstrating that they exert toxic effects through inhalation both in natural environments and in the surroundings of private and public aquaria.

Toxin profile and content of *Ostreopsis* spp. strains from South-East Mediterranean Sea, New Zealand and Australia.

In Chapter 4 the investigation of the toxin profile and content of six strains of *Ostreopsis* sp. from Cyprus Island is reported. The samples were analyzed through an integrated approach based on molecular, chemical and eco-toxicological methods. Cypriot *Ostreopsis* sp. was found to be a species distinct from *O.* cf. *ovata* and *O.* cf. *siamensis*, belonging to the Atlantic/Mediterranean *Ostreopsis* spp. clade. Some variability in toxin profiles emerged: three strains produced OVTX-a, OVTX-d, OVTX-e and isobaric PLTX, so far found only in *O.* cf. *ovata*, the other three strains produced only new PLTX-like compounds, that we named OVTX-i, -j_1, -j_2, and -k. The new OVTXs had the same carbon skeleton as OVTX-a differing primarily for an additional $C_2H_2O_2$ moiety and an unsaturation in the region C49-C52. Other minor structural differences were found, including the presence of a hydroxyl group at C44 (in OVTX-j_1 and -k) and the lack of a hydroxyl group in the region C53-C78 (in OVTX-i and -j_1). Toxin content of the analyzed *Ostreopsis* sp. strains was in the range 0.06-2.8 pg/cell, definitely lower than that of a Ligurian *O.* cf. *ovata* strain cultured under the same conditions. Accordingly, eco-toxicological test on *A. salina* nauplii demonstrated that *Ostreopsis* sp. presents a very low

toxicity compared to *O.* cf. *ovata*. The whole of these data suggest that *Ostreopsis* sp. from Cyprus Island pose a relatively low risk to humans.

Chapter 5 reports the chemical analysis of five strains of *Ostreopsis* spp. collected from Lebanon coasts and of six strains of *Ostreopsis* spp. (*ovata*, *siamensis* and *Ostreopsis* sp.) from New Zealand and Australia. LC-HRMS of Lebanese extracts showed that three strains produced OVTX-a, OVTX-d, OVTX-e in very minute amounts (0.28-0.94 pg/cell), thus presentig a low risk to humans. The toxin profile of these strains quali-quantitatively matched with that of other *Ostreopsis* sp. strains from Cyprus Island. The other extracts did not contain any PLTX congener. Molecular analyses showed that *Ostreopsis* sp. from Lebanon and from Cyprus Island are actually the same species that we named *Ostreopsis fattorussoi*.

LC-HRMS analysis of *Ostreopsis* spp. strains from New Zealand and Australia showed that none of the known PLTX congeners so far known were contained in any of the extracts. Only a new analogue, was present in one of the *Ostreopsis* sp. extracts. It presented a C_5H_7ON moiety as well as 2 unsaturation less than OVTX-a. An extensive LC-$HRMS^n$ study, allowed to locate such modification in the very limited region stretching from the A-side terminal to C-8. This compound presented a characteristic fragmentation behavior: indeed, a formaldehyde loss could be observed from the precursor ion as well as from most of the A-side fragment ions. Formaldehyde losses may occur when a CH_2OH moiety is present in the molecule following a Mac Lafferty-like rearrangement. We located the CH_2OH moiety on the terminal amide.

Application of SPATT for detection of assorted marine biotoxins

Chapter 6 reports on a survey of phytoplankton and algal toxins in Nigerian coastal waters. Seawater samples were obtained from four sites for phytoplankton identification (Bar Beach and Lekki in Lagos State, Port Harcourt in Rivers State and Uyo in Akwa Ibom State), on three occasions between the middle of October 2014 and the end of February 2015. The phytoplankton community was generally dominated by diatoms and cyanobacteria; however, several species of dinoflagellates were also identified: *Dinophysis caudata*, *Lingulodinium polyedrum* and two benthic species of *Prorocentrum*.

Passive samplers (containing Diaion® HP-20 resin) were deployed for several 1-week periods on the same four sites to obtain profiles of algal toxins present in the seawater. Quantifiable amounts of OA and PTX-2, as well as traces of DTX-1 were detected at several sites. The highest toxin concentrations (60 ng OA g/HP-20 resin) were found at Lekki and Bar Beach stations, which had also the highest salinities. Non-targeted

analysis using full-scan HRMS showed that algal metabolites differed from site to site and for different sampling occasions. Screening against a marine natural products database indicated the potential presence of cyanobacterial compounds in the water column, which was also consistent with phytoplankton analysis.

Chapter 7 reports another application of passive samplers in the French lagoon of Ingril. Seawater portions of 30 L were collected and pre concentrated by passive sampling with HP-20 resin over a 48 h period. Detection of lipophilic toxins in the extracts of the resin was carried out using liquid chromatography coupled to tandem mass spectrometry. This combination allowed the detection of sub-ppb levels of dissolved toxins and would permit further studies for accurate modelling of the toxins adsorption behavior by passive sampling devices. In particular, we determined the levels of OA, DTX-1, PTX-2 and PnTX-G in seawater from Ingril lagoon. OA was the most concentrated compound with ca. 8.6 ng/L, followed by DTX-1 with ca. 1.4 ng/L, and both PTX-2 and PnTX-G at ca. 0.2-0.3 ng/L. This is one of the first direct analyses of lipophilic dinoflagellate toxins in seawater. However, these concentrations were observed in a lagoon and should be confirmed in open coastal waters.

Preliminary studies toward isolation of PLTX

Chapter 8 describes preliminary studies aiming to quantitative isolation of palytoxin. Previous reported isolation procedure, provided very poor recoveries of palytoxin congeners as pure compound, with no indication whether such low recoveries were due to instability of the compounds in solution or to irreversible adsorption to materials or to other uncontrolled factors. In view of a large scale isolation work aimed to preparation of PLTX reference material, the causes underlying the huge PLTX loss were investigated. We focused on the evaporation of PLTX under various experimental conditions namely the use of different evaporation systems (Centrifugal Vacuum Concentrator and N_2 stream) versus freeze drying, complete drying versus concentration, the influence of various solvents (aqueous or pure organic), the effect of most common materials (normal and silanized glass vials, polypropylene and Teflon tubes) and of the re-dissolution solvent (nature and quantity) on toxin recovery. Preliminary results on stability of PLTX under various acidic conditions were also obtained. PLTX behaved differently when it was simply concentrated or completely dried down. Recoveries were strongly dependent on solubility of PLTX in the mixtures used as well as on the materials in which evaporation was carried out. We found that, in order to enhance PLTX recovery, freeze drying is an appropriate procedure to be avoided. In general, the highest recoveries were

obtained when PLTX was completely dried down in Teflon carrying out evaporation in aqueous blends or concentration in pure organic solvent. The worst recoveries were obtained using glass materials probably due to the sticking of PLTX on the surface of the vials; in order to reduce this phenomenon water should be used in the mixture. Experiments on stability of PLTX in acid blends demonstrated that PLTX is an acid-sensitive molecule and that, depending on pH, it rapidly degradates forming mainly a PLTX methyl-ester by cleavage of the enamide functionality contained in the A-side terminal of the molecule. Structural insights on the PLTX methyl-ester were gained by LC-HRMS/MS.

The whole of work described has been reported in 4 published articles, 3 manuscripts in preparation, 2 proceedings and several oral/poster communications in international congress.

A list of the publications/oral/poster communications is reported below.

List of published articles

1) Active role of the mucilage in the toxicity mechanism of the harmful benthic dinoflagellate *Ostreopsis* cf. *ovata*

V. Giussani, F. Sbrana, V. Asnaghi, M. Vassalli, M. Faimali, S. Casabianca, A. Penna, P. Ciminiello, C. Dell'Aversano, L. Tartaglione, A. Mazzeo, M. Chiantore

Harmful Algae 2015 Mar;44:46–53. doi: 10.1016/j.hal.2015.02.006 Epub 2015 Mar 20

2) Determination of Palytoxins in Soft Coral and Seawater from a Home Aquarium. Comparison between *Palythoa*- and *Ostreopsis*-Related Inhalatory Poisonings.

Tartaglione L, Dell'Aversano C, Mazzeo A, Forino M, Wieringa A, Ciminiello P

Environ Sci Technol. 2016 Jan 19;50(2):1023-30. doi: 10.1021/acs.est.5b05469. Epub 2015 Dec 23.

3) Chemical, molecular, and eco-toxicological investigation of Ostreopsis sp. from Cyprus Island: structural insights into four new ovatoxins by LC-HRMS/MS.

Tartaglione L, Mazzeo A, Dell'Aversano C, Forino M, Giussani V, Capellacci S, Penna A, Asnaghi V, Faimali M, Chiantore M, Yasumoto T, Ciminiello P.

Anal Bioanal Chem. 2016 Jan;408(3):915-32. doi: 10.1007/s00216-015-9183-3. Epub 2015 Nov 25.

4) Algal toxin profiles in Nigerian coastal waters (Gulf of Guinea) using passive sampling and liquid chromatography coupled to mass spectrometry.
Zendong Z, Kadiri M, Herrenknecht C, Nézan E, Mazzeo A, Hess P.
Toxicon. 2016 Feb 16; 114:16-27. doi: 10.1016/j.toxicon.2016.02.011. [Epub ahead of print]

List of proceeding

In: A. Lincoln MacKenzie [Ed]. Marine and Freshwater Harmful Algae. Proceedings of the 16th International Conference on Harmful Algae, Wellington, New Zealand 27th-31st October 2014.

1) Zendong Z., Abadie E., Mazzeo A., Hervé F., Herrenknecht C., Amzil Z., Dell'Aversano C., Hess P. (2015) Determination of the concentration of dissolved lipophilic algal toxins in seawater using pre-concentration with HP-20 resin and LC-MS/MS detection. Pp. 210-213.

2) Giussani V., Kletou D., Capellacci S., Asnaghi V., Penna A., Ciminiello P., Dell'Aversano C., Mazzeo A., Tartaglione L., Faimali M., Pronzato R., Chiantore M.
New *Ostreopsis* species record along Cyprus coast: toxic effect and preliminary characterization of chemical-molecular aspects Pp. 144-146.

Participation to international congress (presenting author)

1) VII International Conference on Marine Bioprospecting- Tromso, Norway"18-20 February 2015

- Title of poster: Emerging toxin in the Mediterranean Sea. Mazzeo A., Dell'Aversano C., Tartaglione L., Forino M., Ciminiello P.
Awarded from congress committee

2) "Conférence GdR Phycotox - GIS Cyano 2015" 31 March-2 April 2015, Brest (France)

- Title of oral presentation: Extraction of palytoxins from seawater and preliminary stability studies. Mazzeo A., Tartaglione L., Zendong Z., Forino M., Hess P., Ciminiello P., Dell'Aversano C.
Awarded from University of Naples "Federico II"

- Title of oral presentation: The memory of seawater: passive sampling for the profiling of algal toxins in lagoons and open coastal seas. Zendong Z., Herrenknecht C., Abadie E., Jauzein C., Lemée R., Gouriou J., Mazzeo A., Amzil Z., Hess P.

3) "Fifth Joint Symposium and AOAC Task Force Meeting Marine & Freshwater Toxins Analysis" 14-17 June 2015, Baiona, (Spain)

- Title of poster: Toward quantitative isolation of palytoxins. Preliminary stability and purification studies. Mazzeo A., Tartaglione L., Zendong Z., Forino M., Hess P., Ciminiello P., Dell'Aversano C.

- Title of oral presentation: Structural studies on known and novel palytoxin congeners from *Palythoa* spp. and *Ostreopsis* sp. Tartaglione L., Dell'Aversano C., Mazzeo A., Forino M., Ciminiello P.

Chapter 1

1. General introduction

Since the old ages seas and oceans represent a vital source for humans as they provide fishery products. Seafood refers to any marine life form used as source of nutrition by humans, including finfish and shellfish (mollusks, crustaceans, and echinoderms) from open seas as well as from aquacultures. They are very important for humans as they supply proteins, minerals and essential fatty acids. Aquatic food accounts for over 40% of global animal food products [1]. Thanks to the increase of population and urbanization, and the improvement of technologies and more efficient distribution channels, global fish production has grown in the last five decades reaching 158 million tons of fish in 2012 (of which 136.2 for human consumption). Annual per capita apparent fish consumption increased from an average of 9.9 kg in the 1960s to 19.2 kg in 2012 [2]. However, the exploitation of sea resources is a double-edged sword, because these products can also be vectors of potentially harmful substances for humans that represent the last step of the food chain.

The productive base of both marine and freshwater ecosystems is the plankton. It is constituted by living species that can't oppose themselves to the sea currents movement, but that get carried away from these currents. From this comes its name: from the Greek *planktos*, that means "errant". The autotrophic components of the plankton are named phytoplankton (from the Greek word *phyton*, meaning "plant"). They are mostly microscopic, single-celled organisms which transform inorganic carbon in seawater into organic compounds through photosynthesis. This fact makes them an essential part of Earth's carbon cycle representing, therefore, the first ring of the aquatic food chain. In particular, the phytoplankton is constituted by microalgae. The latter can live isolated (unicellular forms) or in groups of little colonies of cells. According to the species, they grow in biomass, by increasing both in dimension and quantity. More than 5000 species of marine microalgae are known to date [3] and can live either in the water column (pelagic) or hung on a substrate (benthic or epiphytic). They can be divided into five main classes:

- *Chlorophyta* (green algae)
- *Chrysophita* (yellow algae and diatoms)
- *Pyrrhophyta* (dinoflagellates)
- *Euglenophy*

- *Cyanophyta* (blue-green algae or cyanobacteria)

These microalgae are vital for filter-feeding bivalve shellfish and usually beneficial for aquaculture. However, about 300 [4] of the previously mentioned marine microalgae species are actually considered harmful to humans. When such species are present at high concentration in the water or proliferate massively, under appropriate climatic and environmental conditions, they cause the so called "Harmful Algal Bloom" phenomenon (HAB). HAB is a natural, world-wide problem, well reviewed already about twenty years ago [5]. It can have a negative impact on the environment. Indeed, when rapid increase in some algal species population occurs, a discoloration of water surface associated with appearance of scums and bad smells may take place. In addition, the depletion of oxygen from the water column due to the action of bacteria on the accumulated biomass results in fish and aquatic invertebrates mortality [6]. Beside the environmental aspect, HABs have a negative socio-economic impact due to economic losses as a result of the closure of fish and shellfish farms infested by toxic algal species and the decline of coastal touristic activities. However, the major concern related to the HABs regards the human health, since there are some microalgae species able to produce toxic secondary metabolites called "phycotoxins", that can be harmful or even lethal to humans. Indeed, the microalgae are the first ring of food chain, since they represent crucial food for the zooplankton, bivalve shellfish, such as mussels, oyster, scallops, clams, etc. and fish [7]; because of phenomena such as the filter-feeding, these species accumulate in their edible tissues all particles in suspension existing in sea water namely microalgae and their relevant toxins. Therefore, algal toxins can find their way through the different levels of the food chain ending up on the table of unaware consumers, thus provoking a variety of gastrointestinal and neurological illness [8]. Skin contact with toxin contaminated water or inhalation of aerosolized toxins are other routes of exposure to these harmful compounds [7]. In the last two decades, the efforts to investigate these phenomena have resulted in a dramatic increase in the number of microalgal species considered "toxic" (or toxin producers): about 40 species were claimed as potentially toxic to humans in 1993 [4], while current databases describe more than 100 eukaryotic species of toxic marine phytoplankton, mostly dinoflagellates and diatoms [9]. Although marine biotoxins have been usually reported for their negative effects, they nonetheless exhibit extensive ranges of bioactivities that make them potential starting points for drugs. Saxitoxin, for example, can be used as a safe and long-acting topical anesthetic [10]. Likewise, tetrodotoxin, a marine toxin found in the pufferfish, is being used in drug dependence research [10].

It is still not clear the reason why some micro-algal species produce toxic compounds which play no explicit role in the internal economy of the producing organisms [11]. These toxins are probably used as a tool for space competition, fighting predation or as a defense against the overgrowth of other organisms [12].

Hundreds of thousands of human poisonings related to exposure of marine biotoxins are reported every year on a global basis [13] due to the expansion in the last decades of HABs in terms of frequency, intensity and geographic distribution [5,7,14-15]. The increase in the number of the HABs signaled, and the increase in the cases of food poisoning, seems due to several causes: sea anthropogenic eutrophication, increase of scientific knowledge of toxic species, wider and better monitoring programs, increase in ship ballast waters which constitute an occasional vectors of microalgae from a geographic area to another and climatic changes [1] In particular, the increase of temperature may substitute the microalgal community by favoring the existence of species fitting life in warmer conditions in certain coastal zones where these species are not historically adapted to live in [16].

As a result, national and local authorities responsible for safeguarding public health have instituted programs of toxin monitoring and risk management with the purpose of limiting adverse impacts of HABs. In this context, several methods were developed and are applied to detect marine toxins in different matrices; these methods can be divided into biological and analytical. Historically, the most commonly used biological detection method is the mouse bioassay (MBA) [17]; it was initially developed by Yasumoto *et al.* [18] and it consists in an intra-peritoneal administration of seafood extracts to laboratory animals followed by monitoring of the symptoms and time to death. However, a number of problems were encountered when dealing with this kind of test, namely unethical issue, lack of sensitivity, specificity and robustness in addition to generation of high rates of false positives and negatives [19-21]. Despite its drawbacks, the MBA is still considered as a good screening tool for unknown toxins and Hess *et al.* (2009) [22] developed a harmonized MBA procedure that provides good reproducibility. Other biological methods including immuno-based technique such as enzyme-linked immunosorbent assay (ELISA), electrochemical and optical immunosensor, receptor-based techniques, cell-based assays and tissue-based methods have been reported for a number of toxin classes [23]. Despite their potential for speed, high sensitivity and low cost, there are some limitations associated with such methods [24]. In this context, FAO/IOC/WHO [25] and European reference control methods for marine toxins in shellfish have chosen to favor the analytical

techniques [26-28]. Actually analytical methods have the potential for sensitive, precise and fully automated quantitation of known toxins as well as identification of new ones. In general, these methods are based on hyphenated techniques, in which Gas chromatography (GC), Thin Layer Chromatography (TLC), Capillary Electrophoresis (CE), and predominantly Liquid Chromatography (LC) are coupled with several detectors such as Ultra-Violet (UV), Fluorescence (FLD) and Mass Spectrometry (MS)detectors. Among all these techniques there are some, which are listed in the reference methods for the detection of marine biotoxins that will be discussed in the following chapters.

2. Phycotoxins

Phycotoxins are metabolites naturally produced by certain microalgal species which proliferate in marine and fresh waters. They are able to concentrate in different marine organisms (including filter-feeding bivalves, herbivorous and predatory fish), ending up in the food chain thus provoking human poisoning. Phycotoxins can be divided in several groups; each group contains often a huge number of analogues which are either produced by the algae or bio-transformed in fish, shellfish or other marine organisms [29]. Traditionally, shellfish poisonings have been classified in five main syndromes (as reviewed in James *et al.* [30]) according to the symptoms recorded in humans, after the ingestion of contaminated bivalve mollusks:

-paralytic shellfish poisoning (PSP);

-amnesic shellfish poisoning (ASP);

-neurotoxic shellfish poisoning (NSP);

-azaspiracid shellfish poisoning (AZP);

-diarrhetic shellfish poisoning (DSP).

However, this classification was found to be inadequate for some kind of toxins (for example regarding the initially classification of pectenotoxins and yessotoxins with the diarrhetic toxins which will be discussed below (see paragraphs 2.5 and 2.6) and it does not consider other types of poisoning that are still not totally characterized (like ciguatera fish poisoning (CFP) as well as Palytoxins related syndrome).

A more suitable classification of marine phycotoxins based on their chemical characteristics (Table I.1), was proposed by Quilliam *et al*. [24] and subsequently adopted by the Joint FAO/IOC/WHO ad hoc Expert Consultation Group on Biotoxins in Bivalve Mollusks in 2005 [31].

Table I.1. Classification of the principal phycotoxins: poisoning syndromes, producer organism, vector to Humans, Formula and molecular weight of the main compound of each group. Reviews (Revs) selected as suggested references were published in the last ten years (2005-2015).

Toxins	Toxic syndrome	Producer	Vector	Chemical class	Formula and molecular weight (g/mol)	Polarity	Revs
Azaspiracid-1 (AZA) and analogs	AZP	*Azadinium spinosum* a *Protoperidinium crassipes*	Bivalve shellfish	Polyether, second amine	$C_{47}H_{71}NO_{12}$ (841)	Lipophilic	[32-33]
Brevetoxin-B and analogs	NSP	*Karenia brevis* *Chattonella* spp.	Bivalve shellfish and marine aerosol inhalation	Ladder-shaped polyether	$C_{50}H_{70}O_{14}$ (894)	Lipophilic	[34]
Ciguatoxin-4B (CTX) and analogs	CFP	*Gamberdiscus toxicus*	Several species of fish ("ciguateric fish")	Ladder-shaped polyether	$C_{60}H_{85}O_{16}$ (1061)	Lipophilic	[35-36]
Domoic acid (DA) and analogs	ASP	*Pseudonitzschia* spp.	Bivalve shellfish and finfish	Cyclic amino acid	$C_{15}H_{21}NO_6$ (311)	Hydrophilic	[37]
Gambierol	CFP	*Gamberdiscus* spp.	Several species of fish ("ciguateric fish")	Ladder-shaped polyether	$C_{43}H_{64}O_{11}$ (757)	Lipophilic	[35-36]
Gymnodimine (GYM)	Not associated with human illnesses	*Karenia selliformis*	Bivalve shellfish	Cyclic imine	$C_{32}H_{45}NO_4$ (507)	Lipophilic	[38-39]
Maitotoxin (MTX)	CFP	*Gamberdiscus* spp.	Several species of fish ("ciguateric fish")	Polyol, 4 fused ring system	$C_{164}H_{256}O_{68}S_2Na_2$ (3422)	Amphiphilic	[35-36]
Okadaic acid (OA) and dinophysistoxins (DTXs)	DSP	*Dinophysis* spp. *Prorocentrum* spp.	Bivalve shellfish	Polyether, spiroketo assembly	$C_{44}H_{68}O_{13}$ (804)	Lipophilic	[40-42]
Palytoxin (PLTX), ostreocins, ovatoxins and mascarenotoxins	PAS	*Ostreopsis* spp.	Bivalve shellfish, marine aerosol inhalation and skin contact	Polyol, 2 amide and 1 primary amine	$C_{129}H_{223}N_3O_{54}$ (2678)	Amphiphilic	[43-45]
Pectenotoxin-2 (PTX) and analogs	-	*Dinophysis* spp. *Prorocentrum* spp.	Bivalve shellfish	Polyether, ester macrocycle	$C_{47}H_{70}O_{14}$ (858)	Lipophilic	[40,46]
Pinnatoxins (PNTX), and analogues	Not associated with human illnesses	*Vulcanodium rugosum*	Bivalve shellfish	Cyclic imine	$C_{41}H_{61}NO_9$ (711)	Lipophilic	[38-39]
Saxitoxin (STX). neosaxitoxins, gonyautoxin and analogs	PSP	*Alexandrium spp., Gymnodinium catenatum Pyrodinium bahamense*	Bivalve shellfish and crustaceans	Tetrahydropurine alkaloid	$C_{10}H_{17}N_7O_4$ (299)	Hydrophilic	[47-48]
13-desmethyl spirolide C (SPX-1)	Not associated with human illnesses	*Alexandrium ostenfeldii*	Bivalve shellfish	Cyclic imine	$C_{41}H_{61}NO_7$ (691)	Lipophilic	[39 .40]
Yessotoxin (YTX) and analogs	-	*Protoceratium reticulatum, Lingulodinium polyedrum, Gonyaulax spinifera*	Bivalve shellfish	Ladder-shaped polyether	$C_{55}H_{82}O_{21}S_2$ (1140)	Lipophilic	[41, 50]

This kind of classification was found to be more appropriate for analytical purposes than the classification based on clinical symptoms. In general, marine microalgal toxins belong to three chemical classes: amino acid derivatives (Domoic acid), alkaloids (Saxitoxins and Tetrodotoxins) and polyketides (the rest). Most of them are lipophilic compounds, except STXs and DA which present acid and basic groups and are therefore classified as hydrophilic compounds. Palytoxins and MTXs have long carbon chains and several polar functions, thus they can be considered as amphiphilic compounds. Yessotoxins also show amphiphilic characteristics, but in Europe they are legally considered as lipophilic toxins [50]. To protect public health and permit the management of shellfish production, for the first time in 2004, European Commission have established maximum levels for marine biotoxins in live bivalve mollusks. [51]. A year later it settled the official testing methods for detecting marine biotoxins. Although bioassays were defined as the reference methods, validated analytical techniques or *in vitro* assays should be applied if they have at least the same efficiency as the biological method [52]. In 2006, the European Commission requested EFSA to provide a scientific opinion on marine biotoxins to assess the current EU limits with regard to human health and methods of analysis for various marine biotoxins, including the new emerging toxins. In this occasion, toxins concentration limits, including exposure due to both regular and occasional consumption of a large portion (400 g) of shellfish [53] Table I.2.

Table I.2 Current EU limits, the exposure levels resulting from consumption of shellfish on the EU market, the acute reference doses (ARfDs) set by EFSA, and the corresponding concentrations in shellfish meat. Extracted from the EFSA Journal (2009) 1306, 7-23

Toxin group	Current EU limits in shellfish meat(A)	Exposure by eating a400 g portion at the EU limits [c]	Exposure from eating a 400 g portion at the 95th percentile of the concentrations in samples currently on the EU market	ARfD	Corresponding dose for a 60 kg adult	Maximum concentration in shellfish meat to avoid exceeding the ARfD, when eating a 400g portion (B)	Ratio B /A
OA and analogues	160 µg OA eq./kg SM[a]	64 µg OA eq./person (1 µg OA eq./kg b.w.)	96 µg OA eq./person (1.6 µg OA eq./kg b.w).	0.3 µg OA eq./kg b.w.	18 µg OA eq./person	45 µg OA eq./kg SM	0.28
AZA	160 µg AZA eq.[c]/kg SM	64 µg AZA1 eq./person (1 µg AZA1 eq./kg b.w.)	16 µg AZA1 eq./person (0.3 µg AZA1 eq./kg b.w.)	0.2 µg AZA1 eq./kg b.w	12 µg AZA1 eq./person	30 µg AZA1 eq./kg SM	0.19
PTX	160 µg OA eq./kg SM[a]	64 µg PTX2/person (1 µg PTX2 eq./kg b.w.)	32 µg PTX2/person (0.5 µg PTX2 eq./kg b.w.)	0.8 µg PTX2 eq./kg b.w	48 µg PTX2 eq./person	120 µg PTX2 eq./kg SM	0.75
YTX	1 mg YTX eq./kg SM	400 µg YTX eq./person (6.7 µg YTX eq./kg b.w.)	320 µg YTX eq./person (IT) (5.3 µg YTX eq./kg b.w.) 125 µg YTX eq./person(NO) (2.1 µg YTX eq./kg b.w.)	25 µg YTX eq./kg b.w	1500 µg YTX eq./person	3.75 mg YTX eq./kg SM	3.75
STX	800 µg PSP/kg SM[b]	320 µg STX eq./person (5.3 µg STX eq./kg b.w.)	< 260 µg STX eq./person (<4.3 µg STX eq./kg b.w.)	0.5 µg STX eq./kg b.w	30 µg STX eq./person	75 µg STX eq./kg SM	0.09
DA	20 mg DA/kg SM	8 mg DA[d]/person (130 µg DA/kg b.w)	1 mg DA[d]/person (17 µg DA/kg b.w)	30 µg DA[d]/kg b.w	1.8 mg DA[d]/person	4.5 mg DA[d]/kg SM	0.23

SM: shellfish meat; eq.: equivalents; b.w.: body weight; ARfD: acute reference dose; PSP: paralytic shellfish poison; EU: European Union; IT: Italy; NO: Norway; OA: okadaic acid; PTX: pectenotoxin; YTX: yessotoxin; STX: saxitoxin; DA: domoic acid.

(a): For OA, dinophysistoxins and PTX, current regulation specifies a combination; however, the CONTAM Panel concluded that PTX should be considered separately.

(b): In the Commission Regulation (EC) No 853/2004 a limit value of 800 µg PSP/kg SM is given. In the EFSA opinion, the CONTAM Panel adopted this figure as being expressed as µg STX equivalents/kg SM.

(c): The CONTAM Panel assumed that AZA equivalent should refer to AZA1 equivalents.

(d): Applies to the sum of DA and epi-DA.

As for the reference methods, in some cases, MBA has been replaced by several analytical techniques: high performance liquid chromatography (HPLC), coupled with UV detection is the reference method for ASP toxins and antibodies based methods (ELISA) can be applied as screening tools [54]. For PSP toxins, HPLC with FLD, (known as the "Lawrence method") is officially accepted, although the reference control method is still the MBA [52,55]. For lipophilic toxins (AZAs, OA and DTXs, PTXs, and YTXs), the current reference control method is based on liquid chromatography coupled to mass spectrometry (LC-MS) [50]. LC-MS method and MBA coexisted until December 31st 2014, when LC-MS became the only reference method for lipophilic toxin control in shellfish in the European Union [50], after being validated in several collaborative (inter-laboratory) exercises [56-57]. BTXs are not currently regulated in EU since to date they have not been reported in shellfish or fish from Europe [58], but they are regulated in USA, Australia and New Zealand.

However, for some toxins the regulations may require revision, since some compounds have been proven not to be related with their original syndrome, such as pectenotoxins (PTXs), no longer considered diarrhetic, or yessotoxins (YTXs), which are even questioned to be toxic for human.

A detailed description of each class of toxins based on their chemical proprieties is reported below.

2.1 The Domoic acid group

Domoic acid (DA) (Figure I.1) is a toxin with anthelmintic activity which was originally isolated from a red marine macroalga, *Chondria armata* [59].

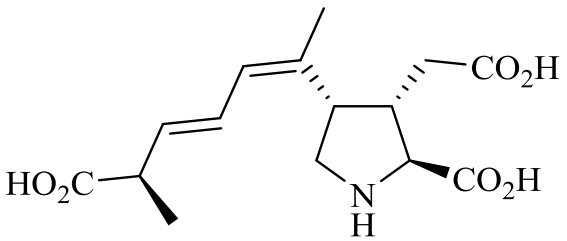

Figure I.1 Structure of Domoic Acid

Thereafter, it was identified in several red macroalgae belonging to the genus *Chondria, Alsidium, Amansia, Digenea* and *Vidalia* as well as by a number of diatoms

belonging to the genus *Pseudo-nitzschia* (*P. pungens* f. *multiseries*, *P. australis, P. pseudo-delicatissima, P. galaxiae, P. multistriata, P. pungens, P. seriata, P. turgidula, P. fraudulenta, P. delicatissima, P. calliantha*) and *Amphora* [37]. These diatom species are distributed worldwide [60]. Consequently, the accumulation of DA in bivalves and fish has been reported from various parts of the world [61]. DA is the causative toxin of Amnesic Shellfish Poisoning (ASP) syndrome [62] resulting in gastrointestinal symptoms (vomiting, nausea, diarrhea, abdominal cramps and hemorrhagic gastritis) and neurological symptoms (disorientation, epilepsy, short-term memory loss, seizures, profuse respiratory secretions, unstable blood pressure, coma and eventually death) [63].

The structure of DA and its stereochemistry were determined in 1966 [64] and then confirmed by total synthesis [65]; DA is a water soluble tricarboxylic aminoacid, belonging to the kainoid class of compounds. A number of congeners have been reported in literature [66-69]; among them three geometrical isomers, isodomoic acids D, E, and F and the C5'-diastereomer have been found in small amounts in both the producing diatom and shellfish tissue [70-71], but only DA and its C5'-diastereomer have been found to have a certain toxicity [29]. DA is structurally similar to the excitatory neuro transmitter glutamic acid thus sharing its mechanism of action which consists in binding predominantly to *N*-methyl-d-aspartate (NMDA) receptors in the central nervous system with a stronger receptor affinity than glutamic acid. This causes depolarization of neurons which increases the permeability to calcium ions inducing cell dysfunction and even death [72].

2.2 The Saxitoxin group

Saxitoxin (SXT) and a number of its congeners (Figure I.2) are produced by several single celled dinoflagellates belonging to genera *Alexandrium* (*A. catenella, A. tamarense, A. tamiyavanichii, A. minutum, A. excavatum, A. fundyense* and *A. cohorticula*) *Gymnodinium catenatum* and *Pyrodinium bahamense* [73-75] as well as by fresh water cyanobacteria such as *Aphanizomenon flos-aquae, Anabaena circinalis, Lyngbya wollei, and Cylindrospermopsis raciborskii* [76].

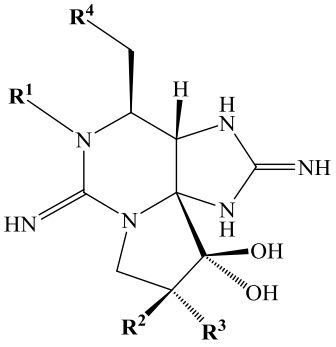

STX = saxitoxin
NEO = neosaxitoxin
GTX = gonyautoxins

R^1	R^2	R^3	R^4	Toxin
H	H	H	$-O-C(=O)-NH_2$	STX
H	H	OSO_3^-		GTX2
H	OSO_3^-	H		GTX3
OH	H	H		NEO
OH	H	OSO_3^-		GTX1
OH	OSO_3^-	H		GTX4
H	H	OH		11a-OH-STX
H	OH	H	$-O-C(=O)-NHSO_3^-$	11b-OH-STX
H	H	H		B1 (GTX5)
H	H	OSO_3^-		C1
H	OSO_3^-	H		C2
OH	H	H		B2 (GTX6)
OH	H	OSO_3^-	$-OH$	C3
OH	OSO_3^-	H		C4
H	H	H		dcSTX
H	H	OSO_3^-		dcGTX2
H	OSO_3^-	H		dcGTX3
OH	H	H		dcNEO
OH	H	OSO_3^-		dcGTX1
OH	OSO_3^-	H		dcGTX4

Figure I.2 Structures of Saxitoxins

STXs have been recognized as the causative toxins of Paralytic Shellfish Poisoning (PSP) syndrome which is a rapid on-set neurological affection. The symptoms can appear 30-60 minutes after ingestion of contaminated seafood and include: paresthesia, cramp, vertigo, numbness, tingling of the face, tongue, and lip. In severe cases, ataxia, inability to use the extremities, blocking of respiration and even death can occur. Saxitoxins are water-soluble molecules which present a perhydropyrrolopurine nucleus having a range of hydroxyl, carbamoyl, and sulfate moieties at four sites of the backbone structure so that they can be subdivided into four groups: the carbamoyl-, the *N*-sulfocarbamoyl-, the decarbamoyl-, and the deoxydecarbamoyl-saxitoxins. Until 2010, 57 analogues have been characterized [76]. The mechanism of action of STXs consists in binding on site 1 of the voltage-gated sodium ion channel in nerve and muscle cells [77] inducing the block of impulse conduction along neurons which results into paralysis [78]. However, for each compound there is a considerable variability in toxicity with the carbamoyl derivatives reported to be the most potent toxins [79].

2.3 The Okadaic acid group

Okadaic acid (OA) and its analogs, the dinophysistoxins (DTXs) (Figure I.3), are lipophilic marine toxins. The parent compound was first isolated from marine sponges of the genus *Halichondria* [80] and subsequently proven to be produced by dinoflagellates belonging to the genera *Dinophysis* mainly (*D. acuta*, *D. acuminate*, and *D. fortii*) [81] and *Prorocentrum* (mainly *P. lima*, but also *P. concavum*) [82-83].

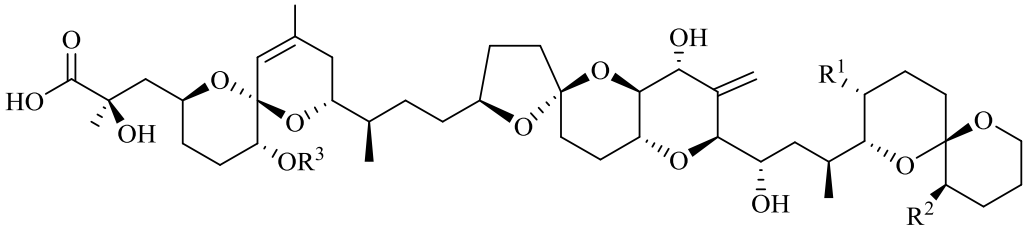

Toxin	R1	R2	R3
OA	CH_3	H	H
DTX-1	CH_3	CH_3	H
DTX-2	H	CH_3	H

Figure I.3 Structures of the principal DSP toxins

These toxins are almost exclusively accumulated in mussel digestive gland and the consumption of these animals provokes the DSP syndrome, that was first defined by Yasumoto and colleagues in Japan at the end of 1970s [84]. Ever since, DSP has spread all over the world. This syndrome is characterized by severe gastrointestinal distress, diarrhea, nausea, vomiting, and abdominal pain, often appearing between 30 min and several hours after ingestion of contaminated seafood [85]. Structurally, OA is a polyether derivative of a C38 fatty acid characterized by a carboxylic acid group and three spiro-keto ring assemblies, one of which connects a five with a six-membered ring. The difference between OA and its analogues stands in the number or the position of some methyl groups (Figure 3). These congeners are also involved in DSP syndrome and most of them are suspected to be either precursors or shellfish-modified metabolites of the active toxin [86-87]. They can have different substituents or conformational change on the skeleton of OA or they can present different long chain esters at the carboxyl group of OA. Among all of them, the most toxic compounds were found to be OA, dinophysistoxin-1 (DTX1), and dinophysistoxin-2 (DTX2) [88]. It has to be mentioned that, beside the diarrhetic effect,

OA and DTXs are found to be potent tumor promoters. Indeed, OA and DTX1 are classified as non-12-O-tetradecanoylphorbol-13-acetate (TPA)-type tumor promoters [89]. Both the aforementioned effects of this class of compounds are mainly explained by the potent inhibitory action against ser/thr protein phosphatases (specific for PP2A and PP1 classes) which are involved in several regulatory process [42,90].

2.4 The Azaspiracid group

Azaspiracids (AZA) (Figure I.4) are marine toxins recently associated with a gastrointestinal human intoxication named Azaspiracid Shellfish Poisoning (AZP).

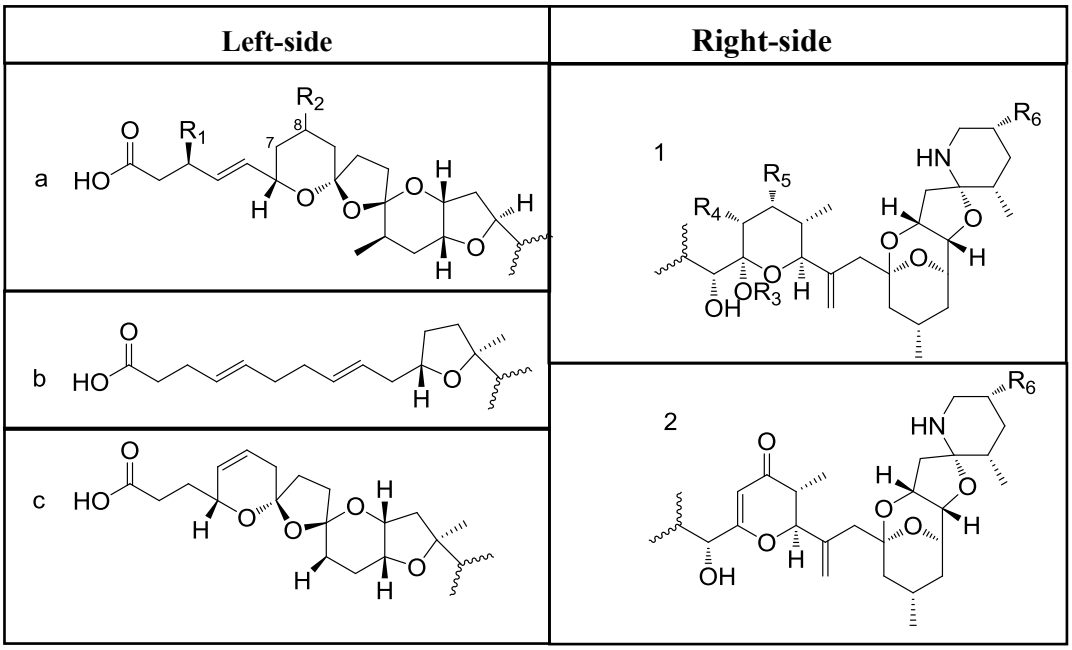

Toxin	Type	R_1	7,8	R_2	R_3	R_4	R_5	R_6	Origin	Status
AZA-1	a1	H	Δ	H	H	CH_3	H	CH_3	*A. spinosum*	Phycotoxin
37-*epi* AZA-1	a1	H	Δ	H	H	CH_3	H	CH_3	*A. spinosum*	Artefact
AZA-2	a1	H	Δ	CH_3	H	CH_3	H	CH_3	*A. spinosum*	Phycotoxin
AZA-3	a1	H	Δ	H	H	H	H	CH_3	Shellfish	Metabolite
AZA-4	a1	OH	Δ	H	H	H	H	CH_3	Shellfish	Metabolite
AZA-5	a1	H	Δ	H	H	H	OH	CH_3	Shellfish	Metabolite
AZA-6	a1	H	Δ	CH_3	H	H	H	CH_3	Shellfish	Metabolite
AZA-7	a1	OH	Δ	H	H	CH_3	H	CH_3	Shellfish	Metabolite
AZA-8	a1	H	Δ	H	H	CH_3	OH	CH_3	Shellfish	Metabolite
AZA-9	a1	OH	Δ	CH_3	H	H	H	CH_3	Shellfish	Metabolite
AZA-10	a1	H	Δ	CH_3	H	H	OH	CH_3	Shellfish	Metabolite
AZA-11	a1	OH	Δ	CH_3	H	CH_3	H	CH_3	Shellfish	Metabolite
AZA-12	a1	H	Δ	CH_3	H	CH_3	OH	CH_3	Shellfish	Metabolite
AZA-13	a1	OH	Δ	H	H	H	OH	CH_3	Shellfish	Metabolite
AZA-14	a1	OH	Δ	H	H	CH_3	OH	CH_3	Shellfish	Metabolite
AZA-15	a1	OH	Δ	CH_3	H	H	OH	CH_3	Shellfish	Metabolite
AZA-16	a1	OH	Δ	CH_3	H	CH_3	OH	CH_3	Shellfish	Metabolite
AZA-17	a1	H	Δ	H	H	COOH	H	CH_3	Shellfish	Metabolite
AZA-19	a1	H	Δ	CH_3	H	COOH	H	CH_3	Shellfish	Metabolite
AZA-21	a1	OH	Δ	H	H	COOH	H	CH_3	Shellfish	Metabolite
AZA-23	a1	OH	Δ	CH_3	H	COOH	H	CH_3	Shellfish	Metabolite
AZA-26	a2	H	Δ	H	-	-	-	-	Shellfish	Metabolite
AZA-29	a1	H	Δ	H	CH_3	H	H	CH_3	Shellfish	Metabolite
AZA-30	a1	H	Δ	H	CH_3	CH_3	H	CH_3	*A. spinosum*	Artefact
AZA-32	a1	H	Δ	CH_3	CH_3	CH_3	H	CH_3	*A. spinosum*	Artefact
AZA-33	b1	-	Δ	-	H	CH_3	H	CH_3	*A. spinosum*	Phycotoxin
AZA-34	c1	-	Δ	-	H	CH_3	H	CH_3	*A. spinosum*	Phycotoxin
AZA-36	a1	OH	Δ	CH_3	H	CH_3	H	H	*A. poporum*	Phycotoxin
AZA-37	a1	OH	-	H	H	CH_3	H	H	*A. poporum*	Phycotoxin

Figure I.4 Structural variants of AZAs; compounds highlighted have had their structures confirmed by NMR. The type refers to variations of the left-side and right-side of the molecule. AZA18, -20, -22, -24 and -27 proposed by Rehmann *et al*. [91] are now known not to exist. AZA25, -28, -31 and -35 have not had their structures well established to date

The first intoxication occurred in The Netherlands in 1995 following consumption of Irish shellfish [92-94]. Some years later, Azaspiracid-1 (AZA-1) was found to be responsible of that poisoning. Its structure was thus elucidated [95] and recently corrected following a total chemical synthesis [96]. AZAs are polyether toxins containing unique spiro-ring assemblies, a cyclic amine and a carboxylic acid. Until 2014, 37 analogues have been reported (Figure I.4) [91,97]. They have been found in several bivalve shellfish species [98-99] and James et al. proposed that the producer organisms was the algae *Protoperidinum crassipe* [100]. It was only in 2009 that the dinoflagellate *Azadinium spinosum* was identified as the producing organism of AZA-1 and -2 [101-102]. Recently, the occurrence of other AZA-like compounds in *A. poporum* [103] and *Amphidoma languida* [104] has also been reported. AZA-3 and some other AZA analogues have been demonstrated to be metabolic products formed in shellfish [105]. To date, limited knowledge about AZAs mechanism of action is available due to the lack of standards and reference material [106]. AZP is characterized by several symptoms including nausea, vomiting, severe diarrhea and stomach cramps, which resembled those exhibited by the classical DSP toxins [107]. Among all the analogues, AZA-1, AZA-2 and AZA-3 are the most important ones based on occurrence and toxicity [95,108].

2.5 The Pectenotoxin group

Pectenotoxins (PTXs) are lipophilic toxins produced by several species of *Dinophysis* (*D. acuta*, *D. fortii* [109], *and Dinophysis* spp. [57]). PTX-1 and -2 were isolated in 1985 from Japanese scallops *Patinopecten yessoensis* [110] and successively it was demonstrated that PTX-1, together with PTX-3 and 6, were metabolites of PTX-2 in the scallops [111]. Another analogue, the PTX-2 seco acid (PTX-2sa) was found to be a different inactive metabolite of PTX-2 in the mussels [112]. PTXs are macrocyclic polyether lactones (Figure I.5) that have some similarities with OA and DTXs sharing the same biogenetical origin as well as some chemical moieties (cyclic ethers and a carboxyl group), thus resulting in their co-extraction.

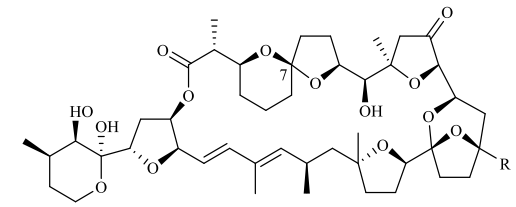

PTX-2

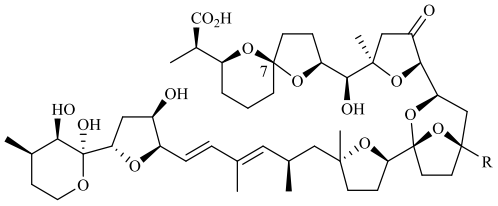

PTX-2sa

Toxin	R	C7
PTX-1	CH_2OH	*7R*
PTX-2	CH_3	*7R*
PTX-3	CHO	*7R*
PTX-4	CH_2OH	*7S*
PTX-6	COOH	*7R*
PTX-7	COOH	*7S*
PTX-2sa	CH_3	*7R*
7-epi-PTX-2sa	CH_3	*7S*

Figure I.5 Structures of Pectenotoxins

Therefore, PTXs have been initially grouped with DSP toxins but animal studies indicate that, although highly cytotoxic [113] and hepatotoxic [114], they are much less toxic than the OA group of toxins by oral route, are inactive against phosphatase PP-1 and PP2A [115], and do not induce diarrhea. So, recently, PTXs (such as YTXs) have been eliminated from the clinical case definition of DSP toxins. As far as we know, PTXs could not be unequivocally associated to any human poisoning, since they are often co-occurring with other toxins in shellfish and there is no information about their real toxicity to humans.

2.6 The Yessotoxin group

Yessotoxins (YTX) are a large group of toxins whose parent compound, Yessotoxin, was first reported in the scallop *Patinopecten yessoensis* [116]. After that, it was proven that YTXs are mainly produced by dinoflagellate *Protoceratium reticulatum* [117], and also by *Lingulodinium polyedrum* [118] as well as *Gonyaulax spinifera* [119]. Some authors suggest that YTXs are actually produced by bacteria associated with dinoflagellates [49]. Since the initial discovery of YTX in Japanese scallops, a significant number of analogues, including homoyessotoxins (homoYTXs), have been identified in toxic shellfish and/or algal cultures from different countries, suggesting their worldwide spread [49]. YTXs (Figure I.6) are a group of polycyclic ether molecules containing 2

sulfate groups and a characteristic ladder-shaped rigid form constituted by 11 cyclic rings and an unsaturated terminal chain with 9 carbon atoms.

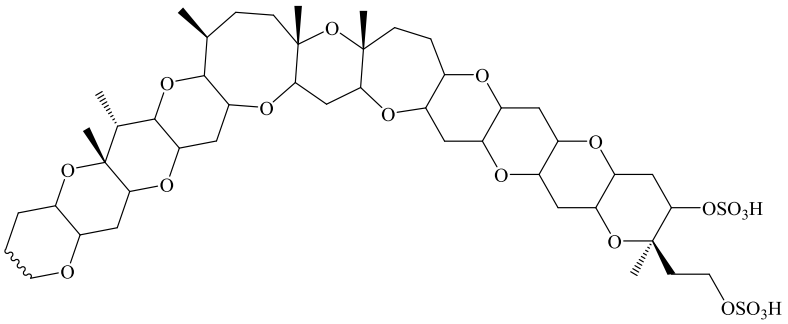

Toxin	Group ~~~~~
YTX	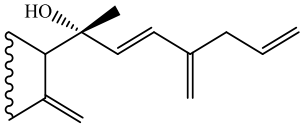
45-hydroxy YTX	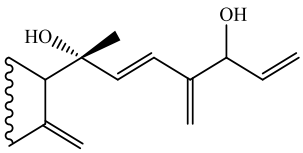
Carboxy YTX	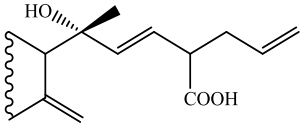

Figure I.6 Structure of Yessotoxins

These toxins are considered as amphiphilic compounds [120], since they present both an apolar moiety (the cyclic rings) and a very polar one (the sulfate groups). However, they are legally considered as lipophilic in Europe [50]. Hundreds of analogues have been identified both in contaminated shellfish and algal culture worldwide [121] and a number of them have been fully characterized either by NMR or LC-MS [122]. As afore mentioned for PTXs, also YTXs were initially included within DSP toxins groups, since they are co-extracted with OA and DTXs. However, they present different toxic activities regarding the lower potency of YTX and its analogues for the inhibition of protein phosphatase 2A [123] in comparison with OA and they do not cause diarrhea. Consequently, they have been removed from DSP toxin group [40]. Actually, no correlation has been established between YTXs and human intoxication. In-vitro studies demonstrated an effect on the

cardiac muscle cells [123] and a modulation of the calcium homeostasis in human lymphocytes [124].

2.7 The Brevetoxin group

Brevetoxins (BTXs) are a large family of compounds mainly produced by the dinoflagellate *Karenia Brevis* (also known as *Gymnodinium breve* or *Ptychodiscus breve*) [125-126]. It is also produced by species of the genera *Chattonella*, *Fibrocapsa*, and *Heterosigma* [127]. BTXs are responsible of Neurotoxic Shellfish Poisoning (NSP) in humans whose symptoms occur within hours and include nausea, emesis, diarrhea, paresthesia, cramps, bronchoconstriction, seizures, paralysis, and coma [34]. Furthermore, the inhalation of brevetoxin aerosols may result in respiratory difficulties and eye and nasal membrane irritation [61,128]. Beside the risk for human health, BTXs affect marine fauna such as fish, birds, dolphins and manatee [129]. BTXs are cyclic lipophilic polyether that are grouped into two classes (type A and B) according to differences in the backbone of the chemical structure: The Type A whose lead compound is BTX-1 presents 10 connected rings while the Type B whose lead compound is BTX-2 exhibits 11 connected rings (Figure I.7).

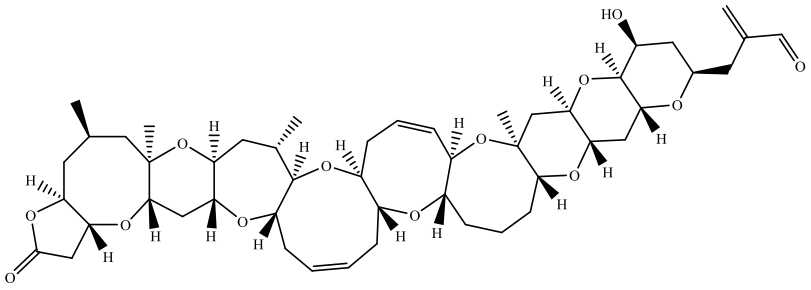

BTX-1

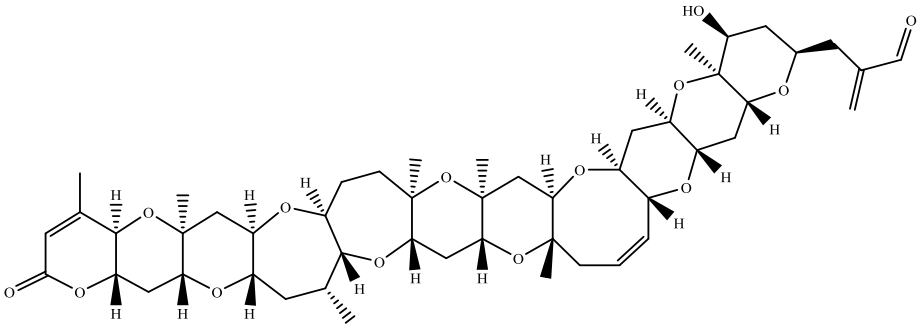

BTX-2

Figure I.7 Structure of Brevetoxins

BTX-1 appears to be a precursor of other NSP toxins [129]. BTX-2 is currently assumed to be the most abundant in algae [34,130]. Fifteen different BTX analogues have been reported so far [1] and some of them are metabolites in shellfish, and finfish [131-132]. Variable toxicity levels were recorded for most of the compounds [133]. BTXs are able to bind voltage-gated sodium channels leading to uncontrolled sodium influx and depolarization of neurons [134] and an increase in intracellular Calcium [135]. Brevetoxin has differential effects on striated, cardiac, and smooth muscle and discrete actions on diaphragm are dominated by blocking of nerve conduction [136].

2.8 Emerging toxins

In this paragraph the so called “emerging toxins “will be described. They include recently discovered toxins (such as pinnatoxins, gymnodimines and spirolides, among others), known toxins that have recently appeared in new locations (such as ciguatoxins), and non-regulated toxins that became a threat to public health (such as palytoxins).

2.8.1 The Cyclic Imines group: spirolides, gymnodimines, pinnatoxins, pteriatoxins, prorocentrolides, and spiro-prorocentrimine

Spirolides (SPXs), gymnodimines (GYMs), pinnatoxins (PnTXs), pteriatoxins (PtTXs), prorocentrolides, and spiro-prorocentrimine (Figure I.8) are marine biotoxins produced by several dinoflagellates that belong to the group of cyclic imines.

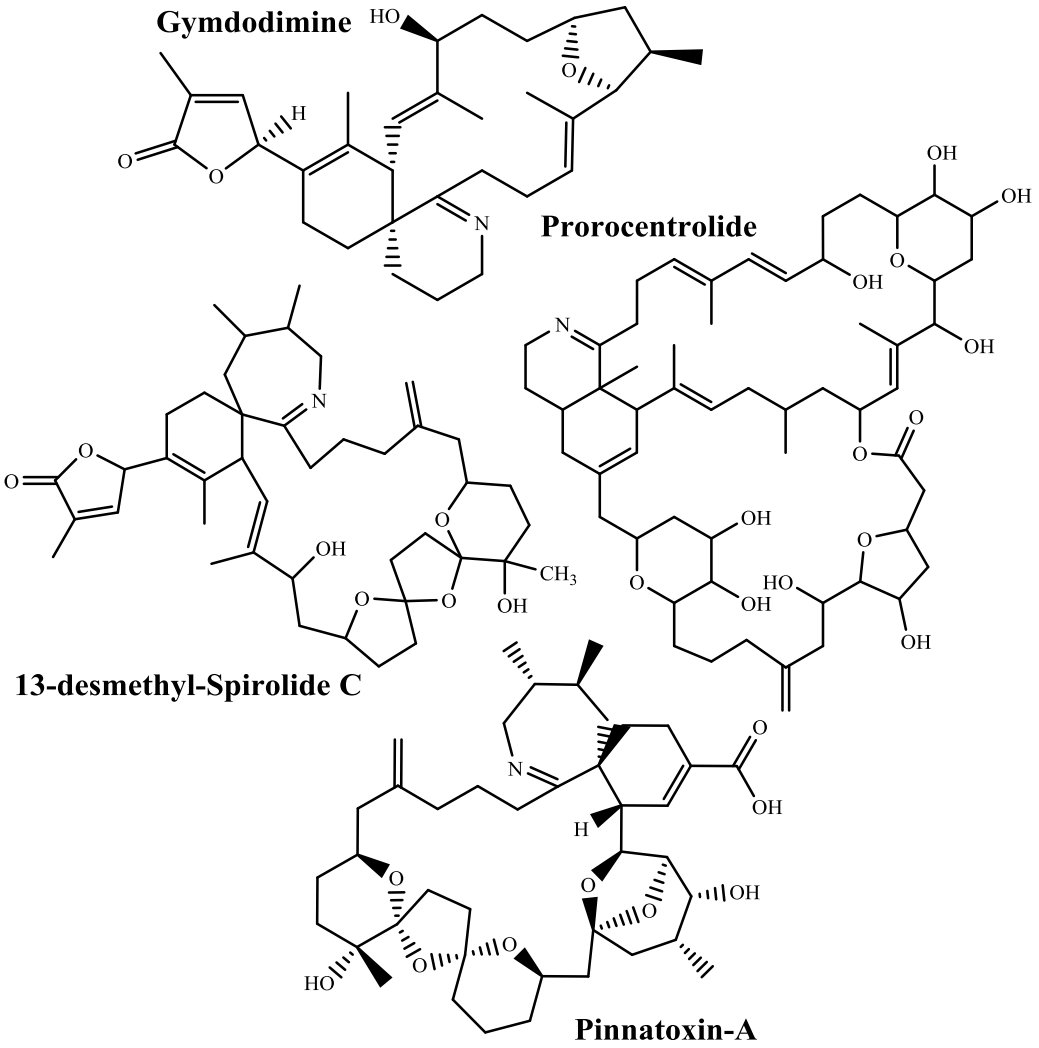

Figure I.8 Structure of Cyclic Imines

All of them are macrocyclic compounds consisting of imine- and spiro-linked ether moieties. In general, they are structurally very similar, e.g., with a 70% structural homology between PnTXs and SPXs [137]. The unique cyclic imine moiety seems to be the pharmacophore responsible for their bioactivity. Indeed, the opening of this ring results in the inactivation of the molecule as described for spirolide E and spirolide F [138]. The cyclic imines are defined as Fast Acting Toxins considering the fast death (within minutes) that occurs in mice after intra-peritoneal injection [139]. However, to date, there are no records of human poisonings due to these toxins [140]. The mechanism+ of action of cyclic imines was deeply investigated for SPXs and GYMs. *In vitro* assays showed that SPXs have a weak activation effect on L type calcium channels [141]. Moreover, it was demonstrated an antagonistic effect of GYM-A and 13-desmethyl-SPX for nicotinic

acetylcholine receptors [142-143], as well as an antagonism of 13-desmethyl-SPX C for muscarinic acetylcholine receptors [144].

SPXs, GYMs and prorocentrolides groups

SPXs, GYMs and prorocentrolides (Figure I.8) are mainly produced by dinoflagellates [145-147]. *Alexandrium ostenfeldii* and *Alexandrium peruvianum* are the principal producer of SPXs [148]. However, important differences in toxicity and toxin profiles have been observed for different strains of these dinoflagellates depending on their geographical origin. For instance, A. *ostenfeldii* cells were found to contain high levels of spirolides in Nova Scotia (Canada) [149] and in Italy, while they contained PSP toxins in populations from New Zealand [150]. As for the GYMs, they are produced by the dinoflagellate *Karenia selliformis* and may persist in shellfish even years after *K. selliformis* blooms [151]. To date only GYM-A, -B and -C have been characterized [39].

PnTXs and PtTXs

PnTXs and PtTXs (Figure I.9) are another group of marine toxins belonging to the cyclic imine family. Pinnatoxins have been the first to be discovered in extracts from the digestive glands of the penshell *Pinna attenuata* in China and *Pinna muricata* in Japan [152-153]. Several PnTXs analogs have been reported (Figure I.9); PnTXs A to D were isolated from *Pinna muricata* [153] and PnTX E to G were detected in oysters.

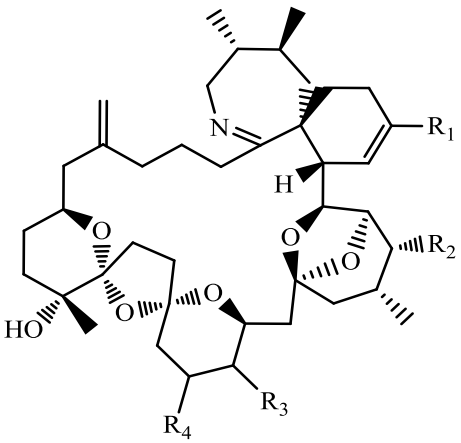

Toxin	R_1	R_2	R_3	R_4
PnTX-A	COOH	OH	H	H
PnTX-B	$CH(NH_2)COOH$ (*S*)	OH	H	H
PnTX-C	$CH(NH_2)COOH$ (*S*)	OH	H	H
PnTX-D	$COCH_2CH_2COOH$	H	OH	CH_3
PnTX-E	$CH(OH)(CH_2)_2COOH$	H	OH	CH_3
PnTX-F	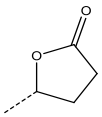	H	OH	CH_3
PnTX-G	$CH=CH_2$	OH	H	H
PnTX-H	CH_2COOH	OH	H	H
PnTX-I	$CH(OH)CH_2OH$	OH	H	H

Figure I.9 Structure of Pinnatoxins

Some of these compounds have been suspected to be algal metabolites [154]. The PnTX biogenetical source currently is thought to be the dinoflagellate *Vulcanodinium rugosum* [154-155]. It is also considered the producer of PtTX (A to C) even if PtTXs may be biotransformation products of PnTXs [154].

2.8.2 The Ciguatoxin and Maitotoxin group

Ciguatoxins (CTXs), gamberiol and maitotoxins (MTXs) (Figure I.10) are toxic compounds linked to the Cigutera Fish Poisoning (CFP) syndrome. The producer species is a benthic dinoflagellate discovered by Yasumoto et al. [156] and designated as a new genus and species, *Gambierdiscus toxicus* [157]. Since the initial discovery of *G. toxicus*, several new species have been added to the genus including *G. belizeanus*, *G. yasumotoi*, *G. pacificus, G. australes, and G. polynesiensis* [158-160]. CFP occurs in humans following consumption of finfish contaminated with ciguatera toxins: indeed, the toxins accumulate along the trophic chain up to attaining the highest concentrations in top predatory fish, such as barracuda, amberjack, grouper and snapper [161]. Ciguatera toxins have been found in the tropical and sub-tropical regions of the Pacific, Atlantic and Indian Ocean. More recently, *Gambierdiscus* spp. Have been found in the Mediterranean [162]. Their mechanism of action consists in an opening of the non-selective, non-voltage-activated ion channels, which elevates intracellular calcium concentration and leads to cellular toxicities [163]. This action generates about 175 symptoms which are in humans classified into four categories: gastrointestinal, neurological, cardiovascular and general symptoms [164]. Since CTXs from the above-mentioned regions have different structures as well as different toxicity/symptomatology, they can be dived into Pacific (P-CTX), Caribbean (C-CTX) and Indian Ocean CTXs (I-CTX). Structurally, they are lipophilic polyether compounds with 13-14 rings (Figure I.10) and more than 30 analogues have been described so far [165]; some of them are metabolites formed in the fish that are more hydrophilic and more toxic than the molecules found in the producing dinoflagellate [166].

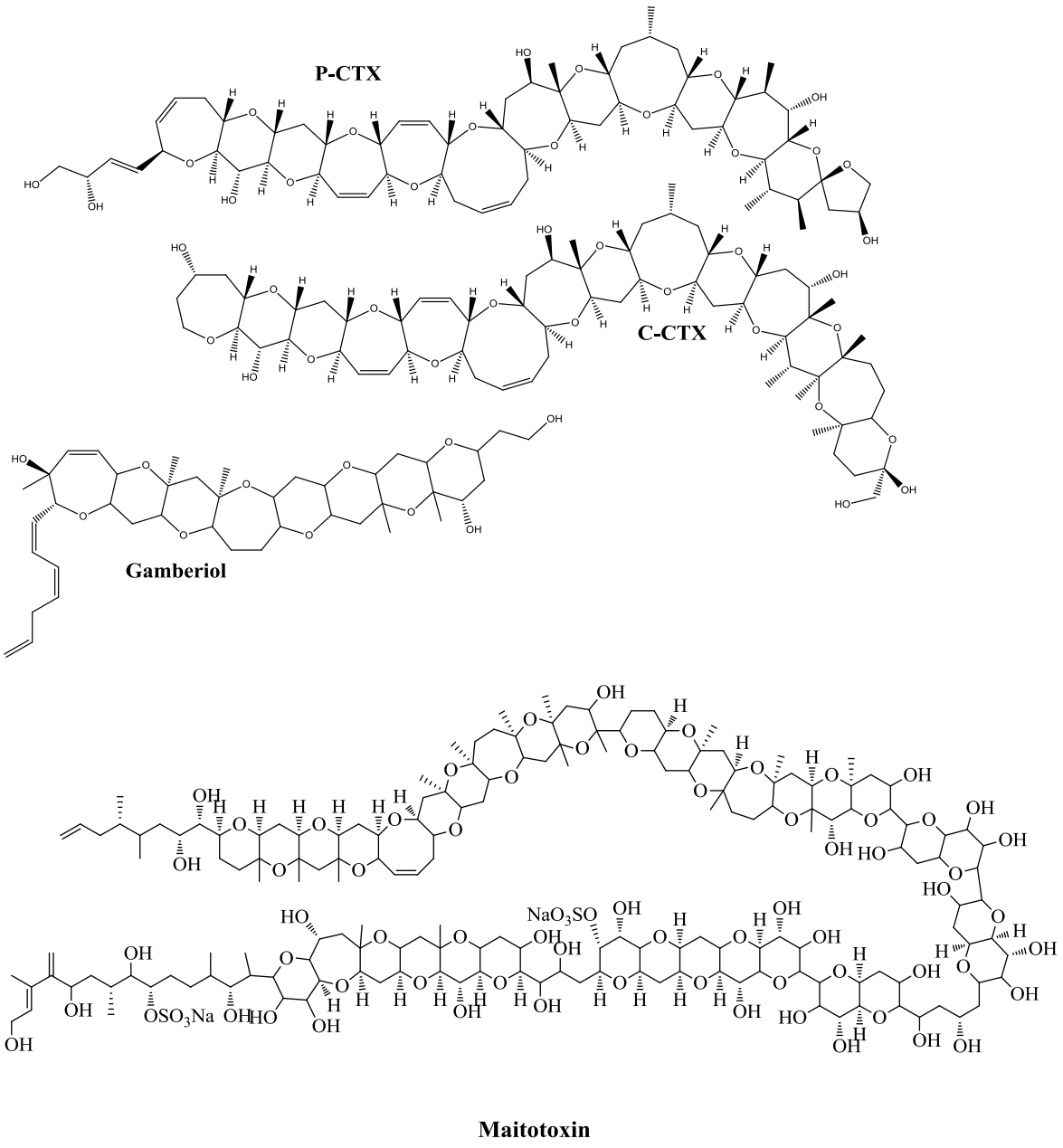

Figure I.10 Structure of Ciguatera toxins

MTXs have the highest molecular weight among the toxins so far known and present a high toxicity. The name Maititoxin derives from "Maito", the Tahitian name for the bristethoot surgeonfish *Ctenochaetus striatus*, in which the toxin was originally detected [167]. MTXs are water soluble, ladder-shaped polycyclic (32 rings) molecules with numerous hydroxyl groups and two sulfate groups. Although three forms of MTXs, MTX-1, MTX-2 and MTX-3 have been identified from *G. toxicus* [168], the structure of only one MTX was determined [169] (Figure I.10). Pharmacological studies demonstrated

that MTX is a potent activator of voltage-gated calcium ion channels. As a consequence of calcium influx, MTX can produce several effects such as hormone and neurotransmitter secretion and phosphoinositides breakdown [170].

3. Palytoxin group

Palytoxins are a group of complex, extremely potent nonproteic marine biotoxins, originally identified in a tropical *Cnidarian* zoanthid, a type of colonial anemone [171].

According to an ancient Hawaiian legend [172], on the island of Maui near the harbor of O' Hana, there was a village of fishermen haunted by a curse. Sometimes, when they returned from the sea, the fishermen would find out that one of them had been missing. One day, the fishermen assaulted a hunchbacked hermit deemed culprit of the town's misery. While they ripped off the cloak from the hermit, they uncovered rows of sharp and triangular teeth within huge jaws. They had caught a shark god. It was clear that the missing man had been eaten by the shark god on their journeys to the sea. The fishermen killed the loner, burned him and threw his ashes into a tidepool nearby the harbor of Hana. Shortly after, a moss started growing on the walls of the tidepool, and the fishermen learnt that the moss, if used on their spears, was able to cause instant death to their victims. The moss growing in the cursed tidepool became known as "limu-make-o-Hana", which literally means "seaweed of death from Hana". The pool became taboo to the local Hawaiians convinced that an ill fate would befall anyone who disturbed the sacred site collecting the deadly seaweed.

Nonetheless, in the '60s, thanks to some local informers, Philip Helfrich, from the University of Hawaii, reached the tidepool, and he was the first to collect some samples of the toxic moss. Ten years later, Prof. P. Scheuer, in collaboration with R. Moore from the University of Hawaii, investigated other toxic samples of the legendary seaweed. They assessed that the sample collected from the Hana tidepool was not a seaweed, as commonly believed, but an unknown type of soft coral, belonging to the family *Zoanthidae*, order *Zoantharia* and phylum *Coelenterata* [171]. This zoanthid was subsequently identified as *Palythoa toxica*, a rare species detected across the Hawaiian Islands [173]. The scientists named the molecule responsible of its high toxicity Palytoxin (PLTX).

Palytoxin several and of its congeners, have also been found in some other species of zoanthids such as *P. tuberculosa* in Pacific Ocean [174], *P. vestitus* from Hawaii [175], *P. caribaeorum* [176] and *P. mammilosa* [177] from the islands of the West Indies [171],

in *Palythoa* spp. from Tahiti [178-179] and Okinawa [180] and recently in Japanese *Palythoa* aff. *margaritae* [181]. The toxin has also been found in zoanthids belonging to the genus *Zoanthus*, such as *Z. solanderi* and *Z. sociatus* [182]. The biogenetic origin of PLTX has been object of speculations for long time due to the significant seasonal and regional fluctuations in its contents [183] as well as for sporadic detection of PLTX in algae [184], crabs [185] and fish [186]. For these reasons, a PLTX origin from microorganisms (microorganisms associated with zoanthids) was proposed [187]. Another hypothesis suggests the coral is simply concentrating the toxin produced by dinoflagellates belonging to the genus *Ostreopsis* [188-193]. This hypothesis is supported by the implication of *O. siamensis* in a case of clupeotoxism in Madagascar where the causative agent was found to be a putative PLTX [194] and, most importantly, by identification of a number of palytoxin-like compounds from various *Ostreopsis* spp. worldwide. Finally, there is another school of thought suggesting that PLTX is produced by bacteria symbiotic with the afore-mentioned organisms [195], as recently highlighted by the discover that some PLTXs are produced also by cyanobacteria of the genus *Trichodesmium* [196].

Structure and chemistry of Palytoxin

Palytoxin is a white, amorphous, hydroscopic solid, insoluble in chloroform, ether and acetone, only sparingly soluble in methanol and ethanol, while totally soluble in water, pyridine, and dimethyl sulfoxide. It has not been crystallized to date; the toxin shows no defined melting point and it is heat resistant but chars at 300°C [194]. It was demonstrated that in aqueous solution PLTX exists as a dimer [198].

After its isolation in 1971 [171], it took nearly 11 years to fully elucidate the complex architecture of PLTX. In 1981, two research groups, from Hawaii and from Japan, independently and almost simultaneously came up with two slightly different planar structures for PLTX. The first group worked on a molecule isolated from *P. tuberculosa* [199], while the second group studied a molecule isolated from a Tahitian *Palythoa* spp. [178]. In 1982 several scientists elucidated the stereochemistry of the natural isomer of PLTX from *Palythoa* spp. [200-204] which encompasses 64 stereogenic center and 8 stereogenic double bond. The basic molecule consisted in a long alkyl chain with spaced cyclic ethers, several hydroxyl groups, two amide groups and one amino group ($C_{129}H_{223}N_3O_{54}$). This structure was subsequently proven correct by a total synthetic study [198]. It exhibits an UV absorption spectrum with λ_{max} at 233 and 263 nm attributed to the presence of respective chromophores (Figure I.11) and a mass fragmentation spectrum

(using ESI as source) with a characteristic ion fragment (A moiety) deriving from cleavage between C-8 and C-9 at *m/z* 327 corresponding at [M-B moiety-H_2O] (Figure I.11).

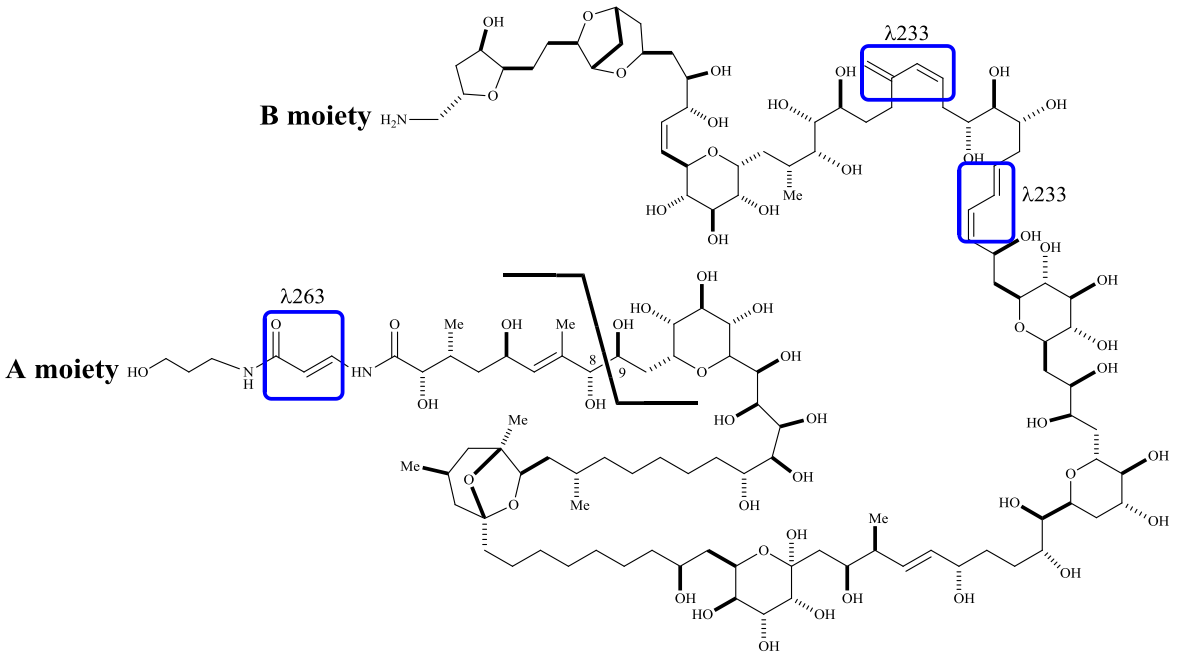

Figure I.11 Structure of Palytoxin

Full MS spectra of PLTX using ESI ion source show a complex ion profile containing pseudo-molecular ions, several cationic adduct (NH_4^+, Na^+, K^+, Ca^{2+}, Mg^{2+}, Fe^{2+}) at different charge states (+1, +2 and +3) and a number of ions due to multiple water losses molecules. In general, two major clusters of tri- and bi- charged ions are present in the mass range *m/z* 900-920 and *m/z* 1240-1370, respectively. Even working at the highest resolutions (that for LTQ Orbitrap XL is 100000), ion assignment may be quite tricky, since several elemental formulae are possible for each ion, even at very low mass accuracy (2-3 ppm). A key role in the ion correct assignment is played by the finding that most of the triply charged ions were adducts with divalent cations. By the way of example, two alternative formulae for the monoisotopic ion of *m/z* 901.1581 are possible, either to $[M+2H+Na]^{3+}$ or $[M+H+Mg]^{3+}$ (Δ=-3.354 ppm and 1.290 ppm, respectively) as well as for the monoisotopic ion of *m/z* 906.4851, for which, either $[M+2H+K]^{3+}$ or $[M+H+Ca]^{3+}$ (Δ=-0.737 ppm and 2.551 ppm, respectively) are possible. To solve this issue, additives of mono and divalent cations as well as EDTA were added to the mobile phases. Indeed, when EDTA, which is able to chelate only the bivalent ions, was added to the mobile

phases at concentration ≥ 4mM, no triply charged ions were present in the spectrum. This indicated that the ions at *m/z* 901 and 906 are adducts with divalent ions, Mg^{2+} and Ca^{2+} respectively. In a similar way, it was demonstrated that doubly charged ions are adduct with monovalent cations (namely Na^{+} and K^{+}) while singly charged ions are protonated ions [205]. LC-HRMS^{n} experiments, using three different fragmentation modes, namely collision induced dissociation (CID), pulsed Q collision induced dissociation (PQD) and high energy collision dissociation (HCD) were carried out in order to interpret the fragmentation pattern of PLTX. Positive HRMS^{n} of PLTX contain a huge number of ions and, even in this case, the key to interpret such spectra was understanding that most of them contained Ca^{+2} in their elemental formulae, not only the triply, but also the doubly and some of the singly charged ions. Fragmentation occurs in many sites of PLTX backbone, originating A-side fragments with 2 Nitrogen atoms, B-side fragments with 1 Nitrogen atom and internal fragments with no Nitrogen atoms. The only region that does not fragment is the part structure stretching from C52 to C78 likely as a consequence of the formation of a conjugated polyene during the fragmentation process [206] (Figure I.12).

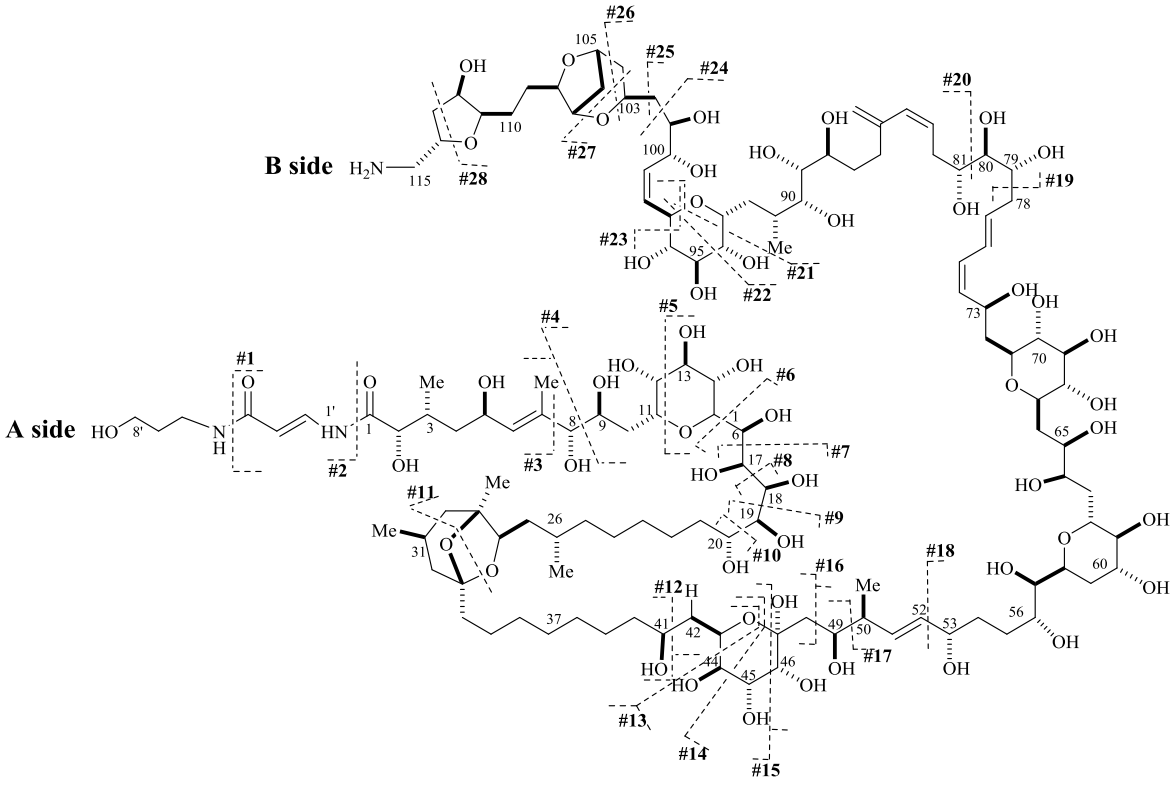

Figure I.12 Planar structure of PLTX including all the cleavages emerging fromits HRMS^{n} spectra

3.1 Identification of PLTX analogues

Since the first report of PLTX in 1971, many compounds which share its same molecular features were detected. In particular, PLTX analogues were found in both *Palythoa* spp. and *Ostreopsis* spp.

Palytoxin's analogues from* Palythoa *spp.

Four minor PLTX-like compounds, were isolated from some Okinawan *P. tuberculosa* extracts. The new PLTX analogues, characterized as homopalytoxin, bishomopalytoxin, neopalytoxin, and deoxypalytoxin, featured little structural differences from the parent compound as shown in Figure I.13 [180].

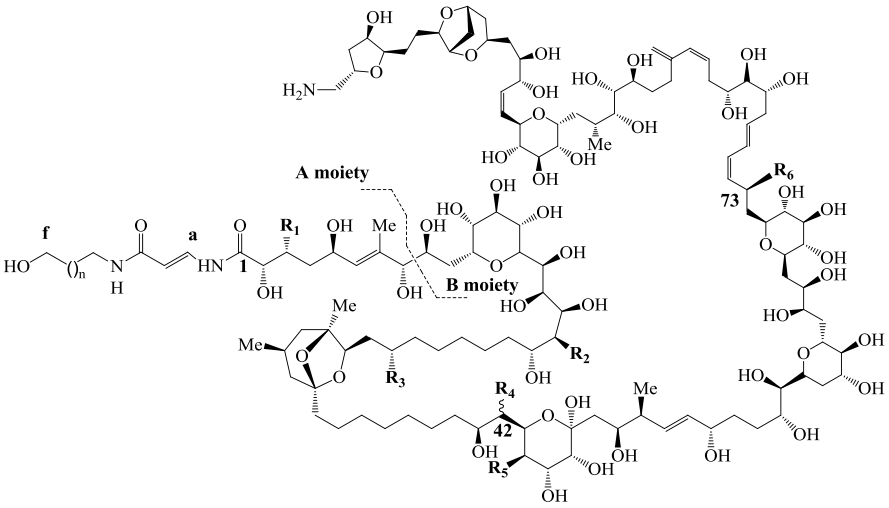

	n	R1	R2	R3	R4	R5	R6
Palytoxin (1)	1	Me	OH	Me	H	OH	OH
Homopalytoxin (2)	2	Me	OH	Me	H	OH	OH
Bishomopalytoxin (3)	3	Me	OH	Me	H	OH	OH
Neopalytoxin (4)	1	-	OH	Me	H	OH	OH
Deoxypalytoxin (5)	1	Me	OH	Me	H	OH	H
42-hydroxypalytoxin (6)	1	Me	OH	Me	OH	OH	OH
Ostreocin D (7)	1	H	H	H	OH	H	OH

A moiety = 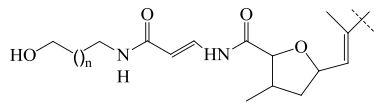

Figure I.13 Strereostructure of Palytoxins

More recently Ciminiello and co-workers, within LC-HRMS analysis of two samples of *P. Tuberculosa* and *P. toxica* provided by the U.S. Army Medical Research and Development Command [207], highlighted the presence in both of the extracts of a new

PLTX analogue. Full 1D- and 2D-NMR investigation allowed to characterize the planar structure of this new analogue as 42-hydroxy PLTX (Figure I.13) [208]. Subsequent NMR-based stereostructural studies disclosed that the two 42-hydroxy PLTX isolated from *P. toxica* and *P. tuberculosa* were indeed diastereoisomers, with inverted configurations at C50 (namely 50*S* in *P. toxica* and 50*R* in *P. tuberculosa* [209].

Palytoxin's analogues from* Ostreopsis *spp.

Ostreopsis spp. are benthic and epiphytic dinoflagellates distributed worldwide. Their normal habitat is the tropical and subtropical areas but they have been regularly detected also in temperate regions of the world. The genus *Ostreopsis* was initially described by Schmidt in 190 [210] and subsequently by Fukuyo in 1981 [211]. To date, 9 different species of *Ostreopsis* are known. Some of them turned out be toxin producers, such as *O. siamensis* [188], *O. ovata* [212], *O. mascarenensis* [190], *O. lenticularis* [213], and *O. heptagona* [214] (Norris et al. 1985); for some others (*O. labens*, *O. marinus*, *O. belizeanus*, and *O. caribbeanus*) toxicity data are not available [215].

Among various PLTX-like molecules, ostreocins were the first compounds to be isolated from biogenetic sources other than *Palythoa* spp. In 1995, Usami and co-workers isolated the major ostreocin (ostreocin-D) from *O. siamensis* [188], whose structure (Figure I.13) was fully elucidated by NMR and MS techniques by Ukena *et al.* [216]. The elemental composition $C_{127}H_{220}N_3O_{53}$, was assigned based on positive ion fast atom bombardment mass spectrometry (FAB-MS) experiments. Since NMR spectra presented a huge number of overlapped signals, in order to reduce the size of the molecule, ozonolysis followed by treatment with $NaBH_4$ was performed and the obtained fragments were chromatographically separated and individually analyzed by ESI-MS and NMR. Thanks to this approach, complete NMR assignment was performed demonstrating that ostreocin-D, compared to palytoxin, lacks two methyls at C-3 and C-26, and two hydroxyls at C-19 and C-44, while presenting an additional hydroxyl at C-42. This structure was further confirmed by application of negative ion FAB collision induced dissociation (CID) tandem MS [217]. Besides ostrecin-D, other minor ostreocins were detected in the Japanese *O. siamensis* culture extract in amounts too low for a complete NMR-based structure elucidation. Tentative structure of ostreocin-B was proposed by Ukena on the basis of NMR data [218] (Ukena 2001b). Compared to ostreocin-D, ostreocin-B presents an additional hydroxyl at C-44, thus being the 42-hydroxy-3,26-didemethyl-19-

deoxypalytoxin. More recently, Ciminiello *et al.* have detected ostreocin-B from Japanese strain of *O. siamensis* and gained structural insights by LC-HRMS^2 [219].

Other PLTX-like compounds were detected in *O. mascarenensis*, thus named mascarenotoxins (McTXs). In 2004, Lenoir *et al*. [191] described the purification and the MS-based characterization of McTX-A and -B. Their structures have not been elucidated and only some observations on their chromatographic and MS behavior have been reported so far. In 2010, Rossi *et al*. [220] reported the presence of monoisotopic ion peaks $[M+H]^+$ at *m/z* 2589.3441 and at *m/z* 2629.2854 in a Mediterranean *O.* cf. *ovata* extract (strain D483). The authors assigned the elemental formulae $C_{127}H_{222}N_3O_{50}$ and $C_{129}H_{222}N_3O_{51}$ to the two ions, respectively, and labeled the peak at m/z 2589.3441 as McTX -A, by interpreting the MS data reported by Lenoir *et al.* [191], and the peak at m/z 2629.2854 as the novel analogue McTX -C. However, errors in the ion assignments exceeded the commonly accepted values (≤ 5 ppm) and were done in absence of a reference sample of McTX.

Several data have been recorded on ovatoxins (OVTXs). Theses toxins are a class of PLTX-like molecules mostly detected in *O.* cf. *ovata* strains. Over the past decades, blooms of this tropical and subtropical dinoflagellates have been steadily detected also across more temperate regions such as the Mediterranean basin [43]. It has to be noted that resolving the taxonomy of *Ostreopsis* species based only on morphology is difficult (Penna et al. 2005) [221] and none of the original *Ostreopsis i*solates from tropical areas has been sequenced yet for the genotype assignment. For these reasons, the designation *O*. cf. (confronta) *ovata* is used when referring to isolates from the Mediterranean Sea. The so called "*Ostreopsis* phenomenon" took place in summer 2005 when an *Ostreopsis* blooms of alarming proportion occurred along the Ligurian coasts in Italy [221-223]. Hundreds of people required medical attention after exposure to marine aerosol, during recreational or working activities on the beach. Plankton samples collected off the Genoa coasts during the toxic outbreak were investigated by applying a newly developed method based on liquid chromatography tandem mass spectrometry specific for PLTXs [212]. Results of the LC-MS analysis highlighted the presence of an isobaric compound of PLTX (so far referred as putative PLTX). One year later, another proliferation of *O.* cf. *ovata* was again detected across the Mediterranean Sea. LC-HRMS analysis revealed – in addition to isobaric PLTX – the presence of another PLTX-like compound, named OVTX-a [192] whose molecular formula was assigned as $C_{129}H_{223}N_3O_{52}$. An extensive LC-HRMS^n study

of the new compound was carried out using fragmentation pattern of PLTX, full of informative cleavages throughout the entire backbone of the molecule, as template to gain detailed structural information on OVTX-a, which was finally characterized as a 42-hydroxy-17,44,64-trideoxy derivative of PLTX. Subsequently, OVTX-a was isolated from an *O. ovata* culture strain the complete elucidation of its stereo-structure was achieved by NMR studies which confirmed the previous structural hypothesis achieved with LC-HRMS^{n}method, demonstrating the validity of such methods to gain stuctural insights on unknown molecules. NMR study also assessed that OVTX-a and PLTX share the same absolute configuration at all of the asymmetric carbon atoms but at C9, C26, and C57, which showed inverted configurations [205,224-225]. (Figure I.14)

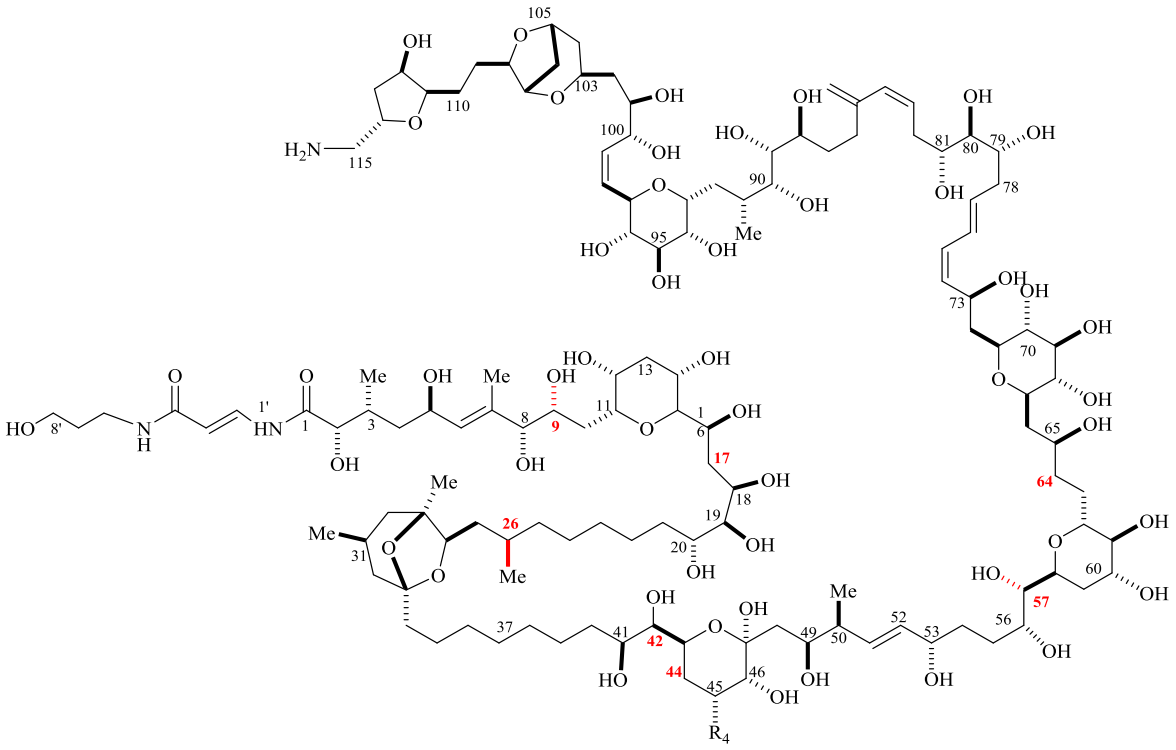

Figure I.14 Stereostructure of OVTX-a. Positions where differences between OVTX-a and palytoxin occur are indicated in red.

In parallel with these studies and more recently, a huge number of OVTXs have been detected, following the LC-HRMS analysis of several *Ostreopsis* spp. strains from all over the Mediterranean [193,226-228]. To date, none of these compounds have been isolated, but structural information were gained through interpretation of their fragmentation patterns in LC-HRMS^n spectra Table I.3 and Figure I.5.

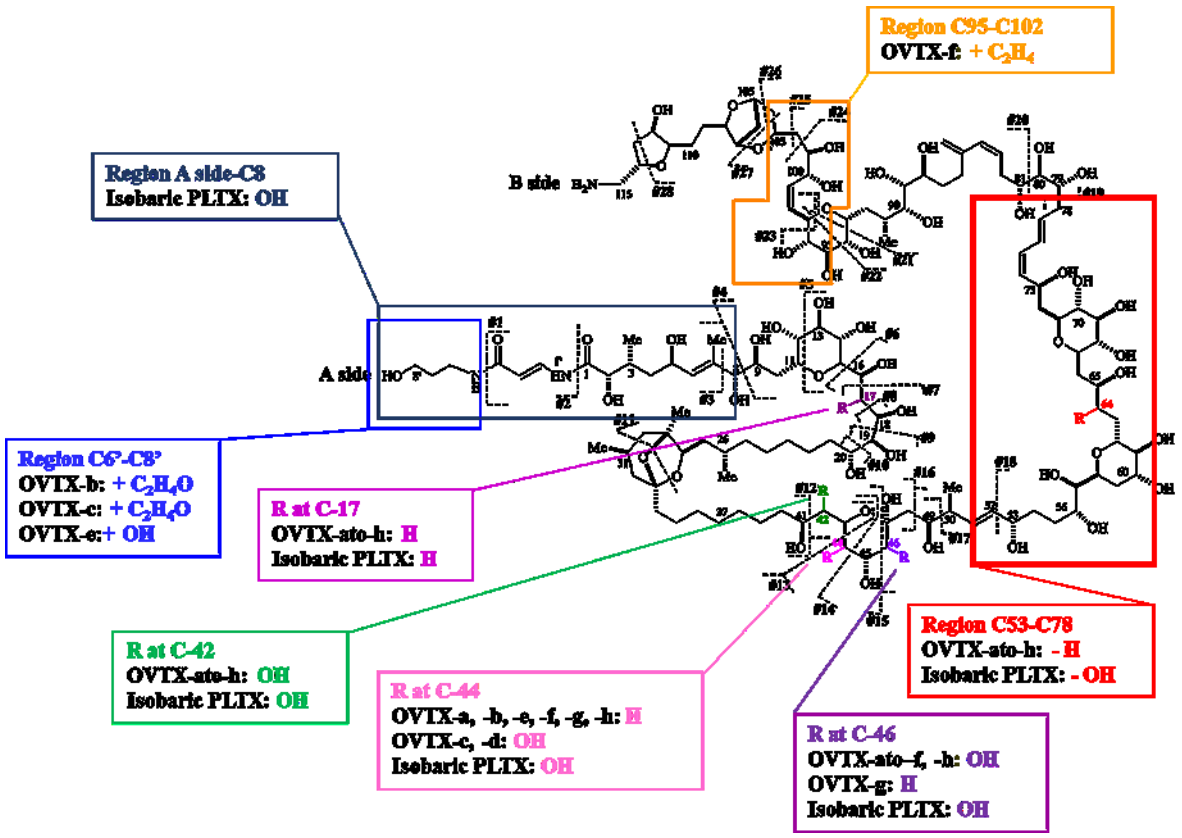

Figure I.15 Structural differences between PLTX (R at C17= OH; R at C42 = H; R at C44 = OH; R at C64=OH) and OVTX-a to –h.

Table I.3 Structural information concerning PLTX and OVTXs: monoisotopic ion peaks of $[M+H]^+$, elemental formulae, elemental composition of A- and B- moieties resulting from cleavage between C8 and C9 and additional water loss.

Toxin	$[M+H]^+$	Elemental formulae	A moiety	$[M+H\text{-B moiety-}H_2O]^+$	B moiety	$[M+Ca\text{-A moiety-2 }H_2O]^{2+}$
PLTX	2679.4893	$C_{129}H_{223}N_3O_{54}$	$C_{16}H_{28}N_2O_6$	327.1919	$C_{113}H_{195}NO_{48}$	1169.1112
OVTX-a	2647.4979	$C_{129}H_{223}N_3O_{52}$	$C_{16}H_{28}N_2O_6$	327.1919	$C_{113}H_{195}NO_{46}$	1153.1194
OVTX-b	2691.5233	$C_{131}H_{227}N_3O_{53}$	$C_{18}H_{32}N_2O_7$	371.2181	$C_{113}H_{195}NO_{46}$	1153.1189
OVTX-c	2707.5173	$C_{131}H_{227}N_3O_{54}$	$C_{18}H_{32}N_2O_7$	371.2181	$C_{113}H_{195}NO_{47}$	1161.1173
OVTX-d	2663.4905	$C_{129}H_{223}N_3O_{53}$	$C_{16}H_{28}N_2O_6$	327.1919	$C_{113}H_{195}NO_{47}$	1161.1157
OVTX-e			$C_{16}H_{28}N_2O_7$	343.1869	$C_{113}H_{195}NO_{46}$	1153.1179
OVTX-f	2675.5054	$C_{131}H_{227}N_3O_{52}$	$C_{16}H_{28}N_2O_6$	327.1908	$C_{115}H_{199}NO_{46}$	1167.1304
OVTX-g	2633.5021	$C_{129}H_{223}O_{51}N_3$	$C_{16}H_{28}N_2O_5$	327.1906	$C_{113}H_{195}NO_{45}$	1163.1261
OVTX-h	2633.5178	$C_{129}H_{225}O_{51}N_3$	$C_{16}H_{28}N_2O_5$	327.1911	$C_{113}H_{197}NO_{45}$	not reported

Recently, three OVTXs have been detected in a toxic clone of *O. ovata* (IK2) collected from Ikei Island, in Japan, by using liquid chromatography/quadrupole time-of-flight mass spectrometry (LC/QTOFMS) [206]. The three new OVTXs are isobaric

compounds of the Mediterranean OVTX-a, OVTX-d, and OVTX-e, but differed from them by their chromatographic behavior. In order to distinguish the Japanese OVTXs from the Mediterranean ones they were named OVTX-a IK2, OVTX-d IK2, and OVTX-e IK2 after the clone's code "IK2". Some insights into their structure were obtained by complementary use of positive and negative ion LC/QTOFMS and finally OVTX-a IK2, OVTX-d IK2, and OVTX-e IK2were tentatively identified as 42-hydroxy-17,44,70-trideoxypalytoxin, 42-hydroxy-17,70-dideoxypalytoxin and 42,82-dihydroxy-17,44,70-trideoxypalytoxin, respectively.

3.2 Toxicity and mode of action of Palytoxin

Palytoxin harms humans through several routes of exposure ranging from ingestion of contaminated seafood to dermal contact, or inhalation of marine aerosol [229-230]. Some fatal human poisonings attributed to PLTX have been reported worldwide [231-232]; the toxin has been suggested as the possible cause of clupeotoxism, a poorly understood syndrome caused by ingestion of edible fish [194]. Intoxication symptoms following ingestion route include bitter/metallic taste, vomiting, diarrhea, muscle cramps, abdominal pain, numbness of the extremities, bradycardia, difficulty breathing, renal failure and death. Symptoms caused by dermal contact or inhalation of contaminated aerosol include erythema and dermatitis, fever (≥38°C), watery rhinorrhea, pharyngeal pain, cough, headache, and bronchoconstriction with dyspnea and conjunctivitis. The Na^+/K^+-ATPase membrane pumps was proposed as the target for PLTX after the observation that PLTX effects were antagonized by cardiotonic steroids such as ouabain [233], transforming that pump in a non-selective cation channel [234].

It was demonstrated that PLTX is a potent tumor promoter in the mouse skin carcinogenesis model [235-236]. In contrast to TPA (12-O-tetradecanoylphorbol-13-acetate), PLTX induces neither ornithine decarboxylase in mouse skin nor HL-60 cell adhesion. Furthermore, PLTX neither binds to protein kinase C *in vitro* nor increases ornithine decarboxylase activity in mouse skin. On the basis of such evidence PLTX was classified as a non-TPA-type tumor promoter [237].

Toxicity strongly depends on administration route [238]. PLTX is exceptionally toxic in mammals when intravenously administrated (LD_{50} ranging between 25-450 ng/Kg); rabbits and dogs are most vulnerable to PLTX, followed by monkeys, rats, guinea pigs and mice [239]. PLTX exhibits lower toxicity when intraperitoneal and intragastric administrations are carried out (e.g. LD_{50} intragastric administration > 40μg/Kg) [239-

240]. Palytoxin toxicity via several other routes of administration has been also investigated: it is highly toxic after intramuscular or subcutaneous injection with LD_{50}observed, similar to that obtained for intraperitoneal injection or following intratracheal instillation [237,239-240]. Severe irritation, involving ulcerations and conjunctivitis, was induced by application of PLTX to the eye [239]. No toxicity was recorded after intrarectal administration of PLTX at 10μg/Kg [240].

Relative toxicity of Palytoxin's analogues

Although very few structural differences exist between PLTX and its analogues, toxicity can be very different. In fact, ostreocin-D, compared to PLTX, presents lower citotoxicity against P388 cells (2.5 pM versus 0.2 pM) and lower hemolytic potency (39.5 nM versus 1.5 nM) [188]. Recently, Ito and Yasumoto [238] have reported that both toxins are toxic by intra-peritoneal injection - with ostreocin-D less potent (5 μg/kg) than PLTX (1.5 μg/kg) - and by intra-tracheal administration causing bleeding and alveolar destruction in the lung and resultant death at 2 μg/kg of PLTX and 11 μg/kg of ostreocin-D. Preliminary toxicological studies have been carried out on the two 42-hydroxy PLTXs. Interestingly, the cytotoxicity of 42*S*-hydroxy-50*R*-palytoxin (from *P. tuberculosa*) toward skin HaCaT keratinocytes appeared approximately two orders of magnitude lower than that of PLTX and one order of magnitude lower than that of 42*S*-hydroxy-50*S* palytoxin (from *P. toxica*). Thus, a single configurational change plays a major role on the cytotoxicity of PLTXs, likely inducing conformational changes that ultimately reduce the potency of the toxin against the HaCaT keratinocytes [241-243]. Regarding the McTXs, preliminary studies carried on purified extracts showed that they present a hemolytic action lower than that of PLTX, with McTX-b more toxic than McTX-a [191]. Toxicological studies on OVTXs are currently in progress; preliminary biochemical studies demonstrated that they significantly increased the levels of mRNAs encoding inflammation-related proteins in immune cells, i.e., monocyte derived human macrophages [244]. Mouse lethality assessment of OVTX-a was tested at a dose level of 7.0 μg/kg. One to 3 min after injection, mice started wriggling and all died within 30 min with paralyzed limbs, leading to the conclusion that the toxin mouse lethality lies below 7.0 μg/kg [224]. Since the other OVTXs have not been isolated yet, no information about their toxicity are available.

3.3 Regulation of Palytoxins

Currently, there are no regulations for PLTXs in shellfish, either in the EU, or in other regions of the world because of lacking in toxicological database for this class of toxins, comprising only acute toxicity studies for PLTX and ostreocin-D via several routes of administration in various animal species. For this reason, CONTAM Panel was only able to derive an oral acute reference dose (ARfD) of 0.2 μg/kg b.w. for the sum of PLTX and ostreocin-D. For a 60 kg adult, in order to avoid exceeding the ARfD, a 400 g portion of shellfish meat should not contain more than 12 μg of the sum of PLTX and ostreocin-D, corresponding to 30 μg/kg shellfish meat. Besides to MBA, cell based assays and HPLC-FLD, LC-MS technique has been indicated by EFSA [245] as a valuable tool for monitoring PLTXs in a regulatory setting since it is rapid, sensitive, can be automated, and permits screening and quantitation in various matrices (plankton, seafood, etc.). However, there are still some drawbacks to overcome before such technique can be used in routine analysis of real samples. An important issue is represented by lacking of certified reference standards of PLTX and its analogues; they are difficult to be obtained in acceptable amounts until a large scale culturing of *Ostreopsis* spp. and efficient isolation procedures of the toxins are developed. To date, quantitation is carried out basing on the tentative assumption that PLTX-like compounds show the same molar response as PLTX itself, but even limited structural features in large molecules as PLTX could significantly impact their ionization efficiency.

3.4 Detection of Palytoxins

Detection and quantitation of PLTXs in environmental or food samples can be accomplished by both biological assays and chemical methods. Biological assays measure a single biological or biochemical response which involves the activity of all toxin congeners contained in the sample. So, they have the advantage to be highly sensitive and to indicate potential global toxicity of a sample, which is the priority for human health protection. Chemical methods are, however, needed for confirmation and unambiguous identification of the involved toxins, for defining toxin profile and for accurate quantitation. So, a combination of methods is sometimes preferable to confirm the presence of PLTXs in a sample.

Biological assays

The simplest way to detect PLTX is the MBA [18]. Within 15 min after intraperitoneal administration, mouse shows several characteristic symptoms namely stretching of hind limbs, lower backs and concave curvature of the spinal column [246]. As recently reviewed by Munday [247], LD_{50} for PLTX in the mouse bioassay is less than 1 µg/kg; Riobó *et al.* recently reported an LD50 value of 294.6 ± 5.4 ng/kg using a 24 h reference time [246]. To the aim of replace MBA, the Hemolysis assay was developed, based on the ability of PLTX to interact with the Na^+/K^+-ATPase. Suppression of hemolysis after pretreatment of samples with ouabain (an ATPase blocker) indicates the presence of hemolytic compounds, such as PLTX in the sample [248]. The hemolysis assay was initially developed by Bignami [249] and then investigated by other authors [246,250-253]. Blood origin (sheep, horse, rabbit, pig, mouse, human, etc.) and other parameters (age, sex, etc.) play a critical role in this assay and may strongly affect the limit of detection (LOD). Aligizaki *et al*. [253] could detect PLTX at concentration as low as 16 pg/mL and reported an LOD of 1.6 ng PLTX equivalents per kg of shellfish tissue. *In vitro* cytotoxicity assays measure morphological changes and cell damage caused by PLTX. Several protocols have been developed based on the use of different cell types, namely MCF-7 breast cancer cell line [254-255] Hela cells [256], or rat 3Y1 cells [181], and the use of different methods to measure citotoxicity, namely release of lactate dehydrogenate [254,256] or MTT-microculture tetrazolium [181]. The assay developed by Bellocci *et al.* presents an LOD of 50 pg/mL (corresponding to about 10 ng of PLTX per kg of shellfish tissue). Citotoxicity assays based on neuroblastoma cells and including ouabain pretreatment have also been reported [257-259]) presenting an LOD of 200 pg/mL and good capability for PLTX detection in *Ostreopsis* spp. extracts and naturally contaminated mussels [258]. Antibody-based methods have good potential for detection of PLTXs in being fast, easy to use and useful to screen many samples for further confirmatory analysis. Anyway, immunoassays present cross-reactivity which does not necessarily parallel toxicity and, similarly to other biological assays, they do not provide any information on toxin profile. So, their accuracy is questionable. A radioimmunoassay as well as ELISA test were developed [260-261]. Recently, Garet *et al*. [262] reported on isolation of single-chain antibodies against PLTX by phage display technology. A competitive ELISA assay was thus optimized with one of these phage antibodies which allowed to detect PLTX in shellfish in a working range 0.5 pg/ml to 500 ng/ml. Afterward, Yakes *et al*. [263] developed an immunoassays using a plasmon resonance biosensor to evaluate a previously

developed PLTX antibody. The assay with this antibody was optimized and it presented an LOD of 520 pg/mL for PLTX standard. Afterward, an electrochemiluminescence-based sensor for the detection of PLTX. The sensor was able to produce a concentration-dependent light signal, allowing quantification of PLTX in mussels, with a limit of quantitation (LOQ) of 220 pg/ml corresponding to 2.2 µg of PLTX per kg of mussels.

Chemical Methods

Although biological methods have the advantage to be highly sensitive and some of them are suitable for regulatory use, they are unable to identify individual components of the toxin profile. Thus, chemical methods are needed for confirmation and unambiguous identification of the involved toxins and for an accurate quantitation with high levels of sensitivity. LC with UV detection [185,190,252] has been largely used for identifying PLTXs in plankton, thanks to the presence of chromophores groups in the molecules. However, this technique is not enough sensitive and it is strongly affected by matrix interferences; thus, it is unsuitable for detection of PLTX in seafood. A pre-column derivatization method followed by LC-FLD has been developed for separation and quantification of PLTX by Riobó *et al*. [252]. It presents an instrumental LOD of 0.75-25 ng of PLTX standard injected being 1000-fold more sensitive than LC-UV. It has been applied to detection of PLTX in plankton samples but data are lacking on its application to seafood analysis. LC-MS has demonstrated great potential for rapid and sensitive identification of PLTXs in contaminated material. Very good results are obtained using ESI-MS^n technique. Indeed, the capability of ESI to produce multiply charged molecules under mild conditions has accessed detection of a high MW compound such as PLTX by extending the mass range for *m/z*-limited mass spectrometers. Fragment ions are also present in full MS spectra and they can provide structural information for identification of PLTX and its analogues. It is largely known that cleavage between carbons 8 and 9 of the molecule is highly favored [180] and divides the molecule in two moieties, A (*m/z* 327) and B (*m/z* 2318). These fragment ions are observed also in product ion spectra. PLTX-like compounds, such as McTXs [190], 42-OH-PLTX [208], and OVTXs [192,227-228] present the above fragmentation behavior that can be employed to gain structural information on potentially new analogues that are usually present in too small quantities in the extracts to carry out NMR studies. Other ionization techniques proved useful in MS detection of PLTX. Particularly, FAB has been used to detect PLTX and ostreocin-D both

in positive [188] and negative [217] ion modes, while Onuma *et al.* [249] used MALDI TOF MS to analyze a toxic extract in comparison to PLTX standard.

The MS instrumentation most appropriate to be used in LC-MS determination of PLTX should be evaluated. Indeed, as previously described, different mass analyzers, operating either at unit (triple quadrupole, ion trap) or high (TOF, hybrid linear ion trap-FTMS) resolution have shown to be capable to detect PLTXs in various matrices. They present different ease-to-use, instrumental sensitivity, and selectivity and their capability to provide accurate and reliable quantitative results should be more in-depth evaluated.

4. Passive sampling for marine biotoxins

The basis for the development of a technique aimed to the passive sampling marine biotoxins came from some observations, during natural events and culture studies on toxic algae, which suggested that significant amounts of polar and non-polar biotoxins are dissolved in the seawater during the algal blooms. This led to the idea that passive adsorption of this dissolved materials coupled to analytical technologies (e.g. LC-MS and ELISA assays) could provide a simples and sensitive means of biotoxins monitoring. In fact, many countries now have marine biotoxins monitoring programmes in place (e.g. EU Regulation 854/2004) aimed to minimize the risk of placing toxic products on the market. These regulations require routine monitoring of shellfish for toxins and the analysis of water samples for the presence of toxin-producing phytoplankton. However, analysis of shellfish has a number of disadvantages: it is a time consuming, technically demanding and expensive process. In addition, many of the toxins are metabolized in shellfish during digestion and assimilation, making toxin quantification more difficult. Finally, there are often matrix problems within extracts and assays and analyses are often slow and relatively insensitive. Phytoplankton monitoring, although being able to provide early warning of developing toxic blooms and having considerably assisted in the development of an understanding of harmful algal bloom ecology, it presents serious limitations: it is difficult to obtain spatially and temporally integrated samples. Most samples provide only a brief snapshot of the composition of the phytoplankton at one time and place that may not be truly representative within a wider context. It requires specialized laboratories and expertise and it can only provide circumstantial evidence regarding the probability of shellfish contamination developing. The intra-specific toxicity of toxic micro-algae species

may vary considerably and toxic and non-toxic species are difficult to definitively identify under the light microscope.

The first one to apply passive sampling to detect marine biotoxins in seawater was MacKenzie, in 2004 [264] who gave the acronym SPATT (solid-phase adsorption toxin tracking) to this technique. The technique is conceptually similar to other passive sampling methods [265-268] designed to monitor the occurrence of organic pollutants in water and shellfish such as the semi-permeable membrane devices (SPMD) and polar organic chemical integrative samplers (POCIS). SPATT technique is assessed for its potential to provide "reliable, sensitive, time-integrated sampling to monitor the occurrence of toxic algal bloom events" [269]. Initially, the SPATT samplers consisted in various polyester mesh, sewn with polyester thread [264]; the practicality of the device was improved by introducing a frame in which the solid phase is restrained to form a "passive sampling disk". This design is simple, cheap, more easily assembled and disassembled than the sewn SPATT bags, and is well suited to high throughput processing of samples [270] (Figure I.16).

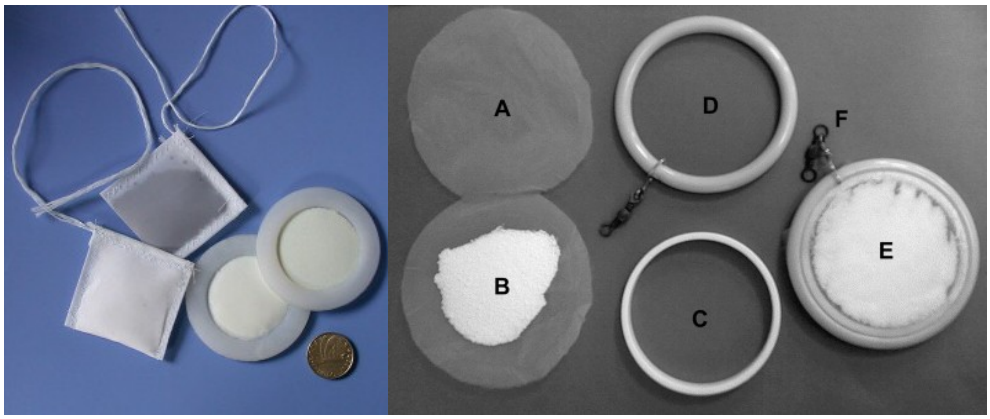

Figure I.16 SPATT bags and disks [264,269]

The SPATT methodology has many advantages including simplicity and low cost with numerous logistical advantages (e.g. storage, transport), time and spatially integrated sampling that simulates shellfish uptake, it is effective where no shellfish exist naturally. In addition, SPATT directly targets the toxic compounds that are not subject to biotransformation and sample matrices are relatively 'clean', which simplifies extraction

and analysis [269]. According to the nature of the solid-phase used to fill the SPATT, biotoxins with different chemistries (polar or nor polar) can be caught by the resin.

SPATT for hydrophilic algal toxins

Although there are some data about the ability of STX-producing *Alexandrium* spp. [271] and DA-producing diatoms [272] to excrete soluble toxins into the water during blooms, studies on the detection of more polar toxins are scarce.

Laboratory experiments have been carried out to investigate the use computationally designed polymers (CDPs) to remove neoSTX and STX from seawater. Good recoveries (97% and 92%, respectively) were achieved using an ethylene glycol methacrylate-phosphate-based polymer [273]. Despite encouraging results obtained in this study, the feasibility of this protocol in the marine environment has to be proven, and it requires very specific skills. More recently field trials have been carried out to evaluate hydrophobic SEPABEADS type resins (SP-700, SP-207, SP-207SS) and HP-20 in the monitoring of DA [274]. The results have shown that they vary in DA adsorption and recovery characteristics and the selection of a particular resin may depend upon the specific purpose for which it is to be used. For example, the weak adsorption (19% in 7 days) and ready dissociation of DA from HP20 may provide a better simulation of shellfish uptake than more strongly adsorbing substrates. However, laboratory experiments showed the presence of DA in the water using to wash the SPATT, leading to consider the wash step as an extraction stage (and thus analyze the wash) to not underestimate the amount of DA captured.

SPATT for lipophilic algal toxins

To date, SPATT devices have allowed the detection of many lipophilic toxins such as OA, PTXs, DTXs, YTXs, AZAs, SPXs, and gymnodimine [264,270,275-278]. The first application of SPATT bags [264] reports the comparison among three different polymeric adsorption resins (DIAION® HP-20, DIAION® SP-70, DIAION® HP-2MG), and HP-20 was found to be superior for the recovery of the major polyether toxins (YTX, OA, DTX1, PTX2). Successively, evaluation of adsorption and desorption behavior of other resins (HP-20, SP 850, SP 825L, XAD-4 andL-493) has been performed [276,279-280] using *Prorocentrum lima* cultures and natural seawater. All resins accumulated AZA-1 and PTX-2 in relatively high amounts. Although HP-20 reached equilibrium in a time longer than SP-850 and SP-825L, probably due to its larger pore size, it always accumulated more OA than other resins in naturally exposed SPATT discs. Marcaillou *et al.* [281] also obtained

good results through experimentation with *P. lima* cultures and HP-20. For this reason, HP-20 resin has been used in a number of studies aimed to develop SPATT methods for lipophilic toxins [282-285].

SPATT and benthic algal toxins

Although among benthic species there are some of the most toxic microalgae (e.g. *Vulcanodinium rugosum* [155], *Prorocentrum lima* [286], *Gambierdiscus* and *Ostreopsis ovata* [287], setting up a SPATT method for benthic algal toxins is a hard challenge; indeed, the benthic microalgae, unlike the pelagic ones, are in general less accessible to sampling since they grow attached to several substrate and it is difficult to find them in the water column. Few studies are present in literature about their detection by application of SAPTT methods. Evaluation of the application of passive samplers filled with HP-20 resin for the detection of dissolved CTXs and MTXs in seawater as a possible mean for the detection of the presence of *Gambierdiscus* toxic blooms in the field, has been carried out [286]. Laboratory experiment with seawater spiked at 100 ng/L of CTX-1B led to excellent recoveries (in the range 91-85%) with no significant differences measured between different times of exposure of the resin to dissolved CTX-1B, while poor recoveries were obtained for MTX spiked in the seawater at 2 μg/L (66%). MacKenzie *et al.* [278] deployed SPATT samplers in New Zealand, within the mangrove and sea-grass habitats and collected pacific oysters and samples of a variety of biological material. Analyses of SPATT extracted showed the presence of high levels of PnTx-E, PnTx-F and OA with trace amounts of other polyether toxins (spirolide desmethyl-C, PnTx-A, G and D, PTX-2 DTX-1). This was one of the first studies showing the ability to capture shellfish toxins produced by benthic microalgae directly in the field, even if the organisms producers are present in low abundance in the water column. Also in Norway, a similar study confirmed the possibility of capturing benthic microalgal toxins through the deployment of SPATTs [289]. Analyses of SPATT extracts allowed the detection PnTX-G and other cyclic imines (13-C and desmethylspirolide 13,19- desmethyl-spirolide-C) produced by *Alexandrium ostenfeldii*. In a recent study [290] alternative resins, such as Oasis HLB, BondElute C18 and STRATA-X together with HP-20, have been evaluated. Comparison in SPE-mode led to the exclusion of BondElute C18 resin. The three remaining sorbents were separately exposed as passive samplers for 24 h to seawater spiked with algal extracts containing known amounts of OA, AZAs, PnTX-G, 13-desmethyl spirolide-C and OVTXs. Irrespective of the toxin group, the adsorption rate of toxins on HP-20 was slower than on

Oasis HLB and Strata-X. However, HP-20 and Strata-X gave higher recoveries after 24h exposure. In all tests, recoveries were generally higher for cyclic imines and OA group toxins, slightly lower for AZAs, and the lowest for OVTXs. The same sorbents were evaluated in closed tanks with mussels exposed to *Vulcanodinium rugosum* or *Prorocentrum lima.* When the different sorbent materials were put in competition for toxins in the same container, Strata-X accumulated higher level of toxins and at higher speed rate than Oasis HLB, and HP-20. The deployment of these three sorbents at Ingril French Mediterranean lagoon to detect PnTX-G in the water column showed accumulation of higher levels on HP-20 and Oasis HLB compared to Strata-X. This study has significantly extended the range of sorbents for passive sampling of marine toxins and it demonstrated for the first time the usefulness of the polymeric Oasis HLB and Strata-X sorbents in laboratory and field studies for various microalgal toxins.

References

1. Daneshian M, Botana LM, Bottein M-YD, Buckland G, Campas M, Dennison N, Dickey RW, Diogene J, Fessard V, Hartung T, Humpage A, Leist M, Molgo J, Quilliam MA, Rovida C, Suarez-Isla BA, Tubaro A, Wagner K, Zoller O, Dietrich D. A roadmap for hazard monitoring and risk assessment of marine biotoxins on the basis of chemical and biological test systems. *Altex-Alternatives to Animal Experimentation.* **2013**, 30(4):487-545

2. Anonymous. The state of world fisheries and aquaculture. In: *World review of fisheries and aquaculture*. **2014**

3. Daranas AH, Norte M, Fernandez JJ. Toxic marine microalgae. *Toxicon : official journal of the International Society on Toxinology.* **2001**, 39:1101-1132

4. Sournia A, Chretiennotdinet MJ, Ricard M. Marine phytoplankton - How many species in the world ocean. *Journal of Plankton Research*. **1991**, 13:1093-1099

5. Hallegraeff GM. A review of harmful algal blooms and their apparent global increase*. *Phycologia.* **1993**, 32(2):79-9

6. Sandra E. Shumway. A Review of the Effects of Algal Blooms on Shellfish and Aquaculture. *Journal of the World Aquaculture Society.* **1990**, 21(2):65–104

7. Van Dolah FM. Marine algal toxins: Origins, health effects, and their increased occurrence. *Environmental Health Perspectives*. **2000**, 108(SUPPL. 1): 133-141

8. Ciminiello P, Dell' Aversano C, Fattorusso E, Forino M. Advances in Molecular Toxicology. Chapter 1 *Recent Developments in Mediterranean Harmful Algal Events*. **2009**, 3:1–41

9. Moestrup Ø, Akselmann R. Fraga S, Hansen G, Hoppenrath M, Iwataki M, Komárek J, Larsen J, Lundholm N, Zingone A. (Eds) (**2009** onwards). *IOC-UNESCO Taxonomic Reference List of Harmful Micro Algae*. Accessed at http://www.marinespecies.org/hab on 2016-03-

10. Kohane DS, Smith SE, Louis DN, Colombo G, Ghoroghchian P, Hunfeld NG, Berde CB, Langer R. Prolonged duration local anesthesia from tetrodotoxin-enhanced local anesthetic microspheres. *Pain*. **2003**, 104(1-2):415-21

11. Hallegraeff GM: Harmful algae and their toxins: progress, paradoxes and paradigm shifts. In: *Toxins and Biologically Active Compounds from Microalgae*. Edited by Rossini GP, vol. 1: CRC press, Taylor and Francis group; **2014**

12. Botana LM, Rodriguez-Vieytes M, Alfonso A. and Louzao MC. In: *Handbook of food analysis - residues and other food component analysis*. Vol. 2 (ed. L.M.L. Nollet), Marcel Dekker Inc., New York, **1996**:1147-1169

13. Aune T. In: *Seafood and Freshwater Toxins Pharmacology, Physiology and Detection.* 2nd ed. (Ed.: L. M. Botana), CRC Press, Boca Raton, FL, **2008**:3-20

14. Anderson DM, Okaichi T, Remoto T. (ed.). Toxic algal bloom and ted tides: a global perspective. *Red tides: biology, environmental science and technology.* New York. Elsevier Science Publishing Co.; **1989**:11-16

15. Brand LE. Toxic harmful algal blooms: natural and anthropogenic causes. In: *New trends in marine freshwater toxins*. Edited by Cabado AG, Vieities JM: Nova Science Publishers, Inc.; **2012**

16. Hallegraeff GM. Ocean climate change, phytoplankton community responses, and harmful algal blooms: a formidable predictive challenge. *Journal of Phycology.* **2010**, 46(2):220-235

17. Stewart I, Mcleod C. The laboratory mouse in routine food safety testing for marine algal biotoxins and harmful algal bloom toxin research: past, present and future. *Journal of AOAC international.* **2014**, 97 (2):356-372

18. Yasumoto T, Oshima Y, Yamaguchi M. Occurrence of a new type of shellfish poisoning in the Tohoku district. *Bulletin of the Japanese Society for the Science of Fish.* **1978**, 1249-1255

19. Combes RD. The mouse bioassay for diarrhetic shellfish poisoning: A gross misuse of laboratory animals and of scientific methodology. *ATLA-Alternatives to Laboratory Animals*. **2003**, 31:595-610

20. Holland P. In: Botana LM (ed) *Seafood and freshwater toxins: pharmacology, physiology and detection*. 2nd edn. Boca Raton, CRC Press. **2008**

21. Sauer U, Spielmann H, Rusche B. Fourth EU report on the statistics on the number of animals used for scientific purposes in **2002**- Trends, problems, conclusions. *Altex 2005*. 22:59-67

22. Hess P, Butter T, Petersen A, Silke J, McMahon T. Performance of the EU-harmonised mouse bioassay for lipophilic toxins for the detection of azaspiracids in naturally contaminated mussel (*Mytilus edulis*) hepatopancreas tissue homogenates characterised by liquid chromatography coupled to tandem mass spectrometry. *Toxicon : official journal of the International Society on Toxinology*. **2009**, 53, 713-722

23. Vilariño N, Louzao MC, Vieytes MR, Botana LM. Biological methods for marine toxin detection. *Analytical and Bioanalytical Chemistry*. **2010**, 397(5):1673-81

24. Quilliam MA. The role of chromatography in the hunt for red tide toxins *Journal of Chromatography A*. **2003**, 1000:527-548

25. FAO. **2004**. Report of the joint FAO/IOC/WHO ad hoc expert consultation on biotoxins in bivalve molluscs, Oslo, Norway

26. Campbell K, Vilarino N, Botana LM, Elliott CT. A European perspective on progress in moving away from the mouse bioassay for marine-toxin analysis. *Trac-Trends in Analytical Chemistry*. **2011**, 30, 239-253

27. Hess P. Requirements for screening and confirmatory methods for the detection and quantification of marine biotoxins in end-product and official control. *Analytical and Bioanalytical Chemistry*. **2010**, 397:1683-1694

28. Christian B, Luckas B. Determination of marine biotoxins relevant for regulations: from the mouse bioassay to coupled LC-MS methods. *Analytical and Bioanalytical Chemistry*. **2008**, 391(1):117-34

29. Ramsdell. In Rossini GP, Hess P. *Phycotoxins: chemistry, mechanisms of action and shellfish poisoning EXS*. **2010**, 100:65-122

30. James KJ, Carey B, O'halloran J, F. N. A. M. van Pelt, Škrabáková Z. Shellfish toxicity: Human health implications of marine algal toxins. *Epidemiology and Infection*. **2010**, 138(7):927-940

31. FAO/IOC/WHO, **2005**. Report of the FAO/IOC/WHO ad hoc expert consultation on biotoxins in bivalve molluscs, Oslo, Norway, Sept. 26-30, 2004

32. Twiner MJ, Rehmann N, Hess P, Doucette GJ. Azaspiracid shellfish poisoning: A review on the chemistry, ecology, and toxicology with an emphasis on human health impacts. *Marine Drugs.* **2008**, 6(2): p. 39-72

33. Furey A, O'Doherty S, O'Callaghan K, Lehane M, James KJ. Azaspiracid poisoning (AZP) toxins in shellfish: Toxicological and health considerations. *Toxicon.* **2010**, 56, (2, 15):173–190

34. Plakas SM, Dickey RW. Advances in monitoring and toxicity assessment of brevetoxins in molluscan shellfish. *Toxicon*. **2010**, 56(2):137-149

35. Caillaud A, de la Iglesia P, Taiana DH, Pauillac S, Aligizaki K, Fraga S, Chinain M, Diogène J. Update on methodologies available for ciguatoxin determination: Perspectives to confront the onset of ciguatera fish poisoning in Europe. *Marine Drugs.* **2010**, 8(6): 1838-1907.

36. Plakas SM, Dickey RW. Ciguatera: A public health perspective. *Toxicon.* **2010**, 56(2):123-136

37. Lefebvre KA, Robertson A. Domoic acid and human exposure risks: A review. *Toxicon*. **2010**, 56(2):218-230

38. Guéret, SM Brimble MA. Spiroimine shellfish poisoning (SSP) and the spirolide family of shellfish toxins: Isolation, structure, biological activity and synthesis. *Natural Product Reports.* **2010**, 27(9):1350-1366

39. Otero A, Chapela M, Atanassova M, Vieites JM, Cabado AG. Cyclic imines: chemistry and mechanism of action: a review. *Chemical Research in Toxicology.* **2011**, 24:1817-1829

40. Dominguez HJ, Paz B, Daranas AH, Norte M, Franco JM, Fernández JJ. Dinoflagellate polyether within the yessotoxin, pectenotoxin and okadaic acid toxin groups: Characterization, analysis and human health implications. *Toxicon.* **2010**, 56(2):91-217

41. Reguera, B, Riobó P, Rodríguez F, Díaz PA, Pizarro G, Paz B, Franco JM, Blanco J. Dinophysis toxins: Causative organisms, distribution and fate in shellfish. *Marine Drugs.* **2014**, 12(1):394-461

42. Vale C, Botana LM Marine toxins and the cytoskeleton: Okadaic acid and Dinophysis toxins. *Federation of European Biochemical Societies Journal.* **2008**, 275(24):6060-6066

43. Ciminiello P, Dell'Aversano C, Fattorusso E, Forino M, Grauso L, Tartaglione L. A 4-decade-long (and still ongoing) hunt for palytoxins chemical architecture. *Toxicon*. **2011**, 57(3):362-367

44. Ciminiello P, Dell'Aversano C, Dello Iacovo E, Fattorusso E, Forino M, Tartaglione L. LC-MS of palytoxin and its analogues: State of the art and future perspectives. *Toxicon.* **2011**, 57(3):376-389

45. Riobó P, Franco JM. Palytoxins: Biological and chemical determination. *Toxicon.* **2011**, 57(3):368-375

46. Liu R, Liang Y. Advances in pectenotoxins studies: A review. *Shengtai Xuebao/ Acta Ecologica Sinica*. **2010**, 30(19):5355-5370

47. Humpage AR, Magalhaes VF, Froscio SM. Comparison of analytical tools and biological assays for detection of paralytic shellfish poisoning toxins. *Analytical and Bioanalytical Chemistry.* **2010**, 397(5):1655-1671

48. Wiese M, D'Agostino PM, Mihali TK, Moffitt MC, Neilan BA. Neurotoxic alkaloids: Saxitoxin and its analogs. *Marine Drugs*. **2010**, 8(7):2185-2211

49. Paz B, Daranas AH, Norte M, Riobó P, Franco JM, Fernández JJ. Yessotoxins, a group of marine polyether toxins: An overview. *Marine Drugs.* **2008**, 6(2):73-102

50. European Commission, Regulation (EC) No 15/2011. *Official Journal of the European Union*. **2011**. L 6(3)

51. European Commission, Regulation (EC) No 853/2004. *Official Journal of the European Union*. **2004**. L 226(22)

52. European Commission, Regulation (EC) No 2074/2005. *Official Journal of the European Union*. **2005**. L 338(27)

53. EFSA Scientific opinion. Marine biotoxins in shellfish – Summary on regulated marine biotoxins. Scientific Opinion of the Panel on Contaminants in the Food Chain. *The EFSA Journal*. **2009**, 1306, 1-23

54. European Commission, Regulation (EC) No 1244/2007. *Official Journal of the European Union*. **2007**. L 281(22)

55. European Commission, Regulation (EC) No 1664/2006. *Official Journal of the European Union*. **2006**. L 320(13)

56. EURLMB, Interlaboratory Validation Study of the EU-Harmonised SOP LIPO LC MS/MS. **2011**

57. Suzuki T, Quilliam MA. LC-MS/MS analysis of diarrhetic shellfish poisoning (DSP) toxins, okadaic acid and Dinophysis toxin analogues, and other lipophilic toxins. *Analytical Sciences.* **2011**, 27(6):571-584

58. Alexander J, Benford D, Boobis A, Ceccatelli S, Cravedi J, Di Domenico A, Doerge D, Dogliotti E, Edler L, Farmer P, Filipič M, Fink-Gremmels J, Fürst P, Guérin T, Knutsen HK, Machala M, Mutti A, Schlatter J, van Leeuwen R. Emerging toxins: Brevetoxin group. Scientific Opinion of the Panel on Contaminants in the Food Chain. *The EFSA Journal*, **2010**, 1677(8(7)):1-29

59. Daigo K. Studies on the constituents of *Chondria armata*. II. Isolation of an anthelmintical constituent. *Yakugaku Zasshi Journal of the Pharmaceutical Society of Japan.* **1959**, 79:353-356

60. Trainer VL, Bates SS, Lundholm N, Thessen AE, Cochlan, WP, Adams NG, Trick CG. *Pseudo-nitzschia* physiological ecology, phylogeny, toxicity, monitoring and impacts on ecosystem health. *Harmful Algae*. **2012**, 14:271-300

61. Paredes I, Rietjens IMCM, Vieites JM, Cabado AG. Update of risk assessments of main marine biotoxins in the European Union. *Toxicon.* **2011**, 58(4):336-354

62. Quilliam MA, Wright JLC. The amnesic shellfish poisoning mystery. *Analytical Chemistry*. **1989**, 6:1053-1060

63. EFSA: Marine biotoxins in shellfish - Domoic acid group, Scientific Opinion of the Panel on Contaminants in the Food chain; adopted on 2 July **2009**. *The EFSA Journal.* 1181, 1-61

64. Takemoto T, Daigo K, Kondo Y, Kondo K. Yakugaku *Zasshi Journal of the Pharmaceutical Society of Japan.* **1966**, 86:874–877

65. Ohfune Y, Tomita M. Total synthesis of (-)-domoic acid. A revision of the original structure. *Journal of the American Chemical Society*. **1982**, 104:3511–3513

66. Holland PT, Selwood AI, Mountfort DO, Wilkins AL, McNabb P, Rhodes LL, Doucette GJ, Mikulski CM, King KL. Isodomoic acid C, an unusual amnesic shellfish poisoning toxin from *Pseudo-nitzschia* australis. *Chemical Research Toxicology*. **2005**, 18:814-816

67. Maeda M, Kodama T, Tanaka T, Yoshizumi H, Takemoto T, Nomoto K, Fujita T. Structures of isodomoic acids A, B and C, novel insecticidal amino acids from the red alga *Chondria armata*. *Chemical and Pharmaceutical Bulletin.* **1986**, 34:4892-4895

68. Walter JA, Falk M, Wright JLC. Chemistry of the shellfish toxin domoic acid: characterization of related compounds. *Canadian Journal of Chemistry*. **1994**, 72:430-436

69. Zaman L, Arakawa O, Shimosu A, Onoue Y, Nishio S, Shida Y, Noguchi T. Two new isomers of domoic acid from a red alga, *Chondria armata*. *Toxicon : official journal of the International Society on Toxinology*. **1997**, 35:205-212

70. Clayden J, Read B, Hebditch KR. Chemistry of Domoic acid, Isodomoic acids, and their analogues. *Tetrahedron*. **2005**, 61:5713–5724

71. Riobò, Franco JM. Chemical methods for detecting phycotoxins: LC and LC/MS/MS. In: *New trends in marine freshwater toxins*. Edited by Cabado AG, Vieites JM: Nova Science Publishers, Inc.; **2012**

72. Berman FW, Murray TF. Domoic acid neurotoxicity in cultured cerebellar granule neurons is mediated predominantly by NMDA receptors that are activated as a consequence of excitatory amino acid release. *Journal of Neurochemistry*. **1997**, 69(2):693-703

73. Lilly EL, Halanych KM, Anderson DM. Phylogeny, biogeography, and species boundaries within the *Alexandrium minutum* group. *Harmful Algae*. **2005**, 4:1004–1020

74. Sako Y, Yoshida T, Uchida A, Arakawa O, Noguchi T, Ishida Y. Purification and characterization of a sulfotransferase specific to N-21 of saxitoxin and gonyautoxin 2 + 3 from the toxic dinoflagellate *Gymodinium catenatum* (Dinophyceae). *Journal of Phycology*. **2001**, 37: 1044–1051

75. Usup G, Kulis DM, Anderson DM. Growth and toxin production of the toxic dinoflagellate *Pyrodinium bahamense* Var. *compressum* in laboratory cultures. *Natural Toxins*. **1994**, 2:254–262

76. Wiese M, D'Agostino PM, Mihali TK, Moffitt MC, Neilan BA. Neurotoxic Alkaloids: Saxitoxin and Its Analogs. *Marine drugs*. **2010**, 8:2185-2211

77. Hall S, Strichartz G, Moczydlowski E, Ravindran A, Reichardt PB. In: *Marine toxins: origin, structure and molecular pharmacology* (Eds.: S. Hall and G. Strichartz), American Chemical Society, Washington, DC, **1990**:29–65

78. Kao CY. Tetrodotoxin, saxitoxin and their significance in the study of excitation phenomena. *Pharmacological Review*. **1966**, 18:997-1049

79. Oshima Y, Blackburn SI, Hallegraeff GM. Comparative study on paralytic shellfish toxin profiles of the dinoflagellate *Gymnodinium catenatum* from three different countries. *Marine Biology*. **1993**, 116:471–476

80. Tachibana K, Scheuer PJ, Tsukitani Y, Kikuchi H, Van Engen D, Clardy J, Gopichand Y, Schmitz FJ. Okadaic acid, a cytotoxic polyether from two marine sponges of the genus *Halichondria. Journal of the American Chemical Society*. **1981**, 103:2469-2471

81. Lee JS, Igarashi T, Fraga S, Dahl E, Hovgaard P, Yasumoto T. Determination of diarrhetic shellfish toxins in various dinoflagellates species. *Journal of Applied Phycology*. **1989**, 1:147–152

82. Rhodes LL, Syhre M. Okadaic acid production by a New Zealand *Prorocentrum lima* isolate. *Journal of Marine & Freshwater Research*. **1995**, 29:367–370

83. Dickey RW, Bobzin SC, Faulkner DJ, Bencsath FA, Andrzejewski D. Identification of okadaic acid from a caribbean dinoflagellate *Prorocentrum concavum*. *Toxicon.* **1990**, 28(4):371-377

84. Murata M, Shimatani M, Sugitani H, Oshima Y, Yasumoto T. Isolation and structural elucidation of the causative toxin of the diarrhetic shellfish poisoning. *Bulletin of the Japanese Society for the Science of Fish.* **1982**, 48:549–552

85. Toyofuku H. Joint FAO/WHO/IOC activities to provide scientific advice on marine biotoxins (research report). *Marine Pollution Bulletin.* **2006**, 52(12):1735-1745

86. Yasumoto T, Murata M, Lee JS, Torigoe K. Polyether toxins produced by dinoflagellates. In: *"Mycotoxins and Phycotoxins '88"*, eds.: Natori S., Hashimoto K.//Ueno Y, **1983**, 375-382

87. Hu T, Doyle J, Jackson D, Marr J, Nixon E, Pleasance S, Quilliam MA, Walter JA, Wright JLC. Isolation of a new diarrhetic shellfish poison from Irish mussels. *Journal of the Chemical Society, Chemical Communications*. **1992**:39–41

88. Opinion of the Scientific Panel on Contaminants in the Food chain on a request from the European Commission on marine biotoxins in shellfish – okadaic acid and analogues, *The EFSA Journal*, **2008**, 589, 1-62

89. Fujiki H, Suganuma M. Tumor promotion by inhibitors of protein phosphatates 1 and 2A: the okadaic acid class of compounds. *Advances in Cancer Research.* **1993**, 61:143–194

90. Sasaki K, Murata M, Yasumoto T, Mieskes G, Takai A. Affinity of okadaic acid to type-1 and type-2A protein phosphatases is markedly reduced by oxidation of its 27-hydroxyl group. *Biochemical Journal*. **1994**, 298:259–262

91. Rehmann N, Hess P, Quilliam MA. Discovery of new analogs of the marine biotoxin azaspiracid in blue mussels *Mytilus edulis* by ultra-performance liquid

chromatography/tandem mass spectrometry. *Rapid Communications in Mass Spectrometry*. **2008**, 22:549–558

92. McMahon T, Silke J. West coast of Ireland: winter toxicity of an unknown etiology in mussels. *Harmful Algae News*. **1996**, 14, 2

93. Ito E, Terao K, McMahon T, Silke J, Yasumoto T. Acute pathological changes in mice caused by crude extracts of novel toxins isolated from Irish mussels. *Harmful Algae*. **1997**:588-589

94. Satake M, Ofuji K, Kevin J, Furey A, Yasumoto T. New toxic event caused by Irish mussels, in: Reguera B, Blanco J, Fernandez ML, Wyatt T (Eds.), *Harmful Algae*. **1998**. IOC of UNESCO and Xunta de Galicia, Santiago de Compostela, Spain.

95. Satake M, Ofuji K, Naoki H, James JK, Furey A, McMahon T, Silke J, Yasumoto T. Azaspiracid, a new marine toxin having unique spiro ring assemblies, isolated from Irish mussels *Mytilus edulis*. *Journal of American Chemical Society*. **1998**, 120:9967–9968

96. Nicolaou KC, Koftis TV, Vyskocil S, Petrovic G, Tang W, Frederick MO, Chen DY, Li Y, Ling T, Yamada YM. Total synthesis and structural elucidation of azaspiracid-1. Final assignment and total synthesis of the correct structure of azaspiracid-1. *Journal of American Chemical Society*. **2006**, 128:2859-72

97. Hess P, McCarron P, Krock B, Kilcoyne J, Miles CO. *Azaspiracids: Chemistry, Biosynthesis, Metabolism, and Detection, Seafood and Freshwater Toxins*. CRC Press, Boca Raton, Florida, USA, **2014**:799-822

98. Furey A, Braña-Magdalena A, Lehane M, Moroney C, James JK, Satake M, Yasumoto T.1 Determination of azaspiracids in shellfish using liquid chromatography–tandem electrospray mass spectrometry. *Rapid Communications in Mass Spectrometry*. **2002**, 16:238–242

99. Furey A, Moroney C, Magdalena AB, Saez MJF, Lehane M, James KJ. Geographical, temporal, and species variation of the polyether toxins, azaspiracids, in shellfish. *Environmental Science and Technology*. **2003**, 37:3078–3084

100. James KJ, Moroney C, Roden C, Satake M, Yasumoto T, Lehane M, Furey A. Ubiquitous 'benign' alga emerges as the cause of shellfish contamination responsible for the human toxic syndrome, azaspiracid poisoning. *Toxicon*. **2003**, 41:145–151

101. Krock B, Tillmann U, John U, Cembella AD. Characterization of azaspiracids in plankton size-fractions and isolation of an azaspiracid-producing dinoflagellate from the North Sea. *Harmful Algae*. **2008**, 8:254–263

102. Tillmann U, Elbrachter M, Krock B, John U, Cembella AD. *Azadinium spinosum* gen. et sp. nov. (Dinophyceae) identified as a primary producer of azaspiracid toxins. *European Journal of Phycology*. **2009**, 44:63-79

103. Gu H, Luo Z, Krock B, Witt M, Tillmann U. Morphology, phylogeny and azaspiracid profile of *Azadinium poporum* (Dinophyceae) from the China Sea. *Harmful Algae*. **2013**, 21–22:64–75

104. Tillmann U, Salas R, Gottschling M, Krock B, O'Driscoll D, Elbraechter M, *Amphidoma languida* sp. nov. (Dinophyceae) reveals a close relationship between *Amphidoma* and *Azadinium*. *Protist*. **2012**, 163:701-719

105. Salas R, Tillmann U, John U, Kilcoyne J, Burson A, Cantwell C, Hess P, Jauffrais T, Silke J. The role of *Azadinium spinosum* (Dinophyceae) in the production of azaspiracid shellfish poisoning in mussels. *Harmful Algae*. **2011**, 10(6):774-783

106 Louzao MC, Lago J, Ferreira M, Alfonso A. Advances in knowledge of phycotoxins, new information about their toxicology and consequences on Europe legislation. In: *New trends in marine freshwater toxins*. Edited by Cabado AG, Vieites JM: Nova Science Publishers, Inc.; **2012**:1-54

107. Campas M, Prieto-Simon B, Marty JL. Biosensors to detect marine toxins: Assessing seafood safety. *Talanta*. **2007**, 72(3):884-895

108. Ofuji K, Satake M, McMahon T, James KJ, Naoki H, Oshima Y, Yasumoto T Two analogs of azaspiracids isolated from mussels, *Mytilus edulis*, involved in human intoxication in Ireland. *Natural Toxins*. **1999**, 7:99-102

109. Suzuki T. In Seafood and Freshwater *Toxins: Pharmacology, Physiology, and Detection*, 2nd Edition (Eds: L. M. Botana), CRC Press, Boca Raton, FL, **2008**:343-359

110. Yasumoto T, Murata M, Oshima Y, Sano M, Matsumoto GK, Clardy J. Diarrhetic shellfish toxins. *Tetrahedron*. **1985**, 41:1019–1025

111. Suzuki T, Igarashi T, Ichimi K, Watai M, Suzuki M, Ogiso E, Yasumoto T. Kinetics of diarrhetic shellfish poisoning toxins, okadaic acid, dinophysistoxin-1, pectenotoxin-6 and yessotoxin in scallops *Patinopecten yessoensis*. *Fisheries Science*. **2005**, 7: 948-955

112. Miles CO, Wilkins AL, Munday R, Dines MH, Hawkes AD, Briggs LR, Sandvik M, Jensen DJ, Cooney JM, Holland PT, Quilliam MA, MacKenzie AL, Beuzenberg V, Towers NR. Isolation of pectenotoxin-2 from *Dinophysis acuta* and its conversion to pectenotoxin-2 seco acid, and preliminary assessment of their acute toxicities. *Toxicon : official journal of the International Society on Toxinology*. **2004**, 43:1-9

113. Ito E, Suzuki T, Oshima Y, Yasumoto T Studies of diarrhetic activity on pectenotoxin-6 in the mouse and rat. *Toxicon*. **2008**, 51:707–716

114. Ishige M, Satoh N, Yasumoto T. Pathological studies on the mice administrated with the causative agent of diarrhetic shellfish poisoning (okadaic acid and pectenotoxin-2). *Bulletin Hokkaido Inst. Public Health*. **1988**, 38:15-19

115. Lun HA, Chen DZ, Magoon J, Worms J, Smith J and Holmes CF. Quantification of diarrhetic shellfish toxins by identification of novel protein phosphatase inhibitors in marine phytoplankton and mussels. *Toxicon*. **1993**, 31:75-83

116. Murata M, Kumagai M, Lee JS, Yasumoto T. Isolation and structure of yessotoxin, a novel polyether compound implicated in diarrhetic shellfish poisoning. *Tetrahedron Letters*. **1987**, 28(47):5869-5872

117. Satake M, MacKenzie L, Yasumoto T. Identification of *Protoceratium reticulatum* as the biogenetic origin of yessotoxin. *Natural toxins*. **1997**, 5:164-167

118. Paz B, Riobò P, Fernandez AL, Fraga S, Franco JM. Production and release of yessotoxins by the dinoflagellates *Protoceratium reticulatum* and *Lingulodinium polyedrum* in culture. *Toxicon : official journal of the International Society on Toxinology.* **2004**, 44:251-258

119. Rhodes L, McNabb P, de Salas M, Briggs L, Beuzenberg V, Gladstone M. Yessotoxin production by *Gonyaulax spinifera*. *Harmful Algae*. **2006**, 5:148-155

120. Hess P, Aasen JB. Chemistry, origins and distribution of yessotoxin and its analogues. In: Botana, L.M. (Ed.), *Chemistry and pharmacology of marine toxins*. Blackwell publishing, Oxford, **2007**:187-2002

121. Ciminiello P, Fattorusso E. In: *Seafood and Freshwater Toxins Pharmacology, Physiology and Detection.* 2nd Edition (Eds.: L. M. Botana), CRC press, Boca Raton, FL, **2008**: 287-314

122. Miles CO, Samdal IA, Aasen JAG, D. J. Jensen, Quilliam MA, Petersen D, M.Briggs L, Wilkins AL, Rise Cooney FJM, MacKenzie L. Evidence of numerous analogs of yessotoxin in *Protoceratium reticulatum*. *Harmful Algae*. **2005**, 4:1075–1091

123. Terao K, Ito E, Oarada M. Murata M. Yasumoto T. Histopathological studies on experimental marine toxin poisoning-5. The effects in mice of yessotoxin isolated from *Patinopecten yessoensis* and of a desulfated derivative. *Toxicon*. **1990**, 28:1095-1104

124. De la Rosa LA, Alfonso A, Vilarino N, Vieytes MR, Botana LM. Modulation of cytosolic calcium levels of human lymphocytes by yessotoxin, a novel marine phycotoxin. *Biochemical Pharmacology*. **2001**, 61:827–833

125. Gunter G, Smith FG, Williams, RH. Mass Mortality of Marine Animals on the lower West Coast of Florida, November 1946-January. *Science* **1947**, 105:256-257

126. Abraham A, Wang Y, El Said KR, Plakas SM. Characterisation of brevetoxin metabolisms in *Karenia brevis* bloom-exposed clams (Mercenaria sp.) by LC-MS/MS. *Toxicon*. **2012**, 60:1030–1040

127. FAO **2004**. The state of world fisheries and aquaculture

128. Pierce RH, Henry MS, Blum PC, Hamel SL, Kirkpatrick B, Cheng YS, Zhou Y, Irvin, CM, Naar J, Weidner A, Fleming LE, Backer LC, Baden DG. Brevetoxin composition in water and marine aerosol along a Florida beach: Assessing potential human exposure to marine biotoxins. *Harmful Algae*. **2005**, 4:965-972.

129. Baden DG, Bourdelais AJ, Jacocks H Natural and derivative brevetoxins: historical background, multi-plicity, and effects. *Environmental Health Perspectives*. **2005**, 113:621-625

130. Landsberg JH. The effects of harmful algal blooms on aquatic organisms. Reviews. In: *Fisheries Science.* **2002**, 10:113-390

131. Plakas SM, Wang Z, El Said KR, Jester ELE, Granade, HR, Flewelling L, Scott P, Dickey RW. Brevetoxin metabolism and elimination in the Eastern oyster (*Crassostrea virginica*) after controlled exposures to Karenia brevis. *Toxicon*. **2004**, 44:667-685

132. Wang Z, Plakas SM, El Said KR, Jester LE, Granade HR, Dickey RW. LC/MS analysis of brevetoxin metabolites in the Eastern oyster (*Crassostrea virginica*). *Toxicon*. **2004**, 43:455-465

133. Scientific Opinion on marine biotoxins in shellfish – Emerging toxins: Brevetoxin group EFSA Panel on Contaminants in the Food Chain (CONTAM) *The EFSA Journal.* **2010**; 8(7):1677

134. Huang JM, Wu CH, Baden DG. Depolarizing action of a red-tide dinoflagellate brevetoxin on axonal membranes. *Journal of Pharmacology Experimental Therapeutics*. **1984**, 229:615-621

135. Watkins SM, Reich A, Fleming LE. Neurotoxic shellfish poisoning. *Marine Drugs*. **2008**, 6:431-455

136. Ramsdell JS. The molecular and integrative basis to brevetoxin toxicity. In: Botana LM (ed.), *Seafood and Freshwater Toxins: Pharmacology, Physiology, and Detection*. Boca Raton, USA: CRC Press. **2008**

137. Hu T, Curtis JM, Walter JA, Wright JLC. Characterization of biologically inactive spirolides E and F: identification of the spirolide pharmacophore. *Tetrahedron Letters*. **1996**, 37:7671-7674

138. Cembella A, Krock B. Cyclic imine toxins: chemistry, biogeography, biosynthesis and pharmacology. In: Botana LM (ed.), *Seafood and Freshwater toxins: Pharmacology, Physiology and Detection*. Boca Raton, Fl, USA: CRC Press **2008**

139. Molgo J, Girard B, Benoit E, Cyclic imines: An insight into this emerging group of bioactive marine toxins, in: L., B. (Ed.), *Phycotoxins, Chemistry and Biochemistry.* Blackwell Publishing, Oxford, **2007**:319-335

140. McCarron P, Rourke WA, Hardstaff W, Pooley B, Quilliam MA. Identification of Pinnatoxins and Discovery of Their Fatty Acid Ester Metabolites in Mussels (*Mytilus edulis*) from Eastern Canada. *Journal of agricultural and food chemistry*. **2012**, 60:1437-1446.

141. Hu TM, Curtis JM, Oshima Y, Quilliam MA, Walter JA, Watsonwright WM, Wright, JLC Spirolide-B and spirolide-D, 2 novel macrocycles isolated from the digestive glands of shellfish. *Journal of the Chemical Society, Chemical Communications*. **1995**, 2159–2161

142. Kharrat R, Servent D, Girard E, Ouanounou G, Amar M, Marrouchi R, Benoit E, Molgò J. The marine phycotoxin gymnodimine targets muscular and neuronal nicotinic acetylcholine receptor subtypes with high affinity. *Journal of Neurochemistry*. **2008**, 107:952–963

143. Bourne Y, Radic Z, Aràoz R, Talley TT, Benoit E, Servent D, Taylor P, Molgò J, Marchot P. Structural determinants in phycotoxins and AChBP conferring high affinity binding and nicotinic AChR antagonism. *Proceedings of the National Academy of Sciences U.S.A*. **2010**, 107:6076–6081

144. Wandscheer CB, Vilarinífo N, Espinífa B, Louzao MC, Botana LM Human muscarinic acetylcholine receptors are a target of the marine toxin 13-desmethyl C spirolide. *Chemical Research in Toxicology*. **2010**, 23:1753–1761

145. Cembella AD, Lewis NI, Quilliam MA. The marine dinoflagellate *Alexandrium ostenfeldii* (Dinophyceae) as the causative organism of spirolide shellfish toxins. *Phycologia*. **2000**, 39:67-74

146. Seki T, Satake M, Mackenzie L, Kaspar HF, Yasumoto T. Gymnodimine, a new marine toxin of unprecedented structure isolated from New-Zealand oysters and the dinoflagellate, *Gymnodinium* sp. *Tetrahedron Letters*. **1995**, 36:7093-7096

147. Torigoe K, Murata M, Yasumoto T, Iwashita T. Prorocentrolide, a toxic nitrogenous macrocycle from a marine dinoflagellate, *Prorocentrum lima. Journal of the American Chemical Society*. **1988**, 110:7876-7877

148. Cembella AD, Lewis NI, Quilliam MA. Spirolide composition of micro-extracted pooled cells isolated from natural plankton assemblages and from cultures of the dinoflagellate *Alexandrium ostenfeldii. Natural Toxins.* **1999**, 7:197-206

149. Cembella AD, Bauder AG, Lewis NI, Quilliam MA. Association of the gonyaulacoid dinoflagellate *Alexandrium ostenfeldii* with spirolide toxins in size fractionated plankton. *Journal of Plankton Research*. **2001**, 23:1413-1419

150. Mackenzie L, White D, Oshima Y, Kapa J, The resting cyst and toxicity of *Alexandrium ostenfeldii* (Dinophyceae) in New Zealand. *Phycologia*. **1996**, 35(2):148-155

151. MacKenzie L, Holland P, McNabb P, Beuzenberg V, Selwood A, Suzuki T. Complex toxin profiles in phytoplankton and Greenshell mussels (*Perna canaliculus*), revealed by LC-MS/MS analysis. *Toxicon : official journal of the International Society on Toxinology.* **2002,** 40:1321-1330

152. Zheng SZ, Huang FL, Chen SC, Tan XF, Zuo JB, Peng J, Xie RW. The isolation and bioactivities of pinnatoxin (in Chinese). *Chinese Journal of Marine Drugs.* **1990**, 33:33–35

153. Chou T, Haino T, Kuramoto M, Uemura D. Isolation and structure of pinnatoxin D, a new shellfish poison from the Okinawan bivalve *Pinna muricata*. *Tetrahedron Letters.* **1996,** 37:4027-4030

154. Selwood AI, Miles CO, Wilkins AL, van Ginkel R, Munday R, Rise F, McNabb P. Isolation, structural determination and acute toxicity of pinnatoxins E, Fand G. *Journal of agricultural and food chemistry*. **2010**, 58:6532-6542

155. Nezan E, Chomerat N. *Vulcanodinium rugosum* gen. nov., sp. nov. (Dinophyceae): a new marine dinoflagellate from the French Mediterranean coast. *Cryptogamie Algologie.* **2011**, 32:3-18

156. Yasumoto T, Nakajima I, Bagnis R, Adachi R. Finding of a dinoflagellate as a likely culprit of ciguatera. *Bulletin of the Japanese Society for the Science of Fish*. **1977,** 43:1021-1026

157. Adachi R, Fukuyo Y. The thecal structure of a toxic marine dinoflagellate *Gambierdiscus toxicus* gen. et spec. nov. collected in a ciguatera-endemic area. *Bulletin of the Japanese Society for the Science of Fish*. **1979,** 45:67-71

158. Faust MA. Observation of sand-dwelling toxic dinoflagellates (Dinophyceae) from widely differing sites, including two new species. *Journal of Phycology*. **1995,** 31:996–1003

159. Holmes MJ. *Gambierdiscus yasumotoi* sp. nov. (Dinophyceae), a toxic benthic dinoflagellate from southeastern Asia. *Journal of Phycology*. **1998,** 34:661–668

160. Chinain M, Faust MA, Pauillac S. Morphology and molecular analyses of three toxic species of *Gambierdiscus* (Dinophyceae): *G. pacificus*, sp. nov., *G. australes*, sp. nov., and *G. polynesiensis*, sp. Nov. *Journal of Phycology.* **1999,** 35:1282–1296

161. FDA **2011**. Fish and Fishery Products Hazards and Controls Guidance http://www.fda.gov/downloads/food/guidance complianceregulatoryinformation/guidancedocuments/seafood/ucm251970.pdf

162. Aligizaki K, Nikolaidis G. Morphological identification of two tropical dinoflagellates of the genera *Gambierdiscus* and *Dinophysis* in the Mediterranean Sea. *Journal of Biological Research-Thessaloniki*. **2008**, 9:75-82

163. Lu XZ, Deckey R, Jiao G, Ren HF, Li M. Caribbean maitotoxin elevates [Ca($^{2+}$)]i and activates non-selective cation channels in HIT-T 15 cells. *World Journal of Diabetes*. **2013**, 4:70-75

164. Terao K. Ciguatera toxins: toxicology In: Botana LM (ed.), *Seafood and Freshwater Toxins: Pharmacology, Physiology and Detection.* **2000** New York, USA: Marcel Dekker

165. Lehane L, Lewis RJ Ciguatera: recent advances but the risk remains. *International Journal of Food Microbiology*. **2000**, 61:91-125

166. Naoki H, Fujita T, Cruchet P. Structural determination of new ciguatoxin congeners by tandem mass spectrometry. *International IUPAC Symposium on Mycotoxins and Phycotoxins.* Wageningen, the Netherlands. Ponsen & Looyen, **2001**, 475-482

167. Yasumoto T, Bagnis R, Vernoux JP. Toxicity of surgeonfishes-II. Properties of the principal water soluble toxin. *Bulletin of the Japanese Society for the Science of Fish*. **1996**, 42:359-365

168. Holmes MJ, Lewis, RJ Purification characterization of large and small maitotoxins from cultured *Gambierdiscus toxicus*. *Natural Toxins*. **1994**, 2:64–72

169. Murata M, Naoki H, Iwashita T, Matsunaga S, Sasaki M, Yokoyama A, Yasumoto T. Structure of Maitotoxins. *Journal of American Chemical Society*. **1993**, 115:2060-2062

170. Wang DZ. Neurotoxins from marine dinoflagellates: A brief review. *Marine Drugs*. **2008**, 6(2):349-371

171. Moore RE, Scheuer PJ. Palytoxin: a new marine toxin from a Coelenterate. *Sci.* (Washington, D.C.) **1971**, 172:495–498

172. Malo D. *Hawaiian Antiquites*, second ed. Bishop Museum Publication, Honolulu, USA. **1951**, 201–226

173. Walsh GE, Bowers RE. A review of Hawaiian zoanthids with description of three new species. *Zoological Journal of the Linnean Society*. **1971**, 50:161–180

174. Kimura S, Hashimoto Y, Yamazato. Toxicity of the zoanthid *Palythoa tuberculosa. Toxicon*. **1972**, 10: 611-612

175. Quinn RJ, Kashiwagi M, Moore RE, Norton TR. Anticancer activity of zoanthids and the associated toxin, palytoxin, against Ehrilich ascites tumor and P-388 lumphocytic leukemia in mice. *Journal of Pharmaceutical Sciences*. **1974**, 63: 257-260

176. Attaway DH Ciereszko LS. Isolation and partial characterization of Caribbean palytoxin. *Proceedings of the 2nd International Symposium for Coral Reefs I, Great Barrier Reef Community*, Brisbane. **1974**, 497-504

177. Béress L, Zwick J, Kolkenbrock HJ, Kaul PN, Wassermann O. A method for the isolation of the Caribbean palytoxin (C-PTX) from the coelenterate (Zoanthid) *Palythoa caribaeorum*. *Toxicon*. **1983**, 2:285-290

178. Moore RE, Bartolini G. Structure of Palytoxin. *Journal of American Chemical Society*. **1981**, 103:2491-2494

179. Moore RE, Woolard FX, Bartolini G. Periodate oxidation of N-(p-bromobenzoyl) palytoxin. *Journal of American Chemical Society*. **1980**, 102:7370-7372

180. Uemura D, Hirata Y, Iwashita T, Naoki H. Studies on palytoxins. *Tetrahedron.* **1985**, 41:1007-1017

181. Oku N, Sata NU, Matsunaga S, Uchida H, Fusetani N. Identification of palytoxin as a principle which causes morphological changes in rat 3Y1 cells in the zoanthid *Palythoa* aff. *margaritae*. *Toxicon*. **2004**, 43(1):21-25

182. Gleibs S, Mebs D, Werding B Studies on the origin and distribution of palytoxin in a Caribbean coral reef. *Toxicon*. **1995**, 33:531-1537

183. Moore RE, Helfrich P, Patterson GML. The deadly seaweed of Hana. *Oceanus*. **1982**, 25:54–63

184. Maeda M, Kodama T, Tanaka T, Yoshizumi H, Nomoto K, Takemoto T Fujiki T. Structure of insecticidal substances isolated from a red alga, *Chondria armata*. *Symposium Papers, 27th Symposium on the Chemistry of Natural Products*, Hiroshima, Japan. **1985**:616–623

185. Yasumoto T, Yasumura D, Ohizumi Y, Takahashi M, Alcala AC, Alcala LC. Palytoxin in two species of xanthid crab from the Philippines. *Agricultural and Biological Chemistry*. **1986**, 50:163-167

186. Fukui M, Murata M, Inoue A, Gawel M, Yasumoto T. Occurrence of palytoxin in the trigger fish *Melichtys vidua*. *Toxicon*. **1987**, 25:1121–1124

187. Halstead BW. The microbial biogenesis of aquatic biotoxins. *Toxicology Mechanisms and Methods*. **2002**, 12(2): 135-153

188. Usami M, Satake M, Ishida S, Inoue A, Kan Y, Yasumoto T. Palytoxin analogs from the dinoflagellate *Ostreopsis siamensis*. *Journal of American Chemical Society*. **1995**, 117:5389-5390

189. Taniyama S, Arakawa O, Terada M, Nishio S, Takatani T, Mahmud Y, Noguchi T. *Ostreopsis* sp., a possible origin of palytoxin (PTX) in parrotfish *Scarus ovifrons*. *Toxicon*. **2003**, 42:29–33

190. Lenoir S, Ten-Hage L, Quod JP, Bernard C, Hennion MC. First evidence of palytoxin analogues from an *Ostreopsis mascarenensis* (Dinophyceae) benthic bloom in southwestern Indian. *Ocean Journal of Phycology*. **2004**, 40:1042–1051

191. Lenoir S, Ten-Hage L, Quod JP, Hennion MC. Characterization of new analogues of palytoxin isolated from an *Ostreopsis mascarenensis* bloom in the south-west Indian Ocean. *African Journal of Marine Science*. **2006**, 28:389–391

192. Ciminiello P, Dell'Aversano C, Fattorusso E, Forino M, Tartaglione L, Grillo C, Melchiorre N. Putative palytoxin and its new analogue, ovatoxin-a, in *Ostreopsis ovata* collected along the Ligurian coasts during the 2006 toxic outbreak. *Journal of The American Society for Mass Spectrometry*. **2008**, 19, 111-120

193. Ciminiello P, Dell'Aversano C, Dello Iacovo E, Fattorusso E, Forino M, Grauso L, Tartaglione L, Guerrini F, Pistocchi R Complex palytoxin-like profile of *Ostreopsis ovata.* Identification of four new ovatoxins by high-resolution liquid chromatography/mass spectrometry. *Rapid Communications in Mass Spectrometry*. **2010**, 24:2735-2744

194. Onuma Y, Satake M, Ukena T, Roux J, Chanteau S, Rasolofonirina N, Ratsimaloto M, Naoki H, Yasumoto T. Identification of putative palytoxin as the cause of clupeotoxism. *Toxicon*. *1999*, 37:55–65

195. Katikou P. *Palytoxin and Analogs: Ecobiology and Origin, Chemistry, Metabolism, and Chemical Analysis.* In: Botana LM [ed.] Seafood and Freshwater Toxins: Pharmacology, Physiology, and Detection. 2nd ed. CRC Press/Taylor & Francis Group; Boca Raton, FL, USA **2008**:631–663

196. Kerbrat AS, Amzil Z, Pawlowiez R, Golubic S, Sibat M, Darius HT, Chinain M, Laurent. First evidence of palytoxin and 42-hydroxy-palytoxin in the marine cyanobacterium *Trichodesmiu. Marine Drugs*. **2011**, 9:543-560

197. Katikou P, Vlamis A. *Palytoxin and analogs: Ecobiology and origin, chemistry and chemical analysis.* In: Seafood and freshwater toxins: Pharmacology, physiology, and detection. Edited by Botana LM, Third edn: CRC Press, Taylor & Francis group; **2014**

198. Armstrong RW, Beau JM, Cheon SH, Christ WJ, Fujioka H, Ham WH, Hawkins LD, Jin H, Kang SH, Kishi Y, Martinelli MJ, McWhorter Jr WW, Mizuno M, Nakata M, Stutz AE, Talamas FX, Taniguchi M, Tino JA, Ueda K, Uenishi J, White JB, Yonaga M. Total synthesis of palytoxin carboxylic acid and palytoxin amide. *Journal of American Chemical Society.* **1989**, 111:7530-7533

199. Uemura D, Ueda K, Hirata Y, Naoki H, Iwashita T. Further studies on palytoxin. *Tetrahedron Letters*. **1981**, 21:1909-1912

200. Klein LL, McWhorter WW Jr, Ko SS, Pfaff KP, Kishi Y, Uemura D, Hirata Y. Stereochemistry of palytoxin. Part 1. C85-C115 segment. *Journal of American Chemical Society.* **1982**, 104:7362-7364

201. Ko SS, Finan JM, Yonaga M, Kishi Y, Uemura D, Hirata Y. Stereochemistry of palytoxin. Part 2. C1-C6, C47-C74, and C77-C83 segments. *Journal of American Chemical Society*. **1982**, 104:7364- 7367

202. Fujioka H, Christ WJ, Cha JK, Leder J, Kishi Y, Uemura D, Hirata Y. Stereochemistry of Palytoxin. Part 3. C7-C51 segment. *Journal of American Chemical Society.* **1982**, 104: 7367- 7369

203. Cha JK, Christ WJ, Finan JM, Fujioka H, Kishi Y, Klein LL, Ko SS, Leder J, McWhorter Jr WW, Pfaff KP, Yonaga M, Uemura D, Hirata Y. Stereochemistry of palytoxin. Part 4. Complete Structure. *Journal of American Chemical Society.* **1982**, 104:7369-7371

204. Moore RE, Bartolini G, Barchi J, Bothner-By AA, Dadok J, Ford J. Absolute stereochemistry of palytoxin. *Journal of American Chemical Society*. **1982**, 104: 3776-3779

205. Ciminiello P, Dell'Aversano C, Dello Iacovo E, Fattorusso E, Forino M, Grauso, L, Tartaglione L. High resolution LC-MSn fragmentation pattern of palytoxin as template to gain new insights into ovatoxin-a structure. The key role of calcium in MS behavior of palytoxins. *Journal of The American Society for Mass Spectrometry*. **2012**, 23:952-963

206. Uchida H, Taira Y, Yasumoto T. Structural elucidation of palytoxin analogs produced by the dinoflagellate *Ostreopsis ovata* IK2 strain by complementary use of positive and negative ion liquid chromatography/quadrupole time-of-flight mass spectrometry. *Rapid Communications in Mass Spectrometry*. **2013**, 27:1999-2008

207. Raybould TJG. Toxin production and immunoassay development Palytoxin (Annual/Final report, Hawaii). DTIC Accession Number: ADA239837. U.S. Army Medical Research and Development Command, Fort Detrick, Frederick, Maryland. **1991**, 21702-5012

208. Ciminiello P, Dell'Aversano C, Dello Iacovo E, Fattorusso E, Forino M, Grauso L, Tartaglione L, Florio C, Lorenzon P, De Bortoli M, Tubaro A, Poli M, Bignami G. Stereostructure and biological activity of 42-hydroxy-palytoxin: a new palytoxin analogue from Hawaiian *Palythoa* subspecies. *Chemical Research in Toxicology*. **2009**, 22, 1851-1859

209. Ciminiello P, Dell'Aversano C, Dello Iacovo E, Forino M, Randazzo A, Tartaglione L Identification of palytoxin-Ca^{2+} complex by NMR and Molecular Modeling Techniques. *Journal of Organic Chemistry*. **2014**, 79:72-79

210. Schmidt J Flora of Koh Chang. Contributions to the knowledge of the vegetation in the Gulf of Siam. Peridiniales. *Botanisk Tidsskrift*. **1901**, 24:212-221

211. Fukuyo Y. Taxonomical study on benthic dinoflagellates collected in coral reefs. *Bulletin of the Japanese Society of Scientific Fisheries*. **1981**, 47(8):967-978

212. Ciminiello P, Dell'Aversano C, Fattorusso E, Forino M, Magno GS, Tartaglione L, Grillo C, Melchiorre N. The Genoa 2005 outbreak. Determination of putative palytoxin in Mediterranean *Ostreopsis ovata* by a new liquid chromatography tandem mass spectrometry method. *Analytical Chemistry*. **2006**, 78:6153–6159

213. Tindall DR, Miller DM, Tindall PM. Toxicity of *Ostreopsis lenticularis* from the British and United States Virgin Islands. In: Toxic *Marine Phytoplankton*. (eds E. Graneli, B. Sundström, L. Edler, and D.M. Anderson) **1990**, 424-429. Elsevier, New York

214. Norris DR, Bomber JW, Balech E. Benthic dinoflagellates associated with ciguatera from the Florida Keys. *Ostreopsis heptagona* sp. nov. In: *Toxic Dinoflagellates*. (eds D.M. White, and Baden D.G.) **1985**, 39-44. Elsevier Scientific, New York

215. Faust MA. Three new *Ostreopsis species* (Dinophyceae): *O-marinus* sp nov., *O-belizeanus* sp nov., and *O-carribeanus* sp nov. *Phycologia.* **1999**, 38(2):92-99

216. Ukena T, Satake M, Usami M, Oshima Y, Naoki H, Fujita T, Kan Y, Yasumot T. Structure elucidation of ostreocin D, a palytoxin analog isolated from the dinoflagellate *Ostreopsis siamensis*. *Bioscience, Biotechnology, and Biochemistry*. **2001**, 65:2585-2588

217. Ukena T, Satake M, Usami M, Oshima Y, Fujita T, Naoki H, Yasumoto T. Structural confirmation of ostreocin-D by application of negative-ion fast-atom bombardment collision-induced dissociation tandem mass spectrometric methods. *Rapid Communications in Mass Spectrometry.* **2002**, 16:2387-2393

218. Ukena T. Chemical studies on ostreocins, palytoxin analogs, isolated from the dinoflagellate Ostreopsis siamensis. *Ph.D. Thesis*, Graduate School of Life Sciences, Tohoku University. **2001**

219. Ciminiello P, Dell'Aversano C, Dello Iacovo E, Fattorusso E, Forino M, Tartaglione L, Yasumoto T, Battocchi C, Giacobbe M, Amorim A, Penna A. Investigation of toxin profile of Mediterranean and Atlantic strains of *Ostreopsis* cf. *siamensis* (Dinophyceae) by liquid chromatography–high resolution mass spectrometry. *Harmful Algae*. **2013**, 23:19–27

220. Rossi R, Castellano V, Scalco E, Serpe L, Zingone A, Soprano V. New palytoxin-like molecule in Mediterranean *Ostreopsis* cf. *ovata* (dinoflagellates) and in *Palythoa tuberculosa* detected by liquid chromatography-electrospray ionization time-of-flight mass spectrometry. *Toxicon*. **2010**, 56:1381-1387

221. Penna A, Vila M, Fraga S, Giacobbe MG, Andreoni F, Riobó P, Vernesi C. Characterization of *Ostreopsis* and *Coolia* (Dinophyceae) isolates in the western Mediterranean Sea based on morphology, toxicity and internal transcribed spacer 5.8S rDNA sequences. *Journal of Phycology*. **2005**, 41:212–245

222. Tognetto L, Bellato S, Moro I, Andreoli C. Occurrence of *Ostreopsis ovata* (Dinophyceae) in the Tyrrhenian Sea during summer 1994. ***Botanica Marina***. **1995**, 38:291–295

223. Sansoni G, Borghini B, Camici G, Casotti M, Righini P, Rustighi C. Fioriture algali di *Ostreopsis ovata* (Gonyaulacales: Dinophyceae): Un problema emergente. *Biologia Ambientale*. **2003**, 17:17-23.

224. Ciminiello P, Dell'Aversano C, Dello Iacovo E, Fattorusso E, Forino M, Grauso L, Tartaglione L, Guerrini F, Pezzolesi L, Pistocchi R, Vanucci S. Isolation and structure elucidation of ovatoxin-a, the major toxin produced by *Ostreopsis ovata*. *Journal of The American Chemical Society*. **2012**, 134:1869-1875

225. Ciminiello P, Dell'Aversano C, Dello Iacovo E, Fattorusso E, Forino M, Grauso L, Tartaglione L. Stereochemical studies on ovatoxin-a. *Chemistry - A European Journal*. **2012**, 18:16836-16843

226. Ciminiello P, Dell'Aversano C, Dello Iacovo E, Fattorusso E, Forino M, Tartaglione L, Battocchi C, Crinelli R, Carloni E, Magnani M, Penna A. Unique toxin profile of a Mediterranean *Ostreopsis* cf. *ovata* strain: HR LC-MSn characterization of ovatoxin-f, a new palytoxin congener. *Chemical Research in Toxicology*. **2012**, 25:1243-1252

227. García-Altares M, Tartaglione L, Dell'Aversano C, Carnicer O, de la Iglesia P, Forino M, Diogène J, Ciminiello P The novel ovatoxin-g and isobaric palytoxin (so far referred to as putative palytoxin) from *Ostreopsis* cf. *ovata* (NW Mediterranean Sea): structural insights by LC-high resolution MSn. *Analytical and Bioanalytical Chemistry*. **2015**, 407:1191-1204

228. Brissard C, Hervé F, Sibat M, Séchet V, Hess P, Amzil Z, Herrenknecht C. Characterization of ovatoxin-h, a new ovatoxin analog, and evaluation of chromatographic columns for ovatoxin analysis and purification. *Journal of Chromatography A*. **2015**, 3(1388):87-101

229. Jonathan R, Deeds JR, Michael D, Schwartz B. Human risk associated with palytoxin exposure. *Toxicon*. **2010**, 56(2):150–162

230. Aligizaki K, Katikou P, Milandri A, Diogene J. Occurrence of palytoxin-group toxins in seafood and future strategies to complement the present state of the art. *Toxicon.* **2011**, 57(3):390-399

231. Alcala AC, Alcala LC, Garth JS, Yasumura D, Yasumoto T. Human fatality due to ingestion of the crab *Demania-reynaudii* that contained a palytoxin-like toxin. *Toxicon*. **1988**, 26(1):105-107

232. Noguchi T, Hwang DF, Arakawa O, Daigo K, Sato S, Ozaki H, Kawai N, Ito M, Hashimoto K. Palytoxin as the causative agent in parrotfish poisonning In: First Asia-Pacific Congress: 1988; Sydney: *Toxicon*. **1988**: 34-34

233. Habermann E. Palytoxin acts through Na^+, K^+-ATPase. *Toxicon*. **1989**, 27(11):1171-1187

234. Vale C. *Palytoxins: pharmacology and biological detection methods*. In: Botana LM. (ed.) Seafood and freshwater toxins, Pharmacology, Physiology, and detection. CRC press, Boca Raton, FL. 2014:675-691

235. Wattenberg EV. Palytoxin: Exploiting a novel skin tumor promoter to explore signal transduction and carcinogenesis. *American Journal of Physiology-Cell Physiology.* **2007**, 292 (1):C24–C32

236. Wattenberg EV, Uemura D, Byron KL, Villereal ML, Fujiki H, Rosner MR. Structure-activity studies of the nonphorbol tumor promoter palytoxin in Swiss 3T3 cells. *Cancer Research*. **1989**, 49(21):5837-42

237. Fujiki H, Suganuma M, Nakayasu M, Hakii H, Horiuchi T, Takayama S, Sugimura T. Palytoxin is a non-12-O-tetradecanoylphorbol-13-acetate type tumor promoter in two-stage mouse skin carcinogenesis. *Carcinogenesis*. **1986**, 7(5):707-10

238. Ito E, Yasumoto T. Toxicological studies on palytoxin and ostreocin-D administered to mice by three different routes. *Toxicon*. **2009**, 54(3):244-251

239. Wiles JS, Vick JA, Christensen MK. Toxicological evaluation of palytoxin in several animal species. *Toxicon : official journal of the International Society on Toxinology*. **1974**, 12(4):427-433

240. Vick JA, Wiles JS. Mechanisms of action and treatment of palytoxin poisoning. *Toxicology and Applied Pharmacology*. **1975**, 34(2):214-223

241. Ciminiello P, Dell'Aversano C, Dello Iacovo E, Forino M, Tartaglione L, Pelin M, Sosa S, Tubaro A, Chaloin O, Poli M, Bignami G. Stereoisomers of 42-Hydroxy Palytoxin from Hawaiian *Palythoa toxica* and *P. tuberculosa*: Stereostructure Elucidation, Detection and Biological Activities. *Journal of Natural Products.* **2014**, 77(2):351-357

242. Del Favero G, Sosa S, Poli M, Tubaro A, Sbaizero O, Lorenzon P. In vivo and in vitro effects of 42-hydroxy-palytoxin on mouse skeletal muscle: Structural and functional impairment. *Toxicology Letters*. **2014**, 225:285-293

243. Pelin M, Boscolo S, Poli M, Sosa S, Tubaro A, Florio C. Characterization of palytoxin binding to HaCaT cells using a monoclonal anti-palytoxin antibody. *Marine Drugs*. **2013**, 11:584-598

244. Crinelli R, Carloni E, Giacomini E, Penna A, Dominici S, Battocchi C, Ciminiello P, Dell'Aversano C, Fattorusso E, Forino M, Tartaglione L, Magnani M. Palytoxin and an *Ostreopsis* toxin extract increase the levels of mRNAs encoding inflammation-related proteins in human macrophages via p38 MAPK and NF-κB. PLoS One 2012, 7 (6), e38139

245. EFSA Journal. Scientific Opinion on marine biotoxins in shellfish – Palytoxin group. *The EFSA Journal*. **2009**; 7(12):1393-1433

246. Riobó P, Paz B, Franco JM, Vazquez JA, Murado MA, Cacho E. Mouse bioassay for palytoxin. Specific symptoms and dose-response against dose-death time relationships. *Food Chemical Toxicology*. **2008**, 46:2639-2647

247. Munday R Palytoxin toxicology: Animal studies. Toxicon. 2011 57(3):470-477

248. Habermann E, Ahnert-Hilger G, Chatwal GS, Beress L. Delayed hemolytic action of palytoxin. General characteristics. *Biochimica et Biophysica Acta*. **1981**, 649:481-486

249. Bignami GS. A rapid and sensitive hemolysis neutralization assay for palytoxin. *Toxicon*. **1993**, 31:817-820

250. Taniyama S, Mahmud Y, Tanu MB, Takatani T, Arakawa O, Noguchi T. Delayed hemolytic activity by the freshwater puffer Tetraodon sp. toxin. *Toxicon*. **2000**, 39(5): 725-727

251. Taniyama S, Arakawa O, Terada M, Nishio S, Takatani T, Mahmud Y, Noguchi T. *Ostreopsis* sp., a possible origin of palytoxin (PTX) in parrotfish *Scarus ovifrons*. *Toxicon*. **2003**, 42:29–33

252. Riobó P, Paz B, Franco JM Analysis of palytoxin-like in *Ostreopsis* cultures by liquid chromatography with precolumn derivatization and fluorescence detection. *Analytica Chimica Acta.* **2006**, 566:217-223

253. Aligizaki K, Katikou P, Nikolaidis G, Panou A. First episode of shellfish contamination by palytoxin-like compounds from *Ostreopsis* species (Aegean Sea, Greece). *Toxicon*. **2008**, 51:418-427

245. Bellocci M, Ronzitti G, Milandri A, Melchiorre N, Grillo C, Poletti R, Yasumoto T, Rossini GP. A cytolytic assay for the measurement of palytoxin based on a cultured monolayer cell line. *Analytical Biochemistry.* **2008**, 374:48-55

255. Bellocci M, G. Ronzitti, A. Milandri, N. Melchiorre, C. Grillo, R. Poletti, T. Yasumoto, Rossini GP. Addendum to "A cytolytic assay for the measurement of palytoxin based on a cultured monolayer cell line". *Analytical Biochemistry*. **2008**, 381: 178

256. Lau CO, Tan CH, Li QT, Ng FH, Yuen R, Khoo HE. Bioactivity and mechanism of action of *Lophozozymus pictor* toxin. *Toxicon*. **1995**, 33(7):901-908

257. Cañete E, Diogène J. Comparative study of the use of neuroblastoma cells (Neuro-2a) and neuroblastoma x glioma hybrid cells (NG108-15) for the toxic effect quantification of marine toxins. *Toxicon*. **2008**, 52(4):541-550

258. Espina B, Cagide E, Louzao MC, Fernandez MM, Vieytes MR, Katikou P, Villar A, Jaen D, Maman L, Botana LM. Specific and dynamic detection of palytoxins by in vitro microplate assay with human neuroblastoma cells. *Bioscience Reports*. **2009**, 29:13-23

259. Ledreux A, Krys S, Bernard C. Suitability of the Neuro-2a cell line for the detection of palytoxin and analogues (neurotoxic phycotoxins). *Toxicon*. **2009**, 53:300-308

260. Levine L, Fujiki H, Gjika HB, Vanvunakis H. A radioimmunoassay for palytoxin. *Toxicon*. **1988**, 26(12):1115-1121

261. Bignami GS, Raybould TJG, Sachinvala ND, Grothaus PG, Simpson SB, Lazo CB, Byrnes JB, Moore RE, Vann DC. Monoclonal antibody based enzyme linked immunoassays for the measurement of palytoxin biological samples. *Toxicon*. **1992**, 30(7):687-700

262. Garet E, Cabado AG, Vieites JM, Gonzalez-Fernandez A. Rapid isolation of single-chain antibodies by phage display technology directed against one of the most potent marine toxins: Palytoxin. *Toxicon*. **2010**, 55(8):1519-1526

263. Yakes BJ, De Grasse SL, Poli M, Deeds JR. Antibody characterization and immunoassays for palytoxin using an SPR biosensor. *Analytical and Bioanalytical Chemistry*. **2011**, 400(9):2865-2869

264. MacKenzie L, Beuzenberg V, Holland P, McNabb P, Selwood A. Solid phase adsorption toxin tracking (SPATT): a new monitoring tool that simulates the biotoxins contamination of filter feeding bivalves. *Toxicon : official journal of the International Society on Toxinology*. **2004**, 44:901-918

265. Greenwood R, Mills G, Vrana B. Wilson and Wilson's comprehensive analytical chemistry (Eds.), *Passive Sampling Techniques in Environmental Monitoring*, Elsevier **2007**, 48:486

266. Boehm PD, Page DS, Brown JS, Neff JM, Bence AE. Comparison of mussels and semi-permeable membrane devices as inter-tidal monitors of polycyclic aromatic hydrocarbons at oil spill sites. *Marine Pollution Bulletin*. **2005**, 50:740–750

267. Alvarez DA, Petty JD, Huckins JN, Jones-Lepp TL, Getting DC, Goddard JP, Manahan SE. Development of a passive, in situ, integrative sampler for hydrophilic organic contaminants in aquatic environments. *Environmental Toxicology and Chemistry*. **2004**, 23:1640–164

268. Bueno MJM, Hernando MD, Aguera A, Fernandez-Alba AR. Application of passive sampling devices for screening of micro-pollutants in marine aquaculture using LC–MS/MS. *Talanta*. **2009**, 77:1518–1527

269. MacKenzie L. In situ passive solid-phase adsorption of micro-algal biotoxins as a monitoring tool Current Opinion in Biotechnology. *Energy biotechnology – Environmental biotechnology*. **2010**, 21(3): 326–331

270. Rundberget T, Gustad E, Samdal IA, Sandvik M, Miles CO. A convenient and cost-effective method for monitoring marine algal toxins with passive samplers. *Toxicon*. **2009**; 53(5):543–550

271. Lefebvre KA, Bill BD, Erickson A, Baugh KA, O'Rouke L, Costa PR, Nance S, Trainer VL. Characterization of intracellular and extracellular saxitoxin levels in both field and cultured *Alexandrium* spp. Samples from Sequim Bay, Washington. *Marine Drugs*. **2008**, 6:103–116

272. Bates SS, Garrison DL, Horner RA. Bloom dynamics and physiology of domoic acid producing *Pseudo-nitzschia* species Anderson DM, Cembella AD, Hallegraeff GM (Eds.), *Physiological Ecology of Harmful Algal Blooms*, Springer-Verlag, Heidelberg. **1998**:267–292

273. Turrel E. Evaluations and method development of solid-phase adsorbents for phycotoxins in the marine environment. In: *Report of the ICES-IOC working group on harmful algal Bloom dynamics*. ICES CN 2008/OCC:03 **2008**, section 7.1.9 :23–24

274. Lane JQ, Roddam CM, Langlois GW, Kudela RM. Application of Solid Phase Adsorption Toxin Tracking (SPATT) for field detection of the hydrophilic phycotoxins domoic acid and saxitoxin in coastal California. *Limnology and Oceanography-Methods*. **2010**, 8:645-660

275. Fux E, Bire R, Hess P. Comparative accumulation and composition of lipophilic marine biotoxins in passive samplers and in mussels (*M. edulis*) on the West Coast of Ireland. *Harmful Algae*. **2009**, 8(3):523–537

276. Fux E, Rode D, Bire R, Hess P. Approaches to the evaluation of matrix effects in the liquid chromatography–mass spectrometry (LC–MS) analysis of three regulated lipophilic toxin groups in mussel matrix (*Mytilus edulis*). *Food Additives & Contaminants*. **2008**, 25.1024–1032

277. Garnett CM, Rafuse CM, Lewis NI, Kirchhoff S, Cullen J, Quilliam MA. Monitroing of lipophilic shellfish toxins using SPATT (solid-phase adsorption toxin tracking) in Nova Scotia, Canada. *Abstract O.19-02 of the 12th International Conference on Harmful Algae*, Copenhagen, Denmark, 4–8 September **2006**:72

278. MacKenzie L, Selwood A, McNabb P, Rhodes L, Boundy M. Dinoflagellate toxins in sea-grass mangrove habitats of a warm-temperate estuary: Rangaunu Harbour, Northland, New Zealand. *Harmful Algae*. **2011**, 10(6):559-566

279. Fux E, McMillan D, Bire R, Hess P. Development of an ultra-performance liquid chromatography-mass spectrometry method for the detection of lipophilic marine toxins. *Journal of chromatography A*. **2007**, 1157:273-280

280. Fux E, Marcaillou C, Mondeguer F, Bire R, Hess P. Field and mesocosm trials on passive sampling for the study of adsorption and desorption behaviour of lipophilic toxins with a focus on OA and DTX1. *Harmful Algae*. **2008**, 7:574–583

281. Marcaillou C, Mondeguer F, Berard JB, Goupil A. Testing of a passive adsorption device in the detection of DTXs under controlled conditions. *Abstract PO.05-07 of the 12th International Conference on Harmful Algae*, Copenhagen, Denmark, 4–8 September **2006**:232

282. Li Z, Mengmeng G, Shouguo Y, Qingyin W, Zhijun T. Investigation of pectenotoxin profiles in the Yellow Sea (China) using a passive sampling technique. *Marine drugs*. *2010*, 8:1263-1272.

283. McCarthy M, van Pelt FNAM, Bane V, O'Halloran J, Furey A. Application of passive (SPATT) and active sampling methods in the profiling and monitoring of marine biotoxins. *Toxicon : official journal of the International Society on Toxinology*. **2014**, 89:77-86

284. Pizarro G, Morono A, Paz B, Franco JM, Pazos Y, Reguera B. Evaluation of passive samplers as a monitoring tool for early warning of dinophysis toxins in shellfish. *Marine drugs*. **2013**, 11:3823-3845

285. Pizarro G, Paz B, Franco JM, Suzuki T, Reguera B. First detection of Pectenotoxin-11 and confirmation of OA-D8 diol-ester in *Dinophysis acuta* from European waters by LC-MS/MS. *Toxicon : official journal of the International Society on Toxinology*. **2008**, 52:889-896

286. Faust MA. Morphological details of 6 benthic species of Prorocentrum (Pyrrophyta) from a mangrove island, twin cays, Belize, including 2 new species. *Journal of Phycology*. **1990**, 26:548-558

287. Besada EG, Loeblich LA, Loeblich AR. Observations on tropical, benthic dinoflagellates from ciguatera-endemic areas - *Coolia, Gambierdiscus*, and *Ostreopsis. Bulletin of Marine Science*. **1982**, 32:723-735

286. Caillaud CA, de la Iglesia P, Barber E, Eixarch H, Mohammad-Noor N, Yasumoto T, Diogène J. Monitoring of dissolved ciguatoxin and maitotoxin using solid-phase adsorption toxin tracking devices: Application to *Gambierdiscus pacificus* in culture. *Harmful Algae*. **2011**, 10:433-446

289. Rundberget T, Aasen JA, Selwood AI, Miles CO. Pinnatoxins and spirolides in Norwegian blue mussels and seawater. *Toxicon : official journal of the International Society on Toxinology*. **2011**, 58:700-711

290. Zendong Z, Herrenknecht C, Abadie E, Brissard C, Tixier C, Mondeguer F, Séchet V, Amzil Z, Hess P. Extended evaluation of polymeric and lipophilic sorbents for passive sampling of marine toxins. *Toxicon*. **2014**, 91(Special Issue: Freshwater and Marine Toxins):57–68

Chapter 2: Active role of the mucilage in the toxicity mechanism of the harmful benthic dinoflagellate *Ostreopsis* cf. *ovata*

1. Introduction

In the last decade, the harmful benthic dinoflagellate *Ostreopsis* cf. *ovata* has been blooming in the Mediterranean region with increasing frequency and distribution, causing mortality of benthic organisms and with additional human health concerns [1-5]. These events have been generated great attention on different aspects of *O*. cf. *ovata* biology (ecology, ecotoxicology, genetics, cytology, etc.).

Ostreopsis genus produces palytoxin-analogs complex (PLTX) that could be involved in ciguatera fish poisoning [6-7], a widespread form of human food poisoning caused by consumption of contaminated finfish, but further studies are required to confirm this hypothesis [8].

Data on the toxic effects of PLTX and some of its analogs on different model organisms have been reviewed in recent papers [9-10]. The toxin profile of *O*. cf. *ovata* can vary but the extent to which production of these toxins is controlled by environmental versus inherent genetic differences among strains has not yet been elucidated [11-12], as well as the role of these drivers on cell proliferation and toxicity. Differently, the increasing toxins production along the growth curve of this species, reaching the maximum during the stationary phase has been proven by Guerrini *et al.*, 2010 [13].Similar evidences has been reported for other toxic benthic dinoflagellates (e.g. *Prorocentrum lima*, *Gambierdiscus toxicus*), which showed higher toxicity effects during stationary phase and/or the blooming phase from field samples [14,11,8].

Field studies suggest that environmental variables, such as temperature and salinity, could play a key role in driving the proliferation of *Ostreopsis* spp. [2,15-19]. However, controversial results in different regions could be either due to different interactions among environmental drivers or different response of local strains. As a consequence, laboratory studies elucidating the role of individual environmental variables on growth and toxicity are increasing [11].

Ostreopsis spp. grow attached to the substrate utilizing a variable amount of mucilage in which they aggregate [20]. *Ostreopsis* mucilage shows a complex structure, formed by a network of long fibers, derived from trychocysts extruded through thecal

pores and by an amorphous matrix of acidic polysaccharides [21-22]. Mucilage increases during cell proliferation in the field, producing a typical brownish mat, visible with the naked eye. Studies focusing on the mucilaginous matrix suggest its key-role in growth strategy and, possibly, in the micropredation activity of *O.* cf. *ovata* cells [23], defense against grazing, increased buoyancy and metabolic self-regulation [24-25].

An active toxicological role for the mucilaginous matrix surrounding the microalgal cells has not been shown yet, although when mass mortalities and or damage of benthic organisms have occurred [5,16,26-28], organisms were reported to be covered by this typical brownish mucilage. Laboratory tests performed on juveniles and larvae of *Paracentrotus lividus*, also describe a mechanical impediment of model organisms due to their being wrapped in the *O.* cf. *ovata* mucilage [29].

A range of laboratory studies have reported much higher toxic effects on model organisms in the presence of intact *Ostreopsis* cells, compared to free cells supernatant (growth medium devoid of cells): *Artemia salina* [30-31], *Paracentrotus lividus* [29], sea bass juveniles [31].

In order to better elucidate toxicity dependence on direct/indirect contact, the role of the mucilaginous matrix and the potential differences in toxicity along the growth curve of *O.* cf. *ovata*, we carried out a toxic bioassay during exponential, stationary and late stationary phases, improving the experimental design described in Faimali *et al.* [30]. The role of the mucilaginous matrix was investigated at the late stationary phase. In fact, at this phase, concurrently with the increase of *O.* cf. *ovata* cell concentration in cultures, a larger production of mucilage matrix is observed in the external medium [32-33].

The experiment was mainly designed to test toxicity effects on *A. salina* nauplii exposed to different conditions of contact with algal cells (whole *O.* cf. *ovata* culture; *O.* cf. *ovata* cells filtered and resuspended in fresh medium; filtered and sonicated cells; growth medium devoid of cells, but containing the mucilage; growth medium devoid of cells and of the mucilage). Concurrently, a real time PCR (qPCR) was performed to quantify intact cells or to exclude cells presence in the treatment corresponding to medium devoid of cells, but containing the mucilage. Furthermore, liquid chromatography-high resolution mass spectrometry (LC-HRMS) analyses were carried out to evaluate toxin profile and content in the different treatments.

Moreover, in order to better elucidate the functional role of the mucilaginous matrix and its links with the *Ostreopsis* cells, the connection between the thecal plates, pores,

trychocysts and the mucilaginous matrix was explored by way of atomic force microscopy (AFM) to investigate cell surface at a sub-nanometer resolution, providing a pioneering description of the inner side of *O.* cf. *ovata* thecal plates.

2. Results

2.1 Toxicity bioassay

Mortality of *A. salina* nauplii exposed for 48 h to A, B, C and D treatments performed along exponential, stationary and late stationary phases are shown in Figure II.1 (a-b-c-d).

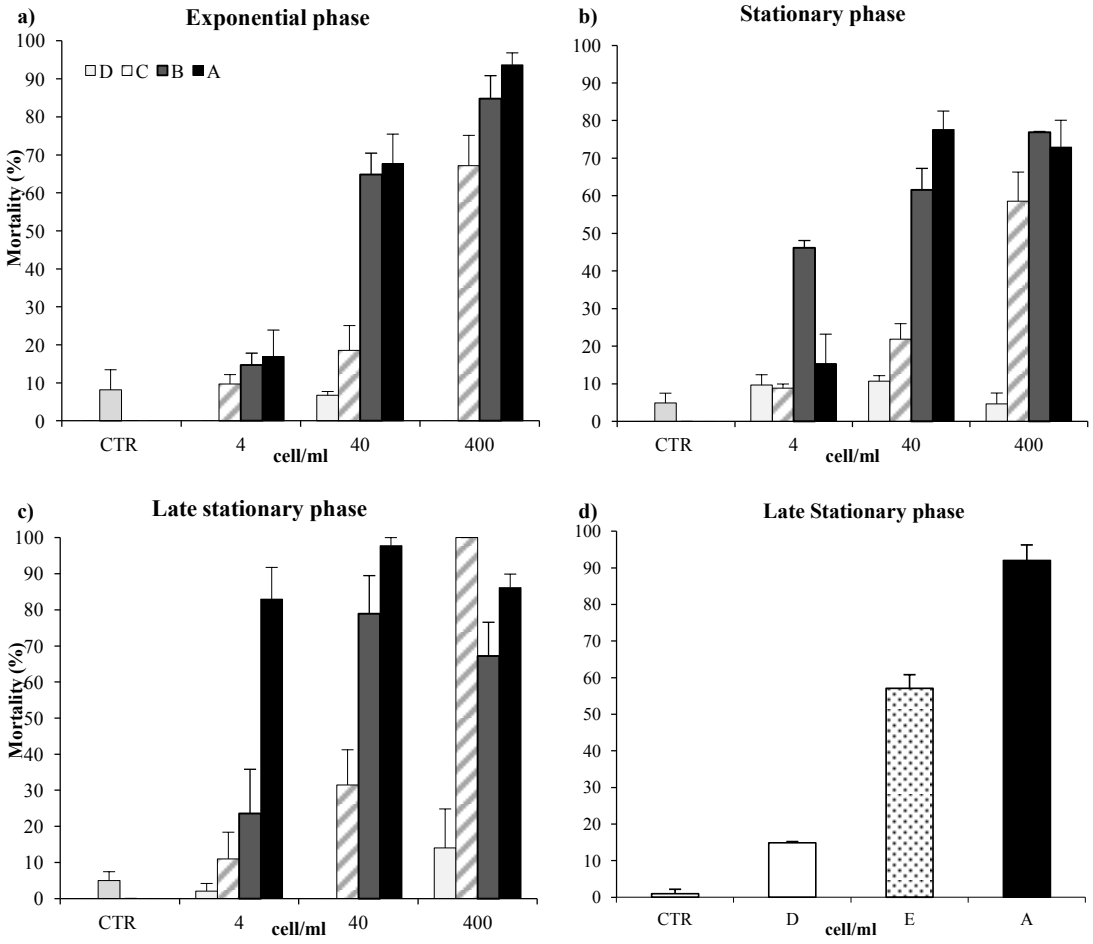

Figure II.1 Mortality (avg ± standard error, N = 3) of *Artemia salina* after 48 h of exposure to 0.22 µm filtered growth medium (D; white bar), sonicated *O.* cf. *ovata* culture (C; striped bar), resuspended *O.* cf. *ovata* culture (B; grey bar) and untreated *O.* cf. *ovata* culture (A; black bar), during exponential (a), stationary (b) and late stationary (c) phases of the growth curve; d) mortality (avg ± standard error, N = 3) of *Artemia salina* after 48 h exposure to 0.22 µm filtered growth medium (D), 6 µm filtered growth medium (E) and untreated *O.* cf. *ovata* culture (A), at the concentration of 400 cells/ml during the late stationary phase. CTR: control in filtered natural seawater.

In general, our data show that the toxicity of *O.* cf. *ovata* increases during the growth curve, causing the higher mortality values during the late stationary phase. In particular, as far as the lower concentrations tested (4 and 40 cells/ml) of untreated *O.* cf. *ovata* culture (A treatment), statistical comparison among the three growth curve phases demonstrates a significantly higher toxic effect during the late stationary phase ($p < 0.01$), with mortality values exceeding 80%. These findings are supported also by the decrease in $LC_{50–48h}$ values: 25 cells/ml during the exponential phase, 17 cells/ml during the stationary phase and < 4 cells/ml during the late stationary phase. The same decreasing trend of $LC_{50–48h}$ values along the three phases of the growth curve is also observed in the B (resuspended *O.* cf. *ovata* cultures) and C (sonicated culture) treatments (Table II.1).

Table II.1 LC_{50-48h} values (cells/ml) and confidence limits obtained exposing nauplii of *A. salina* to A) untreated *O.* cf. *ovata* culture, B) resuspended *O.* cf. *ovata* culture, C) sonicated *O.* cf. *ovata* culture and D) 0.22 μm filtered growth medium, during exponential, stationary and late stationary phases of algal growth curve.

Treatments	LC_{50-48h} (cells/ml)		
	Exponential phase	Stationary phase	Late stationary phase
A	24.83 (18.59 – 33.16)	16.67 (13.46 – 20.63)	< 4 cell/ml
B	30.12 (20.92 – 43.37)	10.19 (3.86 – 26.91)	15.26 (11.56 – 20.15)
C	214.40 (155.96 – 294.75)	266.92 (163.64 – 435.39)	65.48 (51.23 – 83.68)
D	> 400	> 400	> 400

Effects are stronger in A (untreated culture) and B treatments, while C treatment displays higher percentage of mortality (67%, 59% and 100%, during exponential, stationary and late stationary phases, respectively) only at the highest tested concentration (400 cells/ml).

Growth medium devoid of both algal cells and mucilaginous matrix by 0.22 μm mesh size filtration (treatment D) did not show any relevant toxic effect among any concentrations tested throughout all growth curve phases.

Results from the toxicity bioassay performed during the late stationary phase to disentangle the effects of direct contact with cells and the mucous filaments are reported in Figure II.1-d. Also in this case the 0.22 μm filtered growth medium (D treatment) does not show relevant mortality effects, while the growth medium obtained by filtration through 6 μm mesh size nylon net registered almost 60% mortality (57.8%, $p < 0.01$).

This study reports increasing ecotoxicological effects of *O.* cf. *ovata* along its growth curve, with LC_{50} values of *A. salina* lower at the late stationary phase.

The ecotoxicological bioassay provides additional evidence that not only toxin production increases along the growth curve, as reported in literature [13], but also toxic effects on model organisms are more severe. In fact, several studies, mainly focusing on toxin quantification and characterization, report that toxicity of *O.* cf. *ovata*, as for other benthic dinoflagellates, increases along the growth curve, reaching the highest toxin content in the cells at the end of the stationary phase [33-34].

In addition to the increase in toxicity effects along the growth curve, more interestingly, our study shows that toxicity effects on model organisms change drastically according to the presence or not of living cells or mucous filaments. So far, toxicity mechanisms of *Ostreopsis* spp. are still unclear. Faimali *et al.* [30] already observed that toxic effects on marine invertebrates occurred only when they were exposed to direct contact of intact microalgal cells ($LC_{50\text{-}48h}$ at 20 and 25 °C of whole culture equal to 12.43 and < 4 cells/ml, while $LC_{50\text{-}48h}$ at 20 - 25 °C of 0.22 μm filtered growth medium were around 4000 cell/ml, respectively). Moreover, similar trend of toxicity on *Artemia salina* nauplii and juveniles of sea basses has been demonstrated in Pezzolesi *et al.* [31] which show $EC_{50\text{-}24h}$ value of growth medium corresponding to 720 cells/ml versus 8 cells/ml with live cells.

The present study investigates the role of contact with living cells in conveying toxins to the organisms, discriminating between the contact with the whole cells and with the only mucous filaments produced by *O.* cf *ovata*. Honsell *et al.* [31] described *O.* cf. *ovata* mucilage as a network of a very high number of trychocysts embedded with acidic polysaccharides filaments, both secreted through thecal pores, that generate a very resistant extracellular matrix never observed before among microalgal species. This matrix can be extremely thick, especially during the late bloom, when mass mortalities of marine organisms are usually recorded [35-36].

The potential toxic effects of both growth medium and mucilage were tested during the late stationary phase. The results of this test provide the first evidence of a significant toxic effect ($p < 0.01$) on *A. salina* after exposition to growth medium (devoid of microalgal cells) containing only *O.* cf. *ovata* mucilage. Although previous findings report an increase in toxin content in the growth medium at the late stationary phase, possibly due to the large number of broken cells [13], our results on the 0.22 μm filtered growth medium show low mortality values at the late stationary phase as well as undetectable toxin concentrations by

way of chemical analyses. On the contrary, 5% of toxins of the whole culture is present in the 6 μm growth medium, suggesting that toxins are retained in the mucous matrix.

Additional confirmation of the direct involvement of cells (or their filaments) in conveying toxicity to model organisms is provided by the evidence that the sonicated *O.* cf. *ovata* culture, at a concentration comparable to those that often occur in nature (≤ 40 cells/ml), had much lower effects than the intact cells. Only at the highest tested concentration (400 cells/ml, rarely found in nature) a remarkable toxic effect was observed. However, we cannot exclude that sonication may alter the molecular and toxicity properties [30].

Our findings provide additional insights on the role of the microalgal mucilaginous matrix that may represent a defense against grazing, a predation method to capture larger organisms by heterotrophic dinoflagellates [23,37] and/or an adaptation to live in different benthic habitats [8,16]. But, most of all, as reported for other microalgal [38], *Ostreopsis* mucus could be a vehicle through which toxins are released into external medium and/or disseminated into the prey. In fact, the first observed effect on several marine organisms is the interlocking within the mucous [28-29].

2.2 Molecular analysis

The comparison of the pLSUO and cellular standard curves showed the same efficiency (98−100% and $\Delta s < 0.1$, data not shown), thus it was possible to calculate the rDNA copy number per cell of *O.* cf. *ovata*. The normalized copy per cell of *O.* cf. *ovata* was 2859± 175 (Ct mean = 22.95 ± 0.09). The 6 μm filtered growth medium was analyzed by qPCR and was positive for the presence of few *O.* cf. *ovata* cells. In particular, the Ct mean value was 29.39 ± 0.12 (n = 3) corresponding to 8243 ± 658 total LSU rDNA copy number. Thus, only three cells were quantified in the 6 μm filtered growth medium.

2.3 Chemical Analyses: determination of toxin profile and content

Crude extracts of cell pellets and growth media for each treatment (D and E treatments) were directly analyzed by LC-HRMS using a slow gradient elution [39], which allowed to chromatographically separate most of the components of the toxin profile. Full HR MS spectra were acquired in the mass range *m/z* 800-1400 where each palytoxin-like compound produced dominant doubly and triply-charged ions due to $[M+2H-H_2O]^{2+}$ and $[M+H+Ca]^{3+}$, respectively [40]. Under such conditions, accurate quantitation was possible

for most of the palytoxin-like compounds produced by *O.* cf. *ovata*, with the only exception of the structural isomers ovatoxin-d and –e, which were quantified as sum. Instrumental limit of detection for palytoxin was 3.12 ng/ml. Based on extraction volume, the presence of toxins in pellet (1 x 10^6 cells), growth medium D (150 ml), and E (175 ml) could be estimated at levels ≥ 0.13 pg/cell, 0.17, and 0.14 μg/l, respectively.

An Adriatic *O*. cf. *ovata* extract previously characterized [31] was analyzed in parallel under the same experimental conditions and used as reference samples. Palytoxin standard was used in quantitative studies assuming that toxins produced by *O*. cf. *ovata* present the same molar response as palytoxin, which seems quite reasonable based on structural similarities.

Unlike the *O*. cf. *ovata* reference sample, extracts of pellet and 6μm filtered growth medium (E) extract contained only ovatoxin-a, ovatoxin-d and -e and a putative palytoxin, while ovatoxin-b and -c were not detected. No palytoxin-like compound was detected in 0.22 μm filtered growth medium (D). Total toxin content on a per cell basis was 44 pg/cell (pellet), with ovatoxin-a being the major component of the toxin profile (76%), followed by ovatoxin-d and -e (21%) and pPLTX (3%). The highest toxin content was measured in pellet extract (95%) with only 5% being measured in the 6 μm growth medium, while toxins were not detected in the 0.22 μm medium (Table II.2). The chemical analyses on the *O.* cf. *ovata* strain investigated in the present study show that toxin profile of the culture differs from that usually found in Mediterranean *O.* cf. *ovata* strains from both a qualitative and quantitative stand point; more in details, it did not contain ovatoxin-b and -c, versus a previously characterized Adriatic *O.* cf. *ovata* strain containing ovatoxin-a (56%), -b (24%), -d and -e (15%), -c (4%), and putative palytoxin (1%). A similar toxin profile has been reported by Ciminiello *et al.* [41-42] in only one Adriatic *O.* cf. *ovata* strain. The variability in toxin profile of different isolates of this species [11] is stressed by intrinsic (e.g. different strains) and extrinsic (e.g. different habitat) factors [12] that can influence not only toxicity but also amount of mucilage produced.

Table II.2 Toxin content of pellet (pg/cell and µg/l), 6 µm filtered (E) and 0.22 µm filtered (D) growth medium of *O.* cf. *ovata* culture. Conversion between pg/cell and mg/l is calculated according to the cell concentration of 5.40 x 10^3 cells/ml.

Toxin	Pellet pg/cell	Pellet µg/l	Medium 6 µm µg/l	Medium 0.22 µm µg/l
Ovatoxin-a	33.5	180.9	8.0	nd
Ovatoxin-d and -e	9.0	51.3	4.0	nd
Putative Palytoxin	1.5	8.5	trace	nd
Total toxin content	44	240.7	12	nd

2.4 Atomic Force Microscope

Innovative characterization of the inner side of *O.* cf. *ovata* thecal plates, performed by AFM without staining and fissative treatments, is shown in Figure II.2 (a-b-c-d-e). Our investigation highlighted three cellulose layers of the hypothecal plates (specifically on 3''' plate, Figure II.2-b), resulting in 460 nm (for the two inner ones) and 740 nm (for the external one) of thickness. Thecal plates display scattered pores of around 230 nm average diameter (N = 65): on the inner side of the plates, differently from the smooth outer side, the pores are surrounded by a raised edge (around 65 nm height). Moreover, some pores are covered by a conical structure from which channels and filaments (230 nm thick; Figure II.2-c) depart, suggesting that these are structural parts involved in the extrusion mechanism of trychocysts.

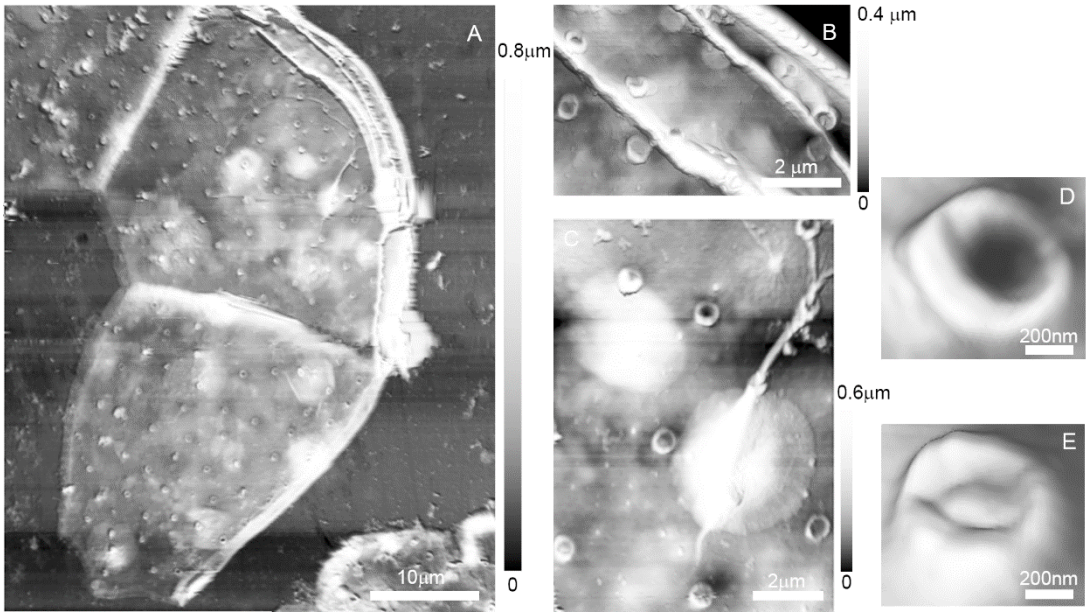

Figure II.2 a) Overview of the inner side of *Ostreopsis* cf. *ovata* hypotheca obtained by atomic force microscopy (AFM); b) zoom on the three cellulose layers of the thecal plate; c) trychocyst and thecal pores on inner side of 3''' thecal plate; d) - e) blowup of thecal pores**.**

The possibly active role of the filaments in conveying toxicity is supported by the innovative images of the *O.* cf. *ovata* theca obtained by atomic force microscopy. AFM images show scattered pores having different structure from their external one (as suggested also in Penna *et al.,* [43]) and, at a higher magnification, highlight conical – tubular structures involved in the trychocyst extrusion mechanism.

3. Materials and methods

3.1 *Ostreopsis* cf. *ovata* cultures and growth curve

Laboratory cultures of *O.* cf. *ovata* were obtained from environmental samples collected during the summer 2012 in Quarto dei Mille (Genoa, NW Mediterranean Sea, Italy). Cell isolation was performed at the laboratory of University of Urbino from the team of Dr. Antonella Penna (strain CBA29-2012). Algal cells were cultured into several 200 ml sterilized plastic flasks closed with transpiring caps, filled with an aliquot of *O.* cf. *ovata* culture from the masters added with filtered (GF/F 0.22 μm) sterilized marine water and Guillard growth medium F/2 (at a concentration of 1 ml/l).

At the start of the toxicity bioassay, six new flasks were prepared with initial cell concentration of 80 cells/ml. All flasks were maintained at 20 ±0.5 °C in a 16:8 h light:dark (L:D) cycle (light intensity 85–135 μE m^{-2} s^{-1}). To set up the growth curve, cell counts were performed in triplicate on 1 ml of samples every two days, using an inverted light microscope.

3.2 Toxicity bioassays

Toxicity tests were performed on II-III stage larvae (nauplii) of the crustacean *A. salina* following the Artoxkit M, obtained from Microbiotest Inc. (Artoxkit, 1990), modified as in Faimali *et al.* [30] during exponential, stationary and late stationary phases.

In order to investigate the toxic effect due to direct or indirect contact with *O.* cf. *ovata* cells along the growth curve, nauplii of *A. salina*(15 – 20 organisms per 2 ml well) were exposed to: A) untreated *O.* cf. *ovata* culture; B) filtered (by 6 μm mesh size nylon net) and resuspended *O.* cf. *ovata* cells in fresh medium; C) filtered, resuspended and sonicated *O.* cf. *ovata* cells in fresh medium; D) growth medium devoid of algal cells by 0.22 μm mesh size filtration, where both cells and mucilaginous matrix were removed (GM 0.22 μm). All treatments (A – D) were tested with concentrations of 4, 40 and 400 cells/ml, at the three phases of the growth curve; three replicates were prepared for each combination of treatments and cell concentrations, including a control (CTR; 0.22 μm Filtered Natural Sea Water).

Moreover, during the late stationary phase, a further investigation was performed to elucidate the role of the mucilaginous matrix. The toxicity bioassay was replicated with treatments A, D and a new one E): growth medium obtained by filtration through a 6 μm mesh size nylon net, which allows the mucilaginous matrix pass through, but retains the cells. These treatments were tested at the concentration of 400 cells/ml; three replicates were prepared for each treatment, including the control (0.22 μm Filtered Natural Sea Water).

Multiwell plates were stored at 20 °C with a 16:8 L:D cycle. After 48 h, the number of dead nauplii was observed under a stereomicroscope.

3.3 Statistical analysis

Three way crossed analysis of variance (three way-ANOVA) and Student-Newman-Keuls (SNK) tests were performed for the comparison of means to check for differences among mortality values for the first experimental set up. Factors tested were:

Phase (exponential, stationary and late stationary; 3 levels), Concentration (4, 40, 400 cells/ml; 3 levels) and Treatment (A - D; 4 levels).

In the second experiment, testing effects of cells, mucous and growth medium during the late stationary phase, a one way-ANOVA was performed to test effects of factor Treatment (A, D, E; 3 levels).

All ANOVAs were performed after checking for homoscedasticity using the Cochran test.

The LC_{50-24h} and LC_{50-48h} values (the concentration of *O.* cf. *ovata* cells causing 50% mortality after 24 and 48 h of exposure) were calculated using trimmed Spearman–Karber analysis.

3.4 Molecular analysis

To check possible presence of algal cells in the treatment E and, therefore, to better understand and validate the interpretation of the ecotoxicological bioassay, 60 ml of *O.* cf. *ovata* culture (harvested during the late stationary phase) was filtered through a 6 μm mesh size nylon, replaced in a new sterilized plastic flask and analyzed by qPCR assay.

In particular, the 6 μm fraction was filtered through a 25 mm diameter Durapore membrane with a pore size of 0.65 μm (Millipore, USA) under gentle vacuum in order to recover possible biological components. Then, the filter was transferred into a new 1.5 ml tube containing 500 μl of lysis buffer as described by Perini *et al.* [44]. Particulate material was washed out from the filter, the filter discharged and the suspension was lysed as described in detail by Casabianca *et al*. [45]. Briefly, after three freeze/thaw cycles the sample was incubated at 55°C for 3h and vortexed every 20 min. A 100°C for 5 min step was performed to inactivate the proteinase K. Finally, the suspension was centrifuged at 12000 rpm for 1 min to precipitate cell debris. The supernatant, or crude extract, was transferred into a new tube, and diluted at 1:10 and 1:100 for the qPCR experiments.

The 6 μm fraction, treated as described above, was analyzed by qPCR following the protocol of Perini *et al.* [44] using primers for the amplification of 204 bp specific fragment targeting LSU rDNA of *O.* cf. *ovata*. A plasmid (pLSUO) standard curve was constructed by amplifying 10-foldscalar dilutions with the copy number ranging from 1×10^6 to 1×10^2 (two replicates), and from 1×10^1 to 2×10^0 (four replicates).

A cellular standard curve was generated with dilutions from 8 to 8×10^{-4} lysed cells. The rDNA copy number per cell of *O.* cf. *ovata* was calculated.

The qPCR assay was carried out in a final volume of 25 µl using the Hot-Rescue Real-Time PCRKit-SG (Diatheva, Fano, Italy) in a StepOne Real-Time PCRSystem (Applied Biosystems, CA), primer sat a final concentration of 200 nM, 0.5 U of Hot-Rescue Taq DNA polymerase, and 2 µl undiluted, 1:10 and 1:100 diluted of culture crude extract. Amplification reactions were carried out using a Step-one Real-time PCR System (Applied Biosystem, Foster City, CA, USA). The thermal cycling conditions consisted of 10 min at 95 °C, followed by 40 cycles at 95 °C for 15 s and 60 °C for 1 min.

Acquisition of qPCR data and subsequent analyses were carried out using StepOne software v. 2.3. A dissociation curve was generated, after each amplification run, to check for amplicon specificity and primers dimer formation. Results from 10-fold dilutions with a Ct difference between 3.3 and 3.4 (ΔCt of 3.3 corresponds to 100% efficiency) were accepted.

3.5 Chemical analysis

In order to characterize and quantify toxins produced by *O.* cf. *ovata*, chemical analyses were performed at the University of Naples on aliquots of D (150 ml), E (175 ml) treatments and on *O.* cf. *ovata* cell pellet (about 1 x 10^6 cells arising from 175 ml culture containing round to 5400 cells/ml) collected during late stationary phase.

Cell pellets and growth media for each treatment were extracted separately as follows. Pellets were added to 30 ml of a methanol/water (1:1, v/v) solution and sonicated for 5 min in pulse mode, while cooling in ice bath. The mixture was centrifuged at 6500 rpm for 10 min; the supernatant was decanted and the pellet was extracted once again with 20 ml of the extraction solvent. The supernatant was decanted and the two extracts were combined (42 ml total). The obtained mixture was analyzed directly by LC-HRMS (5µl injected). Growth media were extracted five times with an equal volume of butanol. The butanol layer was evaporated to dryness, dissolved in 8 ml of methanol/water (1:1, v/v) and analyzed directly by LC-HRMS (5µl injected). Recovery percentages of the above extraction procedures were 98% for the pellet and 75% for the growth medium [46].

LC-HRMS analyses were carried out on an Agilent 1100 LC binary system (Palo Alto, CA, USA) coupled to a hybrid linear ion trap LTQ Orbitrap XL^{TM} Fourier Transform MS (FTMS) equipped with an ESI ION MAX^{TM} source (Thermo-Fisher, San José, CA, USA). Chromatographic separation was accomplished on a 3 µm Gemini C18 (150 X 2.00 mm) column (Phenomenex, Torrance, CA, USA) maintained at room temperature and

eluted at 0.2 ml min^{-1} with water (eluent A) and 95% acetonitrile/water (eluent B), both containing 30 mM acetic acid. A slow gradient elution was used: 20% to 50% B over 20 min, 50% to 80% B over 10 min, 80% to 100% B in 1 min, and hold for 5 min. This gradient system allowed a sufficient chromatographic separation of most palytoxin-like compounds with the only exception of ovatoxin-d and -e. HR full MS experiments (positive ions) were acquired in the range *m/z* 800–1400 at a resolving power of 60,000. The following source settings were used: a spray voltage of 47 V, a capillary temperature of 290 C°, a capillary voltage of 47 V, a sheath gas and an auxiliary gas flow of 38 and 2 (arbitrary units). The tube lens voltage was set at 105 V.

Identification of palytoxin-like compounds contained in the extracts was made on the basis of retention time, elemental formula of the most intense doubly- and triply-charged ions (mono-isotopic ion peak) contained in full HRMS spectrum, and isotopic pattern of each ion cluster. An *O.* cf. *ovata* extract previously characterized [31] was used as reference sample. HR collision induced dissociation (CID) LC-MS^2 experiments were carried out to confirm the identity of individual toxins as reported previously [34,36-37]. Extracted ion chromatograms (XIC) were obtained for each palytoxin-like compound by selecting the most abundant ion peaks of both $[M+2H-H_2O]^{2+}$ and $[M+H+Ca]^{3+}$ ion clusters at a mass tolerance of 5 ppm. Due to commercial availability of the only palytoxin standard, quantitation of the palytoxin-like compounds was carried out by assuming that their molar responses were similar to that of palytoxin. Calibration curve (triplicate injection) of palytoxin standard at four levels of concentration (1000, 100, 50, and 12.5 ng ml^{-1}) was used. Calibration curve equation was y = 10461.3160 x232615.2993 and its linearity was expressed by $R^2 = 0.997$.

3.6 Atomic Force Microscopy (AFM)

A 20 µl drop of *O.* cf. *ovata* culture was deposited directly onto clean glass substrate overnight to allow cells settle and adhere to the surface. Samples were then rinsed in ultrapure water to remove the excess of salt crystals and then placed in Petri dish to allow the excess of water to evaporate. As a consequence of the rinsing procedure the cells disaggregated, breaking down into the separate plates. Stable AFM imaging of the thecal plates, firmly adhered to the glass sheet were then performed. Data acquisition was carried out by using a custom build AFM head [47] based on a three axis closed loop flexure scanner with travel ranges 200 x 200 x 20 µm (mod. PI—527.3CL, PhysikInstrumente,

Karlsruhe, Germany) and driven by R9 digital controller by RHK Technology - Troy, MI (USA), in intermittent contact mode in air at room temperature. Rectangular silicon cantilevers (PPP-NCHR, Nanosensors, Neuchatel, Switzerland) with a nominal tip radius of 10 nm and 330 kHz resonance frequency were used. Topography images were acquired at a resolution of 512 pixels per line using a scan rate of 0.4 Hz. AFM scanner performance and calibration were routinely checked by using a reference grid model STR3-180P (VLSI Standards, CA, U.S.A.) with a lateral pitch of 3 μm and step height of 18 nm. AFM images were pre-processed for tilt correction and scars removal with Gwyddion software.

4. Conclusions

The present study has provided additional evidence on the variability of the toxin profile of *O.* cf. *ovata* strains, highlighting that: i) the toxicity increases along the growth curve; ii) negligible amounts of toxins are released in the growth medium and iii) the mucous filaments play a direct, possibly active, role in conveying toxicity. In fact, the mucous matrix interlocks the organisms, enhances the surface of the contact area, and, most possibly, actively disseminates toxins.

Atomic force microscopy, providing new perspectives on ultrastructure investigations, seems to be a promising technique to highlight cellular features, their connections and role in *O.* cf. *ovata*, and, in general, in other microalgae species [48-51]

References

1. Aligizaki, K., Nikolaidis, G., 2006. The presence of the potentially toxic genera *Ostreopsis* and *Coolia* (Dinophyceae) in the North Aegean Sea, Greece. HarmfulAlgae5, 717–730.

2. Mangialajo, L., Bertolotto, R., Cattaneo-Vietti, R., Chiantore, M., Grillo, C., Lemee, R., Melchiorre, N., Moretto, P., Povero, P., Ruggieri, N., 2008. The toxic benthic dinoflagellate *Ostreopsis ovata*: quantification of proliferation along the coastline of Genoa, Italy. Mar. Pollut. Bull. 56, 1209–14.

3. Penna, A., Fraga, S., Battocchi, C., Casabianca, S., Giacobbe, M. G., Riobò, P., Vernesi, C., 2010. A phylogeographical study of the toxic benthic dinoflagellate genus *Ostreopsis* Schmidt. J. Biogeogr., 37, 380−841.

4. Rhodes, L., 2011. World-wide occurrence of the toxic dinoflagellate genus *Ostreopsis* Schmidt. Toxicon 57, 400–407.

5. Vila, M., Garcés, E., Masó, M., 2001. Potentially toxic epiphytic dinoflagellate assemblages on macroalgae in the NW Mediterranean. Aquat. Microb. Ecol. 26, 51–60.

6. Tosteson, T.R., 1995. The diversity and origins of toxins in ciguatera fish poisoning. P. R. Health Sci. J. 14, 117–129.

7. Richlen, M.L., Morton, S.L., Barber, P.H., 2008. Phylogeography, morphological variation and taxonomy of the toxic dinoflagellate *Gambierdiscus toxicus* (Dinophyceae). Harmf. Algae 7, 614–629.

8. Parsons, M.L., Aligizaki, K., Bottein, M.-Y.D., Fraga, S., Morton, S.L., Penna, A., Rhodes, L., 2012. *Gambierdiscus* and *Ostreopsis*: Reassessment of the state of knowledge of their taxonomy, geography, ecophysiology, and toxicology. Harmful Algae 14, 107–129.

9. Ramos, V., Vasconcelos, V., 2010. Palytoxin and analogs: biological and ecological effects. Mar. Drugs 8, 2021–2037.

10. Munday, R., 2011. Palytoxin toxicology: animal studies. Toxicon 57, 470–7.

11. Pistocchi, R., Pezzolesi, L., Guerrini, F., Vanucci, S., Dell'Aversano, C., Fattorusso, E., 2011. A review on the effects of environmental conditions on growth and toxin production of *Ostreopsis ovata*. Toxicon 57, 421–428.

12. GEOHAB, 2012. GEOHAB core research project: HABs in benthic systems. Organization 64.

13. Guerrini, F., Pezzolesi, L., Feller, A., Riccardi, M., Ciminiello, P., Dell'Aversano, C., Tartaglione, L., Dello Iacovo, E., Fattorusso, E., Forino, M., Pistocchi, R., 2010. Comparative growth and toxin profile of cultured *Ostreopsis ovata* from the Tyrrhenian and Adriatic Seas. Toxicon 55, 211–220.

14. Grzebyk D., Denardou A., Berland B., Pouchus Y.F., 1997. Evidence of a new toxin in the red-tide dinoflagellate *Prorocentrum minimum*. Journal of Plankton Research Vol.19 no.8 pp.1111-1124

15. Shears, N.T. and Ross, P.M., 2009. Blooms of benthic dinoflagellates of the genus *Ostreopsis*: an increasing and ecologically important phenomenon on temperate reefs in New Zealand and worldwide. HarmfulAlgae, 8, 916–925.

16. Totti, C., Accoroni, S., Cerino, F., Cucchiari, E., Romagnoli, T., 2010. *Ostreopsis ovata* bloom along the Conero Riviera (Northern Adriatic Sea): Relationships with environmental conditions and substrata. HarmfulAlgae 9, 233–239.

17. Mangialajo L., Ganzin N., Accoroni S., Asnaghi V., Blanfuné A., Cabrini M., Cattaneo-Vietti R., Chavanon F., Chiantore M., Cohu S., Costa E., Fornasaro D., Grossel H., Marco-Mirailles F., Maso M., Rene A., Rossi A.M., Montserat Sala M., Thibaut T., Totti C., Vila M. &Lemée R., 2011. Trends in *Ostreopsis* proliferation along the Northern Mediterranean coasts. Toxicon 57, 408-420.

18. Asnaghi V., Bertolotto R., Giussani V., Mangialajo L., Hewitt J., Thrush S., Moretto P., Castellano M., Rossi A., Povero P., Cattaneo-Vietti R., Chiantore M., 2012. Interannual variability in *Ostreopsis ovata* bloom dynamic along Genoa coast (North-western Mediterranean): a preliminary modeling approach. Cryptogamie, Algologie, 33 (2), 181-189.

19. Accoroni, S., Romagnoli, T., Pichierri, S., Colombo, F., & Totti, C. (2012). Morphometric analysis of *Ostreopsis* cf. *ovata* cells in relation to environmental conditions and bloom phases. Harmful Algae, 19, 15-22.

20. Besada, E.G., Loeblich, L.A., Loeblich, A.R., 1982. Coral reef paper observations on tropical, benthic dinoflagellates from ciguatera-endemic areas: *Coolia*, *Gambierdiscus*, and *Ostreopsis*. Bull. Mar. Sci. 32, 723–735.

21. Honsell, G., Bonifacio, A., De Bortoli, M., Penna, A., Battocchi, C., Ciminiello, P., Dell'aversano, C., Fattorusso, E., Sosa, S., Yasumoto, T., Tubaro, A., 2013. New insights on cytological and metabolic features of *Ostreopsis* cf. *ovata* Fukuyo (Dinophyceae): a multidisciplinary approach. PLoSOne 8, e57291.

22. Escalera, L., Benvenuto, G., Scalco, E., Zingone, A., & Montresor, M. (2014). Ultrastructural Features of the Benthic Dinoflagellate *Ostreopsis* cf. *ovata* (Dinophyceae). Protist, 165(3), 260-274.

23. Barone R, Prisanzano A (2006) Peculiarita` comportamentale del dinoflagellato *Ostreopsis ovata* Fukuyo (Dinophyceae): la strategia del ragno. Naturalista siciliano 30: 401–418.

24. Reynolds CS, 2006. Ecology of Phytoplankton. Cambridge: Cambridge University Press. 535 p.

25. Reynolds CS, 2007. Variability in the provision and function of mucilage in phytoplankton: facultative responses to the environment. Hydrobiologia 578, 37–45.

26. Granéli, E., Ferraiera C., Yasumoto T., Rodrigues E., Neves B., 2002. Sea urchins poisoning by the benthic dinoflagellate *Ostreopsis ovata* on the Brazilian Coast. In.

Steidinger, K.A. (Ed.), Book of Abstract 10thIntConf on Harmful Algae, 21-25. ST. PETE Beach, PL, p. 113

27 Brescianoni C., Grillo C., Melchiorre R., Bertolotto, Ferrari R.A., Vivaldi B., Icardi G., Gramaccioni L., Funari E., Scardala S., 2006. *Ostreopsis ovata* algal blooms affecting human health in Genova, Italy, 2005 and 2006. Euro Surveill 11 (9) E060907.

28. Shears, N.T., Ross, P.M., 2010. Toxic cascades: multiple anthropogenic stressors have complex and unanticipated interactive effects on temperate reefs. Ecol. Lett. 13, 1149–1159.

29. Privitera, D., Giussani, V., Isola, G., Faimali, M., Piazza, V., Garaventa, F., Asnaghi, V., Cantamessa, E., Cattaneo-Vietti, R., Chiantore, M., 2012. Toxic effects of *Ostreopsis ovata* on larvae and juveniles of Paracentrotus lividus. Harmful Algae 18, 16–23

30. Faimali, M., Giussani, V., Piazza, V., Garaventa, F., Corrà, C., Asnaghi, V., Privitera, D., Gallus, L., Cattaneo-Vietti, R., Mangialajo, L., Chiantore, M., 2012. Toxic effects of harmful benthic dinoflagellate *Ostreopsis ovata* on invertebrate and vertebrate marine organisms. Mar. Environ. Res. 76, 97–107.

31. Pezzolesi, L., Guerrini, F., Ciminiello, P., Dell'Aversano, C., Iacovo, E. D., Fattorusso, E., Pistocchi, R. (2012). Influence of temperature and salinity on *Ostreopsis* cf. *ovata* growth and evaluation of toxin content through HR LC-MS and biological assays. Water research, 46(1), 82-92.

32. Liu, H., & Buskey, E. J. (2000). Hypersalinity enhances the production of extracellular polymeric substance (EPS) in the Texas brown tide alga, *Aureoumbral agunensis* (Pelagophyceae). Journal of Phycology, 36(1), 71-77.

33. Vidyarathna, N. K., &Granéli, E. (2012). Influence of temperature on growth, toxicity and carbohydrate production of a Japanese *Ostreopsis ovata* strain, a toxic-bloom-forming dinoflagellate. Aquatic Microbial Ecology, 65(3), 261-270.

34. Granéli, E., Vidyarathna, N. K., Funari, E., Cumaranatunga, P. R. T., & Scenati, R. (2011). Can increases in temperature stimulate blooms of the toxic benthic dinoflagellate *Ostreopsis ovata*. Harmful algae, 10(2), 165-172.

35. Ferreira, C. E. L. (2006). Sea urchins killed by toxic algae. JMBA global marine environment, 3, 22-23.

36. Nascimento, S. M., França, J. V., Gonçalves, J. E., & Ferreira, C. E., 2012. *Ostreopsis* cf. *ovata* (Dinophyta) bloom in an equatorial island of the Atlantic Ocean. Marine pollution bulletin, 64(5), 1074-1078

37. Kiørboe, T., Titelman, J., 1998. Feeding, prey selection and prey encounter mechanisms in the heterotrophic dinoflagellate *Noctiluca scintillans*. J. Plankton Res. 20, 1615–1636.

38. Blossom, H.E., Daugbjerg, N., Hansen, P.J., 2012. Toxic mucus traps: A novel mechanism that mediates prey uptake in the mixotrophic dinoflagellate *Alexandrium pseudogonyaulax*. Harmful Algae 17, 40–53.

39. Ciminiello, P., Dell'Aversano, C., Dello Iacovo, E., Fattorusso, E., Forino, M., Grauso, L., Tartaglione, L., Guerrini, F., Pistocchi, R., 2010. Complex palytoxin-like profile of *Ostreopsis ovata*. Identification of four new ovatoxins by high-resolution liquid chromatography/mass spectrometry. Rapid Commun. Mass Spectrom. 24, 2735–2744.

40. Ciminiello, P., Dell'Aversano, C., Dello Iacovo, E., Fattorusso, E., Forino, M., Tartaglione, L., 2011. LCMS of palytoxin and its analogues: State of art and future perspectives. Toxicon 57 (3), 376-389.

41. Ciminiello, P., Dell'Aversano, C., Dello Iacovo, E., Fattorusso, E., Forino, M., Grauso, L., Tartaglione, L., Guerrini, F., Pezzolesi, L., Pistocchi, R., Vanucci, S., 2012a. Isolation and structure elucidation of ovatoxin-a, the major toxin produced by *Ostreopsis ovata*. J. Am. Chem. Soc. 134, 1869–75.

42. Ciminiello, P., Dell'Aversano, C., Dello Iacovo, E., Fattorusso, E., Forino, M., Tartaglione, L., Battocchi, C., Crinelli, R., Carloni, E., Magnani, M., Penna, A., 2012b. Unique toxin profile of a Mediterranean *Ostreopsis* cf. *ovata* strain: HR LC-$MS^{(n)}$ characterization of ovatoxin-f, a new palytoxin congener. Chem. Res. Toxicol. 25, 1243–1252.

43. Penna A., Vila M., Fraga S., Giacobbe M.G., Andreoni F., Riobò P., Vernesi C. 2005. Characterization of *Ostreopsis* and *Coolia* (*Dinophyceae*) isolates in the Western Mediterranean Sea based on morphology, toxicity and Internal Transcribed Spacer 5.8s rDNA sequences[1].Journal of Phycology 41 (1), 212-225.

44. Perini F., Casabianca A., Battocchi C., Accoroni S., Totti C., Penna A. (2011). New approach using the real-time PCR method for estimation of the toxic marine dinoflagellate *Ostreopsis* cf. *ovata* in marine environment. PLoS ONE. 6 (3), e17699.

45. Casabianca S., Casabianca A., Riobó P., Franco J.M., Vila M., Penna A. (2013). Quantification of the toxic dinoflagellate *Ostreopsis* spp. by qPCR assay in marine aerosol. Envir. Sci Tech. 47: 3788-3795.

46. Ciminiello, P., Dell'Aversano, C., Fattorusso, E., Forino, M., Magno, G.S., Tartaglione, L., Grillo, C., Melchiorre, N. 2006 The Genoa 2005 outbreak. Determination of putative palytoxin in Mediterranean *Ostreopsis ovata* by a new liquid chromatography tandem mass spectrometry method. Anal. Chem. 78, 6153–6159.

47. Pini, V., Tiribilli, B., Gambi, C. M. C., & Vassalli, M. (2010). Dynamical characterization of vibrating afm cantilevers forced by photothermal excitation. Physical Review B, 81(5), 054302.

48. Morris VJ, Kirby AR, Gunning AP. 1999. Atomic Force Microscopy for Biologist. Imperial College Press: London.

49. Radić, T. M., Svetličić, V., Žutić, V., & Boulgaropoulos, B. (2011). Seawater at the nanoscale: Marine gel imaged by atomic force microscopy. Journal of Molecular Recognition, 24(3), 397-405.

50. Mandal, S. K., Singh, R. P., & Patel, V. (2011). Isolation and characterization of exopolysaccharide secreted by a toxic dinoflagellate, *Amphidinium carterae* Hulburt 1957 and its probable role in harmful algal blooms (HABs). Microbial ecology, 62(3), 518-527.

51. Pletikapić, G., Berquand, A., Radić, T. M., & Svetličić, V. (2012). Quantitative nanomechanical mapping of marine diatom in seawater using peak force tapping atomic force microscopy. Journal of Phycology, 48(1), 174-185.

Chapter 3: Determination of Palytoxins in Soft Coral and Seawater from a Home Aquarium. Comparison between *Palythoa*-and *Ostreopsis*-Related Inhalatory Poisonings

1. Introduction

Inhalatory exposure to palytoxin-producing microalgae represents a major matter of concern in the Mediterranean area where severe respiratory syndromes have affected people exposed to marine aerosols in concomitance to *Ostreopsis* blooms (mainly *O.* cf. *ovata*) [1-6]. The most serious sanitary problems have occurred throughout the Italian coastlines and along the French and Spanish Mediterranean coasts since 1998 [7-8]. On the basis of the concomitance of *Ostreopsis* blooms, respiratory illness in humans, and detection of palytoxins in algal samples, a cause and effect relationship between the cases of malaise and the algal toxins has been postulated. Only very recently, the presence of ovatoxins, and/or *O.* cf *ovata* cells has been demonstrated in marine aerosols [7,9], thus suggesting that *Ostreopsis*-related illness might be a reaction to the palytoxin congeners (ovatoxins) or an allergic-like reaction to cell fragments or even a combination of both.

Further cases of respiratory illness tentatively correlated to palytoxins have been reported for aquarium hobbyists from incidental inhalation of steams generated during cleaning operations of home aquaria containing *Palythoa* spp. [10-18]. These tropical soft-coral species are commonly used in home marine aquaria as decoration or may be even unintentionally introduced as hitchhikers with live rocks [19]. In some of the case reports the presence of palytoxins in the aquarium was proved on the basis of hemolytic and/or chemical evidence [10,13,18]. However, not all the *Palythoa* spp. sold in the aquarium trade have been found to contain palytoxin, which might account for the limited number of *Palythoa*-related poisonings. So the issue still remains controversial in the lack of statistically significant epidemiological studies.

In this study we report on the chemical analyses of the soft coral and the water contained in a home aquarium involved in the poisoning of an entire family [15]. A procedure for the extraction of palytoxins from seawater was developed. Unlike the other few previous such studies on the identification of the likely causative agent, the soft coral and the surrounding water were collected from the aquarium soon after the family

poisoning had occurred and analyzed through LC-HRMS. In addition, considering that both *Palythoa*- and *Ostreopsis*-related poisonings occur by the same exposure route and the toxins have a similar chemical structure, we have also compared the symptoms reported for patients poisoned during handling of home aquaria zoanthids and during *Ostreopsis* outbreaks. Since the environmental parameters during the exposure events were completely different (open-air versus domestic environment), the correlation of symptoms can be of help in clarifying the active role of the toxins in human poisonings.

2. Results and discussion

2.1 Background

An entire family - 2 adults (age 40 and 44) and 2 children (age 14 and 17) – was admitted to the Department of Intensive Care in the Isala Hospital (Zwolle, The Netherlands) with symptoms including high fever, tachycardia, dyspnea, cough, chest pain and nausea. A detailed description of the symptoms and clinical parameters has been recently reported by Wieringa *et al.* [15]. The family entered the hospital approximately 45 minutes after cleaning operation of their home aquarium. Soon after pouring hot water over a piece of rock infested with the zoanthid *Palythoa* sp. and consequent generation of steams, the patients developed cough in 1-2 min and dyspnea after 5 min. No detergent was used during the cleaning operations. All the patients were within 6 meters from the aquarium and the estimated total exposure time to the steams was 5 to 20 min. Considering the rapid onset of the symptoms upon handling the zoanthid, this was suspected to be the cause of the malaise. Therefore, a piece of the rock infested with the *Palythoa* sp. and 0.6 L of the surrounding water (synthetic seawater prepared by mixing water with specially prepared salts to imitate seawater) were collected from aquarium soon after the family poisoning and used for chemical analysis.

2.2 LC-HRMS of the aquarium samples

The zoanthid and the water samples were separately extracted and the crude extracts directly analyzed by LC-HRMS in full scan MS and MS^2 mode. The presence of high levels of palytoxin and very minute amounts of a hydroxypalytoxin was demonstrated in both the extracts and results of the analysis of the zoanthid are shown in Figure III.1 (a-b-c).

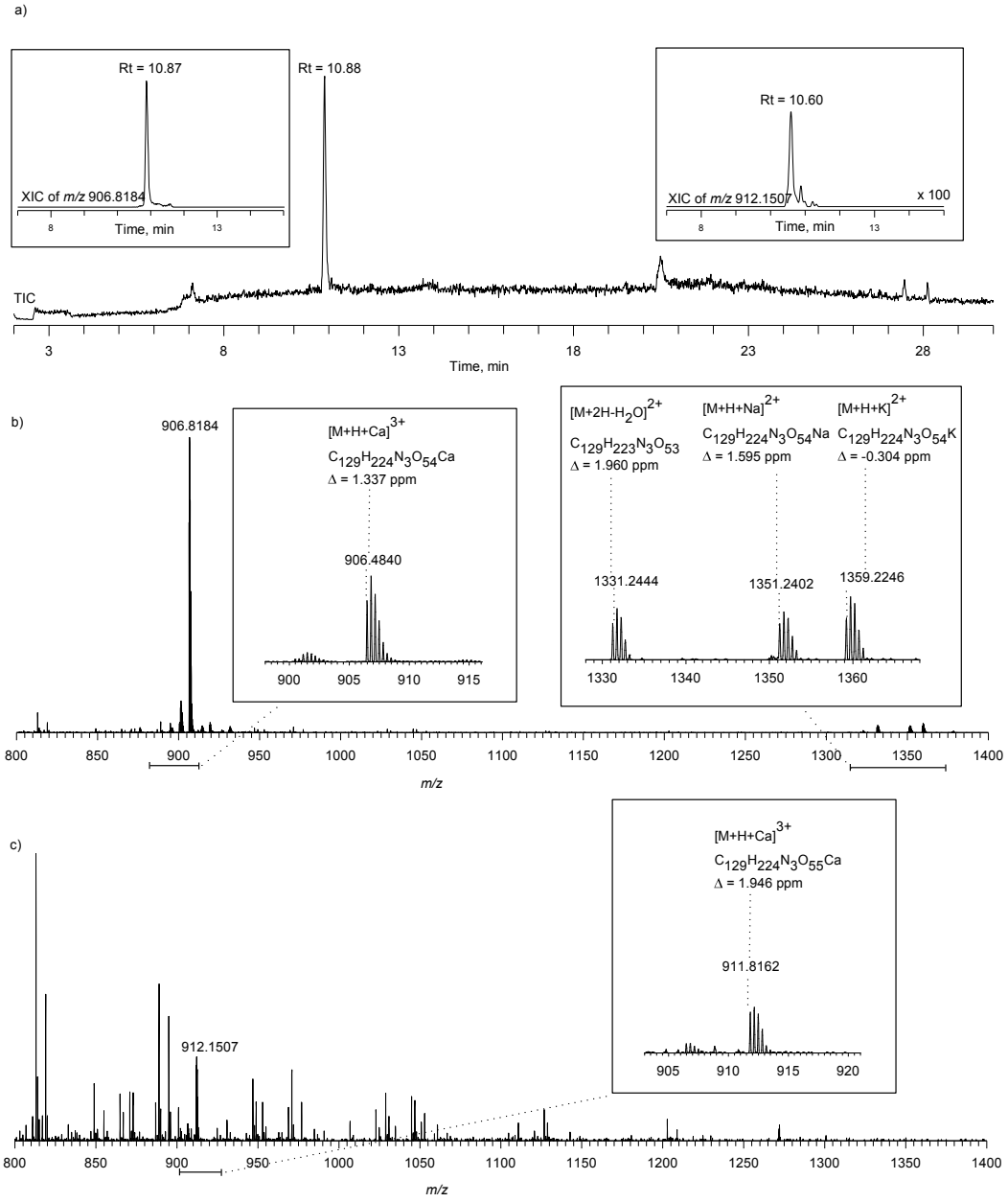

Figure III.1 TIC of the zoanthid (*Palythoa* sp.) extract and XICs of the $[M+H+Ca]^{3+}$ ion at *m/z* 912.1507 (framed on the right) and *m/z* 906.8184 (framed on the left) (a). Full HRMS spectra associated to the peaks at 10.88 min (b) and at 10.60 min (c). Enlargements of the regions *m/z* 900-915 and *m/z* 1320-1370 are shown together with elemental formula of triply and doubly charged ions.

The total ion chromatogram (TIC) (Figure III.1-a) was dominated by a chromatographic peak at 10.88 min. This peak eluted at the same retention time as PLTX standard (from *P. tuberculosa*) and presented a full scan HRMS spectrum (Figure III.1-b) superimposable to that of palytoxin in exact masses, isotopic ion patterns, and relative ion

ratios of triply and doubly charged ions. LC-HRMS^2 spectrum of the $[M+H+Ca]^{3+}$ at *m/z* 906.5 contained all the diagnostic fragment ions of palytoxin which were interpreted according to the approach we recently developed for gaining structural insights into palytoxin-like molecules [20]. All these data clearly indicated that palytoxin ($C_{129}H_{223}N_3O_{54}$) was the major component of the extracts.

Extracted ion chromatograms (XICs) of the triply-charged $[M+H+Ca]^{3+}$ ions of all the palytoxin congeners so far known allowed to highlight only the presence of a hydroxypalytoxin ($C_{129}H_{223}N_3O_{55}$) in the extracts as indicated by XIC of the $[M+H+Ca]^{3+}$ ion at *m/z* 912.1507 (framed in Figure III.1-a) and full MS spectrum associated to the peak eluting at 10.60 min (Figure III.1-c). We attempted to gain structural information on this analogue by a comparative analysis of its LC-HRMS^2 spectrum with that of Palytoxin [20] but, due to the low concentration of the toxin in the extracts, no diagnostic ion was detected. Thus the specific site of the molecule where the additional hydroxyl group was present could not be identified.

Quantitative analyses (Table III.1) indicated a total toxin content of both zoanthid and water extracts of 509 µg of palytoxin and 23.6 µg of a hydroxypalytoxin, with 86% of toxins (palytoxin and hydroxypalytoxin) contained in the water sample. Considering that during the shipment of the samples the zoanthid was immersed in the water, the highest toxin concentration recorded in water was likely due to an active secretion process of the zoanthid under stressful conditions.

Table III.1 Total toxin content of the zoanthid and the aquarium water samples

	Zoanthid		**Water**		**Total**
	µg	µg/cm^2	µg	µg/L	µg
Palytoxin	75	37	434	723	509
Hydroxypalytoxin	0.6	0.3	23	39	23.6

2.3 Optimization of a SPE procedure for extraction of palytoxin from seawater

Liquid/liquid extraction procedure employed in this study for the extraction of palytoxins from water was quite laborious: five extraction steps with butanol were needed to achieve a good recovery of the toxins [21]. As a result, large volumes of butanol (about 2.5 L) had to be evaporated and, considering the high boiling point of butanol, this was a time-consuming step. In addition, due to the high concentration of salts contained in the butanol extract, problems arose in the re-dissolution step with 70 mL of aqueous methanol being necessary. Even if this procedure turned out successful to extract palytoxin from the highly contaminated aquarium water, it is not feasible at relatively low contamination levels. Indeed, while at a spiking level of 2.25 mg/L this procedure provided a 75% recovery, a recovery of 13% was measured at a lower PLTX spiking level (5 µg/L). Poor solubility of the toxin after complete evaporation of the extract and/or adsorption of the toxin onto glass equipment used in the liquid/liquid extraction could be major reasons for toxin loss.

So the need emerged to set up a procedure more rapid, efficient and reliable than liquid/liquid extraction able to provide good recoveries also at relatively low contamination levels. A solid phase extraction (SPE) of palytoxin from seawater was thus optimized, testing four types of stationary phases (Oasis HLB, Strata-X, Sepabeads SP850, and Sepabeads SP205) on natural seawater spiked with PLTX at two spiking levels (2 µg/L and 0.2 µg/L). Compared to synthetic seawater, commonly used in home marine aquaria, natural seawater may contain organic matter that complicates toxin extraction and matrix interference. Different eluting systems (aqueous methanol with and without acid) were tested. Aqueous methanol 80% proved to be the optimum eluting solvent. However, at the highest spiking level of 2 µg/L palytoxin spread over 10 ml elute and the addition of trifluoroacetic acid 0.1% to the eluting solvent was necessary to elute the toxin in a smaller volume (5 mL). At the lowest spiking level, elution with aqueous methanol 80% with 0.1% TFA allowed to concentrate palytoxin in a 1 mL elute. Table III.2 reports recovery obtained for the stationary phases tested. While at the highest spiking level all the tested stationary phases proved able to efficiently recover palytoxin from seawater (recoveries in the range 60-71%), only Oasis HLB provided an acceptable recovery at the lowest spiking level with an average recovery of 50% and an ion suppression of 15%. This SPE procedure is a valid tool to rapidly and efficiently extract palytoxins from sea-water even when

contamination level is low. The observed toxin loss could be related to adsorption onto SPE cartridge material and onto glass vials used to collect eluates as well as to toxin degradation under strong acid conditions. Eluates in aqueous methanol 80% with 0.1% TFA had to be analyzed soon after collection to minimize toxin degradation. Further studies are needed to improve toxin recoveries.

Table III.2 Palytoxin recovery from spiked seawater and ion suppression (IS) using four types of SPE sorbents (n =3)

Stationary phase	Recovery (%)		IS (%)
	[PLTX], 2µg/L	[PLTX], 0.2µg/L	
HLB	71±5	50±3	15
STRATA-X	70±4	nd	51
SP-850	65±2	15±2	21
SP-207	60±3	7±2	21

2.4 Comparison between *Ostreopsis*- and *Palythoa*-related poisonings

Once ascertained the presence of palytoxins in the aquarium as the probable cause of the whole family poisoning, we have correlated the symptomatology shown by the family members with that reported for other inhalatory poisonings tentatively ascribed to palytoxin congeners.

The number of case reports and/or anecdotal references describing human poisonings due to handling of *Palythoa* spp. from home aquarium is quite limited with a total of 42 people involved (Table III.3). Exposure occurred in most cases through inhalation of steam generated during installation or cleaning operation of home aquaria containing *Palythoa* spp. and in 6 cases through dermal contact with the zoanthids and/or the aquarium water. For most of the reported poisonings the possible involvement of palytoxins was postulated based on the assumption that some *Palythoa* spp. (*P. toxica*, *P. tuberculosa*, *P. heliodiscus*, among others) are known to contain palytoxin congeners. To our knowledge, in only one case of skin injury following contact with a *Parazoanthus* sp. high levels of palytoxins were detected through delayed hemolysis assay [13] and in only two cases of inhalation exposure of aquarium hobbyists in Virginia (USA) [10] and in Alaska (USA) [18] the presence of the palytoxins in the zoanthids was confirmed through hemolysis neutralization assay, LC-UV, and LC-MS analyses. Both the exposure route and the symptomatology reported for the Virginia and the Alaska hobbyists were similar to those of the family members in The Netherlands [15].[8]

Table III.3 Symptoms reported for inhalation and dermal poisonings following exposure to *Ostreopsis* spp. in Italy, France, and Spain and to *Palythoa* spp. in home aquaria.

	Ostreopsis-related poisonings						*Palythoa*-related poisonings								
n° of cases	**228**[1]	**28**[2]	**100**[3]	**4**[4]	**43**[5]	**57**[6]	**2**[10]	**3**[11]	**11**[12]	**1**[13]	**6**[14]	**4**[15]	**4**[16]	**1**[17]	**10**[18]
Fever (≥38°C)	x	x	x	x	x	x		x	x		x	x	x		x
Difficulty breathing/dyspnea and/or bronchoconstriction	x	x		x	x	x	x	x	x	x	x	x		x	x
Cough/dry or mildly productive cough	x	x	x			x	x	x	x		x	x			x
Arthralgia/joint pain/myalgia			x		x	x				x	x		x		x
Weakness and discomfort of the extremities/fatigue/ malaise					x	x	x			x	x		x		x
Headache	x				x	x		x	x				x		x
Dysguesia/Bitter metallic taste, nausea and/or vomiting/diarrhea	x	x		x	x			x	x		x	x	x		x
Dizziness/lightheadedness/vertigo					x	x	x			x					x
Mucous hypersecretion/rhinorrhea	x	x			x	x	x								
Dermatitis/skin irritation/ pruritus/erythema/swelling	x				x	x			x	x			x		
Chest Pain						x	x		x	x	x	x		x	
Wheezes		x									x			x	
Conjunctivitis/lacrimation/tearing	x	x			x	x									
Mucosal irritation (eye, nose, lip, tongue)/sneezing			x	x	x	x									
Dry throat/sore throat/ pharyngeal pain/pharyngitis/odynophagia	x			x		x									x
Chills/shivering								x		x	x		x		x
Numbness/paresthesia/glassy eyes/ speech disturbance/collapse							x			x	x		x		x
Rhabdomyolysis							x								
Tachycardia							x	x	x		x	x	x		

Similarities in symptomatology and exposure route (inhalation of steams) stretch also over the other case reports [11-12,14-17] suggesting that the causative agent of all these poisonings is the same, although the presence of palytoxin was not conclusively proven. LC-HRMS detection of palytoxins (palytoxin and hydroxypalytoxin) as the major components of both the soft coral and the aquarium water extracts reported herein suggests that the actual causative agent is the palytoxin-complex.

Inhalatory poisonings following exposure to *Palythoa* spp. in home aquaria resemble those registered in the toxic events occurred in concomitance of *Ostreopsis* spp. blooms (Table III.3) in Italy, [1-3] France 4-5], and Spain [6].It is worth noting that, from a chemical standpoint, toxins involved in *Palythoa*-related poisonings (palytoxin, hydroxypalytoxin, deoxypalytoxin among others) and those involved in *Ostreopsis*

-related poisonings (ovatoxins) differ little in structural details. As a consequence, although relative potencies of individual congeners with respect to the parent compound (palytoxin) might be different [22-23], the overall symptomatology induced by the palytoxin-complex (from *Palythoa* spp.) or the ovatoxin-complex (from *Ostreopsis* spp.) is likely to be the same. Statistically significant epidemiological studies for the *Palythoa*-related poisonings are lacking and for the *Ostreopsis* phenomenon they are quite limited; nonetheless a comparison of the symptoms shown by the patients exposed to either *Palythoa* spp. or to *Ostreopsis* spp. can still be done.

Although some symptomatological differences occur between *Palythoa*- and *Ostreopsis*-related poisonings, there are several symptoms that are definitely common to both poisonings and some others that recur more occasionally. The most common symptoms include fever (≥ 38° C), difficulty in breathing, dyspnea, and/or bronchoconstriction, cough, and assorted flu-like symptoms (arthralgia, joint pain, myalgia, weakness, fatigue, and headache). Some gastro-intestinal signs (dysguesia, nausea and/or vomiting, diarrhea) as well as dizziness, lightheadedness and vertigo have been also reported in most of the *Ostreopsis*- and *Palythoa*-related poisonings. Some symptoms such as mucous hypersecretion, dermatitis, skin irritation, pruritus, erythema, and swelling have been reported more frequently in *Ostreopsis*-related poisonings than in *Palythoa*-related poisonings. Some others were apparently unique of either the *Ostreopsis*-related poisonings (mucosal irritation, conjunctivitis, sore throat, pharyngeal pain) or of the *Palythoa*-related poisonings (chills, numbness, paresthesia, speech disturbance, collapse, rhabdomyolysis, and tachycardia). However, such discrepancies could depend on the

different exposure times and conditions (domestic and open-air environments) which affect the dose of inhaled aerosols as well as on individual sensitivity to the toxic agents.

As for the clinical parameters, in most of the *Palythoa*-related poisonings an increase of creatine kinase (CK), C-reactive protein (CRP) and lactate dehydrogenase (LDH) as well as a significant leukocytosis has been reported indicating the irritating and inflammatory potential of palytoxin (Table III.4). Chest radiograph showed no infiltrates and electrocardiogram (ECG) was normal in most cases with the only exception of 2 case reports [10,13].

Only a limited number of clinical data have been reported for *Ostreopsis*-related poisonings [1] and therefore a reliable comparison of clinical parameters with those reported for *Palythoa*-related illness is not doable. However, the few available clinical data [1] indicated also for *Ostreopsis*-related poisonings a significant leukocytosis (10.1-23.9 x 10^9/L) and neutrophilia (75.2-91.5 x 10^9/L), pointing once again to an irritating and inflammatory potential for palytoxin congeners. Likewise, electrocardiograms and chest-X-rays gave negative results. Values of CK, CRP, LDH were not reported [1].

Table III.4 Clinical parameters reported for *Palythoa*-related poisonings in home aquariums.

	Palythoa-related poisonings								
n° of cases	**2**[10]	**3**[11]	**11**[12]	**1**[13]	**6**[14]	**4**[15]	**4**[16]	**1**[17]	**10**[18]
Creatine Kinase (CK)[a]	508 U/L			198 U/L	184-197 U/L	<170-215 U/L			
C-reactive protein (CRP)[b]		193.3 mg/L		13.8 mg/L		<1-228 mg/L	174 mg/L		
Lactate dehydrogenase (LDH)[c,g]		↑		304 U/L	193-331 U/L				
Leucocytes[d,g]		27.6 x 10^9/L	↑		10.7-34.1 x 10^9/L	15-33.5 x 10^9/L	22.9 x 10^9/L	21.0 x 10^9/L	
Neutrophils[e,g]					87%	15-31 x 10^9/L			
Oxygen saturation (SO_2)[f,g]		93%	↓		98%	88-93%		100%	96%

[a]Normal range CK< 200 U/L
[b]Normal range CRP < 5 mg/L
[c]Normal range LDH= 135-225 U/L
[d]Normal range Leucocytes= 4-10 x10^9/L
[e] Normal range Neutrophils= 2.00-7.20 x10^9/L or 40-75%
[f]Normal range SO_2= 95-100%
[g] ↑and ↓ indicate unspecified levels higher and lower than the normal range, respectively

3. Materials and methods

3.1 Extraction

A stone covered by 2 cm^2 of the zoanthid *Palythoa* sp. was collected, together with 0.6 L of the surrounding water (synthetic seawater), from the home aquarium involved in the case report [15] and used at the Department of Pharmacy, University of Napoli Federico II for chemical analysis. The zoanthid attached to the stone was submerged in 300 mL of methanol/water (8:2) and sonicated thrice for 5 min each round. The resulting extract was centrifuged at 4800 g for 10 min. The supernatant was evaporated, dissolved in 10 ml of methanol/water (1:1) and eventually analyzed by LC-HRMS (5 µl injected). The aquarium water (0.6 L) was extracted five times with an equal volume of butanol. The butanol layer was evaporated to dryness, dissolved in 70 mL of methanol/water (1:1), filtered through Ultrafree MC 0.45 µm centrifugal filter units and analyzed by LC-HRMS (5 µl injected). Accuracy of the liquid/liquid extraction of palytoxin from seawater was measured repeating the above described procedure on 100 mL of blank seawater (natural seawater) spiked with 500 ng of palytoxin (palytoxin spiking level = 5 µg/L). Spiking was carried out adding 25 µL of palytoxin stock solution (20 µg/mL) diluted in methanol/water (1:1). Matrix matched (MM) standards were used for quantitation.

3.2 LC-HRMS

LC-HRMS experiments were carried out on a hybrid linear ion trap LTQ Orbitrap XL™ Fourier Transform MS (FTMS) equipped with an ESI ION MAX™ source (Thermo-Fisher, San Josè, CA, USA) coupled to an Agilent 1100 LC binary system (Palo Alto, CA, USA). LC conditions included the use of a 2.6 µm, 100 × 2.10 mm Kinetex C18 column (Phenomenex, Torrance, CA, USA) maintained at room temperature and eluted at 0.2 mL/min with water (eluent A) and 95% acetonitrile/water (eluent B), both containing 30 mM acetic acid. The following gradient elution was used: 25-30% B in 15 min, 30-100% B in 1 min, 100% B for 5 min. Re-equilibration time was 9 min. Under such conditions, PLTX standard eluted at 10.88 min [24].

HR full scan MS experiments (positive ions) were carried out in the mass range *m/z* 800-1400 at a resolving power of 60,000. The following source settings were used: a spray voltage of 4 kV, a capillary temperature of 290°C, a capillary voltage of 22 V, a sheath gas and an auxiliary gas flow of 35 and 1 (arbitrary units). The tube lens voltage was set at 110 V. $HRMS^2$ data were acquired in collision induced dissociation (CID) mode at a resolving

power of 30,000 by selecting the $[M+H+Ca]^{3+}$ ions of palytoxin (*m/z* 906.5) and hydroxypalytoxin (*m/z* 912.5) as precursors. A collision energy of 25%, an activation Q of 0.250, and an activation time of 30 msec were used. Calculation of elemental formulae of ions contained in HRMS spectra was performed by using the mono-isotopic ion peak of each ion cluster. The isotopic pattern of each ion cluster was considered in assigning molecular formulae. Extracted ion chromatograms (XIC) for palytoxins were obtained by selecting the most abundant ion peaks of $[M+H+Ca]^{3+}$ ion clusters by using a mass tolerance of 5 ppm.

A PLTX standard (100 µg; Lot. LAM7122) from Wako Chemicals GmbH (Neuss, Germany) was dissolved in methanol/water (1:1, v/v) and used for quantitative analyses. It should be noted that this standard is not certified and contains some minor contaminants besides palytoxin itself. Preliminary LC-HRMS analysis of the standard diluted 1:100 showed that it contained 83% of palytoxin itself, 5% of a hydroxypalytoxin, and 12% of other contaminants. PLTX standard was used to generate a five levels calibration curve (100, 50, 25, 12.5, 6.25 ng/mL). Calibration points were the result of triplicate injection and peak areas were used for plotting. Under the used instrumental conditions, measured limit of detection (LOD) and quantitation (LOQ) for PLTX in solvent were 1.3 ng/mL and 2.6 ng/mL, respectively, corrected for the 83% purity of the standard.

3.3 SPE of Palytoxin from seawater

Blank seawater samples were collected from the gulf of Naples and filtered through 0.45 mm Whatman filter to eliminate particulate matter. Blank and spiked (0.2 µg/L or 2 µg/L) aliquots of natural seawater (100 mL) were loaded onto four different 500-mg sorbent bed cartridges - Oasis HLB LP (Waters, USA), Strata-X (Phenomenex, USA), Sepabeads®SP-850 and SP-205 (Sigma Aldrich, Italy) - previously conditioned with MeOH 100%, aqueous MeOH 80% and 10%, and H_2O 100%. Experiments were carried out in triplicate. The sorbent was never allowed to dry during either the conditioning or the sample loading steps. The following washing and eluting conditions were used:

- Wash 1: 3 mL H_2O 100%,
- Wash 2: 3 mL aqueous MeOH 10%
- Elute 1-15: 1 mL aqueous MeOH 80% with or without 0.1 % trifluoroacetic acid (TFA).
- Eluates were collected as 1 mL fractions for 15 mL total volume.

- Elute 16-20: 1 mL MeOH 100%. Eluates were collected as 1 mL fractions for 5 mL total volume.

MM standards of palytoxins were prepared spiking the SPE eluate of the blank seawater with PLTX standard in the range 10-20 ng/mL and used for quantitation.

3.4 Accuracy, Reproducibility, and Matrix effect

Accuracy was expressed in terms of recovery as [(observed concentration/(spiked concentration)] x 100. Reproducibility was expressed in terms of relative standard deviation (RSD) over the three experimental replicates. Ion suppression was assessed as: 100 -[(peak area of Matrix Matched standard)/(peak area of Matrix Free standard)] x 100.

3.5 Literature search

The terms "*Palythoa*, *Ostreopsis*, palytoxin(s), ovatoxin(s), coral, zoanthids" and their combination with "poisoning, intoxication, injury, inhalation exposure, aquarium, fever, trade, aerosols, case report, respiratory impairment, vapor, aquarism, human risk, skin, surveillance, manipulation" were searched using SciFinder and PubMed databases. The search was refined using bibliography cited within each reference.

4. Conclusions

Our study, besides development of a SPE procedure for the extraction of palytoxins from seawater, unequivocally demonstrated the presence of palytoxins in both the soft-coral and the aquarium water collected from a home aquarium soon after the inhalatory poisoning of four family members in the Netherlands. This finding supports the hypothesis that palytoxins may exert their toxic effect by inhalation exposure such as the recent finding of ovatoxins in marine aerosols collected during *O.* cf. *ovata* blooms [7] strongly supports their involvement in *Ostreopsis*-related inhalatory poisonings. Although clinical parameters reported for *Ostreopsis* cases are limited, based on both chemical and symptomatological evidence it seems reasonable to hold palytoxins responsible for the human inhalatory sufferings related either to *Ostreopsis* blooms or to handling of *Palythoa* spp. Accordingly, the short time between exposure and development of symptoms in all the case reports make an infectious etiology unlikely.

Further support to this hypothesis might be obtained by studying the mechanism of palytoxin aerosolization in a laboratory setting, in order to check chemical composition and

particle size distribution of the aerosols. In addition, considering the flu-like nature of the symptomatology, a formal epidemiological study involving both the emergency units and the private pharmacies would be useful. Such interdisciplinary approach (chemical and epidemiological) was already adopted for other microalgal toxins and revealed effective to demonstrate inhalation as a potential way of exposure to microcystins and brevetoxins [25-26], thus allowing their correct risk evaluation [27].

Although the body of evidence points to a palytoxin inhalatory poisoning, the possible involvement of other unidentified toxins cannot be excluded in all cases. The conclusive proofs that palytoxins are the actual culprit of the poisonings would be testing their inhalatory hazard through *in vivo* models and/or detecting such toxins in bodily fluids. Toxicological studies are currently hampered by the lack of sufficient amounts of reference material, while the analysis of palytoxins in biological fluids is prevented by the lack of efficient analytical methodologies able to recover and detect their very low concentrations in such complex organic matrices.

References

1. Durando P, Ansaldi F, Oreste P, Moscatelli P, Marensi L, Grillo, C, Gasparini R, Icardi, G. *Ostreopsis ovata* and human health: epidemiological and clinical features of respiratory syndrome outbreaks from a two-year syndromic surveillance, 2005-2006 in north-west Italy. Euro Surveill. 2007, 12 (23)
http://www.eurosurveillance.org/ViewArticle.aspx?ArticleId=3212

2. Gallitelli M, Ungaro N, Addante LM, Procacci V, Gentiloni N, Sabba C. Respiratory illness as a reaction to tropical algal blooms occurring in a temperate country. JAMA. 2005, 293 (21), 2599-2560

3. Sansoni G, Borghini B, Camici G, Casotti M, Righini P, Rustighi C. Fioriture algali di *Ostreopsis ovata* (*Gonyaulacales: Dinophyceae*): un problema emergente. Biologia Ambientale. 2003, 17 (1), 17-23

4.Kermarec F, Dor F, Armengaud A, Charlet F., Kantin R, Sauzade D, de Haro L. Health risks related to *Ostreopsis ovata* in recreational waters. Environnement, Risques & Santé. 2008, 7, 357−363. [in French]

5. Tichadou L, Glaizal M, Armengaud A, Grossel H, Lemée R, Kantin R, Lasalle JL, Drouet G, Rambaud L, Malfait P, de Haro L. Health impact of unicellular algae of the *Ostreopsis* genus blooms in the Mediterranean Sea: experience of the French

Mediterranean coast surveillance network from 2006 to 2009. Clin Toxicol. 2010, 48 (8), 839−844

6.Barroso García P, Rueda de la Puerta P, Parrón Carreño T, Marín Martínez P, Guillén Enríquez J. Brote con síntomas respiratorios en la provincia de Almería por una posible exposición a microalgas tóxicas. Gac Sanit. 2008, 22, 578−584. [In Spanish]

7. Ciminiello P, Dell'Aversano C, Dello Iacovo E, Fattorusso E, Forino M, Tartaglione L, Benedettini G, Onorari M, Serena F, Battocchi C, Casabianca S, Penna, A. First Finding of *Ostreopsis* cf. *ovata* Toxins in Marine Aerosols. Environ Sci Technol. 2014, 48(6), 3532-3540

8. Tubaro A, Durando P, Del Favero G, Ansaldi F, Icardi G, Deeds JR, Sosa S. Case definitions for human poisonings postulated to palytoxins exposure. Toxicon. 2011, 57, 478–495

9. Casabianca S, Casabianca A, Riobó P, Franco J, Vila M, Penna, A. Quantification of the toxic dinoflagellate *Ostreopsis* spp. by qPCR assay in marine aerosol. Environ Sci Technol. 2013, 47, 3788−3795

10. Deeds JR, Schwartz MD. Human risk associated with palytoxin exposure. Toxicon. 2010, 56, 150–162

11. Bernasconi M, Berger D, Tamm M, Stolz D. Aquarism: An Innocent Leisure Activity? Respiration. 2012, 84, 436–439

12. Dijkman MA, de Vries I. Manipulation of zoanthids in home marine aquarium: unexpected cause of intoxication involving a whole family. Abstracts Toxins 2012/Toxicon. 2012, 60, 146

13. Hoffmann K, Hermanns-Clausen M, Buhl C, Büchler MW, Schemmer P, Mebs D, Kauferstein S. A case of palytoxin poisoning due to contact with zoanthid corals through a skin injury. Toxicon. 2008, 51 (8), 1535-1537

14. Sud P, Su MK, Greller HA, Majlesi N, Gupta A. Case Series: Inhaled Coral Vapor-Toxicity in a Tank. J Med Toxicol. 2013, 9, 282-286

15. Wieringa A, Bertholee D, Ter Horst P, van den Brand I, Haringman J, Ciminiello P. Respiratory impairment in four patients associated with exposure to palytoxin containing coral. Clin Toxicol. 2014, 52 (2), 150-151

16. Snoeks L, Veenstra J. Een gezin met koorts na reiniging van zeeaquarium. Ned Tijdschr Geneeskd. 2012, 156, A4200(1-3). [in Dutch]

17. Majlesi N, Su MK, Chan GM, Lee DC, Greller HA. A case of Inhalation exposure to Palytoxin. Clinical Toxicol. 2008, 46 (7), 637

18. Hamade AK, Deglin SE, McLughlin JB, Deeds JR, Handy SM, Knolhoff AM. Suspected palytoxin inhalation exposures associated with zoanthid corals in aquarium shops and homes – Alaska 2012-2014
http://www.cdc.gov/mmwr/preview/mmwrhtml/mm6431a4.htm

19. Deeds JR, Handy SM, White KD, Reimer JD. Palytoxin Found in Palythoa sp. Zoanthids (Anthozoa, Hexacorallia) Sold in the Home Aquarium Trade. PLoS One. 2011, 6 (4), e18235. DOI 10.1371/journal.pone.0018235

20. Ciminiello P, Dell'Aversano C, Dello Iacovo E, Fattorusso E, Forino M, Grauso L, Tartaglione L. High resolution LC-MSn fragmentation pattern of palytoxin as template to gain new insights into ovatoxin-a structure. The key role of calcium in MS behavior of palytoxins. J Am Soc Mass Spectrom. 2012, 23 (5), 952-963

21. Ciminiello P, Dell'Aversano C, Fattorusso E, Forino M, Magno GS, Tartaglione L, Grillo C, Melchiorre N. The Genoa 2005 outbreak. Determination of putative palytoxin in Mediterranean *Ostreopsis ovata* by a new liquid chromatography tandem mass spectrometry method. Anal Chem. 2006, 78, 6153–6159

22. Ito E, Yasumoto T. Toxicological studies on palytoxin and ostreocin-D administered to mice by three different routes. Toxicon. 2009, 54, 244–251

23. Sosa S, Del Favero G, De Bortoli M, Vita F, Soranzo MR, Beltramo D, Ardizzone M, Tubaro A. Palytoxin toxicity after acute oral administration in mice. Toxicol Lett. 2009, 191, 253–259

24. Ciminiello P, Dell'Aversano C, Dello Iacovo E, Forino M, Tartaglione L. Liquid chromatography–high-resolution mass spectrometry for palytoxins in mussels. Anal Bioanal Chem, 2015, 407, 1463–1473

25. Backer LC, Carmichael W, Kirkpatrick B, Williams C, Irvin M, Zhou Y, Johnson TB, Nierenberg K, Hill VR, Kieszak SM, Cheng YS. Recreational Exposure to Low Concentrations of Microcystins During an Algal Bloom in a Small Lake. Mar Drugs. 2008, 6(2), 389-406

26. Cheng YS, Zhou Y, Irvin CM, Pierces RH, Naar J, Backer LC, Fleming LE, Kirkpatrick B, Baden DG. Characterization of marine aerosol for assessment of human exposure to brevetoxins. Environ Health Persp. 2005, 113, 638–643

27. Fleming LE, Kirkpatrick B, Backer LC, Walsh CJ, Nierenberg K, Clark J, Reich A, Hollenbeck J, Benson J, Cheng YS, Naar J, Pierce R, Bourdelais AJ, Abraham WM, Kirkpatrick G, Zaias J, Wanner A, Mendes E, Shalat S, Hoagland P, Stephan W, Bean J, Watkins S, Clarke T, Byrne M, Baden DG. Review of Florida red tide and human health effects. Harmful Algae. 2011, 10, 224-233

Chapter 4: Chemical, molecular and eco-toxicological investigation of *Ostreopsis* spp. from Cyprus Island. Structural insights into four new ovatoxins by LC-HRMS/MS

1. Introduction

This study is the result of a collaborative effort among chemists, molecular ecologists and eco-toxicologists aimed at defining whether *Ostreopsis* spp. from Cyprus Island is a toxin-producing species. Six strains of *Ostreopsis* spp. were isolated in the summer 2013 in recreational marinas located on Cyprus Island. Molecular methods were used to identify the taxonomy of this microalga and an eco-toxicological assay was used to test its toxicity. The *Ostreopsis* spp. strains were analyzed by LC-HRMS^n (n= 1,2). The employed approach [1] uses the fragmentation pattern of a structurally defined palytoxin congener, such as PLTX [2-3] or OVTX-a [4] (Figure IV.1), as a template for structural characterization of the unknown [5-6] providing tentative structures.

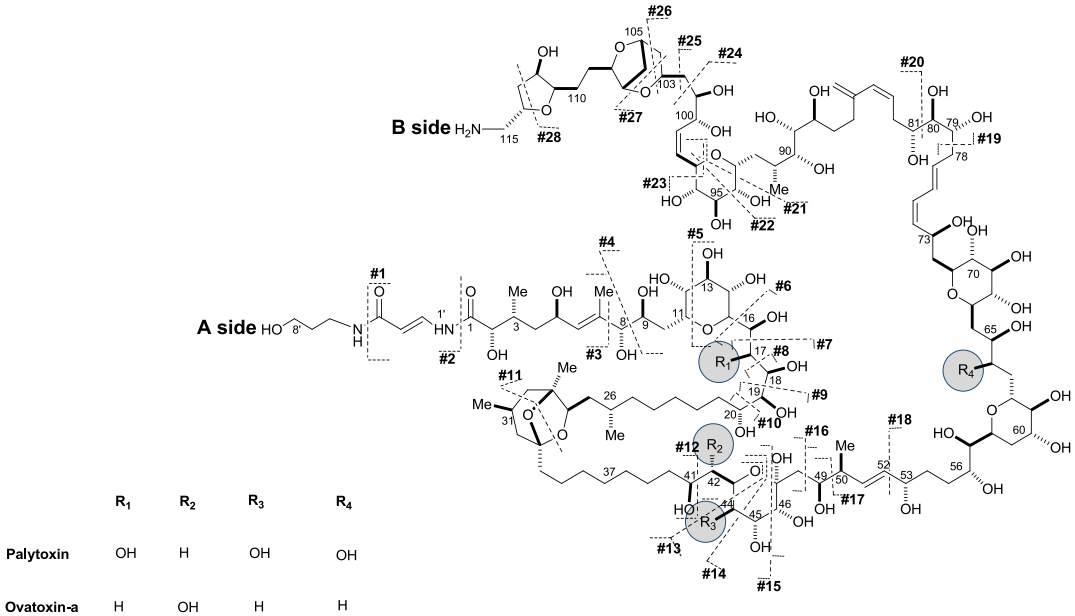

	R_1	R_2	R_3	R_4
Palytoxin	OH	H	OH	OH
Ovatoxin-a	H	OH	H	H

Figure IV.1 Structure of PLTX [2-3] and OVTX-a [4,7] as determined by NMR studies. Cleavage #14, #20, #28 and #6+12 occur only in PLTX [1]. The stereochemistry ofPLTX is depicted. The stereochemistry of OVTX-a is inverted at position

2. Results and discussion

2.1 Chemical analysis

Six strains of *Ostreopsis* spp. were collected during the summer 2013 at Vasiliko Bay (Cyprus). The sequence alignment analysis of ribosomal ITS-5.8S gene of all the *Ostreopsis* spp. strains (CBA-C1012, CBA-C1017, CBA-C1019, CBA-C1020, CBA-C1035 and CBA-C1036) in BLAST silico platform gave the 99-100% identity with other ribosomal sequences of *Ostreopsis* spp. KC86 and KC84 from the Aegean Sea, which belong to the Atlantic/Mediterranean *Ostreopsis* spp. clade [8-9]. This is a different clade from *O.* cf. *ovata* that still remains to be taxonomically named. This clade includes strains from the eastern Mediterranean (including the above Cypriot strains) and the eastern Atlantic regions.

LC-HRMS^n (n=1, 2) experiments were performed on algal extracts to characterize their toxin profiles and measure their toxin content. The analyses were carried out versus a palytoxin standard and two Mediterranean *O.* cf. *ovata* extracts containing most of the ovatoxins previously characterized, namely the Adriatic OOAN0601 extract [10] and the Ligurian CBA-29 extract [11]. Total ion chromatograms (TICs) of all the Cypriot extracts showed peaks barely emerging from the background noise. However, the analysis of the region where palytoxin congeners elute (Rt = 8-16 min) and of the extracted ion chromatograms (XICs) of triply charged ions of all the known PLTX-like compounds (Table IV.1), suggested that three of the analyzed extracts (CBA-C1019, CBA-C1020 and CBA-C1035) contained the known OVTX-a, -d, -e, and isobPLTX while the other three extracts (CBA-C1012, CBA-C1017, and CBA-C1036) contained only new palytoxin-like compounds. Figure IV.2 shows XICs of three representative *Ostreopsis* spp. extracts (CBA-C1012, CBA-C1036 and CBA-C1020) versus the reference Adriatic and Ligurian *O.* cf. *ovata* samples.

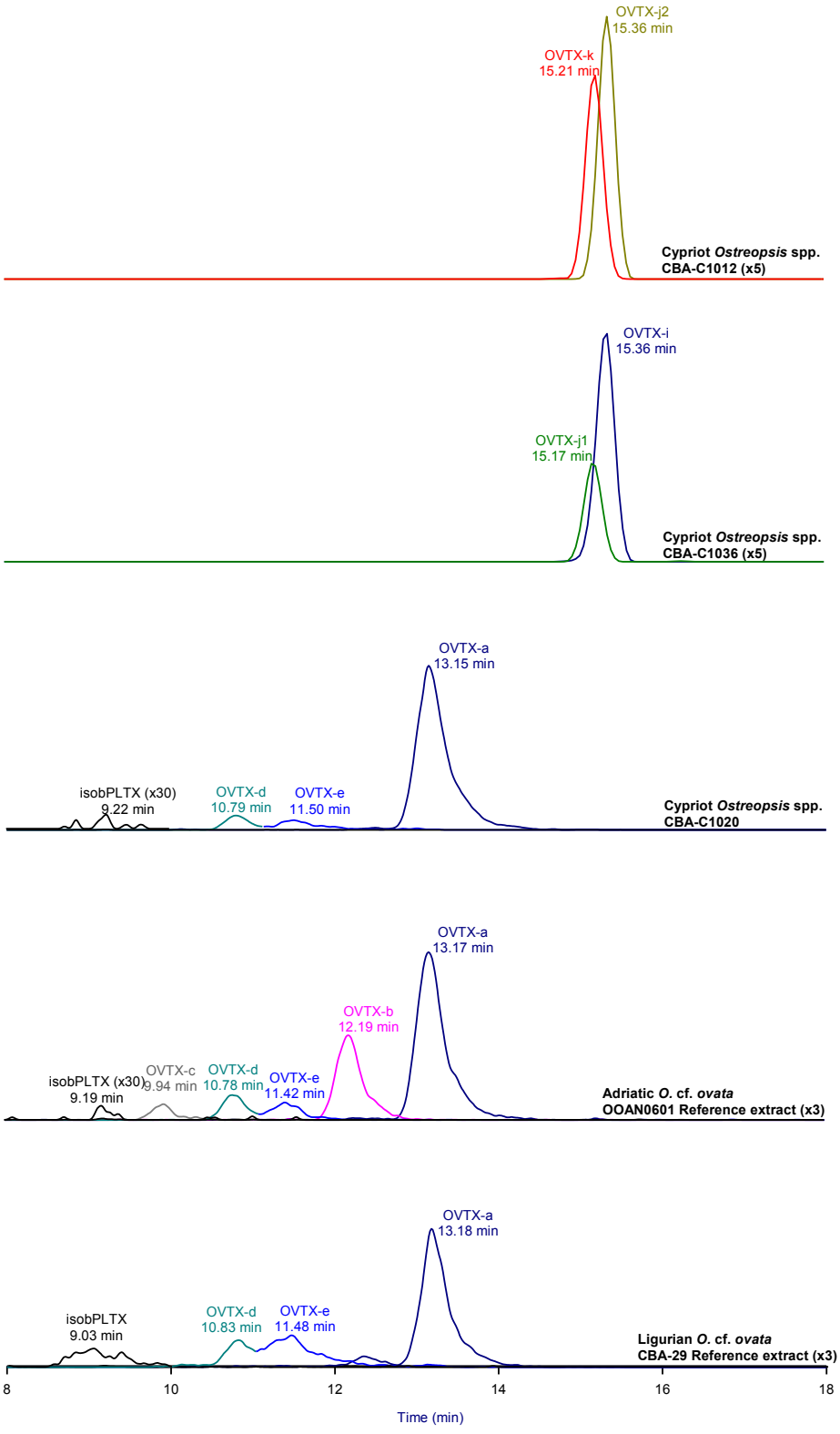

Figure IV.2 Extracted ion chromatograms of $[M+H+Ca]^{3+}$ ions of known and new ovatoxins (OVTXs) contained in some representative *Ostreopsis* spp. extracts from Cyprus Island and in Adriatic and Ligurian *O.* cf. *ovata* extracts which were used as reference.

The identity of OVTX-a, -d, -e, and isobPLTX in CBA-C1019, CBA-C1020 and CBA-C1035 extracts was assessed based on comparison of their retention times (Figure IV.2) and associated full MS spectra (Table IV.1) with those of OVTX-a, -d, -e, and isobPLTX contained in the reference extracts. Further confirmation for the identity of OVTX-a and of the structural isomers OVTX-d and -e was provided by LC-HRMS^2 spectra of their $[M+H+Ca]^{3+}$ ions at *m/z* 896.1 and 901.5, respectively, which were superimposable to those of ovatoxin-a, -d and -e previously characterized [12-13]. Concentration of isobPLTX in the extracts was too low for acquiring HRMS^2 data thus hampering further confirmation based on the analysis of its fragmentation pattern.

Interestingly, although the analyzed *Ostreopsis* spp. strains did not belong to the *O.* cf. *ovata* clade, some of them (CBA-C1019, CBA-C1020 and CBA-C1035) produced known ovatoxins and their toxin profile qualitatively matched that found in about 40% of the Mediterranean *O.* cf. *ovata* strains analyzed so far [13]. So ovatoxins seem not to be species specific compounds.

In-depth investigation of TIC of CBA-C1012, CBA-C1017, and CBA-C1036 extracts highlighted the presence in the range 15-16 min of four new palytoxin-like compounds (Figure IV.2). Even if molecular results identified *Ostreopsis* spp. from Cyprus Island as a species distinct from *O.* cf. *ovata*, we decided to name the new compounds ovatoxin-i, -j_1, -j_2, and k, to highlight that ovatoxins are not typical secondary metabolites of a single *Ostreopsis* species, such as *O.* cf. *ovata*. Full HRMS spectra of the new compounds typically contained triply charged ions in the region *m/z* 830–950 and doubly charged ions in the region *m/z* 1250–1400 (Figure IV.3). A cross check of the elemental formulae of all the ions (error < 3 ppm) contained in the spectra allowed to assign the molecular formulae to the new ovatoxins (Table IV.1).

Table IV.1 Data from HRMS of ovatoxins (OVTX-a, -d, -e, -i, -j_1, -j_2, k) and isobaric palytoxin (isobPLTX) contained in full HRMS spectra (mass range *m/z* 800-1400) of all *Ostreopsis* spp. strains from Cyprus Island. Theoretical molecular mass (M)and elemental formulae assigned to the mono-isotopic ion peaks of the most intense triply and doubly charged ions and relative double bonds equivalents (RDB). Mass errors were below 3 ppm in all cases. n.d. = not detected.

		Theoretical [M]	Triply charged ions					Doubly charged ions					
			$[M+H+Ca]^{3+}$	$[M+H+Mg]^{3+}$	$[M+3H-2H_2O]^{3+}$	$[M+3H-3H_2O]^{3+}$	$[M+H+K]^{2+}$	$[M+H+Na]^{2+}$	$[M+2H]^{2+}$	$[M+2H-H_2O]^{2+}$	$[M+2H-2H_2O]^{2+}$	$[M+2H-3H_2O]^{2+}$
	m/z	2678.4796	895.8189	890.4939	871.1633	865.1598	1343.2250	1335.2413	1324.2418	1315.2465	1303.2413	1297.2351
OVTX-a	Formula	$C_{129}H_{223}O_{52}N_3$	$C_{129}H_{224}O_{52}N_3Ca$	$C_{129}H_{224}O_{52}N_3Mg$	$C_{129}H_{222}O_{50}N_3$	$C_{129}H_{220}O_{49}N_3$	$C_{129}H_{224}O_{52}N_3K$	$C_{129}H_{224}O_{52}N_3Na$	$C_{129}H_{225}O_{52}N_3$	$C_{129}H_{223}O_{51}N_3$	$C_{129}H_{221}O_{50}N_3$	$C_{129}H_{219}O_{49}N_3$
	(RDB)	20.0	19.5	19.5	20.5	21.5	19.0	19.0	19.0	20.0	21.0	22.0
	m/z	2662.4847	901.1497	895.8249	876.4938	870.4904	n.d.	1343.2368	n.d.	1323.2424	1314.2369	nd
OVTX-d	Formula	$C_{129}H_{223}O_{53}N_3$	$C_{129}H_{224}O_{53}N_3Ca$	$C_{129}H_{224}O_{53}N_3Mg$	$C_{129}H_{222}O_{51}N_3$	$C_{129}H_{220}O_{50}N_3$	--	$C_{129}H_{224}O_{53}N_3Na$	--	$C_{129}H_{223}O_{52}N_3$	$C_{129}H_{221}O_{51}N_3$	
	(RDB)	20.0	19.5	19.5	20.5	21.5	--	19.0	--	20.0	21.0	
	m/z	2662.4847	901.1503	895.8257	876.4970	870.4911	n.d.	n.d.	n.d.	1323.2449	1314.2356	n.d.
OVTX-e	Formula	$C_{129}H_{223}O_{53}N_3$	$C_{129}H_{224}O_{53}N_3Ca$	$C_{129}H_{224}O_{53}N_3Mg$	$C_{129}H_{222}O_{51}N_3$	$C_{129}H_{220}O_{50}N_3$	--	--	--	$C_{129}H_{223}O_{52}N_3$	$C_{129}H_{221}O_{51}N_3$	--
	(RDB)	20.0	19.5	19.5	20.5	21.5	--	--	--	20.0	21.0	--
	m/z	2678.4796	906.4810	n.d.	n.d.	n.d.	n.d.	n.d.	n.d.	n.d.	n.d.	n.d.
IsobPLTX	Formula	$C_{129}H_{223}O_{54}N_3$	$C_{129}H_{224}O_{54}N_3Ca$	--	--	--	--	--	--	--	--	--
	(RDB)	20.0	19.5	--	--	--	--	--	--	--	--	--
	m/z	2688.5003	909.8242	904.4991	885.1680	879.1652	1364.2325	1356.2502	1345.2601	1336.2539	1327.2480	n.d.
OVTX-i	Formula	$C_{131}H_{225}O_{53}N_3$	$C_{131}H_{226}O_{53}N_3Ca$	$C_{131}H_{226}O_{53}N_3Mg$	$C_{131}H_{224}O_{51}N_3$	$C_{131}H_{222}O_{50}N_3$	$C_{131}H_{226}O_{53}N_3K$	$C_{131}H_{226}O_{53}N_3Na$	$C_{131}H_{227}O_{53}N_3$	$C_{131}H_{225}O_{52}N_3$	$C_{131}H_{223}O_{51}N_3$	--
	(RDB)	21.0	20.5	20.5	21.5	22.5	20.5	20.0	20.0	21.0	22.0	--
	m/z	2704.4952	915.1564	909.8316	890.5003	884.4960	1372.2323	1364.2494	n.d.	1344.2518	1335.2461	n.d.
OVTX-j_1	Formula	$C_{131}H_{225}O_{54}N_3$	$C_{131}H_{226}O_{54}N_3Ca$	$C_{131}H_{226}O_{54}N_3Mg$	$C_{131}H_{224}O_{52}N_3$	$C_{131}H_{222}O_{51}N_3$	$C_{131}H_{226}O_{54}N_3K$	$C_{131}H_{226}O_{54}N_3Na$	--	$C_{131}H_{225}O_{53}N_3$	$C_{131}H_{223}O_{52}N_3$	--
	(RDB)	21.0	20.5	20.5	21.5	22.5	20.0	20.0	--	21.0	22.0	--
	m/z	2704.4952	915.1555	909.8305	890.4995	884.4960	1372.2295	1364.2465	n.d.	1344.2510	1335.2455	n.d.
OVTX-j_2	Formula	$C_{131}H_{225}O_{54}N_3$	$C_{131}H_{226}O_{54}N_3Ca$	$C_{131}H_{226}O_{54}N_3Mg$	$C_{131}H_{224}O_{52}N_3$	$C_{131}H_{222}O_{51}N_3$	$C_{131}H_{226}O_{54}N_3K$	$C_{131}H_{226}O_{54}N_3Na$	--	$C_{131}H_{225}O_{53}N_3$	$C_{131}H_{223}O_{52}N_3$	--
	(RDB)	21.0	20.5	20.5	21.5	22.5	20.0	20.0	--	21.0	22.0	--
	m/z	2720.4902	920.4871	915.1622	895.8312	889.8276	n.d.	1372.2240	n.d.	1352.2484	1343.2426	1334.2385
OVTX-k	Formula	$C_{131}H_{225}O_{55}N_3$	$C_{131}H_{226}O_{55}N_3Ca$	$C_{131}H_{226}O_{55}N_3Mg$	$C_{131}H_{224}O_{53}N_3$	$C_{131}H_{222}O_{52}N_3$	--	$C_{131}H_{226}O_{55}N_3Na$	--	$C_{131}H_{225}O_{54}N_3$	$C_{131}H_{223}O_{53}N_3$	$C_{131}H_{221}O_{52}N_3$
	(RDB)	21.0	20.5	20.5	21.5	22.5	--	20.0	--	21.0	22.0	23.0

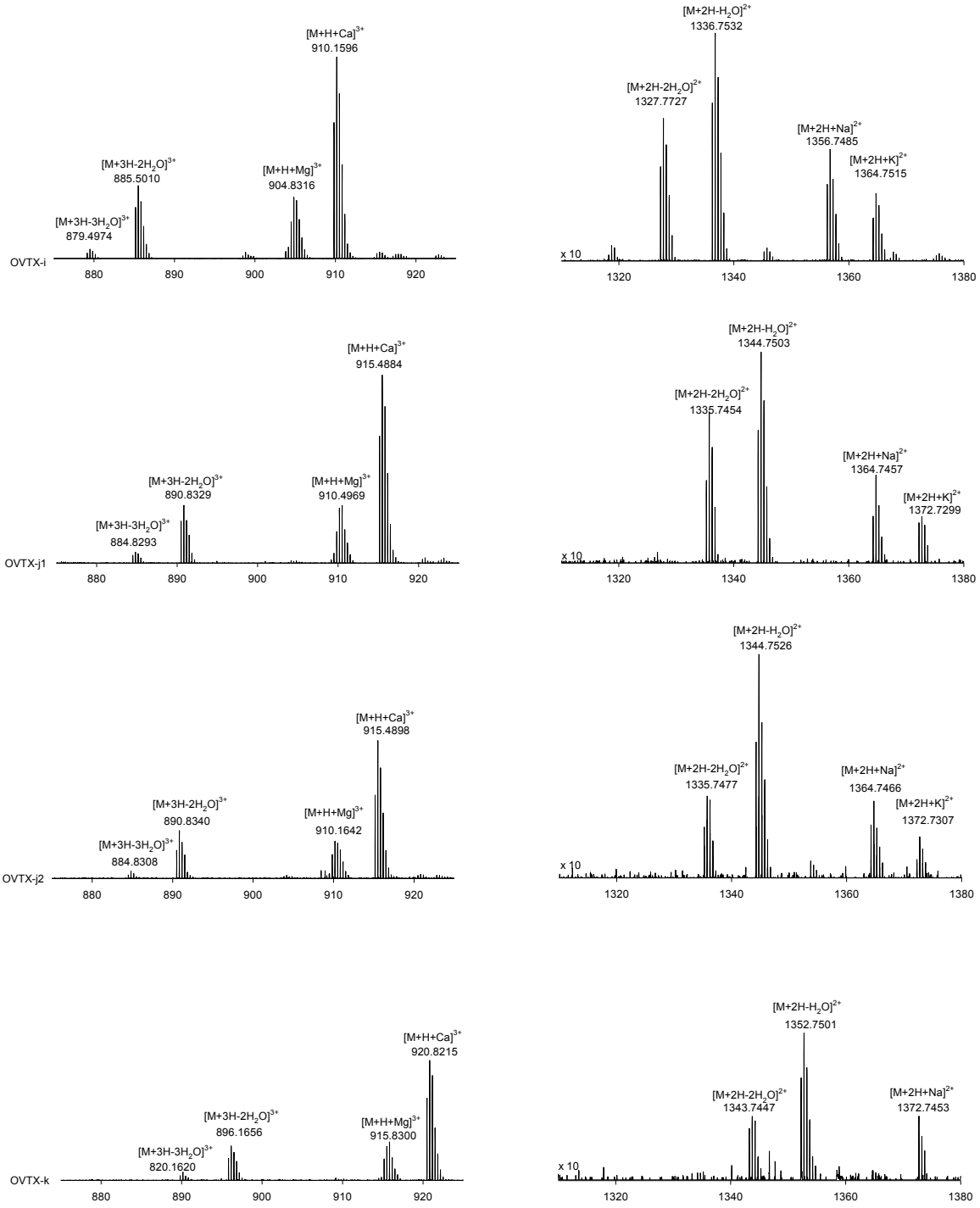

Figure IV.3 Full HRMS spectra of ovatoxin-i, -j_1, -j_2, -k) zoomed in *m/z* 870-930 and *m/z* 1310-1380 ranges. Elemental formula assignments of triply and doubly charged ions are reported in Table IV.3

Since OVTX-i, -j_1, -j_2, and -k were contained in the extracts at levels too low to be isolated and studied by NMR, the LC-HRMS^n approach developed by Ciminiello *et al.* [1] was applied to investigate their structural features. The fundamentals of this approach are that all palytoxin-like compounds share the same MS^2 behavior fragmenting at many sites of their backbone (Figure IV.1). Most of the cleavages generate three types of diagnostic ions of different charge state (1+, 2+, and 3+) which appear in the MS^2 spectrum: A-side fragment ions containing 2 N atoms, B-side fragment ions containing 1 N atom, and internal fragments (containing no N atoms) deriving from the simultaneous occurrence of two cleavages. Most of the fragment ions undergo to several subsequent water losses (see Table IV.3 and IV.5). Interestingly, most of the singly, doubly and triply charged fragment ions appearing in the spectrum of palytoxin-like compounds contain calcium in their elemental formula. In this study, the fragmentation pattern of OVTX-a (Figure IV.1), whose stereo-structure has been fully elucidated [4, 7] was used as template to gain structural insights into the new ovatoxins.

Ovatoxin-i

OVTX-i ($C_{131}H_{225}O_{53}N_3$, RDB= 21) presented two C, two H, and one O atoms more than OVTX-a ($C_{129}H_{223}O_{52}N_3$, RDB= 20), together with an additional unsaturation. The LC-HRMS^2 spectrum of the $[M+H+Ca]^{3+}$ ion at *m/z* 910.1 of OVTX-i was similar to that of OVTX-a since it was dominated by a cluster of $[M+H+Ca-nH_2O]^{3+}$, (n= 2-7) ions due to subsequent water losses from the precursor and it contained many diagnostic ions (Figure IV.4, Table IV.2). This suggested that OVTX-i and OVTX-a shared the same fragmentation pattern reflecting a wide similarity in terms of chemical structure.

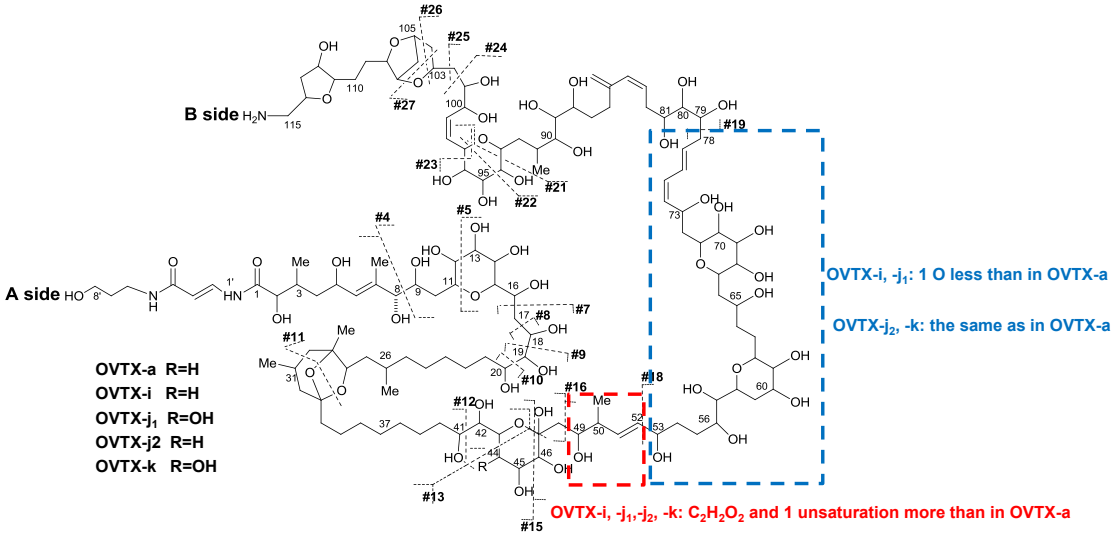

Figure IV.4 Planar structure of ovatoxin-a (OVTX-a) and structural hypotheses for the new ovatoxins (OVTX-i, -j_1, -j_2, -k) based on cleavages detected in CID-HRMS^2 spectra of $[M+H+Ca]^{3+}$ ions (Table VI.4 and VI.5).

Table IV.2 Assignment of A-side, B-side and internal fragments contained in HRMS^2 spectra of ovatoxin-a (OVTX-a) and ovatoxin-i (OVTX-i) to relevant cleavages (#Clv) reported in Figure IV.4. Errors were below 5 ppm in all cases. n.d. = not detected.

	OVTX-a		**OVTX-i**	
	A-side	**B-side**	**A-side**	**B-side**
#Clv	***m/z* (1+, 2+, 3+)(-nH_2O) Formula (RDB)**	***m/z* (1+, 2+, 3+)(-nH_2O) Formula (RDB)**	***m/z* (1+, 2+, 3+)(-nH_2O) Formula (RDB)**	***m/z* (1+, 2+, 3+)(-nH_2O) Formula (RDB)**
#4	327.1906 (1+) (-1H_2O) $C_{16}H_{27}O_5N_2$ (4.5)	1171.1254 (2+) $C_{113}H_{195}O_{46}NCa$ (17.0) 781.0860 (3+) $C_{113}H_{196}O_{46}NCa$ (16.5)	327.1918 (1+) (-1H_2O) $C_{16}H_{27}O_5N_2$ (4.5)	1192.1354 (2+) $C_{115}H_{197}O_{47}NCa$ (18.0) 795.09195 (3+) $C_{115}H_{198}O_{47}NCa$ (17.5)
#11	438.2238 (2+) $C_{40}H_{72}O_{16}N_2$ Ca (6.0)		438.2242 (+1) $C_{40}H_{72}O_{16}N_2Ca$ (6.0)	
#12	536.2965 (2+) $C_{52}H_{92}O_{18}N_2Ca$ (8.0)	799.8905 (2+) (-3H_2O) $C_{77}H_{125}O_{31}NCa$ (16.0)	536.2982 (2+) $C_{52}H_{92}O_{18}N_2Ca$ (8.0)	820.8978 (2+) (-3H_2O) $C_{79}H_{127}O_{32}NCa$ (17.0)
#13	566.3071(2+) $C_{54}H_{96}O_{20}N_2Ca$ (8.0)	787.8919 (2+) (-1H_2O) $C_{75}H_{125}O_{31}NCa$ (14.0)	566.3088 5(2+) $C_{54}H_{96}O_{20}N_2Ca$ (8.0)	n.d.
#15	588.3201 (2+) $C_{56}H_{100}O_{21}N_2Ca$ (8.0)	774.8829 (2+) $C_{73}H_{123}O_{31}NCa$ (13.0) 1510.8122 (1+) $C_{73}H_{124}O_{31}N$ (12.5)	588.3218 (2+) $C_{56}H_{100}O_{21}N_2Ca$ (8.0)	795.8899(2+) $C_{75}H_{125}O_{32}NCa$ (14.0) 1552.8257 (1+) $C_{75}H_{126}O_{32}N$ (13.5)
#16	625.3385 (2+) $C_{59}H_{106}O_{23}N_2Ca$ (8.0)	737.8646 (2+) $C_{70}H_{117}O_{29}NCa$ (13.0) 1436.7757 (1+) $C_{70}H_{118}O_{29}N$ (12.5)	625.3402 (2+) $C_{59}H_{106}O_{23}N_2Ca$ (8.0)	758.8719 (2+) $C_{72}H_{119}O_{30}NCa$ (14.0) 1478.7899 (1+) $C_{72}H_{120}O_{30}N$ (13.5)
#17	639.3359 (2+) $C_{60}H_{106}O_{24}N_2Ca$ (9.0)	1390.7716 (1+) (-1H_2O) $C_{69}H_{116}O_{27}N$ (12.5)	n.d.	n.d.
#18		686.8308 (2+) (-1H_2O) $C_{65}H_{107}O_{27}NCa$ (13.0)	696.3722 (+2) $C_{66}H_{116}O_{26}N_2Ca$ (10.0)	678.8348 (+2) (-1H_2O) $C_{65}H_{107}O_{26}NCa$ (13.0) 1318.7164 (+1) (1-H_2O) $C_{65}H_{108}O_{26}N$ (12.5)

Table IV.2 (continued)

#19	932.5032 (2+)(-1H_2O) $C_{90}H_{156}O_{35}N_2Ca$ (14.0)	804.4365(+1) $C_{39}H_{66}O_{16}N$ (7.5)	953.51104 (2+) (-1H_2O) $C_{92}H_{158}O_{36}N_2Ca$ (15.0)	804.43837(+1) $C_{39}H_{66}O_{16}N$ (7.5)
#21	1113.6005 (2+) $C_{107}H_{186}O_{43}N_2Ca$ (16.0)	406.2216 (1+) (-3H_2O) $C_{22}H_{32}O_6N$ (7.5)	1134.6083(2+) $C_{109}H_{188}O_{44}N_2Ca$ (17.0)	406.2227 (1+) (-3H_2O) $C_{22}H_{32}O_6N$ (7.5)
#22	1128.6053 (2+) $C_{108}H_{188}O_{44}N_2Ca$ (16.0)		1149.6121 (2+) $C_{110}H_{190}O_{45}N_2Ca$ (17.0)	
#23	1158.6164 (2+) $C_{110}H_{192}O_{46}N_2Ca$ (16.0)		1179.6200 (2+) $C_{112}H_{194}O_{47}N_2Ca$ (17.0)	
#24	1199.6367 (2+) (-1H_2O) $C_{115}H_{198}O_{47}N_2Ca$ (18.0)		n.d.	
#25	1206.6449 (2+) (-1H_2O) $C_{116}H_{200}O_{47}N_2Ca$ (18.0)		1218.6493 (2+) (-2H_2O) $C_{118}H_{200}O_{47}N_2Ca$ (20.0)	
#26	1219.6517 (2+) (-1H_2O) $C_{118}H_{202}O_{47}N_2Ca$ (19.0)		1240.6599 (2+) (-1H_2O) $C_{120}H_{204}O_{48}N_2Ca$ (20.0)	
#27	1220.6386 (2+) (-1H_2O) $C_{117}H_{200}O_{48}N_2Ca$ (19.0)		1241.6428 (2+) (-1H_2O) $C_{119}H_{202}O_{49}N_2Ca$ (20.0)	

	Internal fragments	**Internal fragments**
#Clv	***m/z* (1+, 2+, 3+) (-nH_2O) Formula (RDB)**	***m/z* (1+, 2+, 3+) (-nH_2O) Formula (RDB)**
#4+#12	364.1999 (2+) $C_{36}H_{64}O_{12}Ca$ (5.0) 727.3924 (1+) $C_{36}H_{63}O_{12}Ca$ (5.5)	364.2009 (2+) $C_{36}H_{64}O_{12}Ca$ (5.0) 727.3944 (1+) $C_{36}H_{63}O_{12}Ca$ (5.5)
#4+#13	394.2104 (2+) $C_{38}H_{68}O_{14}Ca$ (5.0)	394.2111 (2+) $C_{38}H_{68}O_{14}Ca$ (5.0)
#4+#15	416.2234 (2+) $C_{40}H_{72}O_{15}Ca$ (5.0)	416.2246 (2+) $C_{40}H_{72}O_{15}Ca$ (5.0)
#4+#16	453.2415 (2+) $C_{43}H_{78}O_{17}Ca$ (5.0)	453.2421 (2+) $C_{43}H_{78}O_{17}Ca$ (5.0)
#5+#12	641.3557 (1+) $C_{32}H_{57}O_{10}Ca$ (4.5)	641.3580 (1+) $C_{32}H_{57}O_{10}Ca$ (4.5)
#7+#12	521.3136 (1+) $C_{28}H_{49}O_6Ca$ (4.5)	521.31529 (1+) $C_{28}H_{49}O_6Ca$ (4.5)
#8+#12	507.2979 (1+) $C_{27}H_{47}O_6Ca$ (4.5)	507.2994 (1+) $C_{27}H_{47}O_6Ca$ (4.5)
#9+#12	477.2875 (1+) $C_{26}H_{45}O_5Ca$ (4.5)	477.2894 (1+) $C_{26}H_{45}O_5Ca$ (4.5)
#10+#12	447.2771 (1+) $C_{25}H_{43}O_4Ca$ (4.5)	447.2783 (1+) $C_{25}H_{43}O_4Ca$ (4.5)

In particular, in OVTX-i all the A-side fragments generated by cleavages #4 to #16 and all the internal fragments presented the same elemental composition as those of ovatoxin-a (Table IV.2), suggesting that OVTX-i and OVTX-a share the part structure stretching from the A-side terminal to C-48. The two molecules shared also the part structure stretching from C79 to the B-side terminal, based on the B-side fragments of cleavages #19 and #21, which had the same elemental composition in the two molecules. Thus, we restricted the structural difference between OVTX-i and OVTX-a to the region stretching from C49 to C78. This was confirmed by the A-side fragments of cleavages #19

to #27 and by the B-side fragments of cleavage #4, #12, #15, and #16, all containing in OVTX-i an additional C_2H_2O and an unsaturation compared to those of ovatoxin-a (Table IV.2).

Cleavage #18, that in every palytoxin-like compound analyzed so far originates only a B-side fragment, in OVTX-i originated both A- and B-side fragments. This cleavage was crucial to restrict the region where most of the modifications between OVTX-i and OVTX-a occurred. In particular, the A-side fragment (*m/z* 696.3722, $C_{66}H_{116}O_{26}N_2Ca$, RDB =10.0) due to cleavage #18 in OVTX-i displayed $C_2H_2O_2$ more than the corresponding part structure of OVTX-a. Considering that the A-side fragment of cleavage #16 (*m/z* 625.3402, $C_{59}H_{106}O_{23}N_2Ca$, RDB =8.0) displayed the same elemental composition as in ovatoxin-a, the additional $C_2H_2O_2$ was located in the region stretching from C49 to C52. Consistently, cleavage #18 generated also a B-side fragment ion (*m/z* 678.8348, $C_{65}H_{107}O_{26}NCa$, RDB =13.0) displaying one O less than in ovatoxin-a (*m/z* 686.8308, $C_{65}H_{107}O_{27}NCa$, RDB =13.0). Considering that the B-side fragment due to cleavage #19 matched again that of ovatoxin-a, we could deduce that the oxygen was lacking in the region stretching from C53 to C78. We could not further restrict the region of difference as this part structure does not fragment further, as already observed for other palytoxin-like compounds [1,5,6], likely as a consequence of the formation of a conjugated polyene during the fragmentation process [14].

Table IV.3 Monoisotopic ion peaks of all the fragment ions contained in HR CID MS^2 spectra of $[M+H+Ca]^{3+}$ ions of ovatoxin (OVTX) -a and -i and their assignment to relevant cleavages (Clv).The first ion diagnostic of each cleavage is followed by 1 to 8 ions due to subsequent water losses; the most intense ion of each group is underlined.

	OVTX-a		**OVTX-i**	
	***m/z* (1+, 2+, 3+)**	***m/z* (1+, 2+, 3+)**	***m/z* (1+, 2+, 3+)**	***m/z* (1+, 2+, 3+)**
Precursor	**896.1 (3+)** 883.8109 (-2H_2O) 877.8077 (-2H_2O) 871.8041 (-4H_2O) 865.8007 (-5H_2O) 859.7970 (-6H_2O) 853.7936 (-7H_2O) 847.7886 (-8H_2O)		**910.1 (3+)** 897.8163 (-2H_2O) 891.8123 (-3H_2O) 885.8095 (-4H_2O) 879.8063 (-5H_2O) 873.8028 (-6H_2O) 867.7996 (-7H_2O)	
Clv	**A side**	**B side**	**A side**	**B side**
#4	327.1908 (1+)(-1H_2O) 309.1804 (-2H_2O)	1171.1261 (2+) 1162.1209 (-1H_2O) 1153.1158 (-2H_2O) 1144.1108 (-3H_2O) 1135.1062 (-4H_2O) 1126.1009 (-5H_2O) 1117.0952 (-6H_2O) 1108.0942 (-7H_2O) 781.0867 (3+) 775.0827 (-1H_2O) 769.0792 (-2H_2O) 763.0763 (-3H_2O) 757.0728 (-4H_2O) 751.0699 (-5H_2O)	327.1918 (1+) (-1H_2O) 309.1813 (-2H_2O)	1192.1354 (2+) 1183.1290 (-1H_2O) 1174.1243 (-2H_2O) 1165.1187 (-3H_2O) 1156.1135 (-4H_2O) 1147.1099 (-5H_2O) 1138.1039 (-6H_2O) 1129.0977 (-7H_2O) 795.0919 (3+) (-1H_2O) 789.0884 (-2H_2O) 783.0841 (-3H_2O) 777.0827 (-4H_2O)
#11	438.2239 (2+) 429.2194 (-1H_2O)		438.2242 (2+)	
#12	536.2967 (2+) 527.2914 (-1H_2O) 518.2858 (-2H_2O)	799.8912 (2+) (-3H_2O) 790.8860 (-4H_2O)	536.2982 (2+) 527.2930 (-1H_2O)	820.8977 (2+) (-3H_2O) 811.8934 (-4H_2O)
#13	566.3074 (2+) 557.3021 (-1H_2O) 548.2969 (-2H_2O)	787.8919 (2+) (-1H_2O) 778.8858 (-2H_2O) 769.8802 (-3H_2O)	566.3088 (2+) 557.3030 (-1H_2O)	n.d.
#15	588.3204 (2+) 579.3151 (-1H_2O) 570.3100 (-2H_2O)	774.8833 (2+) 765.8781 (-1H_2O) 756.8727 (-2H_2O) 747.8673 (-3H_2O) 1510.8129 (1+) 1492.8023 (-1H_2O) 1474.7919 (-2H_2O) 1456.7814 (-3H_2O) 1438.7758 (-4H_2O)	588.3218 (2+) 579.3165 (-1H_2O) 570.3114 (-2H_2O)	795.8899 (2+) 786.8850 (-1H_2O) 777.8800 (-2H_2O) 768.8746 (-3H_2O) 1552.8257 (1+) 1534.8158 (-1H_2O) 1516.8050 (-2H_2O) 1498.7947 (-3H_2O) 1480.7910 (-4H_2O)
#16	625.3387 (2+) 616.3335 (-1H_2O) 607.3279(-2H_2O)	737.8650 (2+) 728.8596 (-1H_2O) 719.8543 (-2H_2O) 710.8491 (-3H_2O) 701.8436 (-4H_2O) 692.8384 (-5H_2O) 683.8331 (-6H_2O) 674.8286 (-7H_2O) 1436.7765 (1+) 1418.7659 (-1H_2O) 1400.7555 (-2H_2O) 1382.7446 (-3H_2O) 1364.7341 (-4H_2O) 1346.7232 (-5H_2O) 1328.7132 (-6H_2O)	625.3402 (2+) 616.3352 (-1H_2O) 607.3295 (-2H_2O)	758.8719 (2+) 749.8666 (-1H_2O) 740.8614 (-2H_2O) 731.8566 (-3H_2O) 722.8505 (-4H_2O) 713.8466 (-5H_2O) 1478.7899 (1+) 1460.7790 (-1H_2O) 1442.7698 (-2H_2O) 1424.7581 (-3H_2O) 1406.7478 (-4H_2O)

Table IV.3 (continued)

#17	639.3361 (2+) 630.3310 (-$1H_2O$) 621.3256 (-$2H_2O$)	1390.7711 (1+) (-$1H_2O$) 1372.7605 (-$2H_2O$) 1354.7502 (-$3H_2O$)	n.d.	n.d.
#18		686.8319 (2+) (-$1H_2O$) 677.8256 (-$2H_2O$)	696.3715 (+2) 687.3659 (-$1H_2O$) 678.3608 (-$2H_2O$) 669.3564 (-$3H_2O$)	687.8405 (+2) 678.8348 (-$1H_2O$) 1318.7165 (-$1H_2O$) 1300.7053 (-$2H_2O$)
#19	932.5036 (-$1H_2O$) 923.4983 (-$2H_2O$) 914.4923 (-$3H_2O$)	804.4365 (1+)	953.5110 (+2) (-$1H_2O$) 944.4998 (-$2H_2O$)	804.4383 (1+)
#21	1113.6007 (2+) 1104.5954 (-$1H_2O$) 1095.5591 (-$2H_2O$) 1086.5866 (-$3H_2O$) 1077.5794 (-$4H_2O$)	406.2215 (1+) (-$3H_2O$)	1134.6083 (2+) 1125.6030 (-$1H_2O$) 1116.5974 (-$2H_2O$)	406.2227 (1+) (-$3H_2O$)
#22	1128.6057 (2+) 1119.6021(-$1H_2O$) 1110.5962 (-$2H_2O$) 1101.5869 (-$3H_2O$) 1092.5846 (-$4H_2O$)		1149.6921 (2+) 1140.6116(-$1H_2O$)	
#23	1158.6154 (2+) 1149.6107(-$1H_2O$) 1149.6107 (-$2H_2O$) 1140.6057 (-$3H_2O$) 1131.5990 (-$4H_2O$) 1122.5981 (-$5H_2O$)		1179.6200 (2+) 1170.6180(-$1H_2O$) 1161.6129 (-$2H_2O$)	
#24	1199.6333 (2+) (-$1H_2O$) 1190.6363 (-$2H_2O$)		n.d.	
#25	1206.6488 (2+) (-$1H_2O$) 1197.6399 (-$2H_2O$) 1188.6347 (-$3H_2O$) 1179.6286 (-$4H_2O$) 1170.6232 (-$5H_2O$)		1218.6493 (2+) (-$2H_2O$) 1209.6410 (-$3H_2O$) 1200.6372 (-$4H_2O$)	
#26	1219.6512 (2+) (-$1H_2O$) 1210.6477 (-$2H_2O$) 1201.6436 (-$3H_2O$) 1192.6379 (-$4H_2O$) 1183.6332 (-$5H_2O$) 1174.6263 (-$6H_2O$)		1240.6599 (2+) (-$1H_2O$) 1231.6531(-$2H_2O$) 1222.6467 (-$3H_2O$) 1213.6432 (-$4H_2O$)	
#27	1220.6386 (2+) (-$1H_2O$) 1211.6380 (-$2H_2O$)		1241.6465 (2+) (-$1H_2O$) 1232.6495 (-$2H_2O$)	

It is quite interesting to note that in the region C49-C52 OVTX-i presents structural modifications ($C_2H_2O_2$ and 1 unsaturation more than in OVTX-a) which have never been observed in any of the palytoxins so far known. This results in an atypical fragmentation behavior with regards to cleavage #17. In more detail, cleavage #17, which generally generates clearly detectable A- and B-side fragments in the LC-HRMS^2 spectra [1,5,6], did not occur in OVTX-i. The structural modification could involve oxidation and addition of a C2 unit to methyl group at C50. This is not rare in dinoflagellate products where glycol,

glycine and acetate are used [15]. Nevertheless, in lack of mass spectral evidence, no unambiguous structural hypothesis can be done.

Ovatoxin-j_1, j_2, and -k

The interpretation of LC-HRMS^2 of the $[M+H+Ca]^{3+}$ ions of OVTX-j_1 and -j_2 (at *m/z* 915.4) and of OVTX-k (at *m/z* 920.8) was performed following the same approach described above for OVTX-i. Here below we discuss only the key cleavages highlighting the structural differences among the new analogues.

OVTX-j_1, OVTX-j_2 and OVTX-k presented the same atypical structural features as OVTX-i in the C49-C52 part structure, namely a $C_2H_2O_2$ and an unsaturation more than in ovatoxin-a (Figure IV.4 Table IV.4Table IV.5). OVTX-j_1 and OVTX-j_2 ($C_{131}H_{225}O_{54}N_3$, RDB= 21.0) were structural isomers which, compared to ovatoxin-i, presented an additional O atom, while OVTX-k ($C_{131}H_{225}O_{55}N_3$, RDB= 21.0) contained two more O atoms than ovatoxin-i.

Table IV.4 Assignment of A-side, B-side and internal fragments contained in HRMS^2 spectra of ovatoxin-j_1, -j_2, and –k to relevant cleavages (#Clv) reported in Figure IV.4. Errors were below 5 ppm in all cases. n.d. = not detected

Clv	OVTX-j_1		OVTX-j_2		OVTX-k	
	A side *m/z* **(1+,2+,+3)(-nH2O) Formula, (RDB)**	**B side** *m/z* **(1+,2+,+3) (-nH2O) Formula, (RDB)**	**A side** *m/z* **(1+,2+,+3) (-nH2O) Formula, (RDB)**	**B side** *m/z* **(1+,2+,+3) (-nH2O) Formula, (RDB)**	**A side** *m/z* **(1+,2+,+3) (-nH2O) Formula, (RDB)**	**B side** *m/z* **(1+,2+,+3) (-nH2O) Formula, (RDB)**
#4	327.1917 (1+) (-$1H_2O$) $C_{16}H_{27}O_5N_2$ -(4.5)	1200.1240 (2+) $C_{115}H_{197}O_{48}NCa$ (18.0) 800.4263 (3+) $C_{115}H_{198}O_{48}NCa$ (17.5)	327.1916 (1+) (-$1H_2O$) $C_{16}H_{27}O_5N_2$ (4.5)	1200.1307 (2+) $C_{115}H_{197}O_{48}NCa$ (18.0) 800.4230 (3+) $C_{115}H_{198}O_{48}NCa$ (17.5)	327.1917 (1+) (-$1H_2O$) $C_{16}H_{27}O_5N_2$ (4.5)	1208.1285 (2+) $C_{115}H_{197}O_{49}NCa$ (18.0) 805.7541 (3+) $C_{115}H_{198}O_{49}NCa$ (17.5)
#11	n.d.		438.2250 (2+) $C_{40}H_{72}O_{16}N_2Ca$ (6.0)		438.2253 (2+) $C_{40}H_{72}O_{16}N_2Ca$ (6.0)	
#12	536.2976 (2+) $C_{52}H_{92}O_{18}N_2Ca$ (8.0)	n.d.	536.2978 (2+) $C_{52}H_{92}O_{18}N_2Ca$ (8.0)	828.8956 (2+) (-$3H_2O$) $C_{79}H_{127}O_{33}NCa$ (17.0)	536.2980 (2+) $C_{52}H_{92}O_{18}N_2Ca$ (8.0)	836.8924 (2+) (-$3H_2O$) $C_{79}H_{127}O_{34}NCa$ (17.0)
#13	566.3087 (2+) (-$1H_2O$) $C_{54}H_{96}O_{20}N_2Ca$ (8.0)	n.d.	566.3084 (2+) (-$1H_2O$) $C_{54}H_{96}O_{20}N_2Ca$ (8.0)	816.8951 (2+) (-$1H_2O$) $C_{77}H_{127}O_{33}NCa$ (15.0)	566.3082 (2+) $C_{54}H_{96}O_{20}N_2Ca$ (8.0)	824.8933 (2+) (-$1H_2O$) $C_{77}H_{127}O_{34}NCa$, (15.0)
#15	596.3191 (2+) $C_{56}H_{100}O_{22}N_2Ca$ (8.0)	786.8827 (2+) (-$1H_2O$) $C_{75}H_{123}O_{31}NCa$ (15.0) 1552.8256 (1+) $C_{75}H_{126}O_{32}N$ (13.5)	588.3213 (2+) $C_{56}H_{100}O_{21}N_2Ca$ (8.0)	803.8873 (2+) $C_{75}H_{125}O_{33}NCa$ (14.0) 1568.8211 (1+) $C_{75}H_{126}O_{33}N$ (13.5)	596.3189 (2+) $C_{56}H_{100}O_{22}N_2Ca$ (8.0)	803.8879 (2+) $C_{75}H_{125}O_{33}NCa$ (14.0) 1568.8189 (1+) $C_{75}H_{126}O_{33}N$ (14.0)
#16	633.3378 (2+) $C_{59}H_{106}O_{24}N_2Ca$ (8.0)	758.8721 (2+) $C_{72}H_{119}O_{30}NCa$ (14.0) 1478.7890 (1+) $C_{72}H_{120}O_{30}N$ (13.5)	625.3396 (2+) $C_{59}H_{106}O_{23}N_2Ca$ (8.0)	766.8687 (2+) $C_{72}H_{119}O_{31}NCa$ (14.0) 1494.7825 (1+) $C_{72}H_{120}O_{31}N$ (13.5)	633.3371 (2+) $C_{59}H_{106}O_{24}N_2Ca$ (8.0)	766.8689 (2+) $C_{72}H_{119}O_{31}NCa$ (14.0) 1494.7835 (1+) $C_{72}H_{120}O_{31}N$ (13.5)
#17	nd	nd	nd	nd	nd	nd
#18	704.3657(2+) $C_{66}H_{116}O_{27}N_2Ca$ (10.0)	n.d. 1318.7157 (1+) (-$1H_2O$) $C_{65}H_{108}O_{26}N$ (12.5)	696.3716(2+) $C_{66}H_{116}O_{26}N_2Ca$ (10.0)	686.8324 (2+)(-$1H_2O$) $C_{65}H_{107}O_{27}NCa$ (13.0) 1334.7101 (1+) (-$1H_2O$) $C_{65}H_{108}O_{27}N$, (12.5)	704.3652 (2+) $C_{66}H_{116}O_{27}N_2Ca$ (10.0)	686.8318 (2+)(-$1H_2O$) $C_{65}H_{107}O_{27}NCa$ (13.0) 1334.7057 (1+) (-$1H_2O$) $C_{65}H_{108}O_{27}N$ (12.5)
#19	961.5059 (2+) ($1H_2O$) $C_{92}H_{158}O_{37}N_2Ca$ (15.0)	n.d.	961.5037 (2+) (-$1H_2O$) $C_{92}H_{158}O_{37}N_2Ca$ (15.0)	804.4383 (1+) $C_{39}H_{66}O_{16}N$ (7.5)	969.5067 (2+) (-$1H_2O$) $C_{92}H_{158}O_{38}N_2Ca$ (15.0)	804.4399 (1+) $C_{39}H_{66}O_{16}N$ (7.5)
#21	1142.6052 (2+) $C_{109}H_{188}O_{45}N_2Ca$ (17.0)	406.2212 (1+) (-$3H_2O$) $C_{22}H_{32}O_6N$ (7.5)	1142.6048 (2+) $C_{109}H_{188}O_{45}N_2Ca$ (17.0)	406.2232 (1+) (-$3H_2O$) $C_{22}H_{32}O_6N$ (7.5)	1150.6038 (2+) $C_{109}H_{188}O_{46}N_2Ca$ (17.0)	406.2204 (1+) (-$3H_2O$) $C_{22}H_{32}O_6N$ (7.5)
#22	n.d.		1157.6099 (2+) $C_{110}H_{190}O_{46}N_2Ca$ (17.0)		1156.6012 (2+) (-$1H_2O$) $C_{110}H_{188}O_{46}N_2Ca$ (18.0)	
#23	n.d.		1187.6203 (2+) $C_{112}H_{194}O_{48}N_2Ca$ (17.0)		1186.6064 (2+) (-$1H_2O$) $C_{112}H_{192}O_{48}N_2Ca$ (18.0)	

Table IV.4 (continued)

#24	n.d.	1228.6418 (2+) (-1H_2O) $C_{117}H_{200}O_{49}N_2Ca$ (19.0)	1236.6357 (2+) (-1H_2O) $C_{117}H_{200}O_{50}N_2Ca$ (19.0)
#25	1226.6392 (2+)(-2H_2O) $C_{118}H_{200}O_{48}N_2Ca$ (20.0)	1235.6461 (2+) (-1H_2O) $C_{118}H_{202}O_{49}N_2Ca$ (19.0)	1234.6423 (2+) (-2H_2O) $C_{118}H_{200}O_{49}N_2Ca$ (20.0)
#26	n.d.	1248.6538 (2+) (-1H_2O) $C_{120}H_{204}O_{49}N_2Ca$ (20.0)	1256.6518 (2+) (-1H_2O) $C_{120}H_{204}O_{50}N_2Ca$(20.0)
#27	1249.6436 (+2)(-1H_2O) $C_{119}H_{202}O_{50}N_2Ca$ (20.0)	1249.6385 (2+) (-1H_2O) $C_{119}H_{202}O_{50}N_2Ca$ (20.0)	1257.6445(2+) (-1H_2O) $C_{119}H_{202}O_{51}N_2Ca$ (20.0)
	Internal fragments ***m/z* (-nH_2O)** **Formula (RDB)**	**Internal fragments** ***m/z* (-nH_2O)** **Formula (RDB)**	**Internal fragments** ***m/z* (-nH_2O)** **Formula (RDB)**
#4+#12	364.2000 (2+) $C_{36}H_{64}O_{12}Ca$ (5.0)	364.2008 (2+) $C_{36}H_{64}O_{12}Ca$ (5.0)	364.2005 (2+) $C_{36}H_{64}O_{12}Ca$ (5.0)
	727.3943 (1+) $C_{36}H_{63}O_{12}Ca$ (5.5)	727.3937 (1+) $C_{36}H_{63}O_{12}Ca$ (5.5)	727.3938 (1+) $C_{36}H_{63}O_{12}Ca$ (5.5)
#4+#13	n.d.	394.2109 (1+) $C_{38}H_{68}O_{14}Ca$ (5.0)	394.2089 (1+) $C_{38}H_{68}O_{14}Ca$ (5.0)
#4+#15	n.d.	416.2242 (1+) $C_{40}H_{72}O_{15}Ca$ (5.0)	n.d.
#4+#16	n.d.	453.2419 (1+) $C_{43}H_{78}O_{17}Ca$ (5.0)	n.d.
#5+#12	641.3572 (1+) $C_{32}H_{57}O_{10}Ca$ (4.5)	641.3568 (1+) $C_{32}H_{57}O_{10}Ca$ (4.5)	641.3569 (1+) $C_{32}H_{57}O_{10}Ca$ (4.5)
#7+#12	521.3144 (1+) $C_{28}H_{49}O_6Ca$ (4.5)	521.3144 (1+) $C_{28}H_{49}O_6Ca$ (4.5)	521.3150 (1+) $C_{28}H_{49}O_6Ca$ (4.5)
#8+#12	507.2992 (1+) $C_{27}H_{47}O_6Ca$ (4.5)	507.2991 (1+) $C_{27}H_{47}O_6Ca$ (4.5)	507.2992 (1+) $C_{27}H_{47}O_6Ca$ (4.5)
#9+#12	477.2893 (1+) $C_{26}H_{45}O_5Ca$ (4.5)	477.2886 (1+) $C_{26}H_{45}O_5Ca$ (4.5)	477.2889 (1+) $C_{26}H_{45}O_5Ca$ (4.5)
#10+#12	447.2778 (1+) $C_{25}H_{43}O_4Ca$ (4.5)	447.2781 (1+) $C_{25}H_{43}O_4Ca$ (4.5)	447.2781 (1+) $C_{25}H_{43}O_4Ca$ (4.5)

In OVTX-j_1 the additional O atom was unambiguously located at C44, based on a cross-interpretation of the A-side fragments of cleavages #13 and #15. Indeed, in OVTX-j_1 (Table IV.4) while the A-side fragment of cleavage #13 (*m/z* 566.3087, $C_{54}H_{96}O_{20}N_2Ca$, RDB= 8.0) matched that of ovatoxin-a (Table IV.3), the A-side fragment of cleavage #15 (*m/z* 596.3191, $C_{56}H_{100}O_{22}N_2Ca$, RDB= 8.0) contained 1 more oxygen atom than in ovatoxin-a. Similarly to OVTX-i, OXTX-j_1 presented 1 oxygen atom less than ovatoxin-a in the region stretching from C53 to C78, as deduced by B-side fragments of cleavage #18 and #21.

As for OVTX-j_2, the additional O atom (versus OVTX-i) was contained in the region stretching from C53 to C78 as inferred by cleavages #18 and 19 which gave rise to B-side fragments superimposable to those of ovatoxin-a.

As for OVTX-k, the position of the two additional O atoms (versus OVTX-i) was deduced by interpretation of the key cleavages #13, #15, #18, and #19 in comparison with those of ovatoxin-a. One O atom was located at C44 (such as in OVTX-j_1) and the other in the region stretching from C53 to C78 (such as in OVTX-j_2) (Table IV.4, Table IV.5).

Table IV.5 Monoisotopic ion peaks of all the fragment ions contained in HR CID MS^2 spectra of $[M+H+Ca]^{3+}$ ions of ovatoxin (OVTX) -j_1, -j_2, and -k and their assignment to relevant cleavages (Clv).The first ion diagnostic of each cleavage is followed by 1 to 8 ions due to subsequent water losses; the most intense ion of each group is underlined.

	OVTX-j_1		**OVTX-j_2**		**OVTX-k**	
	***m/z* (1+,2+,+3)**	***m/z* (1+,2+,+3)**	***m/z* (1+,2+,+3)**	***m/z* (1+,2+,+3)**	***m/z* (1+,2+,+3)**	***m/z* (1+,2+,+3)**
Precursor	**915.5** 903.1477 (-$2H_2O$) 897.1443 (-$3H_2O$) 891.1408 (-$4H_2O$) 885.1371 (-$5H_2O$) 879.1331 (-$6H_2O$)		**915.5** 903.1472 (-$2H_2O$) 897.1438 (-$3H_2O$) 891.1401 (-$4H_2O$) 885.1366 (-$5H_2O$) 879.1331 (-$6H_2O$) 873.1293 (-$7H_2O$)		**920.8** 908.4790 (-$2H_2O$) 902.4757 (-$3H_2O$) 896.4720 (-$4H_2O$) 890.4687 (-$5H_2O$) 884.4651 (-$6H_2O$) 878.4613 (-$7H_2O$)	
Clv	**A side**	**B side**	**A side**	**B side**	**A side**	**B side**
#4	327.1917 (1+) (-$1H_2O$) 309.1816 (-$2H_2O$)	1200.1240 (2+) 1191.1251 (-$1H_2O$) 1182.1204(-$2H_2O$) 1173.1152 (-$3H_2O$) 1164.1132 (-$4H_2O$) 800.4263 (+3) 794.4206(-$1H_2O$) 788.4171 (-$2H_2O$)	327.1916 (1+)(-$1H_2O$) 309.1808 (-$2H_2O$)	1200.1307 (2+) 1191.1259 (-$1H_2O$) 1182.1204(-$2H_2O$) 1173.1153 (-$3H_2O$) 1164.1094 (-$4H_2O$) 1155.1064 (-$5H_2O$) 800.4229 (+3) 794.4190(-$1H_2O$) 788.4143 (-$2H_2O$) 782.4124 (-$3H_2O$)	327.1917 (1+)(-$1H_2O$) 309.1812 (-$2H_2O$)	1208.1285 (2+) 1199.1230 (-$1H_2O$) 1190.1177(-$2H_2O$) 1181.1125 (-$3H_2O$) 1172.1087 (-$4H_2O$) 1163.1018 (-$5H_2O$) 1154.0964 (-$6H_2O$) 799.7508(+3) 793.7476 (-$1H_2O$) 787.7406 (-$2H_2O$) 781.7399 (-$3H_2O$)
#11	n.d.		438.2250 (2+)		438.2253 (2+)	n.d.
#12	536.2976 (2+)	n.d.	536.2978 (2+) 527.2931 (-$1H_2O$)	828.8956 (2+) (-$3H_2O$) 819.8894 (-$4H_2O$)	536.2980 (2+) 527.2900 (-$1H_2O$)	836.8924 (2+) (-$3H_2O$)
#13	566.3787 (2+) (-$1H_2O$) 557.3033 (-$2H_2O$)	n.d.	566.3084 (2+) (-$1H_2O$) 557.3015 (-$2H_2O$)	816.8951 (2+) (-$1H_2O$) 807.8893 (-$2H_2O$)	566.3082 (2+) 557.3003 (-$1H_2O$) 548.2971 (-$2H_2O$)	824.8933 (+2) (-$1H_2O$) 815.8839(-$2H_2O$) 806.8783 (-$3H_2O$)

Table IV.5 (continued)

#15	596.3191 (2+) 587.3137 (-1H_2O)	786.8827 (2+) (-1H_2O) 777.8767 (-2H_2O) 1552.8256 (+1) 1534.8147 (-1H_2O) 1516.8059 (-2H_2O) 1498.7925 (-3H_2O	588.3213 (2+) 579.3162 (-1H_2O) 570.3111 (-2H_2O)	803.8873 (2+) 794.8817(-1H_2O) 785.8766 (-2H_2O) 776.8710 (-3H_2O) 1568.8211 (+1) 1550.8089 (-1H_2O) 1532.7989 (-2H_2O) 1514.7898 (-3H_2O	596.3189 (2+) 587.3135 (-1H_2O) 578.3074 (-2H_2O)	803.8879 (2+) 794.8824(-1H_2O) 785.8763 (-2H_2O) 776.8709 (-3H_2O) 1568.8190 (+1) 1550.8099 (-1H_2O) 1532.8014 (-2H_2O) 1514.7854 (-3H_2O)
#16	633.3378 (2+) 624.3321 (-1H_2O) 615.3268 (-2H_2O)	758.8721 (2+) 749.8662(-1H_2O) 740.8620 (-2H_2O)	625.3396 (2+) 616.3344 (-1H_2O) 607.3306 (-2H_2O)	766.8687 (2+) 757.8634(-1H_2O) 748.8581 (-2H_2O) 739.8535 (-3H_2O) 730.8477 (-4H_2O) 721.8418 (-5H_2O)	633.3371 (2+) 624.3320 (-1H_2O) 615.3268 (-2H_2O)	766.8689 (2+) 757.8635(-1H_2O) 748.8581 (-2H_2O) 739.8501 (-3H_2O) 730.8446 (-4H_2O)
#17	n.d.	1478.7890 (+1) 1460.7782 (-1H_2O) 1442.7681 (-2H_2O) 1424.7509 (-3H_2O)	n.d.	1494.7825 (+1) 1476.7724 (-1H_2O) 1458.7620 (-2H_2O) 1440.7522 (-3H_2O)	n.d.	1494.7835 (+1) 1476.7734 (-1H_2O) 1458.7627 (-2H_2O) 1440.7475 (-3H_2O)
#18	704.3657 (2+) 695.3647 (-1H_2O) 686.3587 (-2H_2O)	1318.7157 (1+) (-1H_2O) 1300.7056 (-2H_2O)	696.3716 (2+) 687.3668 (-1H_2O) 678.3606 (-2H_2O)	695.8370 (2+) 686.8324 (-1H_2O) 1334.7101 (1+) (-1H_2O) 1316.6980 (-2H_2O) 1298.6853 (-3H_2O)	704.3652 (2+) 695.3632 (-1H_2O) 686.3567 (-2H_2O)	695.8342 (2+) 686.8318 (-1H_2O) 1334.7057 (+1) (-1H_2O) 1316.6976 (-2H_2O)
#19	961.5059(2+) (-1H_2O) 952.4984 (-2H_2O)	n.d.	961.5037 (2+) (-1H_2O) 952.5000 (-2H_2O)	804.4383 (1+)	969.5067 (2+) (-1H_2O) 960.5002 (-2H_2O)	804.4399 (1+)
#21	1142.6052 (2+) 1133.5993 (-1H_2O) 1124.5932 (-2H_2O)	406.2212 (1+) (-3H_2O)	1142.6048 (2+) 1133.5978 (-1H_2O) 1124.5909 (-2H_2O) 1115.5837 (-3H_2O)	406.2232 (1+) (-3H_2O)	1150.6038 (2+) 1141.5969 (-1H_2O) 1132.5912 (-2H_2O) 1123.5829 (-3H_2O)	406.2204 (1+) (-3H_2O)

Table IV.5 (continued)

#22	n.d.	1157.6099 (2+) 1148.6035 (-1H_2O) 1139.5936 (-2H_2O) 1130.5952 (-3H_2O)	1156.6012 (2+) (-1H_2O)
#23	n.d.	1187.6203 (2+) 1178.6112 (-1H_2O) 1169.6038 (-2H_2O) 1160.6047 (-3H_2O)	1186.6064 (2+) (-1H_2O) 1177.6086 (-2H_2O) 1168.5970 (-3H_2O)
#24	n.d.	1228.6418 (+2) (-1H_2O)	1236.6357 (+2) (-1H_2O)
#25	1226.6392 (+2) (-2H_2O) 1217.6421 (-3H_2O) 1204.6346 (-4H_2O)	1235.6461 (2+) (-1H_2O) 1226.6404 (-2H_2O) 1217.6352(-3H_2O) 1208.6287 (-4H_2O) 1199.6246 (-5H_2O)	1234.6423 (+2) (-2H_2O) 1225.6333 (-3H_2O) 1216.6313 (-4H_2O)
#26	n.d.	1248.6538 (2+) (-1H_2O) 1239.6480 (-2H_2O) 1230.6425 (-3H_2O) 1221.6365 (-4H_2O)	1256.6518 (2+) (-1H_2O) 1247.6471 (-2H_2O) 1238.6402(-3H_2O) 1229.6342 (-4H_2O)
#27	1249.6436 (+2) (-1H_2O) 1240.6458 (-2H_2O)	1249.6468 (+2) (-1H_2O)	1248.6404 (+2) (-1H_2O) 1239.6271 (-2H_2O)

2.2 Quantitative analysis

Based on XICs of $[M+H+Ca]^{3+}$ ions of known and new ovatoxins (Table IV.6), *Ostreopsis* spp. strains from Cyprus Island produced very minute amounts of palytoxin-like compounds (0.06-2.8 pg/cell).

Table IV.6 Molecular formula [M] of the main palytoxin congeners so far known and isotopic ions used in quantitative analyses.

Toxin		Formula [M]	$[M+H+Ca]^{3+}$, *m/z*	
Name	Acronym		Monoisotopic	Most intense
Palytoxin	**PLTX**	$C_{129}H_{223}O_{54}N_3$	906.4828	906.8172
Homopalytoxin	**homoPLTX**	$C_{130}H_{225}O_{54}N_3$	911.4891	911.4891
Bishomopalytoxin	**bishomoPLTX**	$C_{131}H_{227}O_{54}N_3$	911.1547	911.4891
Neopalytoxin	**neoPLTX**	$C_{129}H_{221}O_{53}N_3$	900.4793	900.8137
Deoxypalytoxin	**deoxyPLTX**	$C_{129}H_{223}O_{53}N_3$	901.1511	901.4856
42-hydroxypalytoxin	**42-OHPLTX**	$C_{129}H_{223}O_{55}N_3$	911.8144	912.1489
Ostreocin-D	**OSTR-D**	$C_{127}H_{219}O_{53}N_3$	891.8084	892.1422
Ostreocin-B	**OSTR-B**	$C_{127}H_{219}O_{54}N_3$	897.1403	897.4749
Isobaricpalytoxin	**IsobPLTX**	$C_{129}H_{223}O_{54}N_3$	906.4828	906.8172
Ovatoxin-a	**OVTX-a**	$C_{129}H_{223}O_{52}N_3$	895.8255	896.1572
Ovatoxin-b	**OVTX-b**	$C_{131}H_{227}O_{53}N_3$	910.4976	910.8318
Ovatoxin-c	**OVTX-c**	$C_{131}H_{227}O_{54}N_3$	915.8286	916.1628
Ovatoxin-d	**OVTX-d**	$C_{129}H_{223}O_{53}N_3$	901.1533	901.4884
Ovatoxin-e	**OVTX-e**	$C_{129}H_{223}O_{53}N_3$	901.1533	901.4884
Ovatoxin-f	**OVTX-f**	$C_{131}H_{227}O_{52}N_3$	905.1632	905.4976
Ovatoxin-g	**OVTX-g**	$C_{129}H_{223}O_{51}N_3$	890.4879	890.8223
Ovatoxin-h	**OVTX-h**	$C_{129}H_{225}O_{51}N_3$	891.1598	891.4942
Ovatoxin-i	**OVTX-i**	$C_{131}H_{225}O_{53}N_3$	909.8242	910.1572
Ovatoxin-j_1	**OVTX-j_1**	$C_{131}H_{225}O_{54}N_3$	915.1564	915.4908
Ovatoxin-j_2	**OVTX-j_2**	$C_{131}H_{225}O_{54}N_3$	915.1555	915.4877
Ovatoxin-k	**OVTX-k**	$C_{131}H_{225}O_{55}N_3$	920.4871	920.8189

The toxin levels on a per cell basis of individual samples (Table IV.7) were significatively lower than those recorded in the Ligurian*O.* cf. *ovata* CBA-29 reference sample (44 pg/cell) [11] which had been grown under the same experimental conditions, and of other Adriatic and Tyrrhenian *O*. cf. *ovata* strains reported so far [5, 10].

Table IV.7 Total toxin content on a per-cell basis (pg/cell) and relative abundance (%) of ovatoxins (OVTX-) and isobaric palytoxin (isobPLTX), in the *Ostreopsis* spp. strains from Cyprus Island in comparison with a Ligurian *O.* cf. *ovata* strain used as reference. All the strains were cultured under the same experimental conditions.

	***Ostreopsis* spp.**												***O.* cf. *ovata***	
	CBA-C1012		**CBA-C1017**		**CBA-C1019**		**CBA-C1020**		**CBA-C1035**		**CBA-C1036**		**CBA-29**	
	pg/cell	**%**	**pg/cell**	**%**	**pg/cell**	**%**	**pg/cell**	**%**	**pg/cell**	**%**	**pg/cell**	**%**	**pg/cell**	**%**
isob PLTX	-		-		Trace		Trace		Trace		-		1.5	3.4
OVTX-a	-		-		0.87	96	2.70	97	0.34	96	-		33.5	76.2
OVTX-d	-		-		0.02	3	0.04	2	0.01	3	-		4.35	9.9
OVTX-e	-		-		0.02	2	0.04	1	0.01	2	-		4.62	10.5
OVTX-i	-		0.03	60	-		-		-		0.10	61	-	
OVTX-j_1	-		0.02	40	-		-		-		0.07	39	-	
OVTX-j_2	0.47	47	-		-		-		-		-		-	
OVTX-k	0.54	53	-		-		-		-		-		-	
Total	1.02		0.06		0.91		2.8		0.36		0.17		43.97	

2.3 Growth curve of *Ostreopsis* spp. and eco-toxicity bioassay

One of the *Ostreopsis* spp. strains (CBA-C1036) was used for eco-toxicological bioassays using *A. salina* nauplii. The growth curve, followed for 33 days, reported a specific growth rate of 0.51 per day and a stationary phase reached after 21 day from the initial inoculation, with a maximum density of 9625 cells/mL. Since several studies report that the toxicity of *O*. cf. *ovata* increased along the growth curve [11, 16, 17], we performed the eco-toxicological test of *Ostreopsis* spp. during the late stationary phase (on day 28^{th}) (Figure IV.5).

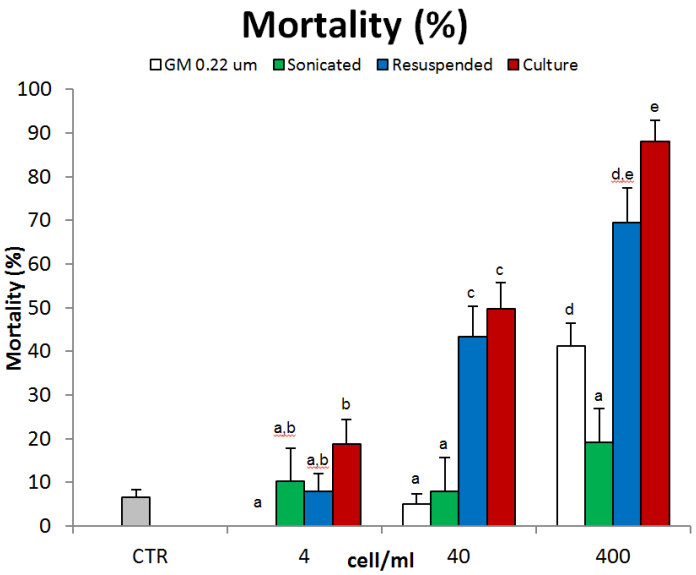

Figure IV.5 Mortality (average ±SE, N=3) of *A. salina* nauplii after 48 h exposure to several treatments of *Ostreopsis* spp. CBA-C1036 cultured strain, namely growth medium filtered at 0.22 µm (GM 0.22 um), filtered, resuspended and sonicated cells in fresh medium (Sonicated), filtered and resuspended cells in fresh medium (Resuspended), and whole culture (Culture). Control (CTR) in natural filtered seawater. Different letters (a – e) represent significant differences (SNK test results).

Overall, our data showed that increasing concentration of algal cells progressively inhibited the nauplii mobility and resulted in increased mortality values. In particular, lethal effects were significantly stronger ($p < 0.05$) with the whole and the resuspended *Ostreopsis* spp. CBA-C1036 treatments, resulting in $LC_{50\text{-}48h}$ values of 45 and 99 cells/mL respectively; the other treatments: the Growth Medium filtered through a 0.22 µm filter mesh free of algal cells (GM 0.22 µm) and the filtered, resuspended and sonicated cells in fresh medium (Sonicated) reported $LC_{50\text{-}48h} > 400$ cells/mL as shown in Table IV.8.

Table IV.8 $LC_{50\text{-}48h}$ (mortality) obtained exposing *A. salina* nauplii to several treatments of *Ostreopsis* spp. CBA-C1036 and *O.* cf. *ovata*CBA-29 strains.

Treatments	***Ostreopsis* spp. CBA-C1036 $LC_{50\text{-}48h}$ (cells/mL)**	***O.* cf. *ovat a*CBA29 $LC_{50\text{-}48h}$ (cells/mL)**
Whole culture	45 (31 – 63)	< 4
Resuspended	99 (40 - 244)	15 (12 – 20)
Sonicated	> 400	66 (51 – 84)
GM 0.22 µm	> 400	> 400

It has to be noted that for the GM 0.22 μm treatment, a 41% mortality value ($p < 0.05$) was observed, but only at the highest concentration tested (400 cells/mL) (Figure IV.5); however the $LC_{50\text{-}48h}$ valueis high and comparable (> 400 cells/mL) to that previously observed for *O.* cf. *ovata* CBA-29 strain [11].

These results describe a toxicity pattern similar to that previously observed for the most widespread species *O.* cf. *ovata* [11]. Indeed, Faimali et al. [18] investigating the toxic effects of this dinoflagellate on invertebrate and vertebrate marine organisms, highlighted that the presence of living algal cells causes significant toxic effects, while the growth medium alone (analogous treatment to GM 0.22 μm described in this study) reported slight or even none effects, independently of the tested organisms. Among all the tested marine organisms, *A. salina* resulted to be the most sensitive species [18] and so, in the present study, we selected it as model organism for investigation on toxicity of one the *Ostreopsis* spp. strains from Cyprus Island.

Comparison of LC_{50} values of each *Ostreopsis* spp. treatment with those obtained by Giussani et al. [11, 19] on *O.* cf. *ovata* showed that *Ostreopsis* spp. CBA-C1036 strain was less toxic than *O.* cf. *ovata* CBA-29 (Table IV.8). This finding is in good agreement with the chemical analyses that measured a lower toxin content in *Ostreopsis* spp. strain CBA-C1036 than in *O.* cf. *ovata* CBA29, together with a different toxin profile (Table IV.7).

3. Material and methods

3.1 Strain collection

Six strains of *Ostreopsis* spp. were isolated from epiphytic seaweed mats collected on July 3rd 2013 from Vasiliko Bay, a heavily impacted coastline in south Cyprus [20]. Surface seawater temperature on the sampling day was 25 °C and salinity was 39. Several samples of macroalgae (mainly *Halopteris scoparia*) with surrounding seawater were collected between 0 and 1 m depth using 500 mL plastic bottles. Samples were vigorously shaken for 10 sec to detach epiphytic cells from the macroalga, then 1 mL replicates of seawater were observed at the light microscope. After confirming the presence of the target species, around 500 mL seawater samples were sieved through a 0.5 mm mesh to remove macrophyte debris and sediments. Finally, several 50 mL sterile plastic flasks were filled with the samples and diluted in 0.2 μm filtered natural seawater (3:1) in order to decrease the potential bacterial density. The samples were shipped to DISB, University of Urbino for strain isolation and identification.

3.2 Strain isolation and microscopy identification

Ostreopsis strains were isolated as described by Penna et al. [21]. The Mediterranean strains were named as CBA-C1012, CBA-C1017, CBA-C1019, CBA-C1020, CBA-C1035, and CBA-C1036. In order to clarify the genus-specific *Ostreopsis* taxonomic identification, cell morphology was studied by light microscopy either under phase contrast, or staining with the Fluorescent Brightener 28, according to Fritz and Triemer [22].

3.3 Taxonomic molecular identification by PCR assay and sequence analysis

Genomic DNA was extracted and purified from 50 mL monoclonal culture of *Ostreopsis* spp. in logarithmic growth phase using DNeasy Plant Kit (Qiagen, CA, USA) according to the manufacturer's instructions. Briefly, cultures were collected by centrifugation at 3000 x *g* for 15 min. The supernatant was removed and the pellets were transferred to a 1.5 mL tube, centrifuged at 13000 x *g* for 10 min and allowed to dry completely at room temperature. The pellets were immediately processed or stored at -80 °C until DNA extraction. The PCR amplification and sequencing of ITS-5.8S rDNA protocols were described in Penna *et al.* [23]. The nucleotide sequences (LN875552; LN875553; LN875554; LN875555; LN875556; LN875557) of ITS- 5.8S rDNA were deposited in ENA-EMBL.

3.4 *Ostreopsis* spp. cultures

Cells were cultured in 1 L glass flasks containing 500 mL sterilized F/4 medium, a derivative of F/2 Guillard growth medium [24], with an initial cell concentration of 1.0×10^3. The temperature was set at 22 °C. Light was provided by cool white fluorescent bulbs (photon flux of 100 $\mu E\ m^{-2}\ s^{-1}$) on a standard 14:10 h light:dark (L:D) cycle. Culture samples were fixed with Lugol's iodine and counted using Utermhöl method [25]. A total volume of 1 L culture was harvested on 10^{th} day of growth by centrifugation at 3000 x *g* for 15 min at room temperature. Pellets containing 6.0×10^6 cells were stored at -80 °C and shipped to the Department of Pharmacy, University of Napoli for chemical analyses.

3.5 Growth curve and eco-toxicological bioassay

Eco-toxicological bioassay was set up at ISMAR-CNR in Genova, using the algal strain CBA-C1036 which had been cultured into natural sterilized marine water and Guillard F/2 medium (at a concentration of 1 mL L^{-1}) and maintained at 20 ± 0.5 °C in a 16:8 h L:D cycle (light intensity 85-135 μE m^{-2} s^{-1}). In order to assess the specific growth parameters of this dinoflagellate, we set up a preliminary growth curve starting with an inoculation of 80 cells/mL. Net exponential growth rate (μ t^{-1}) was calculated as the slope of a regression line of ln (N) versus time (t^{-1}), where N was the estimated cell concentration. Only the exponential portion of the growth curve was used for the calculation [26, 27]. The eco-toxicological experiments were performed according to Faimali et al. [18]. In particular, *Artemia salina* nauplii (15-20 specimens per well) were exposed to 4, 40, 400 cells/mL of the following treatments of the algal culture collected during the late stationary growth phase: a) whole culture, b) filtered and resuspended cells in fresh medium, c) resuspended and sonicated cells in fresh medium, and d) growth medium free of algal cells (0.22 μm filter mesh). Three replicates were prepared for each combination of treatments and cell concentrations, including a control (CTR; 0.22 μm Filtered Natural Sea Water). The lethal end point (% of mortality) was assessed under a stereomicroscope after 24 and 48 h. In particular, mortality is calculated as the sum of dead larvae (not swimming and moving appendages for 10 s of observation) [28]. LC_{50} values were calculated using trimmed Spearman - Karber analysis. Two way ANOVA (Factors: Concentration, 3 levels; Treatments, 4 levels; orthogonal and fixed), and Student-Newman-Keuls tests were performed using R statistical software.

3.6 Reagents and Standards for Chemical Analyses

Chemical analyses were performed at Department of Pharmacy, University of Napoli. All organic solvents and water (HPLC grade) and glacial acetic acid (Laboratory grade) were by Sigma Aldrich (Steinheim, Germany). A palytoxin standard (100μg; lot STJ7776) from Wako Chemicals GmbH (Neuss, Germany) was dissolved in methanol/water (1:1, v/v) and used for quantitative analyses. It should be noted that this standard is not certified and may contain some minor contaminants besides palytoxin itself; quali-quantitative composition of the standard may vary within different lots. The standard used in this study contained 83% of palytoxin itself, 5% of 42- hydroxypalytoxin, and 12% of contaminant(s). Crude extracts of Adriatic OOAN0601 and Ligurian CBA-29 *O.* cf. *ovata* containing a pool of ovatoxins [10, 11] were used as reference samples in chemical analyses.

3.7 Sample extraction

Six cell pellets, namely CBA-C1012 (1.9 x 10^6 cells), CBA-C1017 (1.35 x 10^6 cells), CBA-C1019 (1.71 x 10^6 cells), CBA-C1020 (2.17 x 10^6 cells), CBA-C1035 (3.5 x 10^6 cells), CBA-C1036 (2.65 x 10^6 cells) were extracted by adding 1 mL of a methanol/water (1:1, v/v) solution and sonicated for 10 min in pulse mode, while cooling in ice bath. The mixture was centrifuged at 3000 x *g* for 1 min and the supernatant was decanted. The extraction procedure was repeated again on each pellet to obtain two extracts for each samples that were separately analyzed by LC-HRMS (5 µL injected). For most of the samples toxins were present in quantifiable amounts only in the 1st extract and barely detectable in the 2nd extract. For the sample CBA-C1020, a dilution 1:4 was necessary to quantify the toxins in the 1st extract, while for the sample CBA-C1017 toxins were not detectable in the 2nd extract. Quantitation was made summing the toxin content of the 1st and the 2nd extracts, where possible.

3.8 LC-HRMS^n

LC-HRMS^n (n= 1, 2) experiments were carried out on a Dionex Ultimate 3000 quaternary system coupled to a hybrid linear ion trap LTQ Orbitrap XL^{TM} Fourier Transform MS (FTMS) equipped with an ESI ION MAX^{TM} source (Thermo-Fisher, San Josè, CA, USA). Chromatographic separation was accomplished by using a Poroshell 120 EC-C18, 2.7 µm, 2.1 × 100 mm (Agilent, USA) maintained at room temperature and eluted at 0.2 mL min^{-1} with water (eluent A) and 95% acetonitrile/water (eluent B), both containing 30 mM acetic acid. A slow gradient elution that allowed a sufficient chromatographic separation of most palytoxin-like compounds was used: 28–29 % B over 5 min; 29–30 % B over 10 min; 30–100 % B in 1 min, and hold for 5 min [29].

HR full MS experiments (positive ions) were acquired in the range *m/z* 800-1400 at a resolving power (RP) of 60,000 (FWHM at *m/z* 400). The following source settings were used in all LC-HRMS experiments: a spray voltage of 4.8 kV, a capillary temperature of 290°C, a capillary voltage of 17 V, a sheath gas and an auxiliary gas flow of 32 and 4 (arbitrary units). The tube lens voltage was set at 145 V. HR collision induced dissociation (CID) MS^2 experiments were acquired at a RP= 60,000 using a collision energy (CE)= 35 %, isolation width (IW)= 4.0 Da, activation Q= 0.250, and activation time (At)= 30 ms. The most intense peak of the $[M+H+Ca]^{3+}$ ion cluster of isobaric palytoxin (isobPLTX) and ovatoxins (OVTXs) were used as precursors (Table 1) in HRMS/MS experiments. Calculation of elemental formulae was performed using the mono-isotopic peak of each ion cluster using

Xcalibur software v2.0.7. with a mass tolerance constrain of 5 ppm. The isotopic pattern of each ion cluster was taken into account in assigning molecular formulae.

For quantitative purposes, extracted ion chromatograms (XIC) of all the palytoxin congeners so far known were obtained by selecting the $[M+H+Ca]^{3+}$ ion clusters (Table 1), using a mass tolerance of 5 ppm. Due to availability of the only palytoxin standard, quantitative determination of known and new OVTXs, and isobPLTX in the extracts was carried out by using a calibration curve (triplicate injection) of palytoxin standard at five levels of concentration (100, 50, 25, 12.5, and 6.25 ng mL^{-1}) and assuming that their molar responses were similar to that of PLTX. Calibration curve equation was y=31657x – 211166 and its linearity was expressed by R^2= 0.9987.

4. Conclusions

Based on molecular results, *Ostreopsis* spp. from Cyprus was found to be a species distinct from O. cf. *ovata* and *O.* cf. *siamensis*, belonging to the Atlantic/Mediterranean *Ostreopsis* spp. clade [8-9]. Its toxin profile has been investigated for the first time highlighting some variability in toxin profile among the six *Ostreopsis* spp. analyzed strains. In more detail, three of the analyzed strains produced some of the known ovatoxins (OVTX-a, -d, -e) and isobaric palytoxin, so far found only in O. cf. *ovata* strains [5-6, 12, 30-32]; the remaining strains produced four new ovatoxins (OVTX-i, -j_1, -j_2, and -k). They represent a new addition to the palytoxin group of toxins having the same carbon backbone as ovatoxin-a, all differing for an additional $C_2H_2O_2$ moiety and an unsaturation in the region C49-C52. Further minor structural differences were found, including the presence of a hydroxyl group at C44 (in OVTX-j_1 and -k) and the lack of a hydroxyl group in the region C53-C78 (in OVTX-i and -j_1). All these structural features were deduced from interpretation of $HRMS^2$ spectra of individual ovatoxins contained in crude algal extracts at levels 50-1000 ng/mL, too low for attempting any isolation work.

It is quite surprising that the six strains, collected in the same area and during the same period, present two different toxin profiles: one profile containing only C129-type toxins (OVTX-a, -d, -e, and isobPLTX) and the other one containing only C131-type toxins (OVTX-i, -j_1, -j_2 and k). It would be interesting to investigate whether environmental factors are associated with these two toxin profiles and which other primary or secondary metabolites in the strains are different.

Toxin content of the analyzed *Ostreopsis* spp. strains on a per cell basis was 15-700 times lower than that of a Ligurian *O.* cf. *ovata* strain cultured under the same experimental conditions (Table IV.6). Accordingly, eco-toxicological test on A. salina nauplii demonstrated that *Ostreopsis* spp. presents a very low toxicity compared to *O.* cf. *ovata*. The whole of chemical and eco-toxicological data suggest that *Ostreopsis* spp. from Cyprus Island pose a relatively low risk to humans.

Our results highlight once again the need for an interdisciplinary effort for a correct risk management associated to *Ostreopsis* blooms, involving mainly molecular identification of the species and quali-quantitative determination of the toxin profile.

References

1. Ciminiello P, Dell'Aversano C, Iacovo ED, Fattorusso E, Forino M, Grauso L, Tartaglione L (2012) High resolution LC-MSn fragmentation pattern of palytoxin as template to gain new insights into ovatoxin-A structure. The key role of calcium in MS behavior of palytoxins. J Am Soc Mass Spectrom 23(5):952-963

2. Uemura D, Ueda K, Hirata Y, Naoki H, Iwashita T (1981) Further studies on palytoxin. II. Structure of palytoxin. Tetrahedron Lett 21:2781–2784.

3. Moore RE, Bartolini G (1981) Structure of palytoxin. J Am Chem Soc. 103:2491–2494

4. Ciminiello P, Dell'Aversano C, Dello Iacovo E, Fattorusso E, Forino M, Grauso L, Tartaglione L, Guerrini F, Pezzolesi L, Pistocchi R, Vanucci S (2012) Isolation and structure elucidation of ovatoxin-a, the major toxin produced by *Ostreopsis ovata*. J Am Chem Soc 134(3):1869-1875

5. Ciminiello P, Dell'Aversano C, Dello Iacovo E, Fattorusso E, Forino M, Tartaglione L, Battocchi C, Crinelli R, Carloni E, Magnani M, Penna A (2012) Unique toxin profile of a Mediterranean *Ostreopsis* cf. *ovata* strain: HR LC-MSn characterization of ovatoxin-f, a new palytoxin congener. Chem Res Toxicol 25(6):1243-1252

6. García-Altares M, Tartaglione L, Dell'Aversano C, Carnicer O, de la Iglesia P, Forino M, Diogène J, Ciminiello P (2015) The novel ovatoxin-g and isobaric palytoxin (so far referred to as putative palytoxin) from *Ostreopsis* cf. *ovata* (NW Mediterranean Sea): structural insights by LC-high resolution MSn. Anal Bioanal Chem 407:1191-1204

7. Ciminiello P, Dell'Aversano C, Dello Iacovo E, Fattorusso E, Forino M, Grauso L, Tartaglione L (2012) Stereochemical studies on ovatoxin-a. Chem Eur J 18(52):16836-16843

8. David H, Laza-Martínez A, Miguel I, Orive E (2013) Ostreopsis cf. siamensis and *Ostreopsis* cf. *ovata* from the Atlantic Iberian Peninsula: Morphological and phylogenetic characterization. Harmful Algae 30: 44-55

9. Penna A, Battocchi C, Capellacci S, Fraga S, Aligizaki K, Leme R (2014) Mitochondrial, but not rDNA, genes fail to discriminate dinoflagellate species in the genus *Ostreopsis* 40:40-50. Doi:10.1016/j.hal.2014.10.004

10. Pezzolesi L, Guerrini F, Ciminiello P, Dell'Aversano C, Dello Iacovo E, Fattorusso E, Forino M, Tartaglione L, Pistocchi R (2012) Influence of temperature and salinity on *Ostreopsis* cf. *ovata* growth and evaluation of toxin content through HR LC-MS and biological assays. Water Res 46(1):82-92

11. Giussani V, Sbrana F, Asnaghi V, Vassalli M, Faimali M, Casabianca S, Penna A, Ciminiello P, Dell'Aversano C, Tartaglione L, Mazzeo A, Chiantore M (2015) Active role of the mucilage in the toxicity mechanism of the harmful benthic dinoflagellate *Ostreopsis* cf. *ovata*. Harmful Algae 44:46-53.

12. Ciminiello P, Dell'Aversano C, Dello Iacovo E, Fattorusso E, Forino M, Grauso L, Tartaglione L, Guerrini F, Pistocchi R (2010) Complex palytoxin-like profile of *Ostreopsis ovata*. Identification of four new ovatoxins by high-resolution liquid chromatography/mass spectrometry. Rapid Commun Mass Spectrom 24(18):2735-2744

13. Dell'Aversano C, Tartaglione L, Dello Iacovo E, Forino M, Casabianca S, Penna A, Ciminiello P, *Ostreopsis* cf. *ovata* from the Mediterranean Sea. Variability in toxin profiles and structural elucidation of unknowns through LC-HRMSn. MacKenzie AL [Ed]. Marine and Freshwater Harmful Algae. Proceedings of the 16th International Conference on Harmful Algae, Wellington, New Zealand 27th-31st October 2014. ISBN 978-0-473-33091-0; pp. 70-73

14. Uchida H, Taira Y, Yasumoto T (2013) Structural elucidation of palytoxin analogs produced by the dinoflagellate *Ostreopsis ovata* IK2 strain by complementary use of positive and negative ion liquid chromatography/quadrupole time of flight mass spectrometry. Rapid Commun Mass Spectrom 27(17):1999-2008

15. Kellmann R, Stüken A, Russell JS, Svendsen HM, Jakobsen KS (2010) Biosynthesis and Molecular Genetics of Polyketides in Marine Dinoflagellates. Mar Drugs 8(4): 1011-1048

16. Vidyarathna NK, Granéli E (2012) Influence of temperature on growth, toxicity and carbohydrate production of a Japanese *Ostreopsis ovata* strain, a toxic-bloom-forming dinoflagellate. Aquat Microb Ecol 65(3):261-270

17. Guerrini F, Pezzolesi L, Feller A, Riccardi M, Ciminiello P, Dell'Aversano C, Tartaglione L, Dello Iacovo E, Fattorusso E, Forino M, Pistocchi R (2010) Comparative growth and toxin profile of cultured *Ostreopsis ovata* from the Tyrrhenian and Adriatic Seas. Toxicon 55:211-220

18. Faimali M, Giussani V, Piazza V, Garaventa F, Corrà C, Asnaghi V, Privitera D, Gallus L, Cattaneo-Vietti R, Mangialajo L, Chiantore M (2012) Toxic effects of harmful benthic dinoflagellate *Ostreopsis ovata* on invertebrate and vertebrate marine organisms. Mar Environ Res 76: 97-107

19. Privitera D, Giussani V, Isola G, Faimali M, Piazza V, Garaventa F, Asnaghi V, Cantamessa E, Cattaneo-Vietti R, Chiantore M (2012) Toxic effects of *Ostreopsis ovata* on larvae and juveniles of Paracentrotus lividus. Harmful Algae 18:16-23

20. Orfanidis S, Panayotidis P, Stamatis N (2001) Ecological evaluation of transitional and coastal waters: A marine benthic macrophytes-based model. Medit Mar Sci 2.2:45-66

21. Penna A, Vila M, Fraga S, Giacobbe MG, Andreoni F, Riobo P, Vernesi C (2005) Characterization of *Ostreopsis* and *Coolia* (*Dinophyceae*) isolates in the western Mediterranean Sea based on morphology, toxicity, and internal transcribed spacer 5.8S rDNA sequences. J. Phycol. 41:212-225

22. Fritz L, Triemer RE (1985) A rapid simple technique utilizing calcofluor white M2R for the visualization of dinoflagellate thecal plates1. J Phycol 21(4):662-664

23. Penna A, Fraga S, Battocchi C, Casabianca S, Giacobbe MG, Riobò P, Vernesi C (2010) A phylogeography study of the toxic benthic genus *Ostreopsis* Schmidt. J Biogeogr 37:830-841

24. Guillard RRL (1975) Culture of phytoplankton for feeding marine invertebrates In: Smith WL, Chanley MH (eds) Culture of Marine Invertebrate Animals. Plenum Press, New York pp 29-60

25. Utermöhl VH (1931) Neue Wege in der quantitativen Erfassung des Planktons. Verh Int Ver Theor Angew Limnol 5:567-596

26. Guillard RRL (1973) Division rates In: Stein (ed) Handbook of Phycological Methods V1. Cambridge University Press, Cambridge pp 289-312

27. Berdalet E, Peters F, Koumandou VL, Roldan C, Guadayol O, Estrada M (2007) Species-specific physiological response of dinoflagellates to quantified small-scale turbulence1. J Phycol 43(5):965-977

28. Piazza V, Dragić I, Sepčić K, Faimali M, Garaventa F, Turk T, Berne S (2014) Antifouling activity of synthetic alkylpyridinium polymers using the barnacle model. Mar Drugs 12(4):1959-1976

29. Ciminiello P, Dell'Aversano C, Dello Iacovo E, Forino M, Tartaglione L (2015) Liquid chromatography–high-resolution mass spectrometry for palytoxins in mussels. Anal Bioanal Chem 407:1463–1473. Doi 10.1007/s00216-014-8367-6

30. Ciminiello P, Dell'Aversano C, Fattorusso E, Forino M, Magno GS, Tartaglione L, Grillo C, Melchiorre N (2006) The Genoa 2005 outbreak. Determination of putative palytoxin in Mediterranean *Ostreopsis ovata* by a new liquid chromatography tandem mass spectrometry method. Anal Chem 78:6153-6159

31. Ciminiello P, Dell'Aversano C, Fattorusso E, Forino M, Tartaglione L, Grillo C, Melchiorre N (2008) Putative palytoxin and its new analogue, ovatoxin-a, in *Ostreopsis ovata* collected along the Ligurian coasts during the 2006 toxic outbreak. J Am Soc Mass Spectrom 19(1):111-120

32. Brissard C, Herrenknecht C, Séchet V, Hervé F, Pisapia F, Harcouet J, Lémée R, Chomérat N, Hess P, Amzil Z (2014) Complex toxin profile of French Mediterranean *Ostreopsis* cf. *ovata* strains, seafood accumulation and ovatoxins pre purification. Mar Drugs 12(5):2851-2876

Chapter 5: Chemical analysis of *Ostreopsis* spp. from Lebanon and New Zealand. Structural insights into a new palytoxin like compound by LC-HRMS/MS

1. Introduction

Palytoxins are the major emerging toxins in the Mediterranean area [1-3]. Nonetheless, palytoxin-producing algae have been detected also in coastal waters of Japan, New Zealand, Australia, and Brazil among others [4-5]. In none of these countries, however, the impact on human health seems to be as heavy as in the Mediterranean area. Whether this is due to the chemical features of the involved toxins or to the environmental conditions affecting bloom intensity or aerosols formation is currently unknown. Anyhow, the increasing spread of the phenomenon and the ever-growing number of PLTXs being discovered makes the need of evaluating their toxicity even more urgent.

As a matter of fact, although palytoxins, ostreocins and differ little in structural details - a few methyl, methylene and/or hydroxyl groups over a long polyhydroxylated aliphatic chain - their relative potencies might be very different. Palytoxin itself is exceptionally toxic in-vivo (LD50 iv in mice= 0.045 μg/kg) and in-vitro with several effects being recorded at nanomolar concentrations on cells and tissues (hemolysis, histamine, prostaglandin and norepinephrine release, among others) [6-7]. Ostreocin-D - which overall presents 2 methyl and 1 hydroxyl group less than PLTX - is 3 to 6 fold less toxic than PLTX both in-vivo and in-vitro. In regard to individual ovatoxin analogues, no data on their relative toxicity are currently available. Toxicological studies need to be performed to ensure a correct risk assessment of the *Ostreopsis*-related syndrome and to eventually explore the potential of such molecules or of their biogenetic precursors as pharmacological tools.

This study aimed at defining whether *Ostreopsis* spp. from Lebanon, New Zealand, and Australia are toxin-producing species. Several strains of *Ostreopsis* spp. were collected in such localities and analyzed by LC-HRMS^n (n= 1,2). The employed approach [8] uses the fragmentation pattern of a structurally defined palytoxin congener, such as PLTX [9-10] or OVTX-a [11] (Figure V.1), as a template for structural characterization of the unknown [12-13] providing tentative structures.

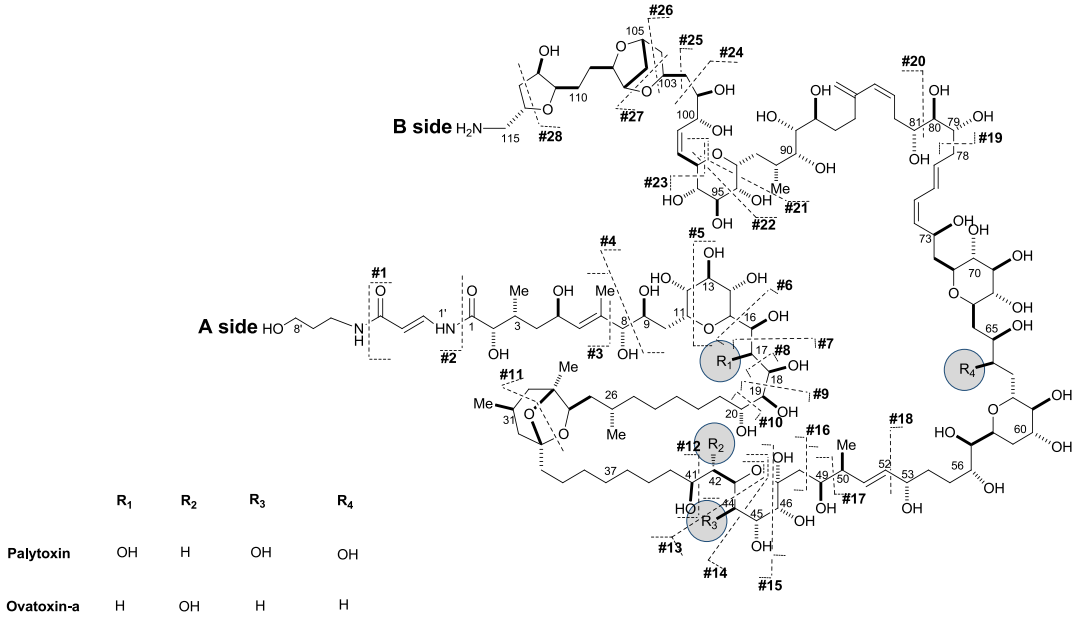

	R_1	R_2	R_3	R_4
Palytoxin	OH	H	OH	OH
Ovatoxin-a	H	OH	H	H

Figure V.1 Structure of PLTX and OVTX-a as determined by NMR studies. Cleavage #14, #20, #28 and #6+12 occur only in PLTX. The stereochemistry ofPLTX is depicted. The stereochemistry of OVTX-a is inverted at position C9, C26, and C57

2. Results and discussion

2.1 Chemical and quantitative analysis of *Ostreopsis* sp. from Lebanon

Five strains of *Ostreopsis* sp. were collected along the Lebanon costs. Crude extracts of L1002, L1007, L1008, L1020, and L1022 strains were analyzed by LC-HRMS^n (n=1, 2) to characterize their toxin profiles and measure their toxin content. The analyses were carried out versus a palytoxin standard and a Ligurian *O.* cf. *ovata* extract containing OVTX-a, -d and –e and isobaric palytoxin [14]. The chromatographic conditions allowed the separation of all of the analogues contained in the extracts.

Extracts L1007, L1020 and L1022 contained OVTX-a, -d and -e. Their identity was ascertained based on comparison of their retention times and associated full MS spectra (Figure V.2) with those of OVTX-a, -d, -e, contained in the reference extract.

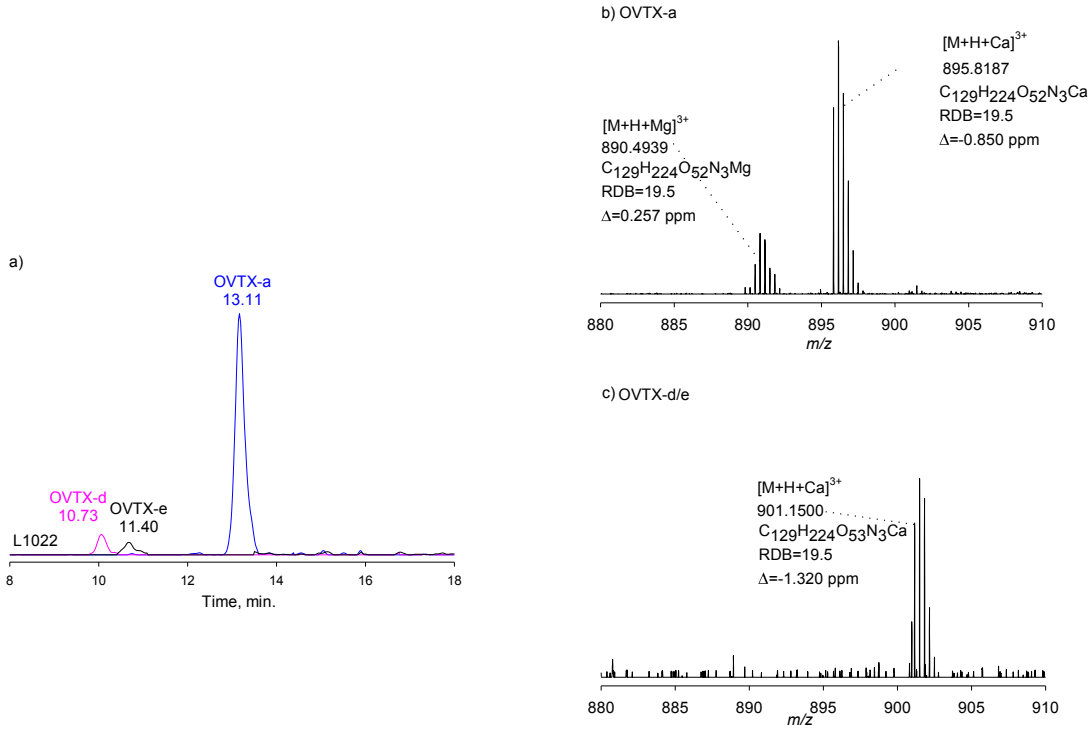

Figure V.2 LC-HRMS analysis of *Ostreopsis* sp. L1022 strain, including (a) extracted ion chromatogram (XIC) of $[M+H+Ca]^{3+}$ ions of ovatoxin-a (OVTX-a) and of the structural isomers ovatoxin-d and -e (OVTX-d, -e). Enlargements of the full HRMS spectra of (b) OVTX-a and (c) OVTX-d/-e.

Further confirmation for the identity of OVTX-a and of the structural isomers OVTX-d and -e was provided by their LC-HRMS^2 spectra which were superimposable to those of OVTX-a, -d and -e previously characterized [15-17]. Extracts L1002 and L1008 did not contain any palytoxin congener. Considering the extraction volume, the absence of toxins in pellet (1 x 10^6 cells), could be estimated at levels ≥ 15 fg/cell.

The results of the quantitative analysis are shown in Table V.1. *Ostreopsis* sp. strains from Lebanon produced very minute amounts of OVTXs (0.28-0.94 pg/cell), thus not representig a threat for human health.

Table V.1 Total toxin content on a per-cell basis (pg/cell) and relative abundance (%) of ovatoxins (OVTX-), in the *Ostreopsis* sp. strains from Lebanon

	Toxin content (pg/cell)	Relative intensities		
		OVTX-a	OVTX-d	OVTX-e
L1002	nd	-	-	-
L1007	0.28	81.6%	11.7%	6.7%
L1008	nd	-	-	-
L1020	0.47	86.7%	8.8%	4.5%
L1022	0.94	87.8%	7.7%	4.5%

The toxin profile of these strains quali-quantitatively matched with that of other *Ostreopsis* sp. strains from Cyprus Island previously characterized [18] and that found in about 40% of the Mediterranean *O*. cf. *ovata* strains analyzed so far [15]. Molecular analysis showed that *Ostreopsis* sp. from Lebanon and that from Cyprus Island are actually the same *Ostreopsis* species that we named *Ostreopsis Fattorussoi*.

2.2 Chemical analysis of *Ostreopsis* spp. from New Zealand

Six culture extracts of *Ostreopsis* spp. collected in New Zealand and Australia, namely CAWD147 (*O. siamensis*), CAWD174 (*O.* cf. *ovata*), CAWD203 (*O. siamensis*), CAWD206 (*O. siamensis*), CAWD208 (*O. siamensis*) and CAWD221 (*Ostreopsis* sp.) were analyzed by LC-HRMS/MS. None of the known PLTX congeners so far known were detected in any of the extracts. The analyses of the full-scan HRMS spectra were performed extracting the ion chromatograms for OVTX-a to –h, ostreocin-d and –b, and all PLTXs from *Palythoa* (PLTX, homoPLTX, NeoPLTX etc.) (see Table IV.6), using exact masses and a mass tolerance of 5 ppm. No peak related to the above PLTX congeners emerged. Then, we proceeded in-depth investigating Total Ion Chromatograms (TIC) of the extracts, in order to highlight the presence of potentially new analogues eluting in proximity of PLTX standard by matching the triply charged ions with the relevant doubly-charged ions.

As a result, the presence of a new PLTX-like compound (preliminarily name Compound-1) in the sample CAWD221 was detected. Full HRMS spectrum of the Compound-1 typically contained a triply charged ions at *m/z* 863.4685 which correspond to $[M+H+Ca]^{3+}$ and several doubly charged ions, including the $[M+2H+Na]^{2+}$ at *m/z* 1286.7161 (Table V.2). A cross check of the elemental formulae of all the ions contained in the spectrum allowed to assign the molecular formula $C_{124}H_{216}O_{51}N_2$ to Compound-1.

Table V.2. Data from HR Full MS of CAWD221 extract: elemental formulae assigned to the mono-isotopic ion peaks of the most intense triply and doubly charged ions, relative double bonds equivalents (RDB) and errors (Δ ppm).

	m/z	Molecular formula	RDB	Δ ppm
$[M+H+Ca]^{3+}$	863.4689	$C_{124}H_{217}O_{51}N_2Ca$	17.5	0.32
$[M+2H+Na]^{2+}$	1286.7161	$C_{124}H_{217}O_{51}N_2Na$	17	-0.54
$[M+2H+K]^{2+}$	1294.7008	$C_{124}H_{217}O_{51}N_2K$	17	-2.25
$[M+2H-5H_2O]^{2+}$	1230.7003	$C_{124}H_{208}O_{46}N_2$	22	0.78
$[M+2H-6H_2O]^{2+}$	1221.6949	$C_{124}H_{206}O_{45}N_2$	23	0.71
$[M+2H-8H_2O]^{2+}$	1203.6819	$C_{124}H_{202}O4_3N_2$	25	-1.36

Interestingly, Compound-1 presented a C_5H_7ON moiety and 2 unsaturation less than OVTX-a ($C_{129}H_{223}O_{52}N_3$, RDB= 20). This suggested that 1 of the 3 Nitrogen atoms, present in all of the PLTX-like compounds so far known, was lacking in compound-1. Since the compound was contained in the extract at levels too low to be isolated and studied by NMR, the LC-$HRMS^n$ approach developed by Ciminiello *et al.* [19] was applied to investigate its structural features.

The HR CID MS^2 spectrum of the $[M+H+Ca]^{3+}$ ion at *m/z* 863.9 revealed that the compound-1 is actually a new PLTX congener. Similarly to OVTX-a, its fragmentation spectrum was dominated by a cluster of $[M+H+Ca-nH_2O]^{3+}$, (n= 2-7) ions due to subsequent water losses from the precursor and contained many diagnostic ions which could be related to those of OVTX-a.

Table V.3 Assignment of A-side, B-side and internal fragments contained in $HRMS^2$ spectra of ovatoxin-a (OVTX-a) and Compound-1 to relevant cleavages (#Clv) reported in **Errore. L'origine riferimento non è stata trovata.**. Monoisotopic ion peaks of all the fragment ions contained in HR CID MS^2 spectra of $[M+H+Ca]^{3+}$ ions for OVTX-a and in HR CID ([a]), HDC ([b]) and PQD ([c]) MS^2 spectra of $[M+H+Ca]^{3+}$ ions for Compound-1. The first ion diagnostic of each cleavage is followed by 1 to 8 ions due to subsequent water losses or formaldehyde losses for Compound-1; the most intense ion of each group is underlined.

	OVTX-a *m/z* **(1+, 2+, 3+) (-nH_2O)**		**Compound-1** *m/z* **(1+, 2+, 3+) (-nH_2O), (-nCH_2O),**	
Precursor	**896.1 (3+)** 883.8109 (-2H_2O) 877.8077 (-2H_2O) 871.8041 (-4H_2O) 865.8007 (-5H_2O) 859.7970 (-6H_2O) 853.7936 (-7H_2O) 847.7886 (-8H_2O)		**863.9 (3+)[a]** 851.4605 (-2H_2O)[a] 845.4572 (-3H_2O)[a] 839.4538 (-4H_2O)[a] 833.4500 (-5H_2O)[a] 827.4465 (-6H_2O)[a] 821.4419 (-7H_2O)[a] **853.4639 (-CH_2O)[a]** 847.4605 (-1H_2O)[a] 841.4571 (-2H_2O)[a] 835.4536 (-3H_2O)[a] 829.4501 (-4H_2O)[a] 823.4464 (-5H_2O)[a]	
Clv	**A side *m/z* (1+,2+,+3) Formula, (RDB)**	**B side *m/z* (1+,2+,+3) Formula, (RDB)**	**A side *m/z* (1+,2+,+3) Formula, (RDB)**	**B side *m/z* (1+,2+,+3) Formula, (RDB)**
#4	327.1908 (1+)(-1H_2O) $C_{16}H_{27}O_5N_2$ (4.5) 309.1804 (-2H_2O)	1171.1261 (2+) $C_{113}H_{195}O_{46}NCa$ (17.0) 1162.1209 (-1H_2O) 1153.1158 (-2H_2O) 1144.1108 (-3H_2O) 1135.1062 (-4H_2O) 1126.1009 (-5H_2O) 1117.0952 (-6H_2O) 1108.0942 (-7H_2O) 781.0867 (3+) $C_{113}H_{196}O_{46}NCa$ (16.5) 775.0827 (-1H_2O) 769.0792 (-2H_2O) 763.0763 (-3H_2O) 757.0728 (-4H_2O) 751.0699 (-5H_2O)	212.1275 (1+)(-3H_2O)[b,c] $C_{11}H_{18}O_3N$ (3.5) 194.1170 (-4H_2O)[b,c] 182.1170 (-CH_2O)[b,c] 164.1064 (-1H_2O)[b,c]	1171.1274 (+2)[a,b,c] $C_{113}H_{195}O_{46}NCa$ 1162.1221 (-1H_2O)[a,b,c] 1153.1169 (-2H_2O)[a,b,c] 1144.1117 (-3H_2O)[a,b,c] 781.0869 (+3)[a,b,c] $C_{113}H_{196}O_{46}NCa$ (16.5) 775.0835 (-1H_2O)[a,b,c] 769.0798 (-2H_2O)[a,b,c] 763.0762 (-3H_2O)[a,b,c] 757.0726 (-4H_2O)[a,b,c] 751.0684 (-5H_2O)[a,b,c]
#5	nd.	nd.	nd.	746.4043 (+3)(-1H_2O)[a,b,c] $C_{109}H_{188}O_{43}Nca$ (16.5) 740.4010 (-2H_2O)[a,b,c] 734.3974 (-2H_2O)[a,b,c]
#11	438.2238 (2+) $C_{40}H_{72}O_{16}N_2$ Ca (6.0) 429.2194 (-1H_2O)		nd.	
#12	536.2965 (2+) $C_{52}H_{92}O_{18}N_2Ca$ (8.0) 527.2914 (-1H_2O) 518.2858 (-2H_2O)	799.8905 (2+) (-3H_2O) $C_{77}H_{125}O_{31}NCa$ (16.0) 790.8860 (-4H_2O)	472.7642 (2+)(-CH_2O)[c] $C_{46}H_{83}O_{16}NCa$ (6.0) 463.7588 (-1H_2O[c]	799.8905 (2+) (-3H_2O)[a] $C_{77}H_{125}O_{31}NCa$ (16.0)
#13	566.3074 (2+) $C_{54}H_{96}O_{20}N_2Ca$ (8.0) 557.3021 (-1H_2O) 548.2969 (-2H_2O)	787.8919 (2+) (-1H_2O) $C_{75}H_{125}O_{31}NCa$ (14.0) 778.8858 (-2H_2O) 769.8802 (-3H_2O)	nd.	nd.
#14	nd.	nd.	nd.	nd.

Table V.5 (continued)

#15	588.3201 (2+) $C_{56}H_{100}O_{21}N_2Ca$ (8.0) 579.3151 (-$1H_2O$) 570.3100 (-$2H_2O$)	774.8829 (2+) $C_{73}H_{123}O_{31}NCa$ (13.0) 765.8781 (-$1H_2O$) 756.8727 (-$2H_2O$) 747.8673 (-$3H_2O$) 1510.8122 (1+) $C_{73}H_{124}O_{31}N$ (12.5) 1492.8023 (-$1H_2O$) 1474.7919 (-$2H_2O$) 1456.7814 (-$3H_2O$) 1438.7758 (-$4H_2O$)	539.7943 (2+)[a,b] $C_{51}H_{93}O_{21}NCa$ (6.0) 524.7889 (-CH_2O)[a,b,c] 515.7824 (-$1H_2O$)[c]	774.8839 (+2)[a,b] $C_{73}H_{123}O_{31}NCa$ (13.0) 765.8785 (-$1H_2O$)[a,b,c] 756.8735 (-$2H_2O$)[a] 1510.8142 (+1)[a] 1492.8026 (-$1H_2O$)[a,b] 1474.7876 (-$2H_2O$)[a]
#16	625.3387 (2+) $C_{59}H_{106}O_{23}N_2Ca$ (8.0) 616.3335 (-$1H_2O$) 607.3279 (-$2H_2O$)	737.8650 (2+) $C_{70}H_{117}O_{29}NCa$ (13.0) 728.8596 (-$1H_2O$) 719.8543 (-$2H_2O$) 710.8491 (-$3H_2O$) 701.8436 (-$4H_2O$) 692.8384 (-$5H_2O$) 683.8331 (-$6H_2O$) 674.8286 (-$7H_2O$) 1436.7765 (1+) $C_{70}H_{118}O_{29}N$ (12.5) 1418.7659 (-$1H_2O$) 1400.7555 (-$2H_2O$) 1382.7446 (-$3H_2O$) 1364.7341 (-$4H_2O$) 1346.7232 (-$5H_2O$) 1328.7132 (-$6H_2O$)	576.8117 (+2)[b] $C_{54}H_{99}O_{22}NCa$ (6.0) 567.8066 (-$1H_2O$)[b] 561.8062 (+2)(-CH_2O)[a,b,c] $C_{53}H_{97}O_{21}NCa$ (6.0) 552.8004 (-$1H_2O$)[b,c]	737.8654 (+2)[a,b,c] $C_{70}H_{117}O_{29}NCa$ (13.0) 728.8601 (-$1H_2O$)[a,b,c] 719.8536 (-$2H_2O$)[b,c] 718.8479 (-$3H_2O$)[b,c] 701.8425 (-$4H_2O$)[b,c] 692.8376 (-$5H_2O$)[b,c] 1436.7771 (+1)[a] $C_{70}H_{118}O_{29}N$ (12.5) 1418.7655 (-$1H_2O$)[a,b]
#17	639.3359 (2+) $C_{60}H_{106}O_{24}N_2Ca$ (9.0) 630.3310 (-$1H_2O$) 621.3256 (-$2H_2O$)	1390.7716 (1+) (-$1H_2O$) $C_{69}H_{116}O_{27}N$ (12.5) 1372.7605 (-$2H_2O$) 1354.7502 (-$3H_2O$)	nd.	nd.
#18		686.8308 (2+) (-$1H_2O$) $C_{65}H_{107}O_{27}NCa$ (13.0) 677.8256 (-$2H_2O$)		nd.
#19	932.5032 (2+)(-$1H_2O$) $C_{90}H_{156}O_{35}N_2Ca$ (14.0) 923.4983 (-$2H_2O$) 914.4923 (-$3H_2O$)	804.4365(+1) $C_{39}H_{66}O_{16}N$ (7.5)	nd.	nd.
#21	1113.6005 (2+) $C_{107}H_{186}O_{43}N_2Ca$ (16.0) 1104.5954 (-$1H_2O$) 1095.5591 (-$2H_2O$) 1086.5866 (-$3H_2O$) 1077.5794 (-$4H_2O$)	406.2216 (1+) (-$3H_2O$) $C_{22}H_{32}O_6N$ (7.5)	1065.0699 (2+)[b] $C_{102}H_{179}O_{42}NCa$ (14.0) 1050.0679 (-CH_2O)[a,b,c]	406.2213 (1+) (-$3H_2O$)[b] $C_{22}H_{32}O_6N$ (7.5)
#22	1128.6053 (2+) $C_{108}H_{188}O_{44}N_2Ca$ (16.0) 1119.6021(-$1H_2O$) 1110.5962 (-$2H_2O$) 1101.5869 (-$3H_2O$) 1092.5846 (-$4H_2O$)		nd.	
#23	1158.6164 (2+) $C_{110}H_{192}O_{46}N_2Ca$ (16.0) 1149.6107(-$1H_2O$) 1149.6107 (-$2H_2O$) 1140.6057 (-$3H_2O$) 1131.5990 (-$4H_2O$) 1122.5981 (-$5H_2O$)		nd.	
#24	1199.6367 (2+) (-$1H_2O$) $C_{115}H_{198}O_{47}N_2Ca$ (18.0) 1190.6363 (-$2H_2O$)		nd.	

Table V.5 (continued)

#25	1206.6449 (2+) (-1H_2O) $C_{116}H_{200}O_{47}N_2Ca$ (18.0) 1197.6399 (-2H_2O) 1188.6347 (-3H_2O) 1179.6286 (-4H_2O) 1170.6232 (-5H_2O)	nd.
#26	1219.6517 (2+) (-1H_2O) $C_{118}H_{202}O_{47}N_2Ca$ (19.0) 1210.6477 (-2H_2O) 1201.6436 (-3H_2O) 1192.6379 (-4H_2O) 1183.6332 (-5H_2O) 1174.6263 (-6H_2O)	nd.
#27	1220.6386 (2+) (-1H_2O) $C_{117}H_{200}O_{48}N_2Ca$ (19.0) 1211.6380 (-2H_2O)	nd.
#4+#12	364.1999 (2+) $C_{36}H_{64}O_{12}Ca$ (5.0)	364.1992 (2+)[c] $C_{36}H_{64}O_{12}Ca$ (5.0)
	727.3924 (1+) $C_{36}H_{63}O_{12}Ca$ (5.5)	727.3931 (1+)[a,b] $C_{36}H_{63}O_{12}Ca$ (5.5)
#4+#13	394.2104 (2+) $C_{38}H_{68}O_{14}Ca$ (5.0)	394.2105 (2+)[c] $C_{38}H_{68}O_{14}Ca$ (5.0)
#4+#15	416.2234 (2+) $C_{40}H_{72}O_{15}Ca$ (5.0)	416.2225 (2+)[c] $C_{40}H_{72}O_{15}Ca$ (5.0)
#4+#16	453.2415 (2+) $C_{43}H_{78}O_{17}Ca$ (5.0)	453.2412 (2+)[c] $C_{43}H_{78}O_{17}Ca$ (5.0)
#5+#12	641.3557 (1+) $C_{32}H_{57}O_{10}Ca$ (4.5)	641.3542 (1+)[b,c] $C_{32}H_{57}O_{10}Ca$ (4.5)
#7+#12	521.3136 (1+) $C_{28}H_{49}O_6Ca$ (4.5)	nd.
#8+#12	507.2979 (1+) $C_{27}H_{47}O_6Ca$ (4.5)	507.2987 (1+)[a,b,c] $C_{27}H_{47}O_6Ca$ (4.5)
#9+#12	477.2875 (1+) $C_{26}H_{45}O_5Ca$ (4.5)	nd.
#10+#12	447.2771 (1+) $C_{25}H_{43}O_4Ca$ (4.5)	nd.

In particular, all the B-side fragments generated by cleavages #4, #12, #15, #16 and #21 and all the internal fragments presented the same elemental composition as those of ovatoxin-a (Table V.3), suggesting that Compound-1 and OVTX-a share the part structure stretching from C-9 to the B-side terminal of the molecule. Therefore, the lack of C_5H_7ON part structure had to occur in the very limited region stretching from the A-side terminal to C-8. Surprisingly, using CID as fragmentation mode, we were not able to detect the A-side fragment generated by cleavage #4, which is normally very abundant in the MS^2 spectrum of PLTX-like compound as well as most of the A-side fragments generated by the aforementioned cleavages. In order to in depth investigate such portion of the molecule, other experiments, using alternative fragmentation modes namely pulsed Q collision induced dissociation (PQD) and high energy collision dissociation (HCD) were carried out. HR PQD and HR HCD MS^2 spectra of the $[M+H+Ca]^{3+}$ ion at *m/z* 863.9 resulted to be very informative in containing the A-side fragments generated by cleavages #4, #12 and #16, which were not present in HR CID MS^2 spectrum as well as most of the internal fragments detected (#4+#12, #4+#13, #4+#15,

#4+#16 and #5+#12). In particular, the A-side fragment due to the cleavage #4 (*m/z* 212.1275, $C_{11}H_{18}O_3N$ RDB = 3.5) displayed a C_5H_7ON moiety less than the corresponding part structure of OVTX-a, confirming that a significant structural change was occurring in the region stretching from the A-side terminal to C8. Interestingly, this compound presented a characteristic fragmentation behavior: indeed, together with water losses that can be generally observed in the fragmentation spectra of all of PLTX congeners, for the first time, formaldehyde losses from the precursor ion as well as from most of the A-side fragment ions, were present. Formaldehyde losses are neutral losses which can occur when a CH_2OH moiety is present in the molecule [20] following a Mac Lafferty-like rearrangement. Since most of the A-side fragments underwent formaldehyde loss, we made a structural hypothesis for Compound-1 locating a CH_2OH moiety at position 1' and suggesting a possible rearrangement in the A-side terminal of the molecule (Figure V.3 and Figure V.4).

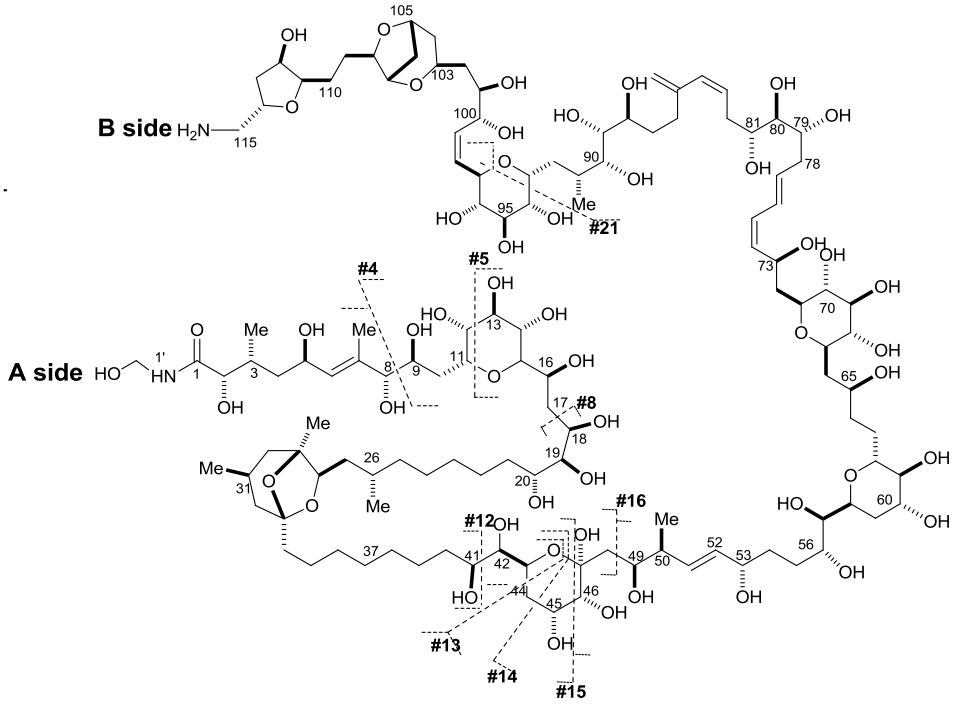

Figure V.3 Tentative structure of Compound-1

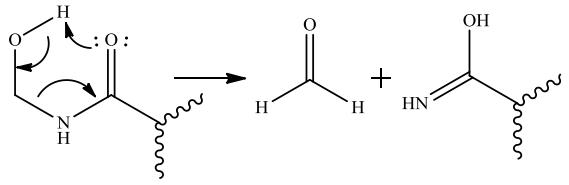

Figure V.4 Hypothesis of rearrangement mechanism resulting in formaldehyde loss

3. Material and methods

3.1 Reagents for Chemical Analyses

All organic solvents and water (HPLC grade) and glacial acetic acid (Laboratory grade) were by Sigma Aldrich (Steinheim, Germany). A palytoxin standard (100µg; lot LAM7122) from Wako Chemicals GmbH (Neuss, Germany) was dissolved in methanol/water (1:1, v/v) and used for quantitative analyses. This standard is not certified and may contain some contaminants besides palytoxin itself; its quali-quantitative composition of the standard may vary within different lots. The standard used in this study contained 83% of palytoxin itself, 5% of 42- hydroxypalytoxin, and 12% of contaminant(s). A crude extract of Ligurian CBA-29 *O*. cf. *ovata* [14] containing a pool of ovatoxins was used as reference sample for identification of ovatoxins in algal extracts.

3.2 Samples extraction

Cell pellets of five *Ostreopsis* sp. strains collected along Lebanon coasts, namely L1002 (8.0 x 10^6 cells), L1007 (1.0 x 10^7 cells), L1008 (3.0 x 10^6 cells), L1020 (4.8 x 10^6 cells), L1022 (1.0 x 10^6 cells), were extracted once by adding 1-10 mL of methanol/water (1:1, v/v) so to have a concentration of about 1.0 x 10^6 cells per mL of extracting solvent. The mixtures were sonicated for 10 min in pulse mode, while cooling in ice bath, and centrifuged at 3000 x *g* for 1 min; the obtained supernatants were then decanted and analyzed by LC-HRMS (5µL injected).

Six strains of *Ostreopsis* spp. collected in New Zealand, namely CAWD147 (3.7 x 10^6 cells), CAWD174 (5.8 x 10^6 cells), CAWD203 (1.5 x 10^6 cells), CAWD206 (5.4 x 10^6 cells), CAWD208 (1.9 x 10^6 cells) and CAWD221 (1.6 x 10^7 cells) were extracted with methanol. The mixtures were sonicated for 10 min in pulse mode, while cooling in ice bath, and centrifuged at 3000 x *g* for 1 min; the obtained supernatants were then decanted and analyzed by LC-HRMS (5µL injected).

3.3 LC- HRMS^n

MS experiments (positive ions) were carried out on a Dionex Ultimate 3000 quaternary system coupled to a hybrid linear ion trap LTQ Orbitrap XL^{TM} Fourier Transform MS (FTMS) equipped with an ESI ION MAX^{TM} source (Thermo-Fisher, San Josè, CA, USA). A Poroshell 120 EC-C18, 2.7 µm, 2.1 × 100 mm column (Agilent, USA) maintained at

room temperature was used. It was eluted at 0.2 mL/min with water (eluent A) and 95% acetonitrile/water (eluent B), both containing 30 mM acetic acid. A slow gradient elution was used: 28–29 % B over 5 min; 29–30 % B over 10 min; 30–100 % B in 1 min, and hold for 5 min.

HR full scan MS experiments (positive ions) were acquired in the range *m/z* 800-1400 at a resolving power (RP) of 60,000 (FWHM at *m/z* 400). The following source settings were used: a spray voltage of 4.8 kV, a capillary temperature of 290°C, a capillary voltage of 17 V, a sheath gas and an auxiliary gas flow of 32 and 4 (arbitrary units). The tube lens voltage was set at 145 V. HR CID, PQD and HCD MS^2 experiments were acquired at a RP= 60,000 using a collision energy (CE) of 35%, 25% and 20% respectively, isolation width (IW)= 3.0 Da, activation Q= 0.250, and activation time (At)= 30 ms. The most intense peak of the $[M+H+Ca]^{3+}$ ion cluster of OVTX-a (*m/z* 896.1), OVTX-d/-e (*m/z* 901.4) and of the new compound (*m/z* 863.9) were used as precursors in $HRMS^2$ experiments. Calculation of elemental formulae was performed using the mono-isotopic peak of each ion cluster using Xcalibur software v2.0.7. with a mass tolerance constrain of 5 ppm. The isotopic pattern of each ion cluster was taken into account in assigning molecular formulae. Extracted ion chromatograms (XIC) of the detected OVTXs were obtained by selecting the $[M+H+Ca]^{3+}$ ion clusters, using a mass tolerance of 5 ppm and employed in quantitative analyses. Due to availability of the only PLTX standard, quantitative determination of OVTX-a, -d, and -e in the extracts was carried out by using a calibration curve (triplicate injection) of PLTX standard at seven levels of concentration (1000, 500, 250, 125, 62.5, 31.2 and 15.6 ng/mL). Ovatoxin molar responses were assumed to be similar to that of PLTX. Calibration curve equation was y = 2455.6x – 19184 and its linearity was expressed by R^2= 0.9976. The instrumental limit of detection of PLTX in pure solvent was13 ng/mL corrected for the 83% purity of the standard.

4. Conclusions

Based on chemical and molecular results, *Ostreopsis* sp. from Lebanon was found to be the same species of *Ostreopsis* sp. from Cyprus Island, distinct from *O.* cf. *ovata* and *O.* cf. *siamensis*, belonging to the Atlantic/Mediterranean *Ostreopsis* spp. clade [21-22]. The strains from Lebanon and some strains from Cyprus Island shared the same toxin profile in producing small amount of known OVTXs (OVTX-a, -d, -e), so far found only in *O.* cf. *ovata* strains [11-12,16,23-25]. This suggests that OVTXs are no species-specific toxins and their

content can vary a lot according to the producing species. Chemical analysis has shown that *Ostreopsis* spp. from Lebanon produce very little amount of toxins compared to *O*. cf. *ovata*. thus not presenting a real risk for humans.

Ostreopsis spp. strains collected in New Zealand did not contain any of the PLTX-like compounds so far known, but a new analogue, likely a precursor or a metabolite, which was detected in only one strain (CAWD221); further studies are ongoing to determine the exact species of *Ostreopsis* producing Compound-1 and to investigate the toxin profile of other *Ostreopsis* spp. strains from New Zealand and Australia with the aim of better characterizing the risk posed by *Ostreopsis* along New Zealand and Australian coasts.

References

1. EFSA CONTAM panel (2009) The EFSA Journal 7(12):1393

2. Mangialajo L, Ganzin N, Accoroni S, Asnaghi V, Blanfuné A, Cabrini M, Cattaneo-Vietti R, Chavanon F, Chiantore M, Cohu S, Costa E, Fornasaro D, Grossel H, Marco-Mirailles F, Maso M, Rene A, Rossi AM, Montserat Sala M, Thibaut T, Totti C, Vila M. &Lemée R, (2011). Trends in *Ostreopsis* proliferation along the Northern Mediterranean coasts. Toxicon 57, 408-420

3. Ramos V, Vasconcelos V, (2010). Palytoxin and analogs: biological and ecological effects. Mar. Drugs 8, 2021–2037

4. Rhodes L, (2011). World-wide occurrence of the toxic dinoflagellate genus *Ostreopsis* Schmidt. Toxicon 57, 400–407

5. Nascimento SM, Corrêa EV, Menezes M, Varela D, Paredes J, Morris S. 2011. Growth and toxin profile of Ostreopsis cf. ovata (Dinophyta) from Rio de Janeiro, Harmful Algae 13. 1-9

6. Munday R. 2011. Palytoxin toxicology: Animal studies. Toxicon. 57(3), 470-477

7. Ito E, Yasumoto T. (2009). Toxicological studies on palytoxin and ostreocin-D administered to mice by three different routes. Toxicon. 54(3), 244-251

8. Ciminiello P, Dell'Aversano C, Dello Iacovo E, Fattorusso E, Forino M, Grauso L, Tartaglione L (2012) High resolution LC-MSn fragmentation pattern of palytoxin as template to gain new insights into ovatoxin-A structure. The key role of calcium in MS behavior of palytoxins. J Am Soc Mass Spectrom 23(5), 952-963

9. Uemura D, Ueda K, Hirata Y, Naoki H, Iwashita T (1981) Further studies on palytoxin. II. Structure of palytoxin. Tetrahedron Lett 21, 2781–2784

10. Moore RE, Bartolini G (1981) Structure of palytoxin. J Am Chem Soc. 103:2491–2494

11. Ciminiello P, Dell'Aversano C, Dello Iacovo E, Fattorusso E, Forino M, Grauso L, Tartaglione L, Guerrini F, Pezzolesi L, Pistocchi R, Vanucci S (2012) Isolation and structure elucidation of ovatoxin-a, the major toxin produced by *Ostreopsis ovata*. J Am Chem Soc 134(3), 1869-1875

12. Ciminiello P, Dellaversano C, Iacovo ED, Fattorusso E, Forino M, Tartaglione L, Battocchi C, Crinelli R, Carloni E, Magnani M, Penna A (2012) Unique toxin profile of a Mediterranean *Ostreopsis* cf. *ovata* strain: HR LC-MSn characterization of ovatoxin-f, a new palytoxin congener. Chem Res Toxicol 25(6), 1243-1252

13. García-Altares M, Tartaglione L, Dell'Aversano C, Carnicer O, de la Iglesia P, Forino M, Diogène J, Ciminiello P (2015) The novel ovatoxin-g and isobaric palytoxin (so far referred to as putative palytoxin) from *Ostreopsis* cf. *ovata* (NW Mediterranean Sea): structural insights by LC-high resolution MSn. Anal Bioanal Chem 407, 1191-1204

14. Giussani V, Sbrana F, Asnaghi V, Vassalli M, Faimali M, Casabianca S, Penna A, Ciminiello P, Dell'Aversano C, Tartaglione L, Mazzeo A, Chiantore M (2015) Active role of the mucilage in the toxicity mechanism of the harmful benthic dinoflagellate Ostreopsis cf. ovata. Harmful Algae 44, 46-53

15. Dell'Aversano C, Tartaglione L, Dello Iacovo E, Forino M, Casabianca S, Penna A, Ciminiello P, *Ostreopsis* cf. *ovata* from the Mediterranean Sea. Variability in toxin profiles and structural elucidation of unknowns through LC-HRMS^n. MacKenzie AL [Ed]. Marine and Freshwater Harmful Algae. Proceedings of the 16th International Conference on Harmful Algae, Wellington, New Zealand 27th-31st October 2014. ISBN 978-0-473-33091-0; pp. 70-73

16. Ciminiello P, Dell'Aversano C, Dello Iacovo E, Fattorusso E, Forino M, Grauso L, Tartaglione L, Guerrini F, Pistocchi R (2010) Complex palytoxin-like profile of Ostreopsis ovata. Identification of four new ovatoxins by high-resolution liquid chromatography/mass spectrometry. Rapid Commun Mass Spectrom 24(18), 2735-2744

17. Ciminiello P, Dell'Aversano C, Iacovo ED, Fattorusso E, Forino M, Grauso L, Tartaglione L (2012) High resolution LC-MS^n fragmentation pattern of palytoxin as template to gain new insights into ovatoxin-A structure. The key role of calcium in MS behavior of palytoxins. J Am Soc Mass Spectrom 23(5), 952-963

18. Tartaglione L, Mazzeo A, Dell'Aversano C, Forino M, Giussani V, Capellacci S, Penna A, Asnaghi V, Faimali M, Chiantore M, Yasumoto T, Ciminiello P. (2016) Chemical, molecular, and eco-toxicological investigation of Ostreopsis sp. from Cyprus Island:

structural insights into four new ovatoxins by LC-HRMS/MS. Anal Bioanal Chem 408(3), 915-932

19. Ciminiello P, Dell'Aversano C, Dello Iacovo E, Forino M, Tartaglione L (2015) Liquid chromatography–high-resolution mass spectrometry for palytoxins in mussels. Anal Bioanal Chem 407(5), 1463-1473

20. Cardozo KHM, Vessecchi R, Galembeck SE, Guaratini T, Gates PJ, Pinto E, Lopes NP, Colepicoloa P. (2009) A Fragmentation Study of Di-Acidic Mycosporine-like Amino Acids in Electrospray and Nanospray Mass Spectrometry J. Braz. Chem. Soc., 20(9), 1625-1631

21. David H, Laza-Martínez A, Miguel I, Orive E (2013) Ostreopsis cf. siamensis and *Ostreopsis* cf. *ovata* from the Atlantic Iberian Peninsula: Morphological and phylogenetic characterization. Harmful Algae 30, 44-55

22. Penna A, Battocchi C, Capellacci S, Fraga S, Aligizaki K, Leme R (2014) Mitochondrial, but not rDNA, genes fail to discriminate dinoflagellate species in the genus *Ostreopsis* 40, 40-50

23. Ciminiello P, Dell'Aversano C, Fattorusso E, Forino M, Magno GS, Tartaglione L, Grillo C, Melchiorre N (2006) The Genoa 2005 outbreak. Determination of putative palytoxin in Mediterranean *Ostreopsis ovata* by a new liquid chromatography tandem mass spectrometry method. Anal Chem 78, 6153-6159

24. Ciminiello P, Dell'Aversano C, Fattorusso E, Forino M, Tartaglione L, Grillo C, Melchiorre N (2008) Putative palytoxin and its newanalogue, ovatoxin-a, in *Ostreopsis ovata* collected along the Ligurian coasts during the 2006 toxic outbreak. J Am Soc Mass Spectrom 19(1), 111-120

25. Brissard C, Herrenknecht C, Séchet V, Hervé F, Pisapia F, Harcouet J, Lémée R, Chomérat N, Hess P, Amzil Z (2014) Complex toxin profile of FrenchMediterranean *Ostreopsis* cf. *ovata* strains, seafood accumulation and ovatoxins prepurification. Mar Drugs 12(5), 2851-2876

Chapter 6: Algal toxin profiles in Nigerian coastal waters (Gulf of Guinea) using passive sampling and liquid chromatography coupled to mass spectrometry

1. Introduction

Toxins from marine micro-algae frequently accumulate in seafood, including fish and shellfish, and maximum concentrations for such toxins have therefore been regulated at global and regional levels [1-4]. As fisheries have only limited potential to increasingly contribute to the global food supply, it is expected that any growth in seafood supply will have to come from aquaculture. Therefore, it is important to investigate the potential of coastal areas for seafood production, and also the risks associated with such production. In terms of public health risks, those originating from harmful algal blooms are particularly common in many parts of the world and must therefore be assessed relatively early on in any survey for aquaculture feasibility.

To our knowledge, no algal toxins have been reported in coastal waters of central Western Africa, except one preliminary report on potentially toxic fish in Cameroon [5]. The southernmost records of algal toxins in Northern Africa are from the Moroccan coastline where an official monitoring program is in place [6-7]. Lipophilic shellfish toxins were shown to accumulate in mussels, cockles, oysters and solen, causing poisoning in the Dakhla region, *i.e.* the South Atlantic Moroccan coast [8]. Toxins of the okadaic acid (OA) group, *i.e*. OA and dinophysistoxins (DTXs) and their associated esters were the agents responsible for those shellfish poisoning events, attributable to the presence of several potentially toxic species of *Dinophysis*. Taleb *et al.* [9] also were the first to report the presence of azaspiracids in mussels, in Morocco.

In southern parts of Africa, regular monitoring is in place in South Africa and Namibia. Production of saxitoxin (STX) off the west coast of South Africa has been attributed to *Alexandrium catenella* [10-11]. Fawcett *et al.* [12] have developed and deployed a bio-optical buoy for monitoring HABs in the southern Benguela Current region off South Africa. These buoys have proved their efficiency in providing both real-time and time-series data, giving interesting information on the occurrence of *Prorocentrum triestinum* in the region. The northernmost records of algal toxins in the southern African region are from [13-14].

Phytoplankton surveys in Nigeria by one of the authors have reported non-toxin producing as well as potentially toxic algae including *Prorocentrum micans*, *Protoperidinium depressum*, *Prorocentrum mite*, *Dinophysis caudata*, *Peridinium gatunense*, *P. cinctum*, *Gymnodinium fuscum* and an array of *Ceratium* species [15-20]. Previous studies by other authors also showed sporadic occurrences of *D. caudata*, *Protoperidinium depressum*, *P. diabolus*, *Prorocentrum micans*, *and Noctiluca scintillans* in Lagos Lagoon [21-22]. A recent report additionally recorded *Lingulodinium polyedrum*, *Prorocentrum minimum*, *P. sigmoides* and *Scrippsiella trochoidea* in Lagos, Cross Rivers and Delta States [23].

As potentially toxic algae have repeatedly been reported from Nigerian coastal waters this study attempted to verify whether algal toxins actually do occur in Nigerian waters. Since there was no algal culturing facility available on site, and as many dinoflagellates are difficult to bring into culture, in particular *Dinophysis*, we have opted for an indirect approach based on passive sampling of algal toxins in Nigerian coastal waters. This approach had been introduced for monitoring of toxins by MacKenzie *et al.* [24]. We have focused on regulated lipophilic toxins known to cause problems in terms of public health but have also used in parallel an approach for untargeted analysis based on high-resolution mass spectrometry as previously described [25].

2. Results and discussion

2.1 Physico-chemical measurements

Water temperatures, salinity and nutrient levels in the study area confirm a strong correlation with seasonality (Table VI.1). Salinity ranged from 2 to 20, all areas and periods confounded, which is comparatively low for marine dinoflagellates. The two stations in the North-west of the study area (Lekki and Bar Beach) displayed the highest salinities, ranging from 17.2 to 18.2 during the end of the wet season (October 2014), and from 18.1 to 19.3 during the dry season (January / February 2015). The stations closer to the Niger delta (off the cities of Port Harcourt and Uyo) showed much lower salinities, with the Port Harcourt station (directly outside the main delta in River States) showing the lowest overall salinity of 2 in wet season (October 2014) but still reaching a salinity of 9 during dry season (February 2015).

Table VI.1 Surface water temperature, dissolved oxygen (DO), salinity and nutrient concentrations at sampling stations in Nigerian coastal waters 2014-15

Parameter	Bar Beach		Lekki		Port Harcourt		Uyo	
	18/10/14	02/02/15	17/10/14	30/01/15	19/10/14	04/02/15	18/10/14	03/02/15
Water Temp (°C)	26	27	27	26	32	30	25.5	31
DO (mg/L)	7.8	9.8	7.8	7.9	7.8	6.5	7.4	6.5
Salinity	18.2	19.3	17.2	18.1	2.0	8.8	6.6	7.8
PO_4^{3-} (mg/L)	0.07	0.51	0.03	0.2	0.07	0.22	0.03	0.51
NO_3^-(mg/L)	1.48	1.61	1.44	1.59	0.37	1.26	1.48	1.61

2.2 Identification of phytoplankton species

Based Phytoplankton samples were generally dominated by diatoms and cyanobacteria, especially filamentous cyanobacteria. However, several species of marine dinoflagellates were also observed (Figure VI.1 (a-b-c-d)). In particular, a few cells of *Dinophysis caudata* were observed in a sample from Bar Beach (21 February 2015). *D. caudata* had previously been reported as a producer of OA and PTX2 in different areas and should thus be considered as a potentially toxic species [26-29]. Interestingly, different regions reported different profiles of toxins in picked cells of *D. caudata*. In Northwestern Spain and China, the toxin profile was dominated by PTX2 [26, 29] while OA was shown to be present in picked cells of *D. caudata* from both Japanese and Singapore waters [27, 28].

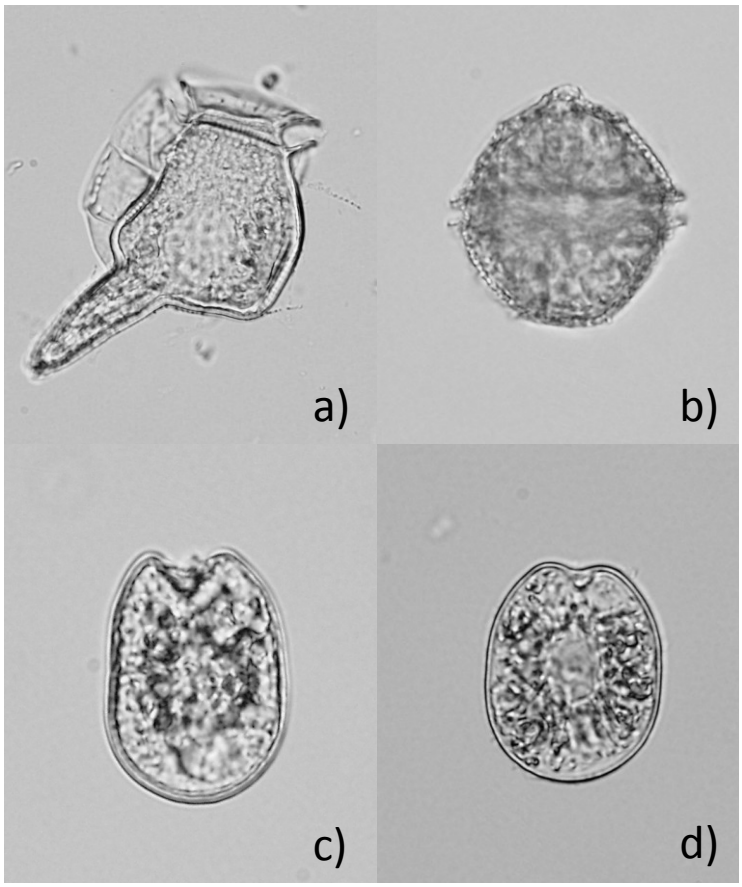

Figure VI.1 Marine dinoflagellates identified on Bar Beach (Lagos State, Nigeria, 21 February 2015): a) *Dinophysis caudata* (L = 100 µm), b) *Lingulodinium polyedrum* (L x W: 40 x 38 µm), c) *Prorocentrum* sp1 (L x W : 37 x 27µm) and d) *Prorocentrum* sp2 (L x W: 36.3 x 28.8 µm)

Another potentially toxic dinoflagellate was observed in the sample from Bar Beach: *Lingulodinium polyedrum*. This species is characterized by its polyhedral shape with a flat antapex lacking any projections, thick thecal plates with ridges along the sutures and circular depressions over the surface of the plates, see also Figure 2. The same organism had also been detected at a concentration of several thousand cells L^{-1} in coastal waters of Atlantic Morocco [30], and cultures of Spanish strains of *L. polyedrum* were shown to produce yessotoxin [31].

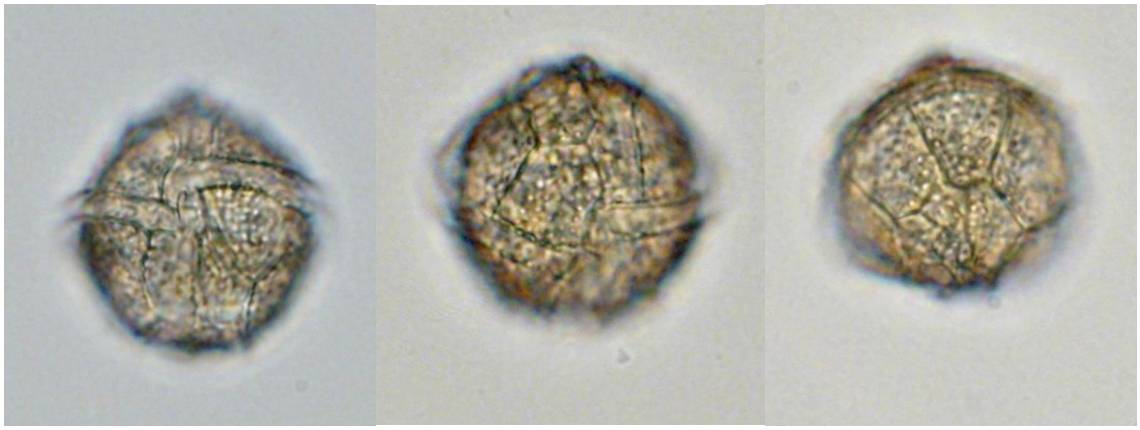

Figure VI.2 Surface focus of a *Lingulodinium polyedrum* cell in ventro-antapical view, in ventro-apical view and, in dorso-apical view showing ornamentation of plates (ridges along the sutures and circular depressions)

Three cells of two unidentified benthic *Prorocentrum* species have also been observed (Figure VI.1-c and -d). A number of benthic *Prorocentrum* species have been associated with the production of toxins of the okadaic acid, the prorocentrolide and the hoffmaniolide groups: *P. lima*, *P. belizeanum*, *P. maculosum*, *P. rhathymum* and *P. hoffmanianum* [32-35], but even a pelagic species of *Prorocentrum* (*P. texanum*) has recently been associated with the production of okadaic acid [36]. Therefore, this observation should be verified to determine the exact species of *Prorocentrum*.

2.3 Quantitative analysis of SPATT samples and toxin confirmation

One Passive samplers were deployed on different dates in November 2014 and February 2015. Analyses of SPATT carried out on System 1 revealed the presence of OA and PTX2 at different concentrations (Figure VI.3-a). Concentrations of OA and PTX2 were significantly higher at Lekki and Bar Beach compared to Port Harcourt and Uyo. This overall pattern seems consistent with the higher potential for *Dinophysis* to survive in areas of higher salinity [37]. *Dinophysis caudata* had also been previously found at Bar Beach and Lekki, sites which at that time had almost oceanic salinity [23]. As abovementioned, *D. caudata* had previously been associated with the production of OA and PTX2, and hence the occurrence of these toxins in Nigerian waters can most likely be attributed to this species. The levels of okadaic acid found (ca. 60 ng OA g^{-1} HP-20 resin) were of a similar order of magnitude than those found by MacKenzie *et al.* [24] in the initial study introducing passive sampling for algal toxins, but comparatively low compared to those reported in a previous study in Ireland

[38]. However, the concentrations in mussels (*M. edulis*) in the latter study also exceeded the regulatory level ca. 6-fold, and hence the actual contamination levels in shellfish in Nigeria should be verified to evaluate the risk for public health or before establishing commercial aquaculture sites. Interestingly, the levels of PTX2 observed in the present study were similar to those observed in the Irish study [38], which may be attributed to the different causative species in both areas: *D. acuminata* and *D. acuta* in Ireland, as compared to *D. caudata* in Nigeria. Rundberget *et al.* [39] had used passive samplers of the same geometry in Norway, and they also found levels of a similar height of order as those in the present study. They also established that SPATTs contained typically three times as much toxin as mussels in a given location, yet occasionally levels in mussels were higher than those in the passive samplers. Since the Irish study did not have the same ratios as those established in the Norwegian study, we anticipate that any correlation between the concentrations observed in passive samplers and a given shellfish species would have to be established locally and verified over time.

The ratio of OA to PTX2 was examined to look for major changes in phytoplankton community structure of OA-producing organisms (Figure VI.3-b). As *Prorocentrum* species have not been found to produce PTX2 but DTX1, a relative increase of OA over PTX2 could be indicative of their increasing importance. The ratio remained relatively constant over the study period indicating that there was either not much change in the population of micro-algae or similar ratios were produced by the organisms present. This is also consistent with the fact that DTX1 was found only in trace amounts at Lekki and Bar Beach, but not found at all in the two other locations. DTX1 has been reported from *P. lima* [40] and the low concentrations in passive samplers deployed at 1 m below the surface could be related to the dilution effect for these toxins if they had been produced by low density benthic species. However, it has been shown that even toxins from *P. lima* can accumulate to significant levels in shellfish locally [41], and hence care should be taken before discarding benthic organisms as a risk to public health.

At Bar Beach, it appeared that toxin concentrations were higher in November and in February which also coincides with a slight increase in salinity and the dry season, for which upwelling had been previously indicated [42]. At Port Harcourt and Uyo, concentrations of OA and PTX2 in the passive samplers were *ca*. 10-fold lower than the maxima observed at Bar Beach and Lekki. This significant difference is understandable from the very low salinities observed at Port Harcourt and Uyo (Table VI.1), which are detrimental for most marine dinoflagellates, in particular *Dinophysis* [37]. The differences in concentrations found

in passive samplers extracts from Port Harcourt and Uyo on one hand and Lekki and Bar Beach on the other are much larger than what could be expected from the simple differences in adsorption due to different salinities. A recent study has shown that kinetics of adsorption may be affected [43], however, this should be negligible for the 1-week deployment periods in the present study. Port Harcourt and Uyo are considered to be brackish water zones and are consequently significantly different from Bar Beach and Lekki (see also section on untargeted analysis).

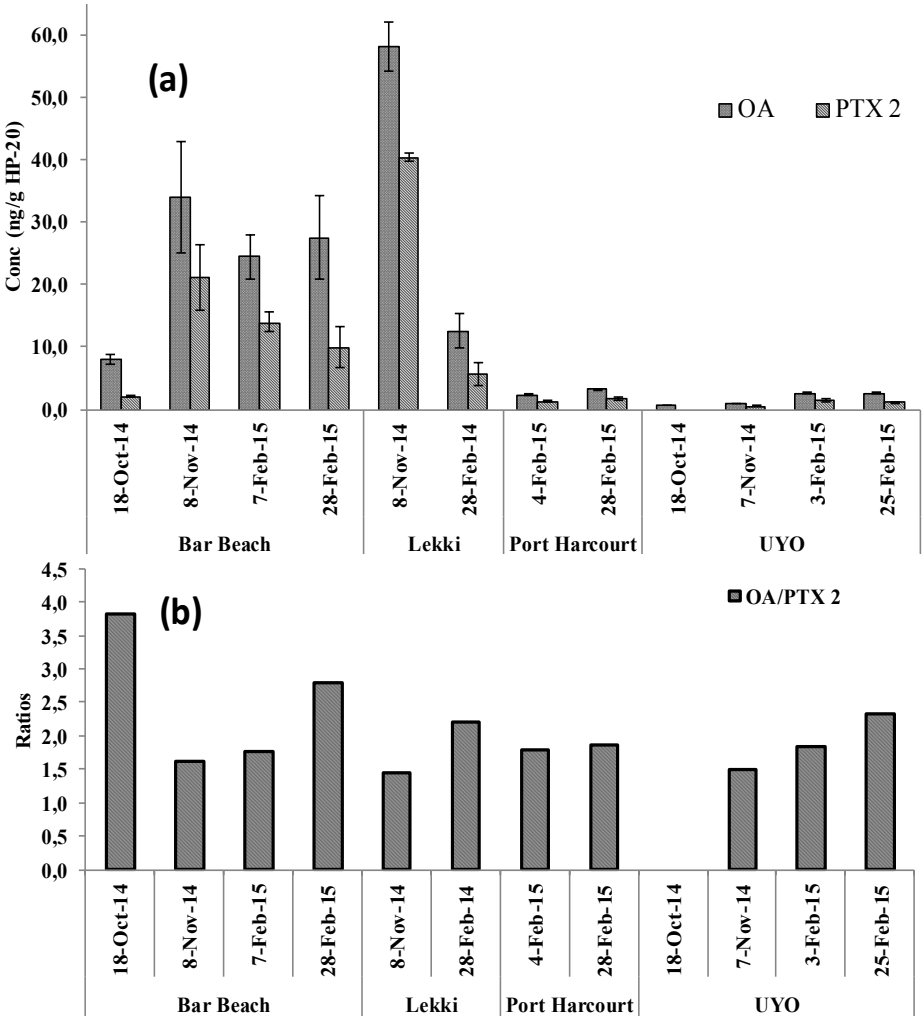

Figure VI.3 Average concentrations (a) and ratios (b) of okadaic acid (OA) and pectenotoxin 2 (PTX2) detected at each deployment site (ng/g of HP-20 resin ± RSD%, n=3)

2.4 Confirmation of okadaic acid and pectenotoxin 2 by high resolution mass spectrometry coupled to liquid chromatography

Comparison For confirmatory purposes, System 3 was used to obtain high resolution spectra from toxins quantified using System 1. For instance, the spectra for OA in negative ionisation mode obtained from a standard solution and a sample from Bar Beach were compared, and showed the same major ions characteristic for OA (Figure VI.4).

Accurate mass measurements for OA for the sample from Bar Beach were also verified and compared well with those of the certified standard of OA: the molecular ion $[M-H]^-$ of OA in the Bar Beach sample (*m/z* 803) showed 1.2 ppm mass error compared to the standard, while the two main fragments *m/z* 113.060 and 255.123 had a mass error of 0.88 and 0.39 ppm, respectively. Mass accuracy for PTX2 was slightly less good, but fragmentation pattern and fragment ion ratios matched very well that of the standard (Figure VI.5). Therefore, the presence of OA and PTX2 can be considered unequivocal as demonstrated by both low and high resolution tandem mass spectrometry.

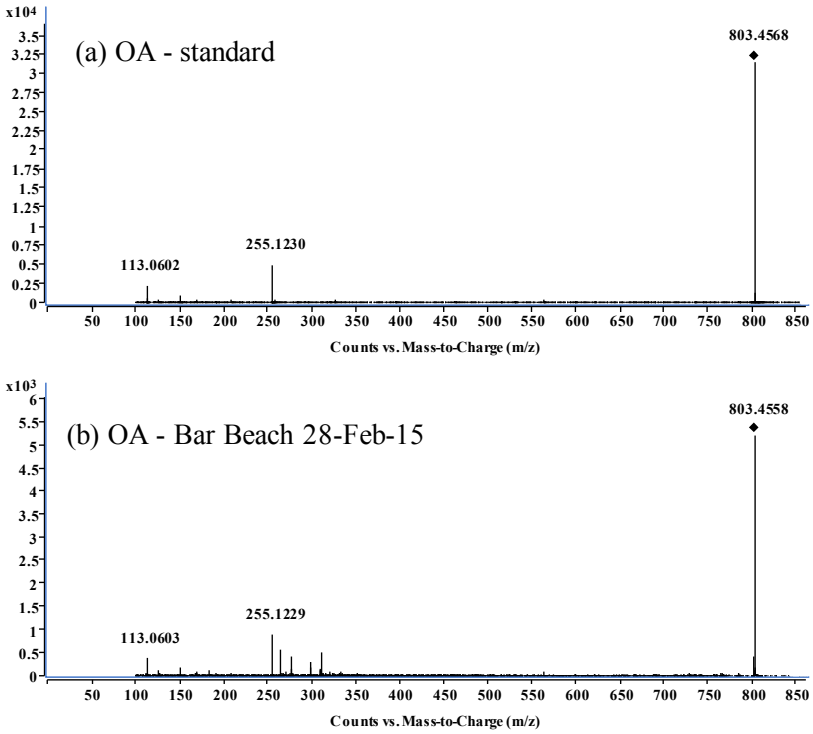

Figure VI.4 Average high resolution spectrum of (a) OA standard and (b) OA in a SPATT extract from Bar Beach. Spectra were obtained on System 3 (QToF 6550) in ESI^- using target MS/MS with collision energies of 20 V, 40 V and 60 eV

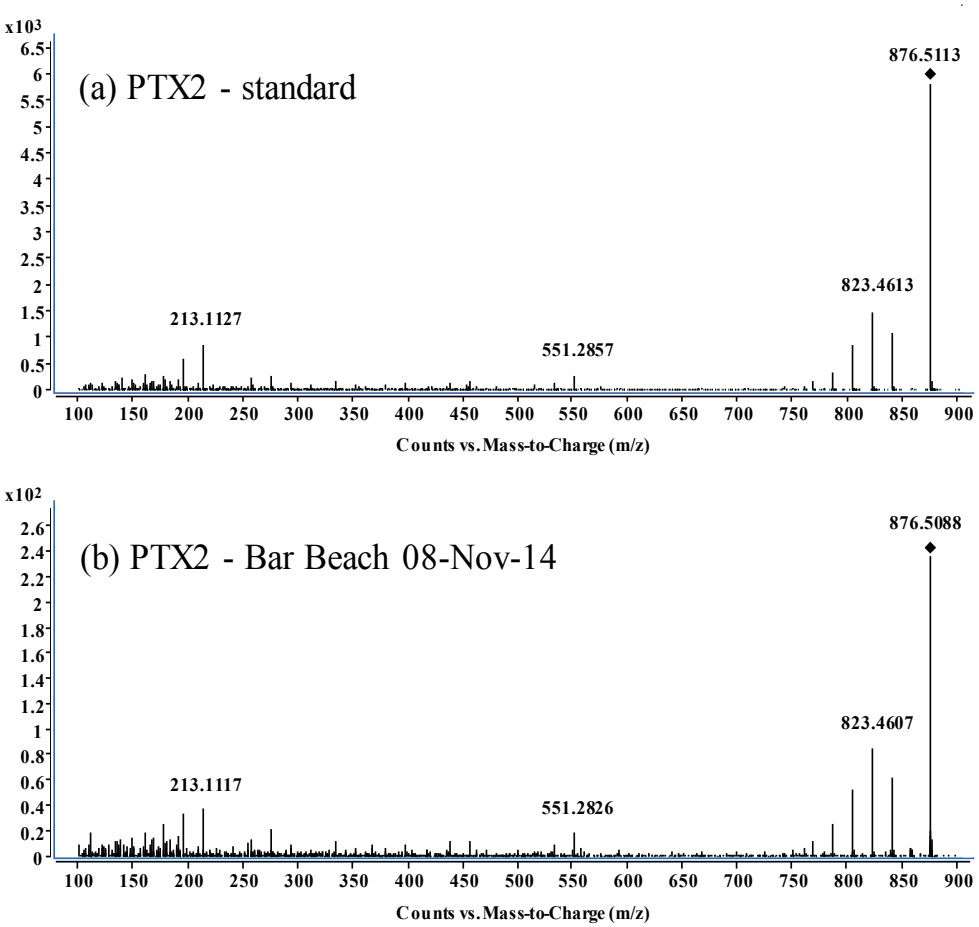

Figure VI.5 Comparison of the high-resolution mass spectrum of PTX2 in a sample from Bar Beach to the spectrum of a certified standard of PTX2

2.5 Untargeted screening approach for passive samplers

Principal component analysis including all masses identified in extracts of the passive samplers clearly showed separation between samples taken at the end of the wet season and those taken during the dry season, irrespective of the sampling site (Figure VI.6).

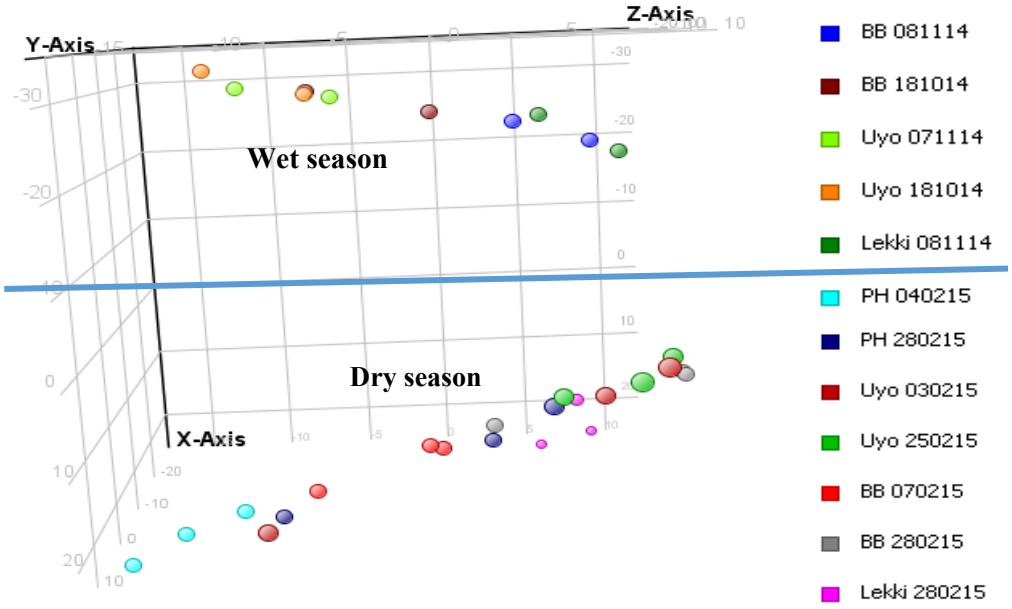

Figure VI.6 Score plot of the principal component analysis of all passive samplers (n=2 for 2014 and n=3 for 2015). Data were acquired by full scan HRMS on System 2. During Molecular Feature Extraction samples were blank-subtracted, ion traces extracted and combined into compounds. The three principal components plotted on the X, Y, and Z axes account for ca. 58% of the total variability in the data set (40.94% for X; 11.18% for Y and 7.06% for Z). *Note:* BB=Bar Beach and PH= Port Harcourt

This separation of seasons in the passive sampler extracts was not as distinct as in the targeted analysis of toxins (Figure VI.3-a) but is consistent with changes expected in the phytoplankton community structures in different seasons. When analysing the trend on a single site, Bar Beach (BB), it was also apparent that each sampling occasion gave a different chemical profile (Figure VI.7).

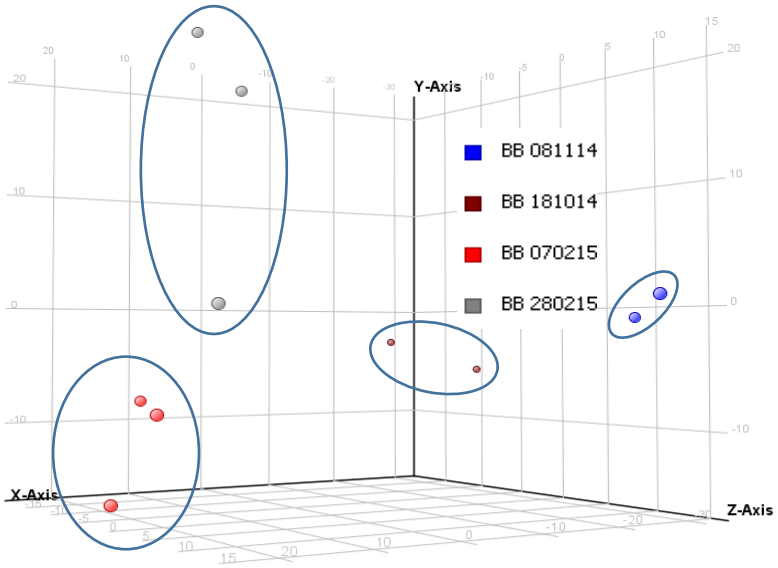

Figure VI.7 Score plot of the principal component analysis of passive samplers from Bar Beach taken on four separate occasions (n=2 for 2014 and n=3 for 2015). Data were acquired by full scan HRMS on system 2. The three principal components plotted on the X, Y, and Z axes account for ca. 83% of the total variability in the data set (69.72% for X; 7.78% for Y and 5.78% for Z)

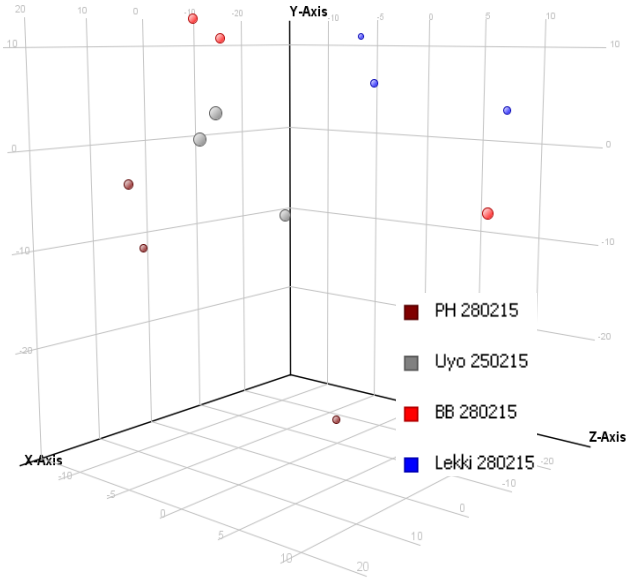

Figure VI.8 Score plot of the principal component analysis of passive samples from all four sites (BB=Bar Beach, PH=Port Harcourt), all taken during week 9 of 2015 (n=3). The three principal components plotted on the X, Y, and Z axes account for ca. 66% of the total variability in the data set (39.04% for X; 18.79% for Y and 9.04% for Z)

Interestingly, all four sites gave also different chemical profiles on a single sampling occasion (Figure VI.8). In this initial untargeted analysis, no identification of compounds was necessary to obtain this trend.

Still, the separation of the sites by PCA is not surprising when considering that the complete set of data for these four sites on a single occasion consisted of 2394 compounds. Amongst those compounds, 1828 occurred only at the two sites of high salinity (Lekki and Bar Beach) and 245 were unique to the sites with low salinity (Uyo and Port Harcourt). This also means that only 321 compounds were common to all four sites during that particular week. This observation also led us to tentatively identify what compounds may occur on the different sites. For this purpose, several samples were also screened against a database derived from the Dictionary of Marine Natural Products [44]. When applying stringent criteria (1 ppm mass accuracy, 5000 count abundance threshold) for matching compounds identified in the Nigerian data set by full scan HRMS, several hundred compounds gave tentative hits.

In particular, we examined what compounds were responsible for distinguishing weeks at Bar Beach station. In the PCA analysis for Bar Beach samples from October/November 2014 were grossly separated from samples taken during February (Figure VI.6). When examining compounds with extreme loadings in the PCA analysis (< -0.03 or > 0.03 normalised loading values, arbitrary choice, (Figure VI.9), 20 compounds of 196 distinctive entities were tentatively identified for the earlier period (October and November 2014, end of wet season), while 20 compounds of 424 distinctive entities were tentatively identified for the later period (February 2015, dry season, TableVI.2). In summary, among the database propositions were many compounds that had initially been identified either in tropical sponges, nudibranches or marine or freshwater cyanobacteria (TableVI.2). The fact that cyanobacterial compounds were identified appears coherent with previous identification of cyanobacteria as a problem in Nigerian waters [45]. These findings also suggest that additional efforts in Nigerian coastal waters should focus on identifying cyanobacterial toxins and source organisms.

Without any pre-selection of compounds on a given site for one sampling occasion (contrarily to the comparative PCA described above), many compounds can be tentatively identified, however, not all are distinctive features of that site – occasion combination. For instance Bar Beach was analysed for identifiable compounds on 08/11/2014 and 170 compounds gave a hit in the Dictionary of Marine Natural Products [44]. Interestingly, these compounds tentatively identified in the non-targeted analysis also included for instance okadaic acid already identified in the targeted analys

Figure VI.9 Principal Component Analysis (PCA) of passive samples taken at Bar Beach, Nigeria, in 2014/2015. The score plot (a) shows good separation of samples from October/November (left-hand side of graph) from those taken in February (right-hand side of graph). As this separation was almost exclusively on principal component 1 (accounting for almost 70% variability in the dataset), compounds most responsible for this separation are those that appear on the left- and right-hand side of the loadings plot (b). An arbitrary cut-off of 0.03 was chosen to select the most "separative" compounds. These compounds were subsequently screened against the Marine Natural Products Dictionary and results are given in TableVI.2 of the manuscript

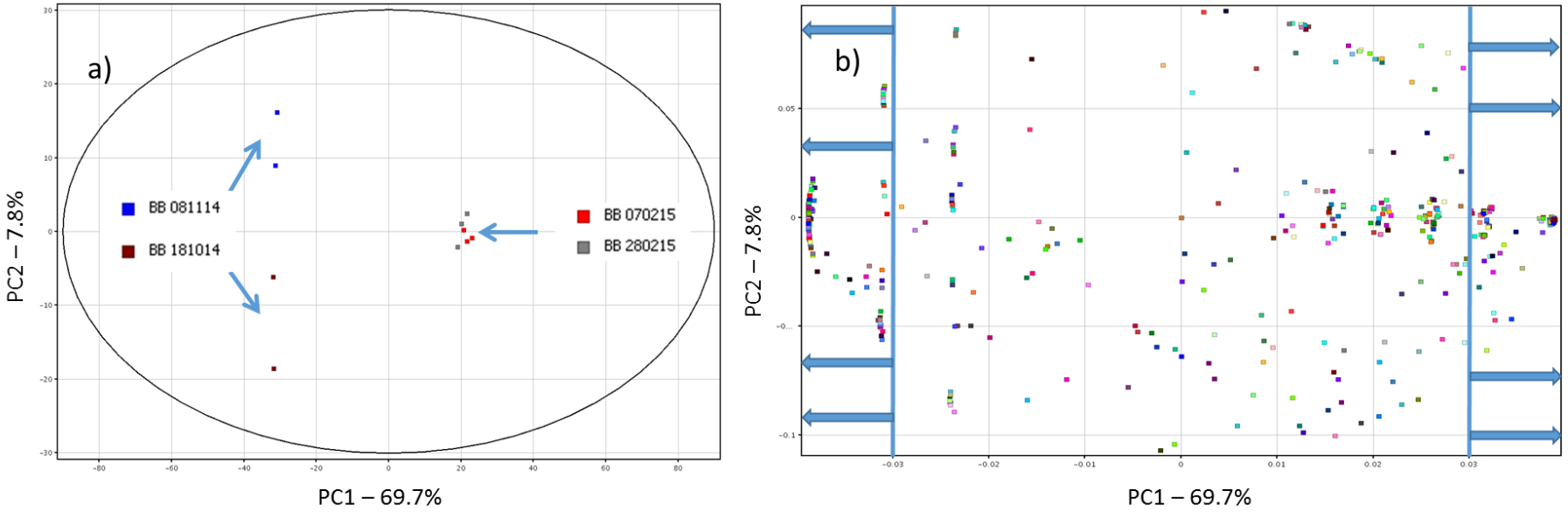

TableVI.2 Compounds tentatively identified in non-targeted analysis using high-resolution mass spectrometry (system 2)

No.	Compound	Month	Freq.	T_R	Mass	Identification Marine Natural Products Dictionary
1	6-Tridecylamine	Feb	6	4.01	199.2296	Isolated from the cyanobacterium *Microcoleus lyngbyaceus*
2	Hedaol B; A5-Isomer(Z-)	Feb	6	7.08	261.1977	Constituent of a *Sargassum sp.*
3	8,11,14-Heptadecatrienal; (all-Z) -form, 14,15-Dihydro	Feb	6	5.27	250.2293	Constituent of cucumber, tobacco and wheat. Also found in the algae *Enteromorpha sp., Scytosiphonlomentaria* and *Ulva pertusa*
4	Glycerol 1-alkyl ethers; Glycerol 1-pentadecyl ether	Feb	6	8.61	302.2818	Constituent of D*esmapsammaanchorata* and *Tethyaaurantiaca*
5	10-Aromadendranol; (1ct,4a,5 13,6a,7a,10a)-form, O -(2-O -	Feb	6	7.21	405.3120	Constituent of *Eucalyptus globulus* (Tasmanian blue gum) and *Thryptomenekochii*
6	Petroformyne 1; 3- or 44- Ketone	Feb	6	3.22	666.5018	Constituent of *Petrosiaficiformis*
7	Dideacetylraspacionin; 10,28- Dihydro, 103-hydroxy, 4,10, 15,21-tetra-Ac	Feb	6	8.16	661.4090	Constituent of sponge *Raspacionaaculeata*
8	Dideacetylraspacionin; 10,28- Dihydro, 103-hydroxy, 21- ketone, 4,10,15-tri-Ac	Feb	6	8.21	634.4068	Constituent of sponge *Raspacionaaculeata*
9	Cholestane-3,5,6,7-tetrol; (3i, 5ct,613,713)-form, 3,7-Di-Ac	Feb	6	8.25	503.3500	Constituent of the gorgonian *Plexaurellagrisea*
10	6-Pentadecyl-1,2,4-benzenetriol; 1-Ac	Feb	6	7.59	400.2594	Constituent of the sponge *Axinellapolycapella*
11	Etzionin; N,O -Di-Ac	Feb	6	7.41	558.3422	cytotoxic & antifungal; isolated from *Didemnumrodriguesi*
12	Fumiquinazoline F; 4-Epimer	Feb	6	7.47	358.1420	Cytotoxin prod. by a marine-derived *Aspergillus fumigatus*
13	Picrotoxinin	Feb	6	3.77	314.0767	Ichthyotoxin isolated from desmosponge*Spirastrellainconstans*

No.	Compound	Month	Freq.	T_R	Mass	Identification Marine Natural Products Dictionary
14	Louludinium(1+)	Feb	6	4.82	294.2211	Isolated from marine cyanobacterium *Lyngbyagracilis*
15	Aeruginosamide	Feb	6	2.66	560.3399	Isolated from *Microcystis aeruginosa* (cyanobacteria)
16	Bengamide Z; 6-Deoxy	Feb	6	2.30	372.2264	Isolated from sponge *Jaspis cf. coriacea*
17	Ulithiacyclamide F	Feb	6	9.26	814.2046	Isolated from the ascidian *Lissoclinum patella*
18	4-Cadinen-10-ol; (1ct,63,7i3,10 13)-form	Feb	6	4.46	222.1987	Isolated from the sponge *Acanthella cavernosa*.
19	Drechslerine G	Feb	6	3.85	270.1823	Metabolite of the algicolous fungus *Drechslerematioidea*
20	Acremonin A; (+)-form	Feb	6	5.25	176.0836	Prod. by a marine-derived micromycte*Acremonium sp*.
21	10-O -(3,4- Dihydroxy-E -cinnamoyl) geniposidic acid	Oct/Nov	4	2.87	536.1535	Constituent of *Genipaamericana* (genipap) and *Premnabarbata* (higher terrestrial plants)
22	6- Sulfate Cholestane-3,6,8,15,24-pentol; (313,5ct,6a,15ct,24S)-form,	Oct/Nov	4	2.1	532.3077	Constituent of *Oreasterreticulatus* (tropical sea star)
23	3-Propanoyl, 12-Ac-3,12-Dihydroxy-20,24-dimethyl-17-scalaren-25,24-olide	Oct/Nov	4	6.36	545.371	Constituent of *Phyllospongialamellosa*
24	1-Tricosene	Oct/Nov	4	9.23	339.3865	Constituent of the alga *Botryococcusbraunii* and various plant spp. incl. *Gardenia tahitensis*
25	4,10-Dimethyldodecanoic acid	Oct/Nov	4	3.85	245.2352	Isolated from a halophilic *Bacillus sp.*
26	2-Amino-11-dodecen-3-ol	Oct/Nov	3	5.50	199.1939	Isolated from a marine sponge *Haliclona n. sp.*
27	N - Eicosanoyl 2-Aminobenzoic acid	Oct/Nov	4	5.65	453.3218	Isolated from aerial parts of *Ononisnatrix* (African terrestrial plant)
28	Dysidazirine; (S ,E)-form	Oct/Nov	4	3.69	307.2516	Isolated from Fijian marine sponge, *Dysideafragilis*
29	Malonganenone B	Oct/Nov	4	6.75	470.3256	Isolated from *Leptogorgiagilchristi* (gorgonian, soft coral)
30	Glanvillic acid A	Oct/Nov	4	6.29	306.2190	Isolated from *Plakortishalichondrioides*

No.	Compound	Month	Freq.	T_R	Mass	Identification Marine Natural Products Dictionary
31	13',14'-Dihydro-amphiasterin B2	Oct/Nov	3	6.72	401.3506	Isolated from *Plakortisquasiamphiaster* (marine sponge)
32	Enterocin	Oct/Nov	4	3.75	444.1060	Isolated from a marine ascidian *Didemnum sp.*
33	Phloeodictyne A; Phloeodictyne 4,6i	Oct/Nov	4	8.59	407.3622	Isolated from the New Caledonian deep water sponge *Phloeodictyon sp.* and shallow-water sponge *Oceanapiafistulosa* (*Phloeodictyonfistulosa*)
34	2-Amino-18-methyl-4- nonadecene-1,3-diol	Oct/Nov	3	8.7	327.3141	Isolated from the sponge *Discodermia calyx*
35	2-Amino-9-hexadecen-3-ol; (2 S ,3R ,9Z)-form	Oct/Nov	4	7.87	255.2563	Isolated from the tunicate *Pseudodistomaobscurum*
36	6-Octadecenoic acid; (E)- form	Oct/Nov	4	7.72	282.2559	Minor constituent of plant oils
37	Choline; O -(2-Methyl-2- propenoyl)	Oct/Nov	4	8.08	194.1157	Monomer. Polymers are used as coagulants in sewage treatment
38	2-Dodecenoic acid; (E)-form, Et ester	Oct/Nov	4	7.12	226.1909	Occurs in pears
39	Hexadecanoic acid; Dimethylamide	Oct/Nov	4	5.74	283.2876	Widely distributed in plants
40	2-Methylpropanoic acid	Oct/Nov	4	7.69	106.0627	The free acid and its esters occur in many plants

3. Material and methods

3.1 Chemicals, reagents and sorbent materials

Certified standard solutions of okadaic acid (OA), domoic acid (DA), dinophysistoxins (DTX1, DTX2), 13-desmethyl spirolide C (13-desmeSPX-C), pectenotoxin 2 (PTX2), gymnodimine A (GYM-A), azaspiracids (AZA1,-2 and -3), yessotoxin (YTX) and homo-yessotoxin (homo-YTX) were obtained from the National Research Council in Halifax, Canada. HPLC grade methanol and acetonitrile as well as ammonium formiate and formic acid (98%) were acquired from AtlanticLabo (Bordeaux, France) and Sigma Aldrich (Steinheim, Germany). Deionized water was produced in-house to 18MΩ cm^{-1} quality, using a Milli-Q integral 3 system (Millipore). For analyses with the high resolution mass spectrometry instrument, acetonitrile and water of LC/MS grade were obtained from Fischer Scientific (Illkirch, France). For passive sampler devices, Diaon® HP-20 polymeric resin was purchased as bulk resin from Sigma-Aldrich and 12 mL capacity polypropylene 2 frits-Reservoirs were from Agilent Technologies.

Brucine-sulfanilic acid reagent was prepared by dissolving 1 g brucine sulfate [$(C_{23}H_{26}N_2O_4)_2$ H_2SO_4, $7H_2O$] and 0.1 g sulfanilic acid ($NH_2C_6H_4SO_3H$, H_2O) into 70 ml of hot distilled water. Concentrated hydrochloric acid (3 mL) was further added and this mixture was cooled, mixed and then diluted to 100 mL with distilled water. The final mixture was stored in a dark bottle at 5 °C. For ascorbic acid, the ready-made PhosVer 3 Hach™ was used.

3.2 Study area

The study area (Figure VI.10), *i.e.* the Nigerian coastal area, is situated in the Guinea Current Large Marine Ecosystem, in the Gulf of Guinea. There are two main seasons in the deploying sites: the rainy (wet) season spanning from May to October and the dry season from November to April. The area is influenced by coastal upwelling which occurs seasonally along the northern and eastern coasts. There are two (major and minor) upwelling seasons. Those seasons occur annually with differing duration and intensities off Ghana and Cote d'Ivoire, in the central part of the large marine ecosystem. The major upwelling season occurs from June to September and transient upwelling events are from January to March [42].

The coastline of Nigeria is approximately 853 km long between latitude 4°10′ to 6°20′ N and longitude 2°45′ to 8°35′ E. The Nigerian coastal area is low-lying of not more

than 3.0 m above sea level, generally covered by fresh water swamp, mangrove swamp, lagoonal mashes, tidal channels, beach ridges and sand bars [46].

The Nigerian coast is composed of four distinct geomorphological units namely: the Barrier-Lagoon complex; the Mud coast; the Arcuate Niger delta; and the Strand coast [47]. The vegetation of the Nigerian coastal area is characterized by mangrove forests, brackish swamp forests and rain forests. The coastal zone is richly endowed with a variety of mineral resources, including oil and gas. The four selected sites are located in the Gulf of Guinea (Atlantic Ocean), two in the Bight of Bonny to the East (Arcuate Niger delta) and two in the Bight of Benin to the West (outside the Barrier-lagoon complex).

Seawater sampling for nutrients and for phytoplankton analysis, as well as passive sampling were carried out at sites and dates as listed in Table VI.3.

Table VI.3 Sampling sites and dates for water and toxin analysis (date format: dd/mm/yy)

Sampling site	Latitude	Longitude	Dates for water sampling	Dates for passive sampling
Bar Beach	N 6° 25.340’	E 3° 26.189’	18/10/14, 02/02/15, 21/02/15	18/10/14, 08/11/14, 07/02/15, 28/02/15
Lekki	N 6° 25.256’	E 3° 32.180’	21/02/15	08/11/14, 28/02/15
Port Harcourt	N 4° 41.828’	E 7° 10.706’	29/01/15, 22/02/15	04/02/15, 28/02/15
Uyo	N 4°33.203’	E 8° 00.202’	17/10/14, 28/01/15, 23/02/15	18/10/14, 07/11/14, 03/02/15, 25/02/15

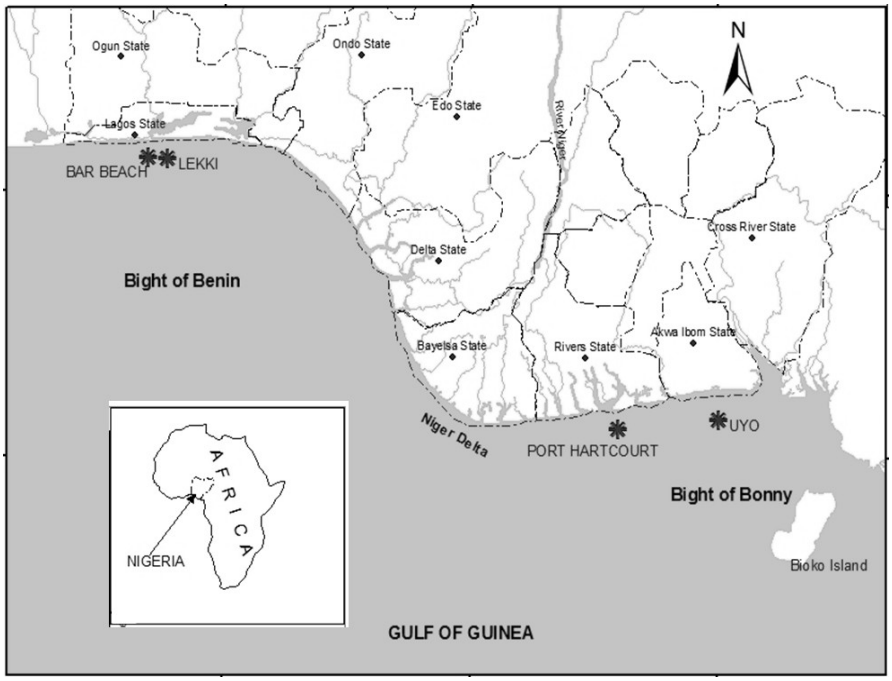

Figure VI.10 Location of sampling sites (stars): Bar Beach and Lekki are both in Lagos State off Lagos lagoon; Port Harcourt is in Rivers State, in the vicinity of the Niger delta, and Uyo is in Akwa Ibom State towards the Eastern Limit of Nigerian waters

3.3 Physico-chemical parameters and water sampling for analysis of nutrients and phytoplankton identification

Water samples (1 L) were obtained for analysis of nutrients at an integrated depth of 10 m to the surface of the ocean, with a lund tube of 2.5 cm diameter. Temperature was measured with a mercury-in-glass thermometer. Dissolved oxygen was measured using a Milwaukee NW 600 probe and salinity was measured with a Hach™ Salinity/Conductivity probe probe (Hach Company, USA).

Nutrients were analyzed according to ASTM [48]. For the determination of nitrate, brucine sulphanilic acid reagent (1 mL) was added to standard solutions as well as to samples (10 mL). The resultant mixtures were mixed thoroughly and allowed to stand for 15 min. Then 10 mL of H_2SO_4 solution were carefully added to 10 mL of distilled water and the resulting solution was added to each of the beakers containing the nitrate standard solutions and the water samples, respectively. This was allowed to stand for 20 min in the dark. Similar treatment was performed on the blank solution, using the same protocol except that no brucine sulphanilic reagent was added to it. The absorbance of standards and samples was determined at 410 nm wavelength using a UV/Visible spectrophotometer.

Phosphate was determined using the ascorbic acid method. The programmed method of Hach was used using the Hach spectrophotometer DR2000™ (Hach Company, USA).

Phytoplankton samples were collected by horizontal and vertical tows using a plankton net made from fine bolting silk (10 µm mesh, length: 107 cm and Diameter: 29 cm). Samples were drained into the plankton bucket and preserved with Lugol's iodine in sample bottles. Light microscopy (LM) observations were carried out from 50 µL of fixed net samples deposited on a glass slide, using an Olympus IX70 inverted light microscope equipped with a digital camera DP72 (Olympus, Tokyo, Japan). Cells were photographed, either directly or after isolation with a micropipette, depending on concentration of organisms and particles.

3.4 Passive sampler design, handling and extraction

Passive sampling devices (Solid Phase Adsorption Toxin Tracking = SPATT) were prepared using a 68 mm embroidery frame (Singer, Nantes, France). Three grams (3 g) of Diaion® HP-20 polymericresin were placed between two layers of a 30 µm nylon mesh (Mougel, France), and clamped in the embroidery frame to form a thin layer of resin. To activate the HP-20 resin, the passive samplers were soaked for 3 h in methanol, rinsed twice with deionized water to remove methanol residues [39, 49] and directly deployed. Three SPATTs were put in three separate compartments cylinders made of steel, to firmly secure them, and deployed in the sea at 1 m depth for 7 days at each site. After deployment, the SPATTs were retrieved, rinsed with seawater to remove residual biofilm and transported in frozen ice packs to the laboratory. The SPATTs were shipped to the analytical laboratory in France on ice and arrived in good condition. They were then stored in a freezer (-20 °C) until analysis. The HP-20 resin was extracted according to previously published methods, with slight changes [49-50]. Briefly, after deployment, the SPATTs were rinsed twice in 500 mL deionized water, transferred into empty polypropylene reservoirs placed on a manifold and eluted dropwise with 24 ml of methanol. The extracts were then evaporated at 45 °C under a gentle nitrogen stream. The dry residue was further reconstituted in 500 µL of 50% methanol, filtered on Nanosep MF centrifugal filters 0.2 µM (Pall) and transferred into HPLC vials for analysis.

3.5 LC-MS analyses

Three different analytical systems were used: (1) for quantitative targeted analysis of toxins; (2) for untargeted screening of unknowns as well as known toxins; (3) for characterization and confirmation of toxins. For all three systems, chromatographic separation was achieved after injection of a 3 µL sample volume onto a Phenomenex Kinetex XB-C18 (100 x 2.6 mm; 2.6 µm) column maintained at 40 °C, with a flow rate of 400 µl/min. The binary mobile phase consisted of water (A) and 95% acetonitrile/water (B), both containing 2 mM ammonium formiate and 50 mM formic acid. The elution gradient rose from 5% to 50% of B in 3.6 min, then 100% B was reached by 8.5 min. After 1.5 min of hold time at 100% B, 5% B was reached within 10 s, followed by 5 min re-equilibration of the column at 5% B. The total chromatographic run time was 15 min. To avoid cross contamination of samples, the needle was washed for 10 s in the flush port with 90% MeOH before each injection. On all analytical systems, mass spectrometric acquisitions were carried out separately in positive (ESI^+) and negative (ESI^-) ionization modes.

System 1: LC-MS/MS for quantitative analysis

A UFLC-XR Shimadzu liquid chromatography system (Champs-sur-Marne, France) was connected to a hybrid triple quadrupole/linear ion-trap mass spectrometer (API4000-Q-Trap™; AB Sciex) equipped with a TurboIonSprayTM ionization source. For quantitation, the mass spectrometer was operated in MRM mode, scanning two transitions for each toxin. Q1 and Q3 resolutions of the instrument were set at Unit (arbitrary terms). Data were acquired in MRM, in separate chromatographic runs, using positive (ESI^+) and negative (ESI^-) ionization modes, respectively with a scan time of 1 s. In ESI^+, the following source parameters were used: curtain gas set at 30 psi, ion spray at 5500 V, a turbogas temperature of 450°C, gas 1 and 2 both set at 50 psi, and an entrance potential of 10 V. In ESI^-, the curtain gas was set at 20 psi, the ion spray at -4500 V, the turbogas temperature at 550°C, gas 1 and 2 at 40 and 50 psi, respectively, and finally the entrance potential at -13 V. MRM transitions used for each toxin are displayed in Table VI.4. Data acquisition was carried out with Analyst 1.6 Software (AB Sciex).

Table VI.4 Multiple Reaction Monitoring (MRM) transitions used for quantitative analysis on System 1 (30 msec dwell in ESI^+ and 80 msec dwell in ESI^-)

Toxin	DP	Q1	Q3 quantifier	CE	Q3 qualifier	CE
DA	61	312.1	266.1	23	161.1	35
GYM-A	86	508.4	490.2	33	392.3	49
13-desmeSPX-C	121	692.5	164.2	69	444.3	53
PnTX-G	141	694.5	164.1	75	458.3	75
AZA1	116	842.5	672.4	69	654.4	69
AZA2	116	856.5	672.4	69	654.4	69
AZA3	116	828.5	658.4	69	640.4	69
PTX2	91	876.5	823.5	31	805.6	37
PTX2sa	91	894.6	823.5	31	805.6	37
OA, DTX2	-170	803.5	255.1	-62	113.1	-92
DTX1	-170	817.5	254.9	-68	112.9	-92
YTX	-120	1141.4	1061.6	-48	855.5	-98
homo-YTX	-120	1155.6	1075.6	-48	869.4	-98

System 2: LC-HRMS for untargeted and targeted screening of toxins and unknowns

A UHPLC system (1290 Infinity, Agilent Technologies) was coupled to a 6540 UHD Accurate-Mass QToF (Agilent Technologies) equipped with a dual ESI source. Full-scan analyses were performed over the range *m/z* 65 to 1700 with an acquisition rate of 2 spectra s^{-1}. In ESI^+ the temperature of the Jet Stream Technologies™ source was set at 205°C with the drying gas flow-rate at 5 L min^{-1}. The sheath gas temperature was 355°C. Other parameters were as follows: capillary voltage, 2000 V; fragmentor voltage, 200 V. The parameters of the Jet Stream Technologies™ source in ESI^- were: gas temperature 305°C, drying gas flow 5 L min^{-1}, nebulizer pressure 50 psi, sheath gas temperature 355 °C, sheath 12 L/min, capillary voltage 3500 V, fragmentor voltage, 180 V.

All experiments were done with reference mass correction using purine (m/z 121.0509 $[M+H]^+$; *m/z* 119.03632 $[M-H]^-$) and HP-921 = hexakis (1H,1H,3H-tetrafluoropropoxy) phosphazine (m/z 922.0099 $[M+H]^+$; *m/z* 966.00072 $[M+HCOO]^-$). The reference ions were infused constantly with an isocratic pump to a separate ESI sprayer in the dual spray source.

System 3: LC-HRMS for toxins confirmation

Analyses were carried out using a UHPLC system (1290 Infinity II, Agilent Technologies) coupled to a 6550 iFunnelQToF (Agilent Technologies) equipped with a dual ESI source. This instrument was operated with a dual electrospray ion source with Agilent Jet Stream Technology™ in positive and negative ionization modes. Analyses were performed over the range *m/z* 100 to 1200 with an acquisition rate of 2 spectra s^{-1}. The parameters of the Jet Stream Technologies™ source in ESI^+ were: gas temperature 205°C, drying gas flow 16 L/min, nebulizer pressure 50 psi, sheath gas temperature 355°C, sheath 12 L/min, capillary voltage 2000 V, fragmentor voltage, 200 V. In ESI^- the parameters were as follows: gas temperature 290°C, drying gas flow 12 L/min, nebulizer pressure 50 psi, sheath gas temperature 355°C, sheath 12 L/min, capillary voltage 3500 V, fragmentor voltage, 180 V. Three collision energies (20, 40 and 60 eV) were applied to the precursor ions to generate fragmentation spectrum. All experiments were done with reference mass correction as described above for System 2. MassHunter Acquisition B05.01 software was used to control the instrument and data were processed with MassHunter B07.00 service pack.

3.6 Data processing and statistical analyses

Raw data files obtained on System 2 were processed using the Agilent *Molecular Feature Extractor* (MFE) algorithm in MassHunterQual software (B.07). This algorithm was used to obtain the *Total Compound Chromatogram* of samples as previously described [25]. This algorithm designed for use with full scan data treats the mass spectral data as a three-dimensional array of retention time, *m/z* and abundance values. Any point corresponding to persistent or slowly-changing background is removed from that array of values. Then the algorithm searches for ion traces that elute at very nearly the same retention times. Those ion traces are then grouped into entities called *Compounds* regrouping all ion traces that are related, *i.e.* those that correspond to mass peaks in the same isotope cluster, or can be explained as being different adducts or charge states of the same entity. The results for each detected *Compound* are a mass spectrum containing the ions with the same elution time and explainable relationships, and an extracted compound chromatogram (ECC) computed using all of these related ion traces in the compound spectrum (and only those traces). The results from the MFE analysis were then uploaded to the Agilent Mass Profiler Professional (MPP) software (B.13.00) as compound exchange

format file (. cef) for further statistical analyses (PCA: Principal Component Analysis). In MPP, feature profiles were aligned with 15 ppm and 0.2 min bins of mass and retention time windows, respectively. Data were log2 transformed, centered and normalized to give features equal weight in classification. Groups/conditions were composed of SPATT samples from the same location and/or the same deployment date. Data were analyzed by univariate and multivariate analysis to detect features of interest. For the multivariate data analysis (MVDA) comparing all samples, all features present in less than 20% of all samples from the data set were discarded. For univariate data analysis comparing only samples from a given site, only entities with p-values > 0.05 and fold-change > 2 were retained. PCA was carried out on conditions *i.e.* to allow for the detection of similarities between samples. Features that were considered characteristic were tentatively identified based on mass and spectral accuracy using the Dictionary of Marine Natural Products (DMNP) library (Blunt and Munro, 2008) (Wolfender et al., 2015).

4. Conclusions

The survey in Nigerian coastal waters confirmed the presence of toxic algae in this area, in particular *Dinophysis caudata*. For the first time, lipophilic toxins were identified in Nigerian coastal waters. Okadaic acid and pectenotoxin 2 have been quantified in passive samplers deployed for 1-week periods and can most likely be attributed to *Dinophysis* species, although a partial contribution by *Prorocentrum* species cannot be excluded. Untargeted analysis using high resolution mass spectrometry also pointed towards the possible accumulation of cyanobacterial metabolites in the passive samplers. Therefore, any further studies investigating the risks for public health from shellfish consumption should examine concentrations of algal as well as cyanobacterial toxins.

References

1. J. Lawrence H. Loreal, H. Toyofuku, P. Hess, K. Iddya, L. Ababouch, Assessment and management of biotoxin risks in bivalve molluscs, FAO Fisheries and Aquaculture Technical Paper No., 551 (2011) 337 pages.

2. P. Hess, Phytoplankton and biotoxin monitoring programmes for the safe exploitation of shellfish in Europe, in: A.G. Cabado, J.M. Vieites (Eds.) New Trends in Marine and Freshwater Toxins: Food Safety Concerns, Nova Science Publishers Inc., 2012.

3. T. Suzuki, R. Watanabe, Shellfish toxin monitoring system in Japan and some Asian countries, in: A.G. Cabado, J.M. Vieites (Eds.) New Trends in Marine and Freshwater Toxins: Food Safety Concerns, Nova Science Publishers Inc., 2012.
4. S.L. DeGrasse, K. Martinez-Diaz, Biotoxin control programmes in North, Central and South American countries, in: A.G. Cabado, J.M. Vieites (Eds.) New Trends in Marine and Freshwater Toxins: Food Safety Concerns, Nova Science Publishers Inc., 2012.
5. P. Bienfang, B. Oben, S. De Felice, P. Moeller, K. Huncik, P. Oben, R. Toonen, T. Daly- Engel, B. Bowen, Ciguatera: the detection of neurotoxins in carnivorous reef fish from the coast of Cameroon, West Africa, Afr. J. Mar. Sci., 30 (2008) 533-540.
6. H. Taleb, P. Vale, M. Blaghen, Spatial and temporal evolution of PSP toxins along the Atlantic shore of Morocco, Toxicon, 41 (2003) 199-205.
7. R. Abouabdellah, H. Taleb, A. Bennouna, K. Erler, A. Chafik, A. Moukrim, Paralytic shellfish poisoning toxin profile of mussels Perna perna from southern Atlantic coasts of Morocco, Toxicon, 51 (2008) 780-786.
8. R. Abouabdellah, A. Bennouna, J. El Attar, K. Erler, M. Dellal, A. Chafik, A. Moukrim, Diarrhetic shellfish poisoning toxin profile of shellfish from Southern Atlantic coasts of Morocco, South Asian Journal of Experimental Biology, 1 (2011) 101-106.
9. H. Taleb, P. Vale, R. Amanhir, A. Benhadouch, R. Sagou, A. Chafik, First detection of azaspiracids in mussels in North West Africa, J. Shellfish Res., 25 (2006) 1067-1070.
10. G.C. Pitcher, D. Calder, Harmful algal blooms of the southern Benguela Current: a review and appraisal of monitoring from 1989 to 1997, South Afr. J. Mar. Sci.-Suid-Afr. Tydsk. Seewetens., 22 (2000) 255-271.
11. G.C. Pitcher, J.M. Franco, G.J. Doucette, C.L. Powell, A. Mouton, Paralytic shellfish poisoning in the abalone Haliotis midae on the west coast of South Africa, Journal of Shellfish Research, 20 (2001) 895-904.
12. A. Fawcett, S. Bernard, G.C. Pitcher, T.A. Probyn, A. du Randt, Real-time monitoring of harmful algal blooms in the southern Benguela, Afr. J. Mar. Sci., 28 (2006) 257-260.
13. P. Vale, I. Rangel, B. Silva, P. Coelho, A. Vilar, Atypical profiles of paralytic shellfish poisoning toxins in shellfish from Luanda and Mussulo bays, Angola, Toxicon, 53 (2009) 176-183.
14. J. Blanco, F. Livramento, I.M. Rangel, Amnesic shellfish poisoning (ASP) toxins in plankton and molluscs from Luanda Bay, Angola, Toxicon, 55 (2010) 541-546.

15. M.O. Kadiri, Phytoplankton distribution in the coastal waters of Nigeria, Nigerian Journal of Botany, 12 (1999) 51-62.

16. M.O. Kadiri, Some marine phytoplankton species from Atlantic Ocean, Nigeria, Biosci. Res. Comm, 13 (2001) 197-207.

17. M.O. Kadiri, A spectrum of phytoplankton flora along salinity gradient in the eastern Niger Delta area of Nigeria, Acta Botanica Hungarica, 44 (2002) 75-83.

18. M.O. Kadiri, Phytoplankton flora and physico-chemical attributes of some waters in the Eastern Niger delta area of Nigeria, Nigerian J. Botany, 19 (2006) 188-200.

19. M.O. Kadiri, Phytoplankton survey in the Western Niger Delta, Nigeria, Afr. J. Environ. Pollut. Health, 5 (2006) 48-58.

20. M.O. Kadiri, Notes on harmful algae from Nigerian coastal waters, Acta Botanica Hungarica, 53 (2011) 137-143.

21. D.I. Nwankwo, A survey of the dinoflagellates of Nigeria. Armoured dinoflagellates of Lagos Lagoon and associated Tidal creeks., Nigerian Journal of Botany 4(1991) 49-60.

22. D.I. Nwankwo, A first list of dinoflagellates (Pyrrhophyta) from Nigerian coastal waters (creek, estuaries lagoons)., Pol. Arch. Hydrobiol 44 (1997) 313-321.

23. C. Ajuzie, G. Houvenaghel, Preliminary survey of potentially harmful dinoflagellates in Nigeria´s coastal waters, Fottea, 9 (2009) 107-120.

24. L. MacKenzie, V. Beuzenberg, P. Holland, P. McNabb, A. Selwood, Solid phase adsorption toxin tracking (SPATT): a new monitoring tool that simulates the biotoxin contamination of filter feeding bivalves, Toxicon : official journal of the International Society on Toxinology, 44 (2004) 901-918.

25. Z. Zendong, P. McCarron, C. Herrenknecht, M. Sibat, Z. Amzil, R.B. Cole, P. Hess, High resolution mass spectrometry for quantitative analysis and untargeted screening of algal toxins in mussels and passive samplers, Journal of Chromatography http://dx.doi.org/10.1016/j.chroma.2015.08.064, (2015).

26. M.L. Fernández, B. Reguera, S. González-Gil, A. Míguez, Pectenotoxin-2 in single-cell isolates of Dinophysis caudata and Dinophysis acuta from the Galician Rías (NW Spain), Toxicon, 48 (2006) 477-490.

27. A.N. Marasigan, S. Sato, Y. Fukuyo, M. Kodama, Accumulation of a high level of diarrhetic shellfish toxins in the green mussel Perna viridis during a bloom of Dinophysis caudata and Dinophysis miles in Sapian Bay, Panay Island, the Philippines, Fish. Sci., 67 (2001) 994 996.

28. M.J. Holmes, S.L.M. Teo, F.C. Lee, H.W. Khoo, Persistent low concentrations of diarrhetic shellfish toxins in green mussels perna viridis from the johor strait, singapore: first record of diarrhetic shellfish toxins from south-east asia, Marine-Ecology-Progress-Series, 181 (1999) 257- 268.

29. A.F. Li, G. Sun, J.B. Qiu, L. Fan, Lipophilic shellfish toxins in Dinophysis caudata picked cells and in shellfish from the East China Sea, Environ. Sci. Pollut. Res., 22 (2015) 3116 3126.

30. A. Bennouna, B. Berland, J. El Attar, O. Assobhei, Lingulodinium polyedrum (Stein) Dodge red tide in shellfish areas along Doukkala coast (Moroccan Atlantic), Oceanologica Acta, 25 (2002) 159-170.

31. B. Paz, P. Riobó, M.L. Fernández, S. Fraga, J.M. Franco, Production and release of yessotoxins by the dinoflagellates *Protoceratium reticulatum* and *Lingulodinium polyedrum* in culture, Toxicon [Toxicon], 44 (2004) 251-258.

32. T. An, J. Winshell, G. Scorzetti, J.W. Fell, K.S. Rein, Identification of okadaic acid production in the marine dinoflagellate *Prorocentrum rhathymum* from Florida Bay, Toxicon, 55 (2010) 653-657.

33. A.E. Jackson, J.C. Marr, J.L. McLachlan, The production of diarrhetic shellfish toxins by an isolate of *Prorocentrum lima* from Nova Scotia, Canada, (1993) 513-518.

34. T. Hu, A.S.W. De Freitas, J.M. Curtis, Y. Oshima, J.A. Walter, J.L.C. Wright, Isolation and structure of *prorocentrolide* B, a fast-acting toxin from *Prorocentrum maculosum*, J. Nat. Prod., 59 (1996) 1010-1014.

35. S.L. Morton, P.D.R. Moeller, K.A. Young, B. Lanoue, Okadaic acid production from the marine dinoflagellate *Prorocentrum belizeanum* Faust isolated from the Belizean coral reef ecosystem, Toxicon, 36 (1998) 201-206.

36. D.W. Henrichs, P.S. Scott, K.A. Steidinger, R.M. Errera, A. Abraham, L. Campbell, Morphology and Phylogeny of Prorocentrum texanum sp nov (Dinophyceae): A New Toxic Dinoflagellate from the Gulf of Mexico Coastal Waters Exhibiting Two Distinct Morphologies, J. Phycol., 49 (2013) 143-155.

37. Delmas, D., Herbland, A., Maestrini, S.Y., 1992. Environmental conditions which lead to increase in cell density of the toxic dinoflagellates *Dinophysis spp* in nutrient-rich and nutrient-poor waters of the French Atlantic Coast Marine Ecology Progress Series 89, 53-61.

38. E. Fux, R. Bire, P. Hess, Comparative accumulation and composition of lipophilic marine biotoxins in passive samplers and in mussels (M. edulis) on the West Coast of Ireland, Harmful Algae, 8 (2009) 523-537.

39. T. Rundberget, E. Gustad, I.A. Samdal, M. Sandvik, C.O. Miles, A convenient and cost-effective method for monitoring marine algal toxins with passive samplers, Toxicon : official journal of the International Society on Toxinology, 53 (2009) 543-550.

40. Y. Pan, A.D. Cembella, M.A. Quilliam, Cell cycle and toxin production in the benthic Dinoflagellate *Prorocentrum lima*, Mar. Biol., 134 (1999) 541-549.

41. J.E. Lawrence, J. Grant, M.A. Quilliam, A.G. Bauder, A.D. Cembella, Colonization and growth of the toxic dinoflagellate *Prorocentrum lima* and associated fouling macroalgae on mussels in suspended culture, Mar. Ecol.-Prog. Ser., 201 (2000) 147-154.

42. A.C. Ibe, T.O. Ajayi, Possible Upwelling Phenomenon off the Nigerian Coast, NIOMR Technical Publication, 25 (1985) 1-30.

43. Fan, L., Sun, G., Qiu, J., Ma, Q., Hess, P., Li, A., 2014. Effect of seawater salinity on pore-size distribution on a poly(styrene)-based HP20 resin and its adsorption of diarrhetic shellfish toxins. Journal of Chromatography A 1373, 1-8.

44. J.W. Blunt, M.H. Munro, Dictionary of Marine Natural Products, with CD-ROM, Chapman & Hall, CRC Press, Taylor and Francis Group, Boca Raton, London, New York, (2008).

45. L.O. Odokuma, J.C. Isirima, Distribution of cyanotoxins in aquatic environment in the Niger Delta, Afr. J. Biotechnol., 6 (2007) 2375-2385.

46. C.O. Dublin-Green, A. Awobanise, E.A. Ajao, Large Marine Ecosystem Project for the Gulf of Guinea (Coastal Profile of Nigeria), Nigeria Institute of Oceanography Encyclopedia Americana, 1994. International Edition, Grolier Incorporated (1997).

47. A.C. Ibe, The Niger Delta and the global rise in sea level., Proc. SCORE Workshop on sea level rise and subsidiary coastal areas. Milliman Press, New York., (1988).

48. ASTM, American Society for Testing and Materials. Annual Book of ASTM Standard, (1980) pp. 547-549.

49. Z. Zendong, C. Herrenknecht, E. Abadie, C. Brissard, C. Tixier, F. Mondeguer, V. Sechet, Z. Amzil, P. Hess, Extended evaluation of polymeric and lipophilic sorbents for passive sampling of marine toxins, Toxicon : official journal of the International Society on Toxinology, 91 (2014) 57-68.

50. E. Fux, C. Marcaillou, F. Mondeguer, R. Bire, P. Hess, Field and mesocosm trials on passive sampling for the study of adsorption and desorption behavior of lipophilic toxins with a focus on OA and DTX1, Harmful Algae, 7 (2008) 574-583.

Chapter 7: Determination of the concentration of dissolved lipophilic algal toxins in seawater using pre-concentration with HP-20 resin and LC-MS/MS detection

1. Introduction

A decade ago, passive sampling has been introduced as a tool to monitor algal toxins [1]. Since then, a number of field studies have shown the use of the technique to trace an array of algal or cyanobacterial toxins in algal cultures or marine and coastal environments, including hydrophilic toxins such as saxitoxins and domoic acid, and lipophilic toxins, e.g. azaspiracids, brevetoxins, ciguatoxins, microcystins and okadaic acid, [2-9].

It was already shown [10] the capability of passive samplers to capture toxins from both pelagic and benthic or epiphytic microalgae (Figure VII.1). In particular, PnTX-G and DTX-1 had been accumulated in significant amounts, indicating the presence of both *Vulcanodinium rugosum* and *Prorocentrum lima* in this lagoon.

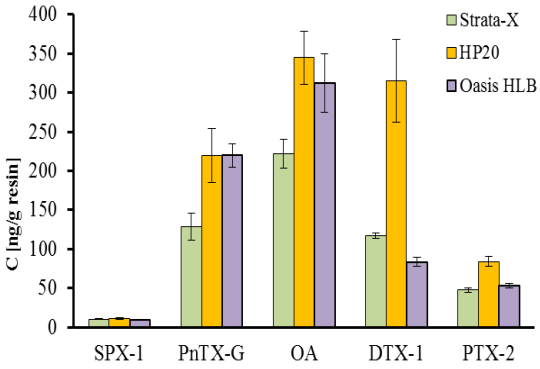

Figure VII.1 Accumulation of SPX1, PnTX-G, OA, DTX1 and PTX2 on Oasis HLB, Strata-X and HP-20 SPATTs exposed in July at Ingril Lagoon on a weekly basis (expressed as [ng/g dry resin])

However, very little is known about the quantitative relationship of the levels of dissolved toxins in seawater and either the levels in shellfish or the levels in the passive samplers. Only few studies have been able to determine the concentrations of dissolved toxins in the field [11-13]. Especially, no studies were known to us that have determined

absolute concentrations of lipophilic toxins in seawater. Thus, we designed an experiment to quantitatively determine the concentrations of lipophilic toxins produced by dinoflagellates in seawater. Our approach consisted in the collection of large volumes of filtered seawater and concentration of the toxins on a lipophilic resin (HP-20), followed by analysis using liquid chromatography coupled to tandem mass spectrometry (LC-MS/MS).

2. Results and discussion

Four toxins were quantifiable in at least one of the portions of seawater: OA, DTX-1, PTX-2 and PnTX-G. Traces of 13-desmethyl spirolide C were also detected. This profile is coherent with previous results obtained with passive sampling directly in this lagoon [10]. Okadaic acid was the most concentrated toxin, with a maximum of ca. 6.9 ng/L determined in the first extraction (S1-30L) of the 30 L portion (Table VII.1). The second extraction (S2, Table VII.1) yielded typically around 20% of the cumulative total for all toxins but DTX-1, for which slightly higher proportions were detected in the second extraction. The other toxins were less abundant but all were above limit of quantification (LOQ), except PTX-2 in the second extraction of the two larger seawater portions. The highest LOQs were those for OA and DTX-1, *i.e.* both ca. 5 ng/mL of injected solution (or ca. 0.2 ng/L seawater), and the lowest LOQ was the one for PnTX-G, *i.e.* 0.5 ng/mL injected solution (or ca. 0.02 ng/L seawater). The concentrations of all of the toxins were lower in the larger water portions, typically by ca. 50%, than those in the 30 L portion. We believe that this is due to an artefact of adsorption of the dissolved toxins to the container wall of the polyethylene carboys, and subsequent loss when the 30 L portions were combined into the larger containers of 90 and 150 L, respectively. The fact that both the 90 L and the 150 L portion yielded the same toxin concentration also suggests that container adsorption may be a dominant factor in the losses observed. Therefore, future exercises should attempt extraction of the water portions directly in the sampling container, as was done with the 30 L portion in this experiment. Seawater collection in transportable containers of 20 to 30 L is practical and as several portions were deployed in each of the containers anyhow, and extracted separately to pre-concentrate the toxins from seawater, such a procedure would not constitute a major obstacle.

Table VII.1. Concentrations of toxins in seawater of Ingril Lagoon, September 2nd 2014 (in [ng/L of seawater]); S1-volume refers to the seawater concentration as determined by the first resin portion (T0 to 48 h), S2-volume refers to the seawater concentration as determined by the second resin portion (48 h – 96 h); n.d. = not detected

Sample	OA	DTX-1	PTX-2	PnTX-G
S1-30L	6.9	1.0	0.2	0.2
S1-90L	3.5	0.7	0.1	0.1
S1-150L	3.5	0.9	0.1	0.1
S2-30L	1.7	0.4	0.1	0.05
S2-90L	1.1	0.5	*n.d*	0.02
S2-150L	0.9	0.5	*n.d*	0.02
Total-30L	8.6	1.4	0.3	0.25
Total-90L	4.6	1.2	0.1	0.12
Total-150L	4.4	1.4	0.1	0.12

The fact that 20% of the toxins were still recovered in the second extraction suggests that both adsorption dynamics and kinetics may play a significant role for this experimental design. This is consistent with the observations mentioned above for the losses in transferring the seawater from several 30 L carboys to larger containers. As previously shown, salinity also appears to affect adsorption kinetics of lipophilic toxins on HP-20 resin [14] . Seawater salinity at Ingril Lagoon during the present study was quite elevated (ca. 40). Therefore, future studies should also take this factor into consideration.

3. Material and methods

3.1 Seawater sampling in Ingril Lagoon

Seawater samples (nine portions of 30 L) were collected from Ingril Lagoon on 2 September 2014. Raw seawater was pumped over two sieves in series of 125 μm and 20 μm phytoplankton mesh using a submersible electric galley pump (GP1352 13 L Whale, USA), operated with FD-7011 batteries (12 V, Lohuis, The Netherlands) into 30 L carboys (polyethylene). A total of nine carboys were filled in this way on the shore. Once in the laboratory, one carboy of filtered seawater was kept separately, while the other eight were combined into a 90 L portion and a 150 L portion. Portions of HP-20 resin (3 g) were prepared in embroidery frames and activated as previously described [8, 10]. Two, four and six portions of resin were placed into the 30 L, 90 L and 150 L portions of seawater,

respectively. The 30 L portion of seawater was stirred using a stir bar with a magnetic stirrer (VCM-C7, VWR, France), while seawater in the two larger containers was circulated using peristaltic pumps equipped with 15 mm flexible plastic tubing (7549-40 Masterflex Cole-Parmer Instrument Co., Chicago, Illinois, USA). Stirring or circulation of seawater was maintained for 48 h before replacing the resin portions with the same number of fresh frames which were deployed for a further 48 h.

3.2 Extraction and LC-MS/MS analysis of resins

The portions of HP-20 resin were extracted as previously described [8, 10]. All 3 g portions were extracted on separate SPE cartridges for ease of handling. Subsequently, elutes were combined into single fractions for each of the three seawater portions, keeping the extracts from the first and second deployment separate. Thus a total of six final extracts were obtained for LC-MS/MS analysis (three different volumes of seawater each consecutively extracted twice). Final extract volume was kept to 1 mL of 50% aqueous methanol for all six fractions.

Analysis was performed on a UHPLC-system (UFLC, Shimadzu) coupled to a triplequadrupole mass spectrometer (4000 Qtrap, ABSciex, Les Ulis, France). Chromatography was performed with a Hyperclone MOS C8 column (50 × 2.0 mm, 3μm) with a C8 guard column (4 × 2.0 mm, 3 μm, Phenomenex). A binary mobile phase was used, phase A (100%aqueous) and phase B (95% aqueous acetonitrile), both containing 2 mM ammonium formiate and 50 mM formic acid. The flow rate was 0.2 mL/min and injection volume was 5 μL. The column and sample temperatures were 25°C and 4°C, respectively. Two different gradients were employed, one for the negative mode (to analyze OA, DTX-1 and dinophysistoxin-2 (DTX2-)) starting with 30% B, rising to 95% B over 8 min, held for 2 min, then decreased to 30% B in 0.5 min and held for 4.5 min to equilibrate the system; and a second gradient for the positive mode (for PTX2, 13-desmethyl spirolide C, PnTX-G and pinnatoxin A (PnTX-A)) starting with 30% B, rising to 95% B over 2.5 min, held for 5 min, then decreased to 30% B in 0.1 min and held for 2.5 min to equilibrate the system. Analytes were detected by negative or positive ion mode using multiple reaction monitoring (MRM). The following negative transitions (precursor ion→product ion) were used for quantification and confirmation (confirmatory ions shown in parentheses): OA and DTX-2: *m/z* 803.4→255.1 (803.4→113.1); DTX-1: *m/z* 817.5→254.9 (817.5→112.9). Positive ionization transitions were as follows, PTX-2: *m/z* 876.6→823.5 (876.6→805.6); 13-desmethyl spirolide C: *m/z* 692.6→164.2

(692.6→444.3); PnTX-G: *m/z* 694.4→164.1 (694.4→458.3); PnTX-A: *m/z* 712.4→164.1 (712.4→458.3).

PnTX-A and -G were quantified against a well characterized standard of PnTX-G from NRCC (Halifax, CA), assuming that PnTX-A had the same response factor as PnTX-G. All other toxins were quantified against certified calibrants (NRCC, Canada).

The ESI interface was operated using the following parameters, in negative mode: curtain gas 20 psi, temperature: 550°C, gas1: 40 psi; gas2: 50 psi, ion spray voltage: -4500 V; in positive mode: curtain gas: 30 psi, temperature: 450°C, gas1: 50 psi; gas2: 50 psi, ion spray voltage: 5500 V.

4. Conclusions

The experiments settled up in this study have overcome the typical limitations of classical solid-phase extraction (SPE) of seawater which is known to suffer from break-through phenomena for volumes greater than 1 L. Overall, these results are encouraging to apply a similar design to the analysis of coastal seawater from open bays, since the limits of quantitation were surpassed by ca. 10 to 15-fold in the first extraction, even for the smallest volume of seawater used here (30 L).

References

1. L. MacKenzie, V. Beuzenberg, P. Holland, P. McNabb, A. Selwood, Solid phase adsorption toxin tracking (SPATT): a new monitoring tool that simulates the biotoxin contamination of filter feeding bivalves, Toxicon : official journal of the International Society on Toxinology, 44 (2004) 901-918.

2. D. Shea, P. Tester, J. Cohen, S. Kibler, S. Varnam, Accumulation of brevetoxins by passive sampling devices, African Journal of Marine Science, 28 (2006) 379-381.

3. L.A. Stobo, J.P.C.L. Lacaze, A.C. Scott, J. Petrie, E.A. Turrell, Surveillance of algal toxins in shellfish from Scottish waters, Toxicon, 51 (2008) 635-648.

4. E. Fux, S. Gonzalez-Gil, M. Lunven, P. Gentien, P. Hess, Production of diarrhetic shellfish poisoning toxins and pectenotoxins at depths within and below the euphotic zone, Toxicon, 56 (2010) 1487-1496.

5. J.Q. Lane, C.M. Roddam, G.W. Langlois, R.M. Kudela, Application of Solid Phase Adsorption Toxin Tracking (SPATT) for field detection of the hydrophilic

phycotoxinsdomoic acid and saxitoxin in coastal California, Limnology and Oceanography-Methods, 8 (2010) 645-660.

6. R.M. Kudela, Characterization and deployment of Solid Phase Adsorption Toxin Tracking (SPATT) resin for monitoring of microcystins in fresh and saltwater, Harmful Algae, 11 (2011) 117-125.

7. E. Fux, C. Marcaillou, F. Mondeguer, R. Bire, P. Hess, Field and mesocosm trials on passive sampling for the study of adsorption and desorption behaviour of lipophilic toxins with a focus on OA and DTX1, Harmful Algae, 7 (2008) 574-583.

8. E. Fux, R. Bire, P. Hess, Comparative accumulation and composition of lipophilic marine biotoxins in passive samplers and in mussels (M. edulis) on the West Coast of Ireland, Harmful Algae, 8 (2009) 523-537.

9. A. Caillaud, P. de la Iglesia, E. Barber, H. Eixarch, N. Mohammad-Noor, T. Yasumoto, J. Diogène, Monitoring of dissolved ciguatoxin and maitotoxin using solid-phase adsorptiontoxin tracking devices: Application to Gambierdiscus pacificus in culture, Harmful Algae, 10 (2011) 433-446.

10. Z. Zendong, C. Herrenknecht, E. Abadie, C. Brissard, C. Tixier, F. Mondeguer, V. Sechet, Z. Amzil, P. Hess, Extended evaluation of polymeric and lipophilic sorbents for passive sampling of marine toxins, Toxicon : official journal of the International Society on Toxinology, 91 (2014) 57-68.

11. K.A. Lefebvre, B.D. Bill, A. Erickson, K.A. Baugh, L. O'Rourke, P.R. Costa, S. Nance, V.L. Trainer, Characterization of intracellular and extracellular saxitoxin levels in both field and cultured Alexandrium spp. samples from Sequim Bay, Washington, Mar. Drugs, 6 (2008) 103-116.

12. V.L. Trainer, M.L. Wells, W.P. Cochlan, C.G. Trick, B.D. Bill, K.A. Baugh, B.F. Beall, J. Herndon, N. Lundholm, An ecological study of a massive bloom of toxigenic Pseudonitzschia cuspidata off the Washington State coast, Limnol. Oceanogr., 54 (2009) 1461-1474.

13. J.D. Liefer, A. Robertson, H.L. MacIntyre, W.L. Smith, C.P. Dorsey, Characterization of a toxic Pseudo-nitzschia spp. bloom in the Northern Gulf of Mexico associated with domoic acid accumulation in fish, Harmful Algae, 26 (2013) 20-32.

14. L. Fan, G. Sun, J. Qiu, Q. Ma, P. Hess, A. Li, Effect of seawater salinity on pore-size distribution on a poly(styrene)-based HP20 resin and its adsorption of diarrhetic shellfish toxins, Journal of Chromatography A, 1373 (2014) 1-8.

Chapter 8: Preliminary studies toward isolation of palytoxin

1. Introduction

Several cases of inhalatory poisonings and/or skin injuries have been reported in beachgoers concomitantly with massive blooms of *O.* cf. *ovata* as well as in aquarium hobbyists from incidental contact with PLTX-producing *Palythoa* spp. Symptom similarities between *Ostreopsis*- and *Palythoa*-related poisonings suggest that the etiological agent is the same [1]. As a matter of fact, PLTXs and OVTSs differ little in structural details- a few methyl, methylene and/or hydroxyl groups over a long polyhydroxylated aliphatic chain. So, they are likely to cause the same overall symptomatology although their relative potencies might be different [2].

The increasing spread of the *Ostreopsis* phenomenon and the ever-growing number of palytoxin congeners being discovered makes the need of evaluating their toxicity urgent. The availability of sufficient amounts of well characterized reference material is the cornerstone for the achievement of toxicity data. To achieve this goal, we are developing an isolation procedure for quantitative recovery of individual PLTX-congeners from *Palythoa* spp. grown in marine aquarium and we are evaluating the stability of PLTXs under different conditions.

Our previous work on isolation of OVTX-a from *O.* cf. *ovata* [3], although successful in recovering 700 μg of pure toxin from 80 liters of algal culture, provided an overall recovery of about 12% following extraction, 4 chromatographic separations and multiple evaporation steps. Similarly, Brissard *et al*. [4], although reported an 85% recovery of OVTXs from algal extracts following a single Sephadex-LH20 chromatography, highlighted that only 1/3 of the expected toxin could be recovered after total evaporation. Zendong *et al.* [5] in the evaluation of polymeric and lipophilic sorbents for passive sampling of marine toxins reported poor recoveries for OVTX-a from passive samplers, consistent with the low recoveries obtained by solid phase extraction (SPE). There is no indication in literature whether generally low recoveries for PLTX and its congeners are due to instability of the compounds in solution or to irreversible adsorption to materials or to other uncontrolled factors. Only Taylor *et al.* [6] suggested a non-specific binding of palytoxin to polyethylene (PE) tubings that was attenuated by adding 0.1% rat serum albumin. In view of a large scale isolation work aimed to preparation of PLTX

reference material, the causes underlying the huge PLTX loss needs to be investigated. In this study, we focused on the evaporation of PLTX under various experimental conditions namely the use of different evaporation systems (Centrifugal Vacuum Concentrator and N_2stream) versus freeze drying, complete drying versus concentration, the influence of various solvents (aqueous or pure organic), of most common materials (normal and silanized glass vials, polypropylene and Teflon tubes), and of the re-dissolution solvent (type and volume) on toxin recovery. Preliminary results on stability of PLTX under various acidic conditions were also obtained.

2. Results and discussion

2.1 Effect of drying techniques on PLTX recovery

In order to substantiate the observed heavy loss of PLTXs reported in literature [3-5], and to exclude a systematic bias due to operators, a preliminary evaporation experiment was carried out by mixing PLTX with okadaic acid (OA), a diarrhetic shellfish poisoning toxin which was used as reference to compare evaporation recoveries. Both PLTX and OA were mixed at equimolar concentration in 80% aqueous MeOH- the solvent most commonly employed to extract PLTXs from mussels [7] and seawater [1] - and the mixture was evaporated to dryness under N_2 stream at room temperature. LC-MS analysis of the dry residue reconstituted in 50% aqueous MeOH showed a recovery of 62%±6 for PLTX and of 103%±2 for OA. The poorer recovery of PLTX than OA clearly confirmed the previously reported data and suggested that at least one of the reasons for such losses could be related to the evaporation that, thus, represents a key step to optimize within the isolation work.

In order to investigate the effect of drying techniques on PLTX recovery, PLTX was dissolved in 80% aqueous MeOH (125 ng/mL) and evaporated to dryness using either N_2 stream at room temperature or Centrifugal Vacuum Concentrator at T= 30°C. The latter device consists in the combination of vacuum, centrifugal force, and heat resulting into solvent evaporation. At the same time, PLTX dissolved in 10% aqueous methanol 125 ng/mL) was freeze dried. Experiments were carried out in triplicate in glass vials without cap (as routinely done) and with perforated cap (see experimental) over 1 day and repeated over 4 different days. LC-MS analyses were performed in triplicate on the same day as preparation.

Recoveries obtained for evaporation of PLTX in vials with no cap were quite similar using N_2 stream (62%±6) and Centrifugal Vacuum Concentrator (64% ± 5), suggesting that evaporation method has a negligible influence on the recovery of PLTX. Inter-day repeatability was indicated by RSD values of 15% for both evaporation systems. Comparison of recoveries obtained with and without cap indicated that an additional 13% and 7% of the toxin could be recovered carrying out evaporation with perforated cap under N_2 stream and Centrifugal Vacuum Concentrator, respectively.

Recovery of PLTX following freeze-drying was 37% ± 4, significantly lower than those obtained by the aforementioned evaporation techniques, with an inter-day repeatability (RSD) of 21%. However, in the experiments carried out with perforated cap recovery increased to 55% ± 6. So, even freeze drying without cap resulted into a quite heavy toxin loss. Comparison of the results obtained with and without cap, suggests that some aerosolization of PLTX occurs within the dry-down process (either evaporation of freeze drying), contributing to toxin loss. This supports the hypothesis that PLTXs could be aerosolized thus representing the probable cause of several inhalatory poisonings occurred in humans concomitantly to *Ostreopsis* spp. blooms and during cleaning operation of marine aquarium containing *Palythoa* spp. [1,8].

2.2 Complete Drying versus Concentration in different solvents. Solubility issue

Based Palytoxin (125 ng) was diluted in 6 different solvent mixtures –pure MeOH, EtOH and IsoPrOH and 80% aqueous solutions of each solvent– and evaporated to dryness under N_2stream in PP tubes. Residues were re-dissolved either in the original solvent mixtures or in 50% aqueous MeOH, which is commonly used to dissolve PLTX and to extract PLTX-like compounds from algal pellets [9]. This to the aim of testing both the influence of the solvent within the evaporation step and the solubility of the toxin in the different solvents. The obtained recoveries are reported in Table VIII.1.

Table VIII.1 Recoveries of PLTX following complete evaporation in various solvents and subsequent re-dissolution either in the original solvent or in 50%aqueous MeOH. ± represents standard deviation (n= 3)

Complete drying in	Recovery % (original solvent)	Recovery % (MeOH 50%)
MeOH 80%	40±13	56±11
EtOH 80%	59±8	61±4
IsoPrOH 80%	23±2	60±6
MeOH 100%	27±1	42±8
EtOH 100%	16±7	46±9
IsoPrOH 100%	nd	40±13

The When PLTX was re-dissolved in the original solvent mixture, the lowest recoveries were observed when pure organic solvents were used, in the order IsoPrOH<<EtOH<MeOH (Table VIII.1). Although all polar protic solvents were used, they present quite different dielectric constants (MeOH, ε = 32.7; EtOH, ε = 24.5; IsoPrOH, ε = 17.9) related to the length of the alkyl chains.So, the lipophilic moieties of PLTX play a minor role in the solubility processthan the hydrophilic groups able to establish hydrogen bonds.

When PLTX was re-dissolved in 80% aqueous solvents, higher recoveries than in pure organic solvents were obtained, in the order 80% EtOH>80% MeOH>80% IsoPrOH (Table VIII.1). This suggests that a significant percentage of water significantly improve re-dissolution ofPLTX. However, it seems that solubility of PLTX in aqueous blends does not depend only on dielectric constant of each solvent mixture.This is in agreement with Gorman and Hall [10] who demonstrated that the extent of solubility of polar compounds is not related just to the dielectric constant of the solvent blend but varies with the particular solvent mixture used, although the bonding characteristic of each blend are somewhat similar.

The whole of these data suggests that solubility of PLTX in different solvents plays an important role in the recovery of the evaporation step. For this reason, this experiment was repeated evaporating PLTX in the above mentioned different solvents and usingas re-dissolution solvent 50% aqueous MeOH, which is the most employed mixture for dissolving PLTXs. Higher recoveries than those obtained in the previous experiment were observed for all samples especially for those evaporated in pure organic solvents (Table VIII.1). However, recoveries still remained poor with the highest recovery not exceeding 61% for the 80% aqueous EtOH sample. This indicated that solubility is not the only factor

affecting recovery since a significant toxin loss occurred anyway during the evaporation process.A co-factor contributing to the toxin loss could be the aerosolization of the toxin. This hypothesis is substantiated by the observation that the lowest recoveries (40-46%) were obtained for samples evaporated in pure organic solvents, for which the evaporation process occurs faster than in aqueous solvents, resulting in a more pronounced aerosol formation and subsequent toxin loss.

To in-depth investigate the solubility issue, an experiment of 1:10-dilutionof PLTX in various solvent mixtures and subsequent LC-HRMS analysis was carried out (Figure VIII.1).

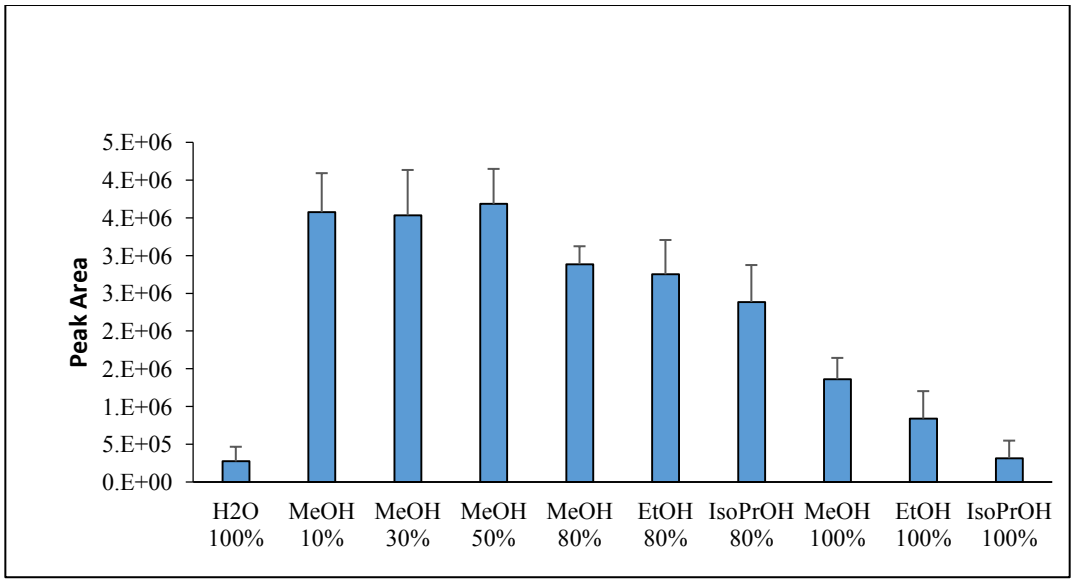

Figure VIII.1 Chromatographic peak areas obtained from LC-HRMS analysis of PLTX 1:10 dilution in various solvents mixtures. Error bars represent standard deviation (n= 3)

The highest responses were obtained when PLTX was diluted in 50%, 30% and 10% aqueous MeOH with no significant differences being observed among the three solvent mixtures. A decreasing trend in the response was observed in 80% aqueous blends, in the order MeOH>EtOH>IsoPrOH. A significantly lower response than 50% aqueous MeOH ($p<0.001$) was observed for dilutions carried out in pure organic solvents ε (MeOH>EtOH>IsoPrOH) as well as in pure water. So, this suggests that PLTX in pure water as well as in pure organic solvent is not fully soluble.

A slight contribution to the low response could be due to the formation of PLTX dimer in water [11]. To investigate this issue, Full HRMS spectra of concentrated PLTX

standard (10 µg/ml) were recorded in pure water and in 50% aqueous MeOH. In both samples the presence of a PLTX dimer $[2M+H+Ca]^{3+}$at *m/z* 1799.3102 (Δ =0.479 ppm) and trimer $[3M+3H+Ca]^{5+}$ at *m/z* 1615.6828 (Δ =-0.997ppm) (Figure VIII.2) emerged, together with the most abundant monomeric form of PLTX $[M+H+Ca]^{3+}$ at *m/z* 906.4824. Considering that the dimer was 2.4 times more abundant in pure water than in 50% aqueous MeOH (monomer/dimer ratio 38:1 and 67:1 in pure water and 50% aqueous MeOH, respectively), the lower response observed for PLTX in pure water could be likely due to both lower solubility and increased dimer formation.

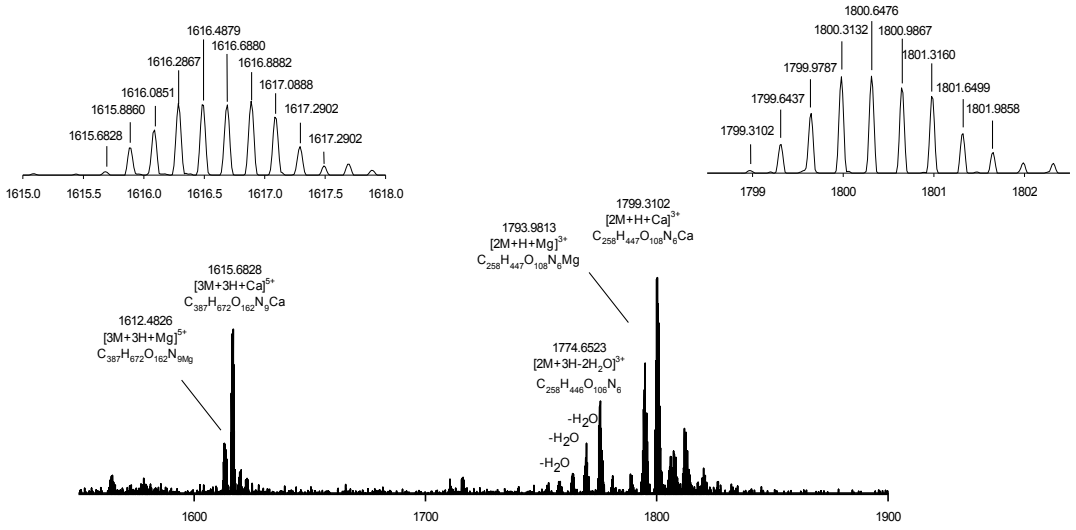

Figure VIII.2 Full HRMS spectrum of PLTX dimer and trimer zoomed in m/z 1510-1900 range with elemental formula assignment of the triply and quintuple charged monoisotopic ions. Further enlargements of the $[3M+3H+Ca]^{5+}$ and $[2M+H+Ca]^{3+}$ ions are present to show isotopic ion pattern

When samples were simply concentrated in the solvent mixtures previously described a relevant toxin loss as well as a low inter-day reproducibility was observed when water was present in the mixture (Table VIII.2). In particular, PLTX was not detected in 80% aqueous MeOH, while low but significant recoveries were observed in 80% aqueous EtOH and IsoPrOH. Addition of an equal volume of the relevant organic solvent to the concentrated samples resulted into an improved but still unsatisfactory recovery for 80% aqueous MeOH (10%). Better recoveries were obtained for 80% aqueous EtOH and IsoPrOH samples.

Table VIII.2 Recoveries of PLTX following concentration in various solvents and recoveries of aqueous blends after adding 200 μL of the relevant organic solvent.± represents standard deviation (n= 3)

	Recovery %	Recovery % after adding 200μL organic solvent
MeOH 80%	n.d.	10±1
EtOH 80%	50±9	88±20
IsoPrOH 80%	58±19	150±30
MeOH 100%	86±2	-
EtOH 100%	83±6	-
IsoPrOH 100%	47±17	-

Considering that during the concentration of aqueous mixtures PLTX remained mainly in water, these results confirm that solubility of PLTX in pure water is low and that some organic solvent is necessary to keep it in solution.

Higher recoveries than in aqueous blends were obtained when PLTX was concentrated in pure organic solvents, namely 86% in MeOH and 83% in EtOH. Recovery and reproducibility was still low when PLTX was concentrated in pure IsoPrOH (47%).

Comparison between concentration and complete drying results in pure organic solvents, shows that concentration leads to higher recoveries than dry-down. On the contrary, when PLTX is in aqueous blends, dry-down leads to higher recoveries than concentration. This suggests that besides the solubility and the aerosolization issues some other factors play a role. A possible interaction with tube materials has been thus investigated.

2.3 Complete Drying versus Concentration in different materials. Adsorption issue

In order to investigate the role of materials during the evaporation procedures, complete drying and concentration of PLTX in the aforementioned mixtures was tested in different tubes and vials, namely: normal glass and silanized glass vials, PP and Teflon tubes.

Results obtained concentrating PLTX in glass (either normal or silanized) and plastic materials (either PP or Teflon) suggested that PLTX behaves differently in the 2 types of materials. However, in most cases no significant differences were observed between normal and silanized glass vials as well as between PP and Teflon tubes (Figure VIII.3).

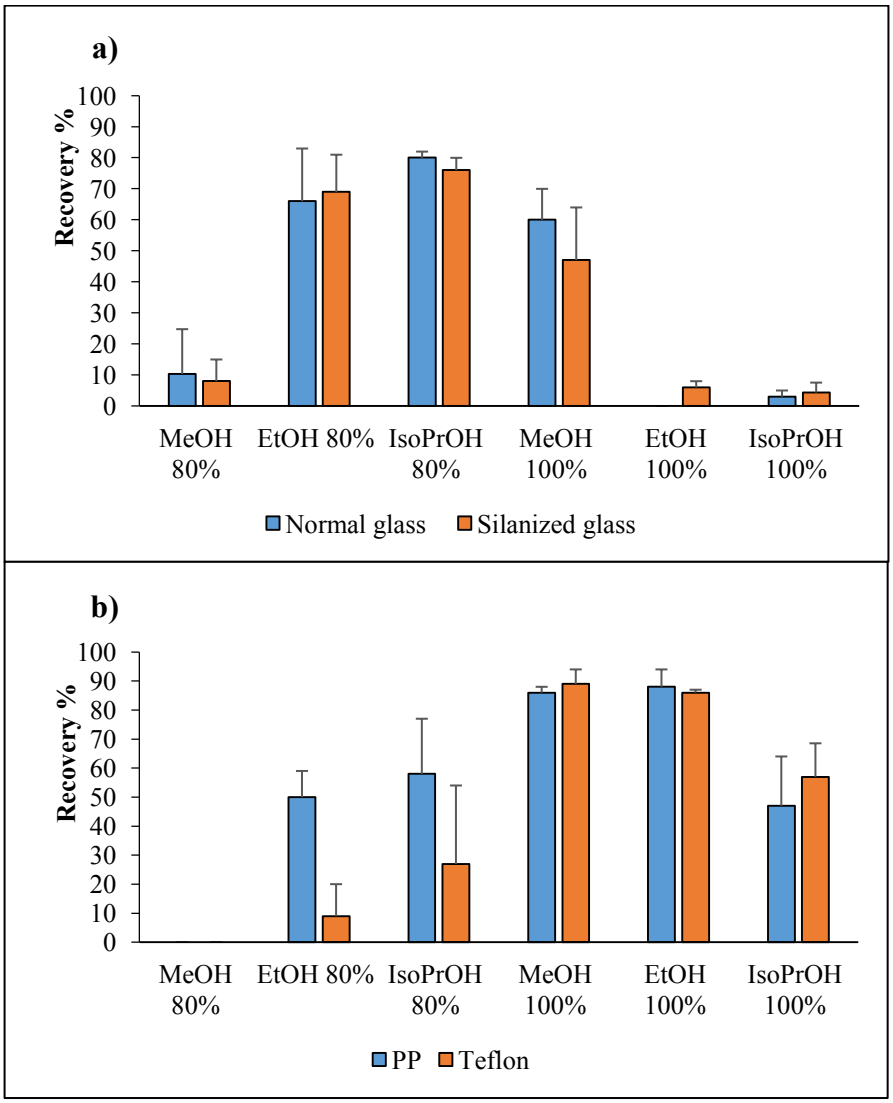

Figure VIII.3 Recoveries of PLTX following concentration in various solvents using both normal and silanized glass vials (3a) or PP and Teflon tubes (3b). Error bars represent standard deviation (n= 3)

In PP and Teflon, best recoveries (in the range 86-89%) were obtained when PLTX was concentrated in pure organic solvent (mainly MeOH and EtOH) while poor recoveries and reproducibility were obtained when PLTX was concentrated in aqueous blends (Figure VIII.3b). Surprisingly, while PLTX in pure IsoPrOH showed the poorest recovery among the tested organic solvents, aqueous 80% IsoPrOH led to higher PLTX recovery than aqueous 80% EtOH and MeOH.

In glass materials (either normal or silanized), PLTX was barely detectable after concentration in pure EtOH and IsoPrOHwhile its recovery was lower than in plastic materials when PLTX was concentrated in pure MeOH (60% in normal glass versus 86% in PP). Unlike plastic tubes, when PLTX was concentrated in aqueous blends in glass,

relatively better recoveries were obtained (Figure VIII.3a) with an improvement in glass compared to plastic materials of about 8% for 80% aqueous MeOH, and 20% for 80% aqueous EtOH and IsoPrOH. Similarly to plastic materials, concentration in 80% aqueous IsoPrOH leads to the highest recoveries among the tested aqueous blends.

The whole of such data suggests that, in addition to the PLTXsolubility issue in the used solvents, a phenomenon of interaction/adsorption with the material might occur. McGinley *et al.* [12] summarized the interactions between solute and sorbent into the following three categories of sorption: a) physical sorption which includes interactions between dipole moments (permanent or induced) of solute and sorbent molecules; b) chemical sorption which involves covalent bond and hydrogen bond; and c) electrostatic sorption which involves ion–ion and ion–dipole forces. Sorption of organic compounds sometimes can be explained with the simultaneous contribution of two or more of these mechanisms.We can hypothesize that in glass vials hydrogen bonds might be formed between OH and NH groups of PLTX and the oxygen atoms of the glass silanols. This could result into PLTX sticking to the walls of the glass vials. However, solubility and adsorption are competitive factors. Focusing on pure organic solvents, adsorption is more evident when PLTX is concentrated in a poor solvent, such as pure EtOH and IsoPrOH, which actually produce the worst recoveries (in the range 0-6%) (Figure VIII.3a). Adsorption can be instead minimized when the toxin isconcentrated in a good solvent such as pure MeOH, with recoveries of 47 and 60% being observed in normal and silanized glass, respectively. In the plastic materials where the only possible interactions are hydrophobic type, adsorption of PLTX on the material seems to play a minor role compared to solubility.

Adsorption on glass of PLTX concentrated in aqueous blends is minor than in pure organic solvents.One possible explanation could be that water molecules could compete with PLTX in the adsorption process on glass and thus resulting in satisfactory recoveryfor PLTX (e.g. 80% of recovery in 80% aqueous IsoPrOH). A similar behavior has been reported by Delle Site [13] who described a strong competition in hydrogen bonds formation between water molecules and some analytes (aniline, acetanilide and carbamate pesticide analogues) occurring in soil. When concentration is carried out in aqueous solvents in Teflon and PP tubes, leading to an increase percentage of water of the initial mixture, PLTX recoveriesare worse than in the glass materials, being in the range 0-27% and 0-58% respectively (Figure VIII.3b). This suggests that in such materials

poorsolubility of PLTX in H_2O plays a major role. An increase of PLTX recovery was observed when 200 µL of relevant organic solvent were added to these samples.

Figure VIII.4 shows results of complete drying of PLTX in glass vials and in plastic tubes and subsequent re-dissolution in the original solvents.

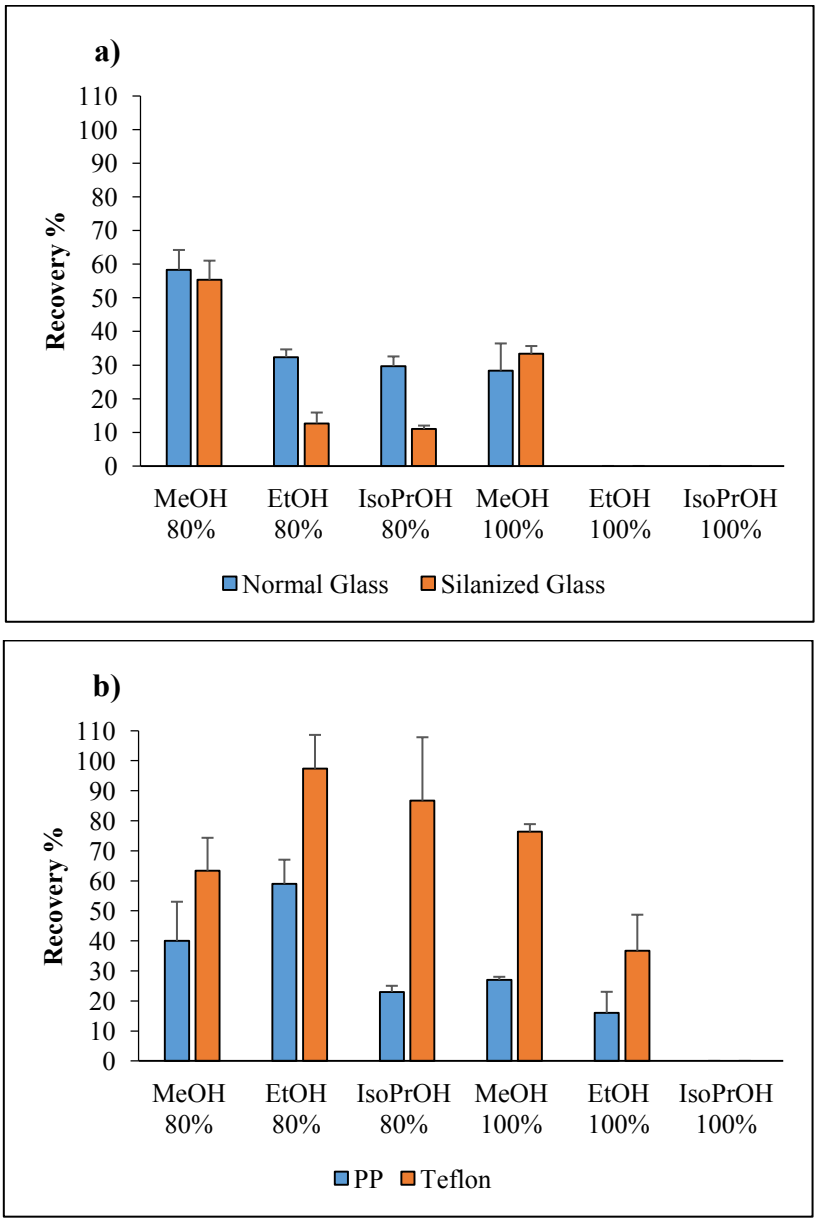

Figure VIII.4 Recoveries of PLTX following complete drying in various solvents using both normal and silanized glass vials (4a) or PP and Teflon tubes (4b). Error bars represent standard deviation (n= 3)

Similarly to the concentration experiment, recoveries in plastic tubes (either PP or Teflon) followed the same general trend. The highest recoveries were obtained when PLTX was evaporated to dryness in Teflon tubes, with a 97% recovery for the 80% aqueous EtOH sample. This in contrast with the results obtained just concentrating PLTX in aqueous blends, among 80% aqueous IsoPrOH emerged as the preferred concentrating solvent. In plastic materials recoveries in pure organic solvents paralleled solubility of PLTX in the used solvents. Indeed PLTX was not detected in pure IsoPrOH.

Unsatisfactory recoveries (in the range 11-58%) were obtained completely drying PLTX in glass vials (normal and silanized). In this case, adsorption seems to play a major role. Considering that PLTX was not detected after drying in pure EtOH and IsoPrOH, aqueous solvents are necessary but not sufficient to re-dissolve PLTX. This trend was opposite to that observed in the concentration experiment. Among the pure organic solvents, only MeOH succeeded to dissolve PLTX.

Finally,both in concentration and drying experiments, there are two competing factors, namely adsorption and solubility. In plastic materials, the behavior seems to be governed primarily by the solubility; in the glass materials adsorption affects recoveries more than solubility.

2.4 Dry-down of PLTX at different concentration levels

Adsorption is a concentration dependent phenomenon; for this reason, evaporation of different concentration of PLTX solutions in 80% aqueous MeOH was carried out under N2 flow in PP tubes. The obtained results (Figure VIII.5) showed that adsorption significantly increased at lower concentrations and that higher loss of PLTX occurred at concentrations <250 ng/mL.

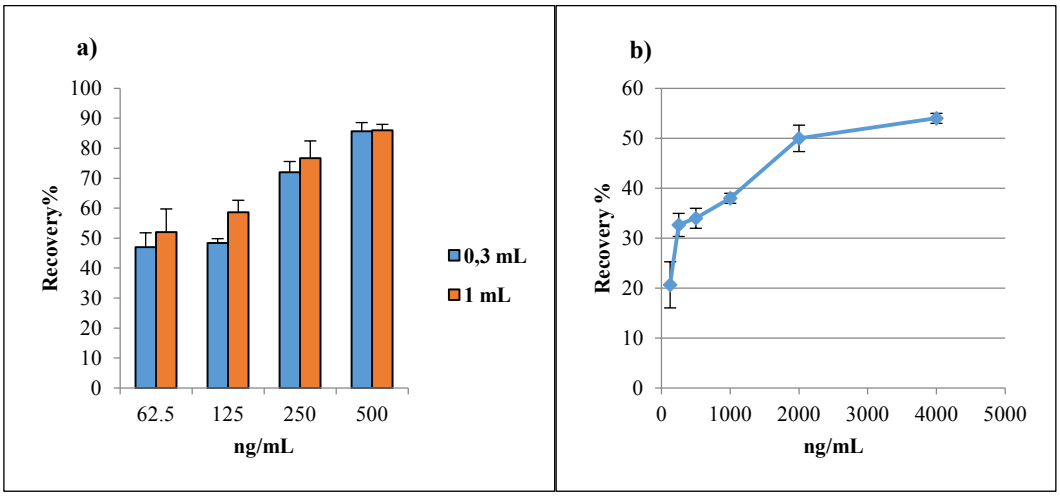

Figure VIII.5 Recoveries of PLTX following complete drying in 80% aqueous MeOH at different spiking concentrations (62.5, 125, 250 and 500 ng/mL) and subsequent re-dissolution either in 0.3 or 1 mL of 50% aqueous MeOH (5a). Recoveries of PLTX following freeze-drying in 10% of aqueous MeOH at different spiking concentrations (125, 250, 500, 1000, 2000 and 4000 ng/mL) and subsequent re-dissolution in 0.3 mL of 50% aqueous MeOH (5b). Error bars represent standard deviation (n= 3)

A similar trend was observed when PLTX was freeze-dried in glass vials in a wider concentration range (125-4000 ng/mL) (Figure VIII.5b). Although, consistently with data reported in the paragraph 2.1, recoveries following freeze-drying were definitely lower than that obtained using N_2 flow (Eg. 34% recovery versus 86% at 500 ng/mL), the amount of PLTX adsorbed was higher at lower concentration and the increase in recovery from 125 ng/ml to 500 ng/mL was steeper using PP tubes (38% increase) than using normal glass vials (13% increase). This confirms that adsorption in glass is stronger than in PP tubes.

We also tested the influence of the re-dissolution volume on recovery of PLTX: an increase of 5-11% in recovery was observed for the less concentrated samples (62.5 to 250 ng/mL) when1 mL of re-dissolution volume (50% aqueous MeOH) was used instead of 0.3 mL. However no difference in recoveries was observed at the highest tested concentration of 500 ng/mL.

2.5 Preliminary study on stability of PLTX in acids

In order to investigate PLTX behavior under different acid conditions, PLTX was dissolved in 80% aqueous MeOH mixtures containing either 0.2% acetic acid (AA, pH 3.25), 2% formic acid (FA, pH 2.66), or 0.1% trifluoroacetic acid (TFA, pH 1.20). The solutions were analyzed by LC-MSand LC-HRMS/MS soon after preparation and after 2

weeks versus control (PLTX in 80% aqueous MeOH) to check whether any degradation of PLTX due to acid addition had occurred. No statistically significant difference was measured at day 0 among the different treatments, although response of PLTX in AA presented a 17% enhancement versus control. At day 14,while a 19% enhancement was still observed between PLTX in AA and control, a 64% and a 29% decrease of PLTX versus control was observed for samples inTFA and FA respectively, suggesting that aexposure to strong acidic condition ($pH \leq 2.66$) caused the degradation.

The effect of the total evaporation under N_2 stream on PLTX in the above mentioned acid solutions was also investigated (Figure VIII.6a and b). All the tested acid solutions (AA, TFA, and FA samples) as well as the control sample were re-dissolved in 80% aqueous MeOH after total drying and analyzed versus PLTX calibration curve. According to previous observations, a 74% recovery of PLTX was measured for the control sample. A similar recovery (72%) was recorded for the AA sample, while a strong degradation occurred for the TFA and FAsamples with recoveries of 28% and 58%, respectively. The degradation was likely due to a progressiveincrease of acid concentration due to the evaporation of the solvent and consequent decrease in pH.

Another aspect we considered was the influence of temperature on PLTX. All the samples (control, AA, TFA, and FA) were kept at 60°C for 1 hour (Figure VIII.6b) and soon after analyzed versus a PLTX calibration curve: 16% and 68% of PLTX recoveries were observed in TFA and FA samples, respectively, while no significant difference was measured between PLTX in acetic acid and in control.

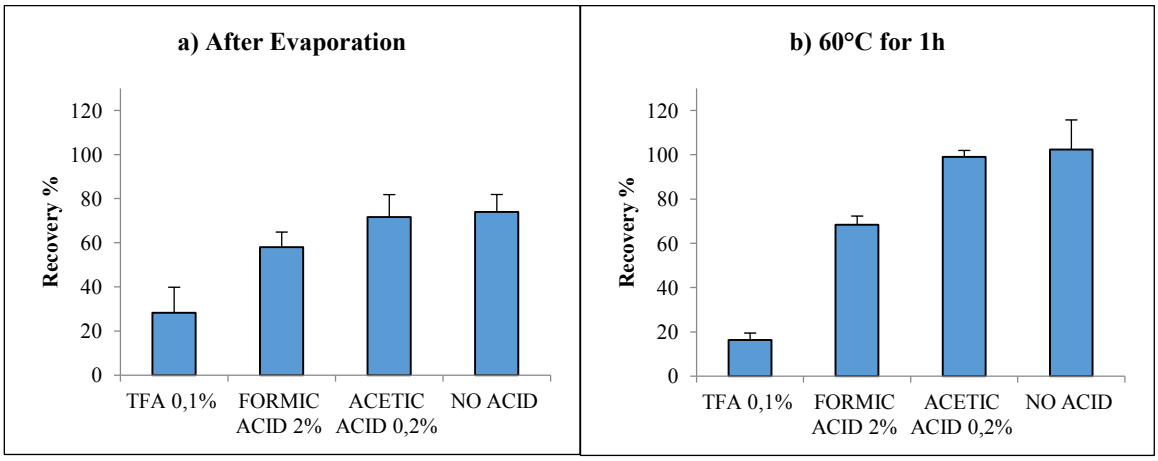

Figure VIII.6 Recoveries of PLTX (125ng) following complete drying in three different 80% aqueous MeOH mixtures containing respectively 0.2% of acetic acid, 0.1% of trifluoroacetic acid and 2% of formic acid and subsequent re-dissolution in 1 mL of 80% aqueous MeOH (6a). Recoveries of the same PLTX acidic mixtures following a heat-treatment (60° C for 1 hour) (6b). Error bars represent standard deviation (n= 3)

The degradation observed for PLTX in the stronger acidic conditions tested could be explained considering that PLTX contains several acid sensitive functionalities (ketal, emiketal, enamide, hydroxyls).

In order to check for the presence of degradation products we in-depth investigatedfull HRMS spectra of PLTX in those samples that presented the lowest recoveries, namely 0.1% TFA samples obtained at day 0 and 14 and at 60°C. A close comparison between these samples and control was carried out. The presence of a triply-charged ion at *m/z* 869.1261 ($C_{124}H_{216}NO_{53}Ca$, RDB 17.5, Δ= -2.432) eluting in the vicinity of PLTX emergedonly in the acidified samples. This ion increased in the XIC overtime as well as with temperature.The difference of $C_5H_8N_2O$ between molecular formula of this compound ($C_{124}H_{215}NO_{53}$) and PLTX ($C_{129}H_{223}N_3O_{54}$) suggested that structural modifications likely occurred in the A-side terminal of the molecule where 2 N were present. HRMS/MS of *m/z* 869.4 confirmed this hypothesis since the characteristic B-side fragments of all diagnostic cleavages (#4, #5, #12, #13, #15, #17) as well as the internal fragments (#4+12, #4+15, #4+16) were superimposable to those of PLTX while all the relevant A-side fragments of these cleavages presented the same mass difference of $C_5H_8N_2O$. In addition the characteristic A-side fragment of cleavage #4 (m/z 327) was totally lacking [14-18]. (Table VIII.3). The whole of these data suggested that the molecule could be a PLTX methyl ester at C1. Its formation under strong acidic conditions could be explained according to the tentative mechanism reported in Figure VIII.7 **Hypotetical**

mechanism formation of PLTX methyl-ester. The first step of the mechanism could involve protonation of the carbonyl oxygen at C1' leading to an *N*-acylimminium cation fully conjugated. In methanol, the presence of a good conjugated leaving group in this compound, could favour formation of a methyl ester at C1 instead of the hydrolysis of the iminium group [19] which would lead to the formation of an amide at C1 and a ketone.

The presence of PLTX congeners lacking the moiety 1'-8' has been recently highlighted also for natural occurring PLTX congeners.

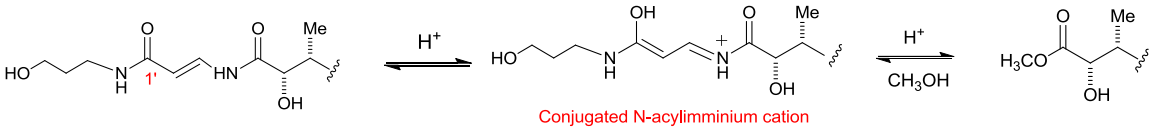

Figure VIII.7 Hypotetical mechanism formation of PLTX methyl-ester

Table VIII.3 Assignment of fragments contained in HR CID MS^2 spectra of palytoxin methyl Ester to relevant cleavages (Clv). Elemental formulae of the mono-isotopic ion peaks (*m/z*) are reported with ion charge state (1+, 2+ or 3+) and relative double bonds (RDB). Errors were below 5 ppm in all cases.

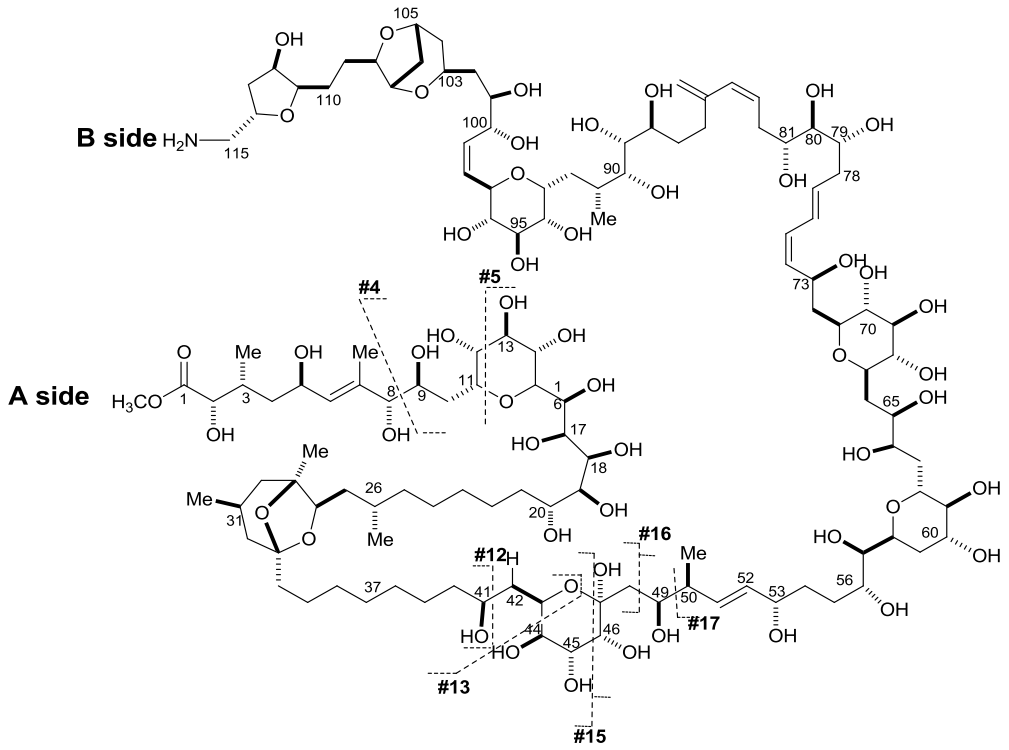

	Palytoxin Methyl Ester		
Clv	**A side**	**B side**	
	***m/z* (1+,2+,+3)** **Formula** **RDB**	***m/z* (1+,2+,+3)** **Formula** **RDB**	
#4		1178.1179 (2+) $C_{113}H_{193}O_{47}NCa$ 17.0, -1.664	
#5		791.7502 (3+) $C_{113}H_{196}O_{48}NCa$ 16.5, -1.274	
#12	488.2636 (2+) $C_{47}H_{84}O_{18}Ca$ 6.0	-	
#13	510.2767 (2+) $C_{49}H_{88}O_{19}Ca$ 6.0	-	
#15	540.2873 (2+) $C_{51}H_{92}O_{21}Ca$ 6.0	782.8752 (2+) $C_{73}H_{123}O_{32}NCa$ 13.0	1526.8181 (1+) $C_{73}H_{124}O_{32}N$ 12.5
#16	568.3004 (2+) (-1H2O) $C_{54}H_{96}O_{22}Ca$ 7.0	745.8638 (2+) $C_{70}H_{117}O_{30}NCa$ 13.0	1452.7733 (1+) $C_{70}H_{118}O_{30}N$ 12.5
#17	647.3343 (2+) $C_{60}H_{106}O_{25}N_2Ca$ 9.0	1388.7573 (1+) (-1H2O) $C_{69}H_{114}O_{27}N$ 13.5	
#4+#12	372.1981 (2+) $C_{36}H_{64}O_{13}Ca$ 5.0		
#4+#15	424.2218 (2+) $C_{40}H_{72}O_{16}Ca$ 5.0		
#4+#16	452.2349 (2+) (-1H2O) $C_{43}H_{76}O_{17}Ca$ 6.0		

In order to check for the presence of the methyl ester in the other acidified samples (AA and FA), XIC of the ion at *m/z* 869.1268 were obtained. Table VIII.4 reports the relative percentage of PLTX and its methyl ester. Accordingly to the previous observations, the methyl ester was detected in all the acidified samples with the only exception of AA at day 0 and gradually increased overtime and with the acid strength.

.

Table VIII.4 Recoveries following LC-HRMS analysis of PLTX and PLTX Methyl Ester at day 0 and day 14 in control and acidic solvents

	Control		Acetic Acid		Formic Acid		Trifluoroacetic Acid	
	% PLTX	% Methyl Ester	% PLTX	% Methyl Ester	% PLTX	% Methyl Ester	% PLTX	% Methyl Ester
Day 0	100	0	100	0	89	11	84	16
Day 14	100	0	94	6	61	39	37	63

The analysis of the full HRMS spectra of the TFA sample at 60° after several weeks after preparation showed that, beside the methyl ester, other ions emerged, likely due to other degradation products. Investigation on these compounds is undergoing.

3. Material and methods

3.1 Reagents, materials and standards for chemical analyses

All organic solvents (HPLC grade) were obtained from AtlanticLabo (Bordeaux, France) and Sigma Aldrich (Steinheim, Germany). Trifluoroacetic, Acetic and Formic acid were also acquired from Sigma–Aldrich. Milli-Q water was produced in-house to 18 MΩ/cm quality, using a Milli-Q integral 3 system (Millipore). Normal glass vials (1.5 mL) were obtained from Agilent Technologies; Silanized glass vials (1.5 mL) were obtained from Macherey-Nagel, Polypropylene (PP) and Teflon tubes (1.5 mL) were obtained from Merck Millipore. Certified standard solution of Okadaic acid (OA), obtained from the National Research Council in Halifax, Canada, and was dissolved in pure methanol. A PLTX standard (100 µg; lot LAM7122), obtained from Wako Chemicals GmbH (Neuss, Germany), was dissolved in methanol/water (1:1,v/v) and used for quantitative analyses. It should be noted that this standard is not certified and may contain some minor contaminants besides PLTX itself; quali-quantitative composition of the standard may vary within different lots. The standard used in this study contained 83 % of PLTX itself, 5 % of 42-hydroxypalytoxin, and 12 % of contaminant(s).

3.2 Liquid chromatography mass spectrometry

Mass spectrometry experiments were carried out on two different systems:

System 1: A UFLC-XR Shimadzu liquid chromatography system (Champs-sur-Marne, France) was coupled to a hybrid triple quadrupole/ion-trap mass spectrometer (API 4000 Qtrap, ABSCIEX, Les Ulis, France) equipped with a TurboIonSpray^{TM} ionization source. Mass spectrum detection for was carried out in multiple reactions monitoring (MRM) mode (positive ions). MRM experiments were established using source setting: curtain gas set at 30 psi, ion spray at 5000 V, a turbogas temperature of 300 °C, gas 1 and 2 set at 30 and 40 psi, respectively and an entrance potential of 10 V. For PLTX the following transitions were monitored: *m/z* 1340.9/327.3 ($[M + 2H]^{2+}$), 1331.9/327.3 ($[M + 2H - H_2O]^{2+}$) and 887.8/327.3 ($[M + 3H - H_2O]^{3+}$). The collision energy was applied at 47 eV for bi-charged ions and at 31 eV for the tri-charged ion. Declustering potential (DP) was set at 56 V for all transitions and cells exit potential (CXP) were at 20 V and 18 V for bi-charged ions and tri-charged ions, respectively. All the transitions were monitored with a dwell time of 500ms. For OA the transitions monitored were showed in **Table VIII.5**:

Table VIII.5 Multiple reaction monitoring (MRM) transitions used for quantitative analysis on System 1

	Declustering Potential (V)	Q1	Q3	Dwell Time (ms)	Entering Potential (V)	Collision energy (eV)	Cells Exit Potential (V)
PLTX	56	1340.9	327.3	500	10	47	20
	56	1331.9	327.3	500	10	47	20
	56	887.8	327.3	500	10	31	18
OA	86	822.5	787.3	250	10	17	20
	86	822.5	769.4	250	10	23	12
	86	822.5	751.8	250	10	29	18
	86	822.5	805.4	250	10	13	12

System 2: a Dionex Ultimate 3000 quaternary system coupled to a hybrid linear ion trap LTQ Orbitrap XL^{TM} Fourier TransformMS (FTMS) equipped with an ESI ION MAX^{TM} source (Thermo-Fisher, San Josè, CA, USA). HR full MS experiments for PLTX (positive ions) were acquired in the range m/z 800–1400 at a resolving power (RP) of 60,000 (FWHMat *m/z* 400). The following source settings were used: a spray voltage of 4.8 kV, a capillary temperature of 290 °C, a capillary voltage of 17 V, and a sheath gas and an auxiliary gas flow of 32 and 4 (arbitrary units). The tube lens voltage was set at 145 V.

Liquid chromatography was carried out by using a Poroshell 120 EC-C18, 2.7 μm, 2.1×100 mm (Agilent, USA) thermostated at 25°C. The solvents using for the elution were water (eluent A) and 95% acetonitrile/water (eluent B), both containing 2 mM ammonium formiate and 50 mM formic acid for OA, and eluent A and, both containing 30 mM acetic acid for PLTX at 0.2 mL/min flow rate. The gradient was raised from 20% to 100% B in 10 min and was held over 5 min before dropping down to the initial conditions.

PLTX standards at eight levels of concentration (1000, 500, 250, 125, 62.5, 31.25, 15.625 ng/mL) and OA standards at six concentration levels (58.5, 40.9, 22.2, 10.5, 5.8, 2.9 ng/mL) were used to generate a calibration curve that was employed in quantitative analyses. Sum of MRM peak areas was used to express peak intensity. The average of triplicate measurements was used for plotting.

3.3 Instrumentation for drying down processes

Multiple Nitrogen evaporator equipped with a metal block thermostat was obtained from Liebisch, Labortechnik, (Germany); Rotational Vacuum Concentrator RVC 2-18 and Freeze Dryer Epsilon 1-4 LSCplus were obtained from Martin Christ (Germany).

3.4 Preliminary OA and PLTX evaporation experiment

Both PLTX (125 ng/mL) and OA (25 ng/mL) were mixed at equimolar concentration in 80% aqueous MeOH and the mixture was evaporated to dryness under N_2 stream at room temperature. The dry residue was reconstituted in 300 μL of 50% aqueous MeOH and transferred into PP vials for LC-MS analysis.

3.5 Effect of drying techniques on PLTX recovery

Palytoxin (125 ng) was diluted in 1 mL of 80% aqueous MeOH: 3 samples were evaporated to dryness under N_2 stream at room temperature and 3 samples were evaporated to dryness using vacuum concentrator (temperature was set at 30°C for 5 hours); to test freeze drying, PLTX (125 ng) was diluted in 1 mL of 10% of MeOH to allow the freezing of the mixture and 3 samples were evaporated to dryness using the fallowing program:

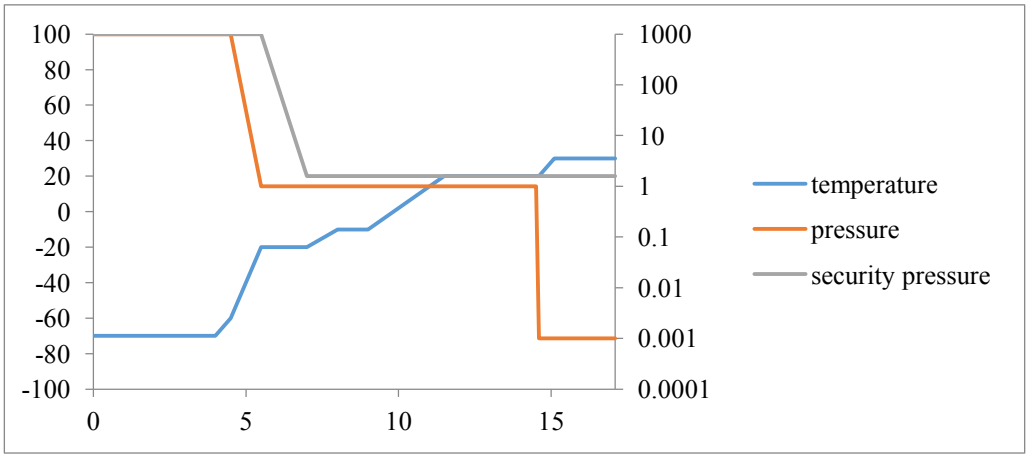

All the samples were dried in Normal glass vials. All the residues were re-dissolved in 300 µL of 50% aqueous MeOH and transferred into PP vials for LC-HRMS analysis.

In order to test the aerosolization phenomenon during evaporation procedures, another set of similar samples was prepared. The samples were evaporated to dryness with or without lid. For the samples evaporated under N_2 stream, the evaporation was performed piercing the lid and hanging it directly into the hole of the nozzle leakage of Nitrogen, with the lid slightly unscrewed to avoid an overpressure inside the vials. For the samples evaporated with vacuum concentrator and freeze drier, the lid was slightly unscrewed. All the residues were re-dissolved in 300 µL of 50% aqueous MeOH and transferred into PP vials for LC-HRMS analysis.

3.6 Complete Drying versus Concentration in different solvents

Palytoxin (125 ng) was diluted in 1 mL of six solvent mixtures: 80% aqueous MeOH, 80% aqueous EtOH, 80% aqueous IsoPrOH, pure MeOH, pure EtOH and pure IsoPrOH. PP tubes were chosen as containers. Each mixture was evaporated to dryness under N_2 stream at room temperature. All the experiments were carried out in triplicate. The obtained residues were re-dissolved either in the same volume (1 mL) of the original solvent mixture or in 50% aqueous MeOH and transferred into PP vials for LC-HRMS analysis.

To test the concentration process, PLTX (125 ng) was diluted in 1 mL of six afore mentioned mixtures into PP tubes. Each mixture was concentrated under N_2stream at room temperature, up to a volume of about 200 µL which was transferred into PP vials for LC-HRMS analysis. After the analysis, all the aqueous samples were added with 200 µL of the relevant organic starting solvent and reanalyzed.

3.7 Complete Drying versus Concentration in different materials

Palytoxin (125 ng) was diluted in 1 mL of six solvent mixtures: 80% aqueous MeOH, 80% aqueous EtOH, 80% aqueous IsoPrOH, pure MeOH, pure EtOH and pure IsoPrOH. Four different materials were tested both in complete drying and concentration mode: normal glass and silanized glass vials, PP and Teflon tubes. To test complete drying, each mixture was evaporated to dryness under N_2 stream at room temperature. The obtained residues were re-dissolved in the same volume (1 mL) of the original solvent mixture and transferred into PP vials for LC-HRMS analysis. All the experiments were carried out in triplicate.

To test the concentration process, PLTX (125 ng) was diluted in 1 mL of six afore mentioned mixtures into the four materials. Each mixture was concentrated under N_2stream at room temperature, up to a volume of about 200 µL which was transferred into PP vials for LC-HRMS analysis. After the analysis, all the aqueous samples were added with 200 µL of the relevant organic starting solvent and reanalyzed.

3.8 Dry-down of PLTX at different concentration levels and influence of the re-dissolution volume

Four different PLTX 80% aqueous MeOH solutions (62.5, 125, 250 and 500 ng/mL) were evaporated to dryness under N_2 stream at room temperature in Teflon tubes. The obtained residues were re-dissolved either in 0.3 mL or 1 mL or 80% aqueous MeOH and transferred into PP vials for LC-HRMS analysis.

Six different PLTX 10% aqueous MeOH solutions (125, 250, 500, 1000, 2000 and 4000 ng/mL) were freeze dried in normal glass vials. The obtained residues were re-dissolved in 0.3 mL of 50% MeOH and transferred into PP vials for LC-HRMS analysis.

3.9 Preliminary study on stability of PLTX in acids

Palytoxin (125 ng) was diluted in three different 80% aqueous MeOH mixtures containing respectively 0.2% of acetic acid (AA), 0.1% of trifluoroacetic acid (TFA) and 2% of formic acid (FA). Simultaneously, 80% aqueous MeOH was spiked with the same quantity of PLTX to serve as control. Teflon tubes were chosen as containers. Each mixture was evaporated to dryness under N_2 stream at room temperature. All the experiments were carried out in triplicate. All the residues were re-dissolved in 1 mL of 80% aqueous MeOH and transferred into PP vials for LC-MS and LC-HRMS/MS analysis.

The same acidic mixtures have been kept at 60°C for 1 hour and after transferred into PP vials for LC-MS and LC-HRMS/MS analysis.

4. Conclusions

This work represents one of the first studies of PLTX behavior in different experimental conditions. In the aim of an isolation work, the evaporation step has been in-depth investigated, highlighting that PLTX behaves differently whether it is simply concentrated or completely dried down. Recoveries are strongly dependent on solubility of PLTX in the mixtures used as well as on the materials in which evaporation is carried out. We demonstrated that, in order to maximally recover PLTX, freeze drying is a procedure that should be avoided. In general, better results were obtained when PLTX was completely dried down in Teflon materials carrying out evaporation in aqueous blends or concentration in pure organic solvent; worse recoveries were obtained using glass materials probably because PLTX sticks to the walls of the vials; in order to reduce this phenomenon water should be used in the mixture. Stability of PLTX in acidic blends was also investigated. We demonstrated that PLTX is an acid-sensitive molecule and we are able to find one of the degradation products which could be a PLTX methyl-Ester.

References

1. Tartaglione L, Dell'Aversano C, Mazzeo A, Forino M, Wieringa A, Ciminiello P. Determination of Palytoxins in Soft Coral and Seawater from a Home Aquarium. Comparison between *Palythoa*- and *Ostreopsis*-Related Inhalatory Poisonings. (2016) Environmental Science and Technology, 50(2), 1023-103

2. Ito E, Yasumoto T: Toxicological studies on palytoxin and ostreocin-D administered to mice by three different routes. Toxicon 2009, 54(3):244-251

3. Ciminiello P, Dell'Aversano C, Dello Iacovo E, Fattorusso E, Forino M, Grauso L, Tartaglione L, Guerrini F, Pezzolesi L, Pistocchi R, Vanucci S. Isolation and structure elucidation of Ovatoxin-a, the major toxin produced by *Ostreopsis ovata* (2012) J. Am. Chem.Soc. 134, 1869−1875

4. Brissard C, Herrenknecht C, Sechet V, Herve F, Pisapia F, Harcouet J, Lemee R, Chomerat N, Hess P, Amzil Z. (2014). Complex Toxin Profile of French Mediterranean Ostreopsis cf. ovata Strains, Seafood Accumulation and Ovatoxins Prepurification. Marine Drugs, 12(5), 2851-2876

5. Zendong Z, Herrenknecht C, Abadie E, Brissard C, Tixier E, Mondeguer F, Sechet V, Amzil Z, Hess P. (2014). Extended evaluation of polymeric and lipophilic sorbents for passive sampling of marine toxins. Toxicon, 91, 57-68

6. Taylor TJ, Gerald PW, Abram FB, Mereish, Kay MA. Non-specific binding of palytoxin to plastic surfaces. (1991). Toxicology Letters, 57(3), 291-296

7. Ciminiello P, Dell'Aversano C, Dello Iacovo E, Fattorusso E, Forino M, Tartaglione L, Rossi R, Soprano V, Capozzo D, Serpe L. Palytoxin in seafood by liquid chromatography tandem mass spectrometry: investigation of extraction efficiency and matrix effect. (2011) Anal Bioanal Chem 401:1043–1050

8. Ciminiello P, Dell'Aversano C, Dello Iacovo E, Fattorusso E, Forino M, Tartaglione L, Benedettini G, Onorari M, Serena F, Battocchi C, Casabianca S, Penna A. First Finding of *Ostreopsis* cf. *ovata* Toxins in Marine Aerosols. (2014) Environ. Sci. Technol., 48 (6), 3532−3540

9. Ciminiello P, Dell'Aversano C, Fattorusso E, Forino M, Magno GS, Tartaglione L, Grillo C, Melchiorre N. (2006) The Genoa 2005 outbreak. Determination of putative palytoxin in Mediterranean *Ostreopsis ovata* by a new liquid chromatography tandem mass spectrometry method. Anal. Chem. 78, 6153–6159

10. Gorman WG, Hall GD. Dielectric constant correlations with solubility and solubility parameters. (1964) J Pharm Sci 53, 1017-1020

11. Armstrong RW, Beau JM, Cheon SH, Christ WJ, Fujioka H, Ham WH, Hawkins LD, Jin H, Kang SH, Kishi Y, Martinelli MJ, McWhorter WW, Mizuno JrM, Nakata M, Stutz AE, Talamas FX, Taniguchi M, Tino JA, Ueda K, Uenishi J, White JB, Yonaga M. 1989. Total synthesis of palytoxin carboxylic acid and palytoxin amide. J. Am. Chem. Soc. 111: 7530-7533

12. McGinley PM, Katz LE, Weber JrWJ. Competitive sorption and displacement of hydrophobic organic contaminants in saturated subsurface soil systems. (1996) Water resources research, 32(12), 3571-3577

13. Delle Site A. Factors affecting sorption of organic compounds in natural sorbent/water systems and sorption coefficients for selected pollutants. A Review. (2001) J. Phys. Chem. 30 (1)

14. Ciminiello P, Dell'Aversano C, Dello Iacovo E, Fattorusso E, Forino M, Grauso L, Tartaglione L. High resolution LC-MS^n fragmentation pattern of palytoxin as template to

gain new insights into ovatoxin-A structure. The key role of calcium in MS behavior of palytoxins. (2012) J Am Soc Mass Spectrom 23(5):952–963

15. Ciminiello P, Dell'Aversano C, Dello Iacovo E, Fattorusso E, Forino M, Tartaglione L, Battocchi C, Crinelli R, Carloni E, Magnani M, Penna A. The unique toxin profile of a Mediterranean *Ostreopsis* cf. *ovata* strain. HR LC-MS^n characterization of ovatoxin-f, a new palytoxin congener. (2012) Chem Res Toxicol 25:1243–1252

16. Brissard C, Hervé F, Sibat M, Séchet V, Hess P, Amzil Z, Herrenknecht C. Characterization of ovatoxin-h, a new ovatoxin analog, and evaluation of chromatographic columns for ovatoxin analysis and purification. (2015) J Chromatogr A. 3, 1388:87-101

17. García-Altares M, Tartaglione L, Dell'Aversano C, Carnicer O, de la Iglesia P, Forino M, Diogène J, Ciminiello P. (2015) The novel ovatoxin-g and isobaric palytoxin (so far referred to as putative palytoxin) from *Ostreopsis* cf. *ovata* (NW Mediterranean Sea): structural insights by LC-high resolution MS^n. Anal Bioanal Chem 407, 1191–1204

18. Tartaglione L, Mazzeo A, Dell'Aversano C, Forino M, Giussani V, Capellacci S, Penna A, Asnaghi V, Faimali M, Chiantore M, Yasumoto T, Ciminiello P. Chemical, molecular, and eco-toxicological investigation of *Ostreopsis* sp. from Cyprus Island: structural insights into four new ovatoxins by LC-HRMS/MS (2015) Anal Bioanal Chem 408(3), 915-932

19. Katrizky A. Advances in heterocyclic chemistry 1st edition (2014). Imprint: Academic Press. eBook ISBN: 9780124202092 Print BookISBN: 9780124201606